ABSTRACT OF THESIS

Name of Candidate John Ernest Jackson, B.Sc.,

Address

Degree Doctor of Philosophy *Date* May 1964.

Title of Thesis Studies on the Catalytic Thermal Decomposition of Solids

A brief outline has been given of the present knowledge of the kinetics of the thermal decomposition of inorganic solids.

The effect of NiO, Fe_2O_3, CuO, ZnO, MnO_2 and α-Al_2O_3 on the decomposition of potassium permanganate in the solid state has been studied using pelleted samples of 1.1 mixtures, by weight, of permanganate and oxide. The decomposition in all cases, could be accurately represented by the equation

$$KMnO_4 \longrightarrow K_2MnO_4 + MnO_2 + O_2$$

The oxides were found to catalyse the initial stages of the decomposition but their effect was exhausted, with the exception of NiO, after α = c 0.15. The decomposition in the later stages, α = 0.15 - 0.9 followed the Prout-Tompkins equation, viz.

$$\log \alpha/1-\alpha = kt + c$$

two values of k being required. This requires the acceleration or autocatalytic stage α = 0.15 - 0.5 to proceed by a "branching plane" mechanism in which the planes interfere, k being a measure of the probability of branching. The second value, k_2, is required for the decay stage of the decomposition α = 0.5 - 0.9.

Since in the α- range 0 - 0.10 a common kinetic equation did not hold for all the systems studied, it was necessary, in order to measure the relative catalytic efficiency of the oxides, to resort to arbitrarily selecting the inverse of the time required for α to reach 0.03, as a measure of the catalysis. This procedure gave the following "activity series"

$$NiO > Fe_2O_3 > CuO > ZnO, \alpha\text{-}Al_2O_3 > MnO_2$$

The activation energy for the decomposition in this region, as measured by oxygen evolution, was 38±3 k. cals/mole; irrespective of system. The catalytic action of the oxides is therefore due to a change in the pre-exponential term of the Arrhenius equation. Their action would appear to be dependent on an "active surface" and on oxide surface area, since heating to 1000°C, in the case of NiO and ZnO, destroyed the catalysis. The semi-conductor properties of the oxides do not appear to be important: the incorporation of altervalent lithium and chromic oxide into the lattices of nickel and zinc oxide respectively led to no significant change in catalytic activity or kinetics.

The changes in electrical conductivity of the permanganate - oxide pellets were measured during the decomposition of the permanganate. The results have been explained within the mechanism proposed by Smirnova, although the exact identity of the intermediate given as MnO_4 or of the conducting species assumed to be an electron, could not be established. These results suggested that the rate determining step of the decomposition is probably the removal of an electron from the permanganate ion. The activation energy for the production of the charge carrier, 38±2 k. cals/mole, is not significantly different from that for the initial decomposition as measured by oxygen evolution. The presence of oxides, with the exception of ZnO (1000°), ZnO + Cr_2O_3 and α-Al_2O_3 did not alter the activation energy of conduction, confirming that the catalysis is due to changes in the A factor.

Use other side if necessary.

STUDIES on THE CATALYTIC THERMAL DECOMPOSITION of SOLIDS

Thesis presented for the degree of Doctor of Philosophy

by

JOHN E. JACKSON, B.Sc.

University of Edinburgh

July, 1964.

EX BIBL UNIV. EDINBURGEN

TO MY PARENTS

PREFACE

This thesis is primarily concerned with studying the effect of certain oxides on the isothermal decomposition of potassium permanganate and to see if electrical conductivity measurements in conjunction with studies using "doped" oxides would allow any insight into the mechanism of the decomposition.

ACKNOWLEDGMENTS

I should like to thank my supervisor, Dr. Duncan Taylor, for his unceasing guidance, advice and encouragement throughout the course of this work.

I thank Professor T.L. Cotterell for the interest he has shown in this work, and him and Professor E.L. Hirst for the provision of laboratory facilities.

Acknowledgment is made for the award of a Research Studentship (1961-64) from the Department of Scientific and Industrial Research.

I should also like to take this opportunity to thank my parents for their help and encouragement throughout my years of study.

CONTENTS

GENERAL INTRODUCTION

In studies of the thermal decomposition of solids, it is convenient to use reaction of the type

$$A(s) \longrightarrow B(s) + C(gas) \quad 1$$

Endothermic reactions of this type, however, may present experimental and theoretical difficulties due to the possible occurrence of both dissociation and recombination processes. Nevertheless such investigations are worthwhile since the information gained concerning nucleation and the interface reaction is not readily obtainable elsewhere. A comprehensive review of such reactions has been given by Garner[1].

Because of these difficulties, most of the reactions studied fall into the category of irreversible exothermic decompositions, the kinetics of which can easily be followed by measuring the increase in pressure of the evolved gas or the loss in weight of the solid. The thermal decomposition of potassium permanganate is an example of this type of reaction.

The first stage of the experimental study of a thermal decomposition is usually the determination of the form of the α/Time curve (Fig. 1) where α represents the fraction decomposed. These curves are normally sigmoidal, indicating an autocatalytic reaction (a) and can usually be divided into three stages: - (1) An induction or slow reaction period AB, (2) an acceleration stage BC and a decay stage CD. However if the initial accelatory period is short and the final decay stage more pronounced, then an asymetric curve (b) results. Type (b) is given by lead styphanate[2] and mercuric oxalate[3]; in other cases e.g. lead azide[4] the induction period is virtually absent (c).

The general form of these curves can be explained by considering the formation and growth of "nuclei" of the decomposition product B, decomposition

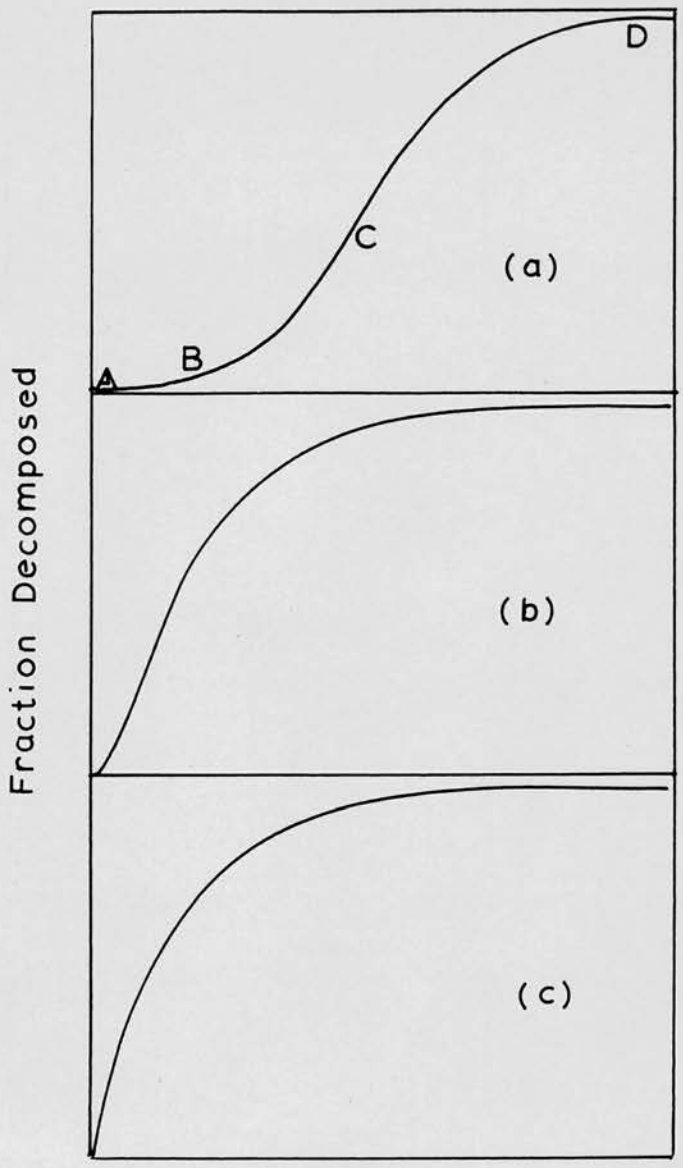

Fig. 1

beginning at special sites in the crystal lattice of A, where local fluctuations in lattice energy supply the necessary free energy of nucleation. The rate of decomposition, however, cannot be calculated purely in terms of probability theory since the molecules of B have finite size. Thus while the first fragments of B may have superimposed on them the molecular volume and lattice type of A, larger particles of B will almost certainly have a different molecular volume and lattice type. This will cause local deformation in the lattice which is referred to as "strain". The associated energy is termed "strain energy". For a fragment of B containing m molecules and a strain energy per unit area of interface γ, the free energy of formation is

$$\Delta G_1 = m\Delta G_B + \sigma\gamma \quad (1)$$

where σ is a shape factor and G_B is the bulk free energy per molecule. Assuming spherical particles of radius r and that the volume per molecule of the product phase is v_m,

$$m = 4\pi r^3/3v_m \quad (2)$$

Equation (1) can now be written

$$\Delta G_1 = m\Delta G_B + \gamma (36\pi v_m^2)^{1/3} m^{2/3}$$
$$= am^{2/3} - bm \quad (3)$$

where a is proportional to the strain energy and b is the negative of the bulk free energy charge per molecule. Such an expression, providing γ is positive, shows that ΔG, must pass through a maximum at $m = m^*$, when a fragment has the critical size to be in equilibrium with its surroundings. Small fragments of B would thus appear to be unstable reverting back to A, whereas large fragments of B are stable with respect to the reaction $A \rightarrow B + C$. Further reaction therefore tends to take place at the interface of the two solid phases. The products B thus spreads from those points where the reaction first began. It is these points which are referred to as "nuclei" or growth nuclei. The unstable nuclei where

$m < m^*$ are known as "germ nuclei".

If we assume that the free energy of activation of the interface reaction is substantially less than that for nucleus formation, then the reaction proceeds by the formation of compact nuclei distributed throughout, the matrix of A. This has been observed by Wischin[5] with barium azide. The general autocatalytic nature of such reactions can now be explained in terms of the slow formation of nuclei at localised spots in the reactant followed by their relatively fast growth. Curves of type (b) would result if there was no great difference between the activation free energy for growth and nucleus formation, since in this case a large number of small nuclei could be formed, none of which would grow to visable size; hence the reduction in the acceleratory period. Curve (c) which is the limiting case of (b) would result of the probability of nucleation was enhanced e.g. by grinding. This enhancement probably occurs because grinding (c.f. the cold working of metals) will produce a high concentration of ion vacancies[6 7] and increase the number of dislocations[8 9]; and because the energy required for nucleation is least at lattice imperfections such as dislocations[10], vacancies, Smekal cracks. Growth of nuclei is also preferred at these sites, since large lattice stresses cannot be supported in their vicinity. This last point was experimentally shown by Hedges and Mitchell[11] in the photolysis of silver bromide.

Kinetic equations, expressing α as a function of time, can be derived also by considering the production and growth of nuclei. If we assume that the decomposition of a single molecule leads to the formation of a growth nucleus, then the rate of nucleation can be given by

$$dN/dt = k_1 N_0 \exp. (-k_1 t)$$

where N is the number of nuclei at time t; N_0 is the number of potential nucleus

forming sites. This is known as the exponential law.

If however several successive decompositions or the reaction of several intermediates are required; the rate of nucleation is given by a power law

$$dN/dt = Dt^{\beta}$$

The growth nuclei so formed then grow either one, two or three dimensionally and assuming that the nuclei grow at a constant rate, as visual observation of copper sulphate pentahydrate[13], nickel sulphate heptahydrate[14] and barium azide[15] has shown; a power law

$$\alpha = At^{n} + C$$

is derived.

This law represents normal growth, the value of n depending on the dimensions of growth and the rate of nucleation. The power law holds well for barium azide[5], silver, oxide[15] and aged mercury fulminate[16]. However since no allowance is made for possible overlap between growing nuclei nor for the complications caused by cracking of the crystals due to strain, departures from the law are to be expected.

Avrami[17], by allowing for overlapping of nuclei derived an equation

$$\alpha = 1 - e^{kt^{n}}$$

which should apply for both the acceleration and decay periods providing the reaction interface remains intact. Should the interface collapse, then, since each molecule can now be considered to have an equal chance of decomposition, a unimolecular decay law would be required.

Garner and Hailes[18], in order to explain the high values of n (11.2 - 22.8) they found with whole crystals of mercury fulminate, introduced the concept of nuclei as linear branching chains. Such a supposition leads to the derivation of an exponential increase of α with time, $\alpha = Ce^{kt}$.

This exponential law held up to $\alpha = 0.5$ for large crystals of lead

styphanate[2] and up to $\alpha = 0.3$ for freshly prepared silver oxalate[19]. Although there was thus experimental verification for the exponential law, the concept on which it was based was doubtful.

There are two accepted explanations for an exponential law. The first assumes that the reaction spreads by a "branching plate" mechanism whereby the reaction interface is increased by the formation of new surfaces by cracking and not by the production and growth of new nuclei. Such a mechanism is thought to occur due to the product molecules forming decomposition spikes on the surface of the crystal which exert a lateral stress on the crystal. This is relieved by cracking, thus revealing fresh surfaces. Such cracking would be expected to be facilitated by the presence of dislocations in the crystal. Then, provided the rate of reaction is dependant on the rate of branching, an exponential law can be derived

$$\alpha = De^{kt}$$

k being the probability of branching.

Prout and Tompkins[20] extended this theory by introducing the concept of interference between the branching plates which would result in the termination of the chains involved. This altered the exponential law to

$$\log_e \alpha/1-\alpha = kt + C.$$

They found that this expression held throughout the decomposition of potassium permanganate excluding the induction period. The Prout-Tompkins equation also holds for a series of alkali and alkaline earth permanganates[21 22 23], ammonium dichromate[24], lead oxalate[25] and small crystals of mercury fulminate[26].

The second explanation of an exponential law was first postulated by Garner[27] and has been developed by Hill[28] in his investigation involving potassium permanganate and its self-sustained reactions with iron and molybdenum. Here nuclei

are thought to be produced by diffusion of product into the lattice, thus increasing the number of growth nuclei.

During the later stages of any solid decomposition considerable overlapping of nuclei must occur, leading to the formation of a continuous interface surrounding fragments of unreacted solid. If this interface remains intact the Avrami[17] equation will hold. If, as is to be expected, there are differences in molecular volume the interface will collapse, leading to a unimolecular law since each molecule may now have an equal chance of decomposition. Should this assumption, however, be modified by requiring that an unreacted molecule must be adjacent to a product molecule before decomposition can occur, then the Prout-Tompkins equation is required.

The present work is primarily directed towards the investigation of the effect of various oxides on the thermal decomposition of potassium permanganate. While decomposition of potassium permanganate itself has been widely studied, the effect of oxides and other additives, has, up to the present, received much less attention. The work carried out on potassium permanganate alone will therefore be reviewed first, followed by a review of the results obtained with various additives on the decomposition and on the decomposition of other solids.

The decomposition can be represented by

$$2\ KMnO_4 \rightarrow K_2MnO_4 + MnO_2 + O_2.$$

As already mentioned Prout and Tompkins[20] first applied their equation to this decomposition. Using fresh crystals in the temperature region 200-225°C they found that this equation held overall, excluding the induction period and that it required two constants as a result of the assymetry about the point of inflexion in the α/Time curve. Grinding the crystals reduced the induction period but did not essentially alter the main acceleratory process; it did however significantly

alter the activation energy for whole crystals from E_1 = 38.5 kcals/mole E_2 = 38.8 kcals /mole to E_3 = 34.5 kcals/mole E_4 = 33.1 kcals/mole where E_1, E_2 represent activation energies for whole crystals and E_3, E_4 those for ground material. The similarity between the activation energies, in both cases, for the acceleration and decay stages supports the view that the same chemical processes occurs in both stages. The grinding effect they explained by arguing that this would produce a larger initial concentration of nuclei; hence the reduction in induction period.

The slow initial reaction or induction period was later re-examined in conjunction with the study of the thermal decomposition of Rubidium permanganate[21]. In the case of Potassium permanganate it was described by

$$p = kt + c$$

where p is the pressure of 0_2 evolved, and for Rubidium by the expression

$$p^{\frac{1}{2}} = kt + c.$$

In both cases grinding eliminated this slow reaction. The Arrhenius plot of 'k' for this slow reaction with whole crystals gave the activation energy as 25.5 kcals/mole which is considerably less than that for the main reaction. A similar discreprancy was found for Rubidium. This slow stage they suggested was due to reaction of a fixed number of nuclei and proceeded along the crystal dislocations. Such a reaction would be energetically more preferable; hence the lower activation energy.

Erofeev and Smirnova[29] similarly found grinding affected the result, in the temperature range 211.5 - 227.6°; the acceleration being more marked with finely ground crystals. Their results fitted the Avrami equation giving values of n = 4-5 for whole crystals and n= 4 for ground crystals. In the initial stage of their reaction there was considerable deviation from the equation, especially with ground material. The value of n is represented as related to the number of "stages" by which the initial growth nuclei grow in three dimensions thus $n = \sigma + 3$, a value of four thus

indicating one "stage" and n = 5, two"stages" for nuclei growth. These values of n were obtained by plotting log (log 1/1 $-\alpha$) as a function of log t. Such a technique is insensitive so that any differentiation between the values of n is suspect. However in a study of aged material[30] they obtained a value of n = 2, representing two dimensional growth of a fixed number of nuclei. This difference between fresh and aged material is significant.

The importance of the initial surface area of the material was further brought out by B.V. Erofeev[31] who reported that at 218° the initial decomposition rate increased directly with the specific surface area of potassium permanganate, the maximum rate depending only slightly on the surface area. Komatsu[32] has also shown that the rate of decomposition is dependant on crystal size.

The results of Prout and Tompkins have been confirmed by Hill and Welsh[33], for fresh material. Their results could be fitted by an exponential relationship

$$\alpha = A\exp(kt + c).$$

Aged material however gave poor exponential relationships.

The only systematic study of the effect of oxides on the thermal decomposition of potassium permanganate has been carried out by Roginsky and Shultz[34]. Using a gradually rising temperature and mainly powdered mixtures of permanganate crystals and oxides they found that the oxides catalysed the decomposition and that this catalysis was more pronounced with powdered permanganate. They found that the oxides could be divided into three groups depending on their efficiency. Thus NiO, Co_3O_4, Fe_2O_3 and CuO were very efficient; somewhat weaker were Mn_3O_4, Ag_2O, SnO_2 and PbO, much less effective were Sb_2O_5, Cr_2O_3, SnO, Al_2O_3, CdO and PbO_2.

The oxides activity, however, also depended on its mode of preparation and could be destroyed by heating. Thus while ferric oxide prepared from the oxalate was very efficient that prepared from the sulphate or hydroxide was only average. This gradation in the catalytic activity of ferric oxide was paralleled by changes

in other physical properties such as solubility and colour.

Since these oxides also acted as catalysts for, other reactions - decomposition of potassium chlorate, ozone and barium peroxide - forming a similar "activity series" Roginsky and Shultz attampted to correlate their activity with their physical properties. They reached the conclusion that the most effective catalysts were dark coloured paramagnetic oxides. This they believed pointed to the reaction occurring by an electronic mechanism.

Ossinovik and Bel'kevich[35] have found that aluminium powder catalyses the reaction at 350° but not at 265°.

Smirnova[36] argues from the difference between the activation energy of growth of the nuclei and that for their formation, both in whole and powdered crystals, that the solid products act catalytically.

Simchen[37] reports that the decomposition is not catalysed by manganese dioxide or by the reaction products. Prout and Tompkins also found that the products had no catalytic effect on $KMnO_4$[20] and $RbMnO_4$[21] while with $AgMnO_4$[38] they found that traces of water catalysed the reaction and that mixing with the end products shifted the pressure/time curves to shorter times but had no effect on the rate in the acceleration or decay stage.

A similar series of investigations into the effect of oxides on the decomposition of ammonium perchlorate has been carried out by Solymosi and Kris[39,40 & 41], Galwey and Jacobs[42] and Hermoni and Salmon[44]. The effect of the oxides on this reaction, however, are much more pronounced. Thus while pure ammonium perchlorate below 240° gives only 30% conversion, in the presence of the oxides conversions of 80 - 100% are obtained and the "explosion temperature" is lowered by approximately 200°. Since most of the effective oxides are of p-type character Solymosi and Kris argue thatthis supports the electron-transfer mechanism proposed by Galwey and Jacobs[45]

with the rate determining stage the removal of an electron from the perchlorate ion

$$ClO_4^- \quad ClO_4 + e.$$

Certainly their results with doped CuO[39] supports this view. Increasing the defect electron concentration by incorporating lithium oxide decreased the induction period and increased the reaction rate with respect to the reaction with pure CuO. Incorporating chromic oxide, which decreases the "defect electron concentration", led to an increase in induction period and a slight decrease of reaction rate.

Their results with zinc oxide[40] and doped zinc oxide tend however to contradict this. Zinc oxide is an n-type semi-conductor and therefore would not promote the above electron transfer. Similarly any doping, with alumina to increase the oxides conductivity will hinder the electron transfer, while doping with lithium oxide to decrease the conductivity will aid the transfer. Their results completely contradicted this. Thus not only did zinc oxide catalyse the reaction but doping with alumina shortened the induction period and increased the reaction rate, while doping with lithium oxide increased the induction period and decreased the reaction rate. Solymosi and Kris explain this contradiction by arguing that the increased reaction rate in the presence of zinc oxide is due to the melting of ammonium perchlorate which takes place during the solid phase reaction with zinc oxide. Similarly the effect of doping can be attributed, instead of to changes in electron concentration, to the change in the rate of solid phase reaction between the perchlorate and zinc oxide, which in turn is probably related to the degree of sintering the zinc oxide has undergone. In agreement with this is the known fact that lithium oxide promotes the sintering of zinc oxide while aluminium oxide hinders it.

Solymosi and Kris[43] have also studied the effect of oxides on the thermal

decomposition of potassium chlorate. In this case the oxides used were NiO, ZnO, CuO, MgO and TiO_2. A similar "activity series" to that found by Roginsky and Shultz[34] was the result. The most effective was the defect conductor NiO followed by the intrinsic conductor CuO, then the insulator MgO and finally the electron conductors ZnO and TiO_2. This again points to the reaction occurring by an electron transfer mechanism. Nickel oxide was found to be the only oxide whose efficiency depended on its heat treatment.

Smirnova[46] has suggested that the decomposition of potassium permanganate could be represented by a mechanism

$$MnO_4^- \rightarrow MnO_4 + e \quad (1)$$

$$MnO_4 \rightarrow MnO_2 + O_2 \quad (2)$$

$$MnO_4^- + e \rightarrow MnO_4^{2-} \quad (3)$$

with the rate determining stage step (1). If such a mechanism did hold, then the role of the oxides could be regarded as aiding or hindering the electron transfer process. An insight into the possibility of this could perhaps be obtained by measuring the change in conductivity of pure permanganate and permanganate/oxide mixtures during the decomposition. It would also provide the opportunity to compare the activation energy for the conduction process with that for the rate determining stage of the reaction as measured by oxygen evolution. For these reasons the second section of this work is concerned with measuring the changes in electrical conductivity during the decomposition.

2 Experimental

2.1. Apparatus

The apparatus is shown in (fig. 2) and is similar to that used by Phillips[47]. The decompositionswere carried out in a closed system, the increase in pressure, in a known volume, being continuously monitored by a Pirani gauge. This was of the compensating type and was operated at a constant voltage by a Wheatstone bridge method, the out of balance voltage being fed through a shunt into a Sunvic recorder. The gauge was calibrated against a standard McLeod gauge and was found to give a linear response up to 100 μ.

The Pyrex reaction vessel, incorporating the thermocouple pocket, was centrally situated in an electrically heated furnace which was stabilised to better than 0.1°C by an electronic controller and a Sangamo Weston platinum resistence thermometer. The basic A.C. mains supply was stabilised by a voltage stabiliser.

The sample was contained in a small bucket constructed from 2 sq. cms. of 0.0025 cm. thick platinum foil and could be lowered into the furnace by means of the winch, to which the bucket was attached by a fine platinum wire.

The thermocouple was constructed from British Driver Harris T_1/T_2 thermocouple alloys by electric arc welding. It was then calibrated, with one junction at the bottom of the reaction vessel and the other held at 0°C in ice, in steps of 5°C from 100° - 270°C against a standard Platinum/Platinum - Rhodium thermocouple; the voltage was read to 0.001 mv. on a Tinsley potentiometer type 3184D.

The gases from the reaction vessel passed through trap T_1, into the vacuum line. V consisted of three bulbs, any of which could be connected to the vacuum line to give pressures in the desired range.

The volume of each section of the system was found by expanding a known

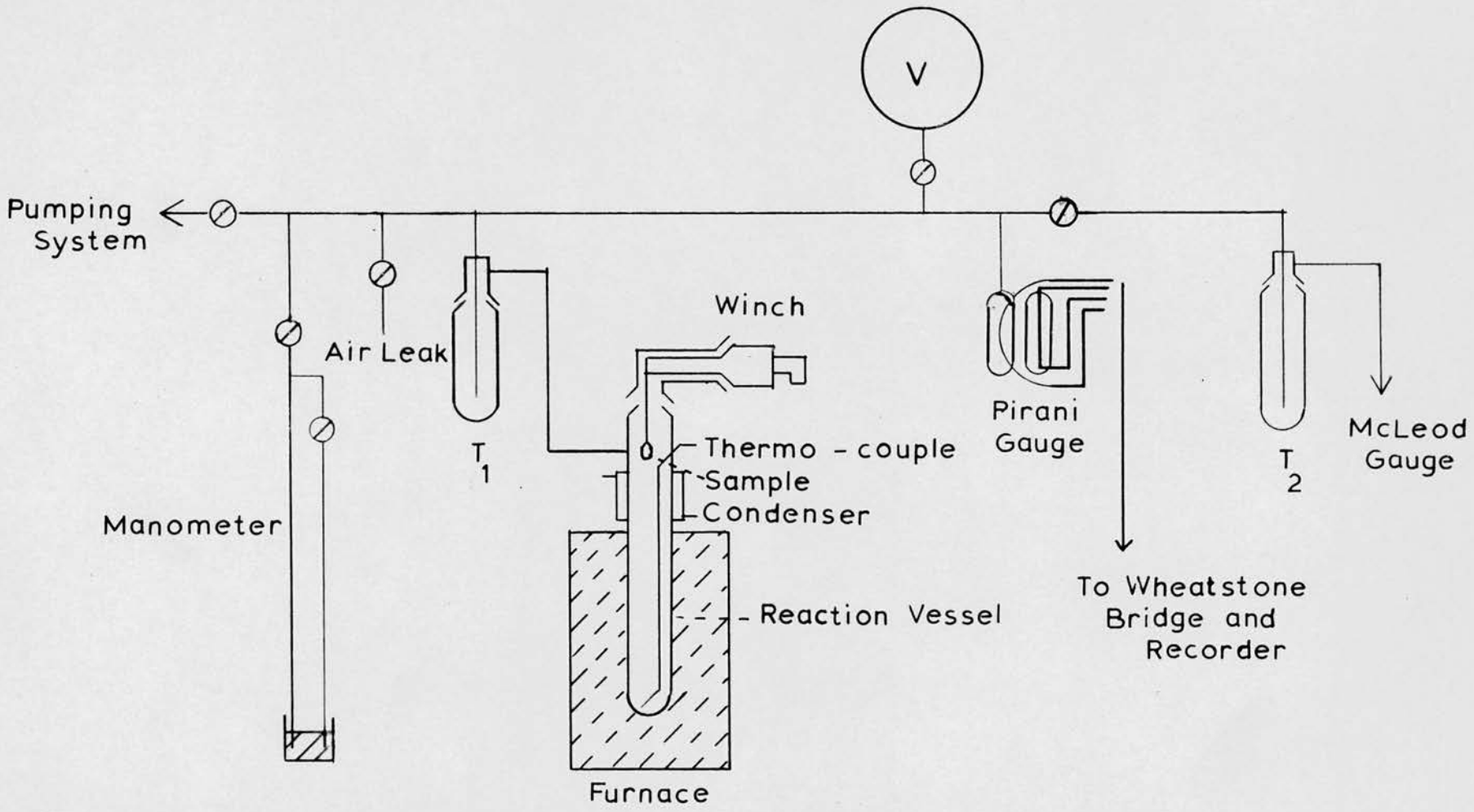

Apparatus for Oxygen Evolution Measurements

Fig. 2

pressure of dry air from a known volume, through the air leak into each section and measuring the resulting pressure on the manometer. From Boyle's Law, the volume of each section was calculated. Small volumes, where necessary, were calculated from the tubing dimensions. The volumes given in Table 1 are the mean of three determinations and were obtained with the reaction vessel and both traps at room temperature. The pressures read on the McLeod or Pirani gauge were converted to pressures at $0^{o}C$ by a correction factor calculated from the respective volumes and temperatures of the reaction vessel, of the cold traps and of the remaining volume of the system.

Table 1

Section of System	Mean Volume mls.	$\frac{p\ 273^{o}K}{p\ measured}$ = correction factor
Reaction line + T_1	542	1.19
McLeod gauge + T_2	519	1.19
Bulb No. 1	1100	1.03
Bulb No. 2	2303	-
Bulb No. 3	2335	-
Total Volume (added)	6799	0.96

The pumping system consisted of a glass two stage mercury diffusion pump, backed by a Speedivac rotary oil pump, the unit giving a vacuum of 10^{-3} μ. Apieson 'L' grease was used for all joints and taps

2.2. Preparation of the Oxides

Nickel Oxide

Black nickel oxide was prepared by heating basic nickel carbonate for 4 hours, in an atmosphere of air, at 400°C in an electric furnace.

Ferric Oxide

Ferric oxide was prepared, (cf. Roginsky's[34] "active" ferric oxide), from the oxalate by heating it in an electric furnace for 4 hours at 400°C, again in an atmosphere of air.

Zinc Oxide

Normal "Analar" zinc oxide was used but for standardisation this was heated for 4 hours at 400°C.

α Alumina

α Alumina was prepared by heating normal chromatographic alumina for 3 hours at 1200°C.

Cupric Oxide

Cupric oxide was prepared from the basic carbonate by heating, in air, for 4 hours at 400°C.

Manganese Dioxide

Manganese dioxide was prepared from the hydrated manganous sulphate by the method given in Palmers, Inorganic Chemistry[48]. It was finally dried by heating for 4 hours at 400°C. The purity of the manganese dioxide was then determined by titration with oxalic acid and potassium permanganate and found to be 78% pure.

Nickel oxide + 1 Mole% Lithium Oxide

The "doped" oxide was prepared by adding the calculated amount of lithium carbonate, as a solution in water, to the nickel oxide. This slurry was then dried overnight in an oven at 130°C. The dried mixture was then thoroughly mixed

by a mortar and pestle, pelleted and fired for 3 hours at 1000°C to ensure complete incorporation of the lithium oxide in the lattice structure of the nickel oxide. For comparison purposes a sample of "pure" nickel oxide was fired for 3 hours at 1000°C.

Zinc Oxide + 1 Mole% Chromic Oxide

This was prepared in an analogous manner. The calculated weight of ammonium dichromate was added to the zinc oxide again as a solution in water. This was then dried as above, mixed, pelleted and fired for 3 hours at 1000°C. Again a sample of "pure" zinc oxide was given the same heat treatment.

All the oxides were finally ground to a fine powder and stored, until required, in a desiccator over phosphorous pentoxide.

2.3. Experimental Procedure

Since it was intended to make electrical conductivity measurements at a later stage of the work and since this would entail working with small pellets of sample it was decided to work entirely with "pelleted" samples.

These samples were prepared by compressing, unless otherwise stated, (1:1) mixtures by weight of Potassium permanganate and the oxide under study, in the following way. The permanganate crystals were first finely ground by hand in a mortar for a fixed period of time; 5 minutes. The correct amount of oxide was then added and the mixture thoroughly mixed for 10 minutes. The sample was now loaded into a Perkin-Elmer dye type 1860002 and compressed at 10 tons pressure on the ram. This resulted in circular pellets 13 mm. in diameter and approximately 1 mm. thick. Small pieces of such a pellet were then used in the subsequent decomposition runs.

Since the grinding of the potassium permanganate crystals required by this procedure exposes "new" surfaces of permanganate, recrystallised material was not used. All samples were taken from one batch of "Analar" potassium permanganate.

By the above procedure the following oxide/permanganate systems were prepared.

A. Pure $KMnO_4$

B. $KMnO_4/\alpha Al_2O_3$

C. $KMnO_4/MnO_2$

D. $KMnO_4/CuO$

E. $KMnO_4/Fe_2O_3$

F. $KMnO_4/ZnO$

G. $KMnO_4/ZnO(1000^o)$

H. $KMnO_4/ZnO$ + 1 Mole% Cr_2O_3

I. $KMnO_4/NiO$

J. $KMnO_4/NiO$ (1000^o)

K. $KMnO_4/NiO$ + 1 Mole% Li_2O

L. $KMnO_4/10$ - 80% NiO

With the weighed sample (approximately 10mg. $KMnO_4$) in the platinium bucket, the system was pumped out overnight, a vacuum of 10^{-3} μ being obtained. The system was then isolated from the pumps and the taps to the volume bulbs were closed. If after an hour the pressure remained below 10^{-2} μ the sample was lowered into the furnace and care taken that it made good contact with the bottom of the thermocouple pocket. The thermocouple indicated a maximum heating up time of 4 minutes and gave no evidence of self-heating in the sample during the decomposition.

With liquid nitrogen surrounding T_1 and T_2 the Pirani continuously measured the pressure of oxygen evolved during the decomposition. The volume of the system was increased as required. The final pressure was recorded at least one hour after the apparent end point had been reached. Thus the fraction decomposed α at any time could be calculated by dividing the pressure at that time by the final pressure.

By this procedure a continuous record of the reaction was obtained. In many cases only the first 10% of the reaction was studied. In these cases full scale deflection of 10" on the recorder with appropriate choice of system volume represented on average 10% decomposition and as the recorder chart was subdivided into 0.1", it was estimated that the percentage decomposition, as read from the traces, was accurate to 0.03%, as this represented 0.03". Thus the course of the reaction through a given 1% decomposition was accurately known.

2.4. Preliminary Experiments

Preliminary kinetic experiments on the various systems were carried out in an identical manner to that described in section 2.3. Graph 1 shown a typical example of the results obtained.

The presence of the oxides greatly enhanced the initial reaction rate. This catalytic effect was however exhausted or greatly reduced by the time the reaction had proceeded to circa 20% decomposition. The effect of the oxides was also reflected in the fact that the shape of the initial section of the "α" - Time curves was dependent on the oxide present. However, with the exception of nickel oxide, this "shape dependancy" also vanished after $\alpha \doteq 0.2$. In the case of nickel oxide the effect persisted to the end. This will be discussed more fully in the discussion. The final volume of oxygen produced in all these runs, irrespective of system, was in agreement within a few percent with the results of Prout-Tompkins; 1 mole of potassium permanganate producing 0.5 moles Oxygen.

Thus the decomposition can be represented by

$$2KMnO_4 \rightarrow K_2MnO_4 + MnO_2 + O_2.$$

No results supporting the further decomposition of the manganate, as suggested by Simchen[37]

$$4KMnO_4 \rightarrow 2K_2O + 3MnO_2 + MnO_3 + 2\tfrac{1}{2}O_2$$

were obtained.

It was therefore decided to carefully study, in the first section of this work, the first 10% of the decomposition, taking only the high temperature runs to completion and utalising these results to calculate final pressures for the other runs.

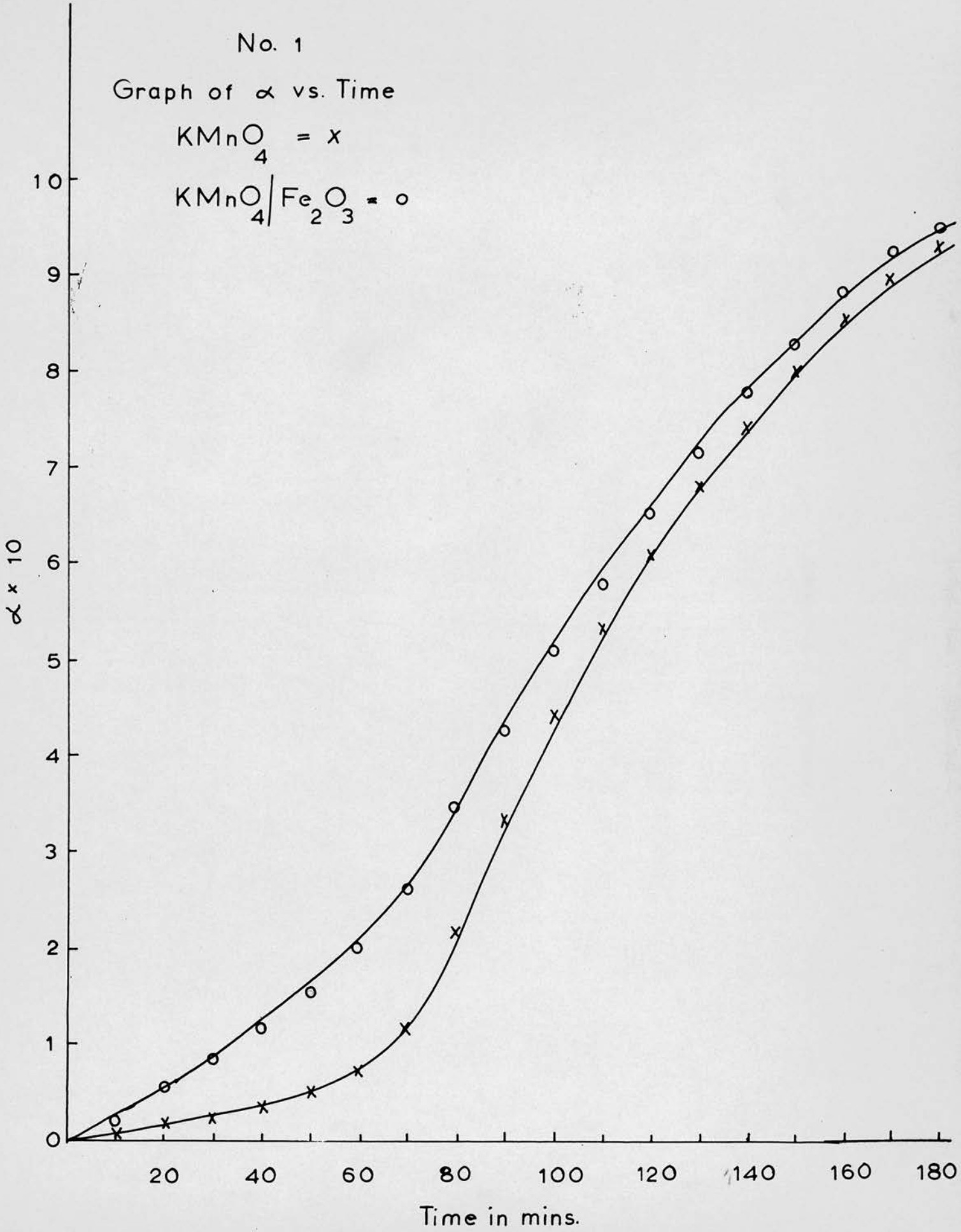
No. 1
Graph of α vs. Time
KMnO4 = X
KMnO4/Fe2O3 = o
α x 10
0
1
2
3
4
5
6
7
8
9
10
20
40
60
80
100
120
140
160
180
Time in mins.

2.5. Kinetics of the Decomposition

Since as has already been stated the shape of the initial section of the "α" - time curves is dependent on the system used examples of these are included in the appropriate sub-section. Similarly, the kinetic equations required to fit the initial stages, up to approximately 10% decomposition, are dependent on the system being studied.

A complication thus arises in trying to investigate the relative efficiency of the oxides used since no one kinetic equation covers all the systems studied. Thus resort had to be made to the technique of arbitrarily selecting the inverse of the time required for α to reach 0.03 as a measure of the initial rate and thus of any catalytic effect. This rate is denoted in the following sub-sections as k_x. The main acceleration and decay stages were however found, in all the systems studied, to give a reasonable fit to the Prout-Tompkins equation

$$\log_{10} \alpha/1-\alpha = kt + c.$$

The use of the rate constants derived from this equation, particularly from the runs carried out in the second section of this work, to construct an Arrhenius diagram for a 45° temperature range gave more conclusive proof of the limited catalytic effect of the oxides, since all the points lay, within experimental error, on one straight line, irrespective of the system used.

The following tables and graphs show a cross-section of the runs performed at various temperatures in the range 177 - 223°C. The tables give the respective functions of 'α' as required for the analysis used and the graphs show the plots of the different functions.

The following abbreviations have been used in the subsequent tables:

log = $\log_{10}$; $\underline{PT} = \log_{10} \alpha/1-\alpha$; k_x = rate derived from time to 3% decomposition; $k_{\frac{1}{3}}$ = constant from $\alpha = kt^3$; $k_{\frac{1}{2}}$ = constant from $\alpha = kt^2$;

k_{α} = constant from $\alpha = kt$; $k_{(1-\alpha)}$ = constant from log $1/1-\alpha = kt$;

$k_{(1-\alpha)^{\frac{1}{3}}}$ = constant from contracting sphere $\alpha = 1 - \left[c - k(t-t_o)\right]^3$

k_1 is the Prout-Tompkins branching coefficient from the equation

$\log_{10} \alpha/1-\alpha = kt + C$;

k_2 = constant from the Prout-Tompkins equation, applicable to the decay stage;

t_o = extrapolated time for initial fast growth;

k_o = constant derived from $1/t_o$.

2.5.1. Kinetics of the decomposition for pure potassium permanganate.

In tables 2, 3 and 4 and graphs 2, 3, 4 and 5 and 6 the kinetics are illustrated for pure potassium permanganate (A). The main features are that after the induction period, which is temperature dependent, the curves are acceleratory.

The initial slow reaction was best fitted, in the region $\alpha = 0.01 - 0.10$ by the power law

$$\alpha = kt^n \qquad \text{where } n = 3$$

The later stages of the reaction were fitted by the Prout-Tompkins equation, two values of "k" being required.

Tables 2 and 3	Analysis of system A.
Table 4	Rate constants for system A.
Graph 2	The initial stage of the "α" - time curves .
Graph 3	The initial slow reaction, a plot of $\alpha^{\frac{1}{3}}$ vs, Time.
Graph 4	The initial slow reaction extrapolated back to estimate the time required for the initial fast growth (t_o).
Graph 5	Arrhenius diagram for the initial fast growth.
Graph 6	Arrhenius diagram for normal growth which gives an activation energy E = 37±2 K cals./mole.

Table 2 System A $KMnO_4$

Run	A1			A2		A3	
Temp.	212.2°C			205.8°C		201.8°C	
Time Min	$\alpha \times 10^2$	$\alpha^{\frac{1}{3}} \times 10$	P.T.	$\alpha \times 10^2$	$\alpha^{\frac{1}{3}} \times 10$	$\alpha \times 10^2$	$\alpha^{\frac{1}{3}} \times 10$
5	0.15	1.14		0.27	1.39	0.10	1.01
10	0.27	1.39		0.63	1.84	0.35	1.52
15	0.39	1.57		0.99	2.15	0.60	1.82
20	0.56	1.78		1.38	2.40	0.83	2.02
25	0.83	2.02		1.83	2.63	1.09	2.21
30	1.12	2.24.		2.38	2.88	1.36	2.39
35	1.57	2.50		3.02	3.11	1.75	2.59
40	2.24	2.82		3.77	3.35	2.15	2.78
45	3.78	3.36		4.67	3.68	2.59	2.96
50	5.58	3.82		5.71	3.85	3.12	3.15
55	8.23	4.35		6.90	4.10	3.72	3.34
60	11.49	4.86		8.11	4.33	4.34	3.51
65				9.60	4.58	5.06	3.70
67			$\bar{1}.55$				
70				11.25	4.83	5.79	3.87
75						6.61	4.04
77			$\bar{1}.90$				
80						7.44	4.21
85						8.37	4.37
87			0.21				
90						9.25	4.52
97			0.46				
117			0.66				
127			0.89				
137			1.09				
147			1.31				
157			1.62				

Table 3 System A $KMnO_4$

Run	A4		A5		A6	
Temp.	197.9°C		194.1°C		194.2°C	
Time Min	$\alpha \times 10^2$	$\alpha^{\frac{1}{3}} \times 10$	$\alpha \times 10^2$	$\alpha^{\frac{1}{3}} \times 10$	$\alpha \times 10^2$	$\alpha^{\frac{1}{3}} \times 10$
5	0.04	0.76				
10	0.25	1.35	0.28	1.42	0.28	1.41
15	0.37	1.54				
20	0.49	1.70	0.07	1.87	0.56	1.78
25	0.61	1.83				
30	0.77	1.97	0.09	2.09	0.77	1.97
35	0.91	2.09				
40	1.05	2.19	1.17	2.27	1.03	2.17
45	1.25	2.32				
50	1.48	2.46	1.50	2.47	1.30	2.35
55	1.76	2.60				
60	2.04	2.73	1.88	2.66	1.59	2.51
65	2.40	2.88				
70	2.79	3.04	2.33	2.86	1.96	2.70
75	3.16	3.16				
80	3.63	3.31	2.84	3.05	2.37	2.87
85	4.12	3.45				
90	4.62	3.59	3.48	3.26	2.87	3.06
95	5.20	3.73				
100	5.80	3.87	4.15	3.46	3.37	3.23
105	6.41	4.00				
110	7.06	4.13	4.89	3.66	3.99	3.42
115	7.91	4.26				
120	8.48	4.39	5.66	3.84	4.65	3.60
125	9.32	4.53				
130	10.15	4.67	6.48	4.02	5.36	3.77
135						
140			7.31	4.18	6.15	3.95
145						
150			8.18	4.34	6.96	4.11
155						
160					7.77	4.27

Table 4 Rate constants for System A $KMnO_4$

Run	$1/T^{\circ}A \times 10^3$	$k_{\frac{1}{3}} \times 10^2$	$t_{\frac{1}{3}}$	$k_o \times 10^2$	$k_x \times 10^2$	$k_1 \times 10^2$	$k_2 \times 10^2$
A1	2.062		20.5	4.88	2.36	3.50	2.10
A2	2.088	4.86	13.0	7.69	2.89		
A3	2.106	3.75	8.0	12.5	2.06		
A4	2.123	2.73	14.5	6.90	1.40		
A5	2.141	1.97	38.5	2.60	1.21		
A6	2.140	1.79	39.0	2.57	1.08		

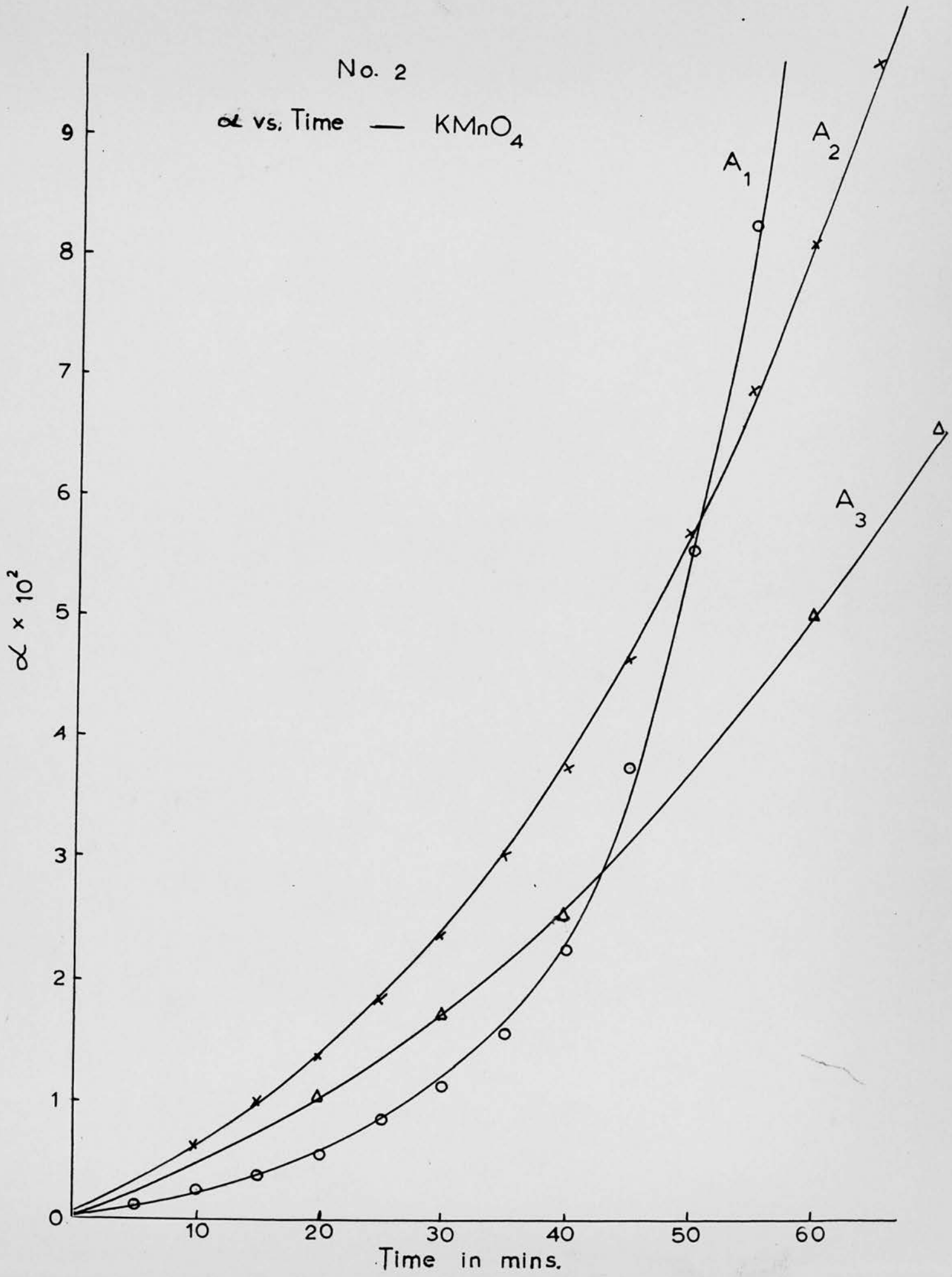
No. 2
α vs. Time — KMnO4
A1
A2
A3
α × 10²
Time in mins.
0
1
2
3
4
5
6
7
8
9
10
20
30
40
50
60

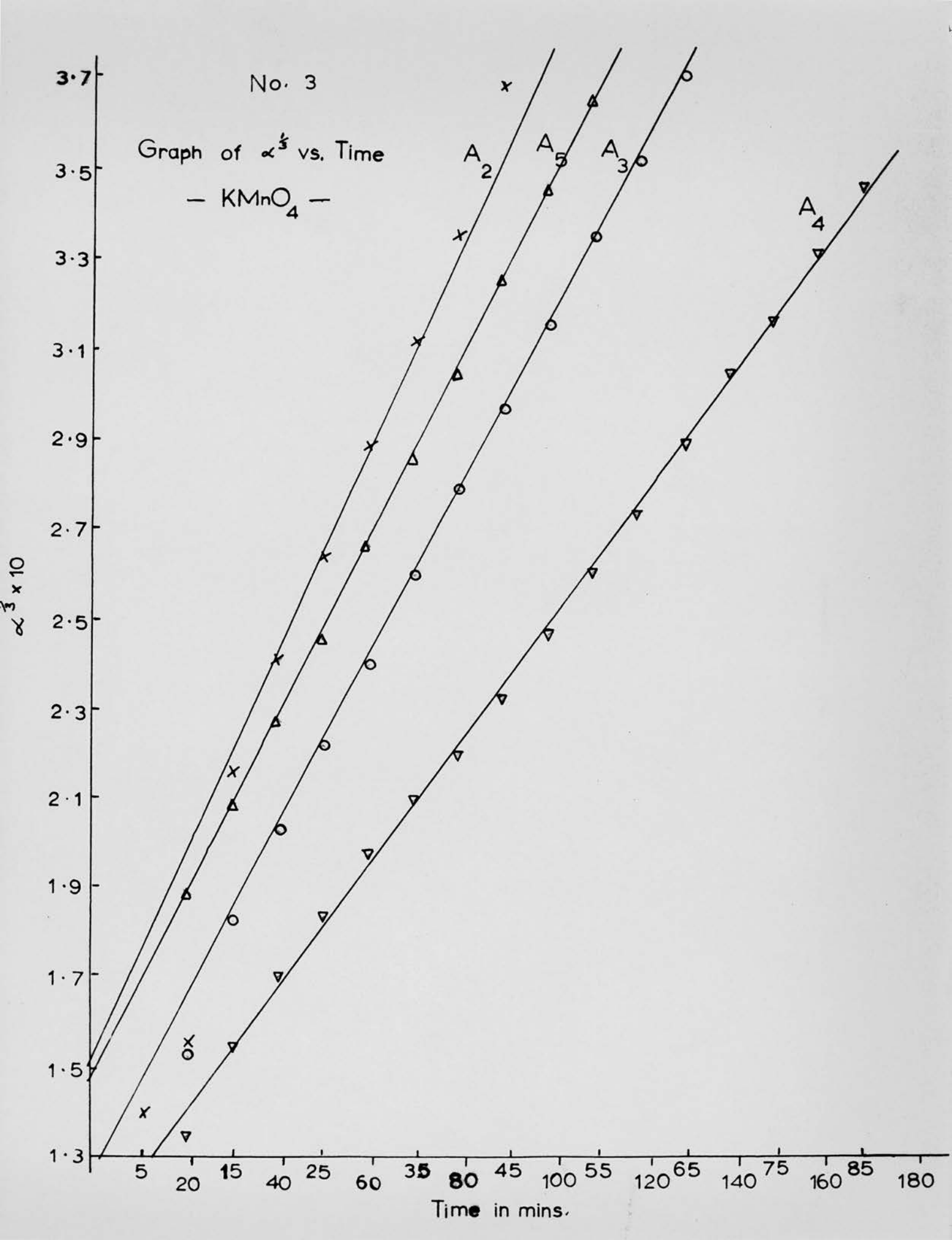
No. 3
Graph of $\alpha^{\frac{1}{3}}$ vs. Time
— $KMnO_4$ —
A_2
A_5
A_3
A_4
$\alpha^{\frac{1}{3}} \times 10$
3·7
3·5
3·3
3·1
2·9
2·7
2·5
2·3
2·1
1·9
1·7
1·5
1·3
5
20
15
40
25
60
35
80
45
100
55
120
65
140
75
160
85
180
Time in mins.

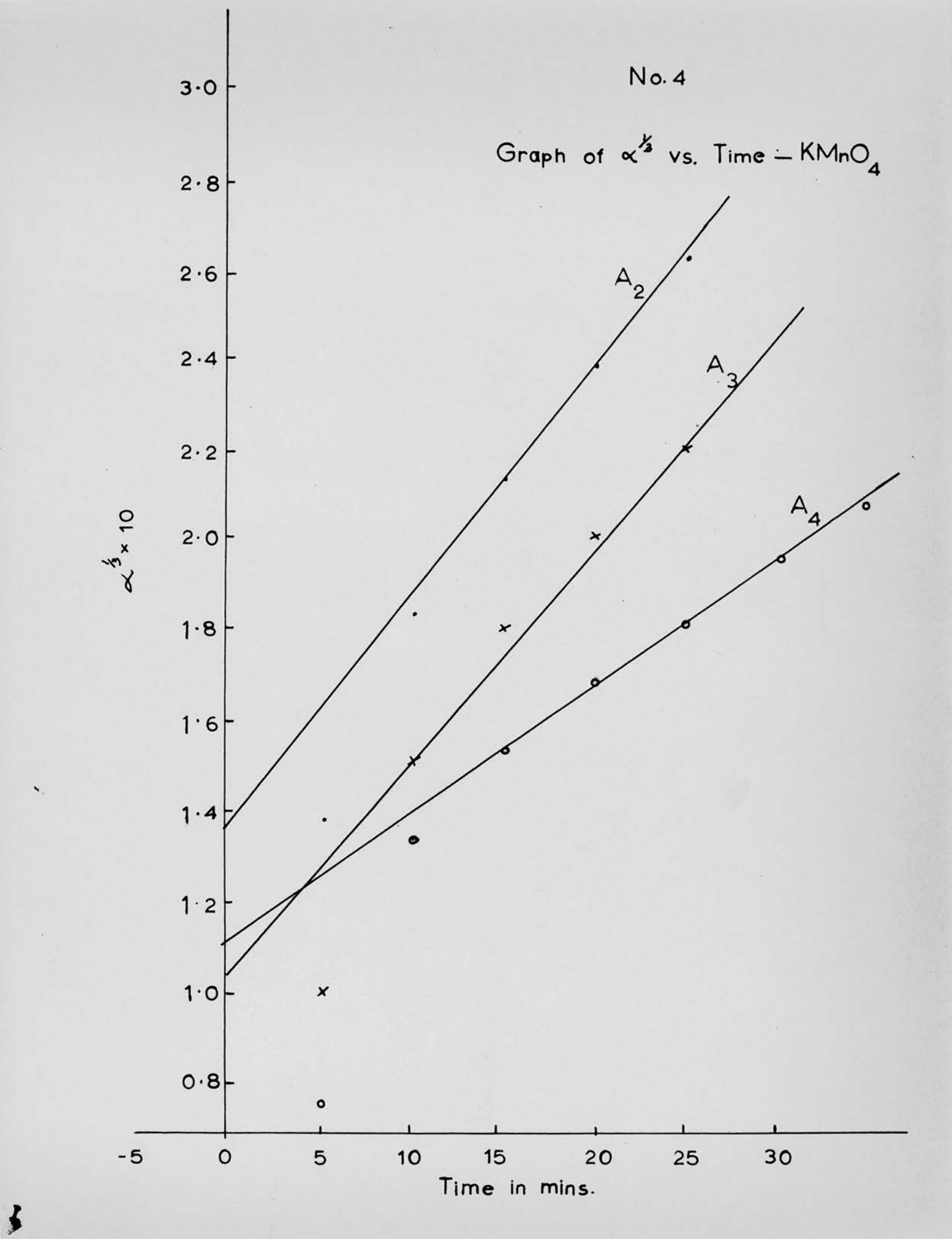
No. 4
Graph of $\alpha^{1/3}$ vs. Time – $KMnO_4$
A_2
A_3
A_4
$\alpha^{1/3} \times 10$
3·0
2·8
2·6
2·4
2·2
2·0
1·8
1·6
1·4
1·2
1·0
0·8
-5
0
5
10
15
20
25
30
Time in mins.

No. 5

Graph of $\text{Log}k_o$ vs. $\frac{1}{T^\circ_A}$ – $KMnO_4$

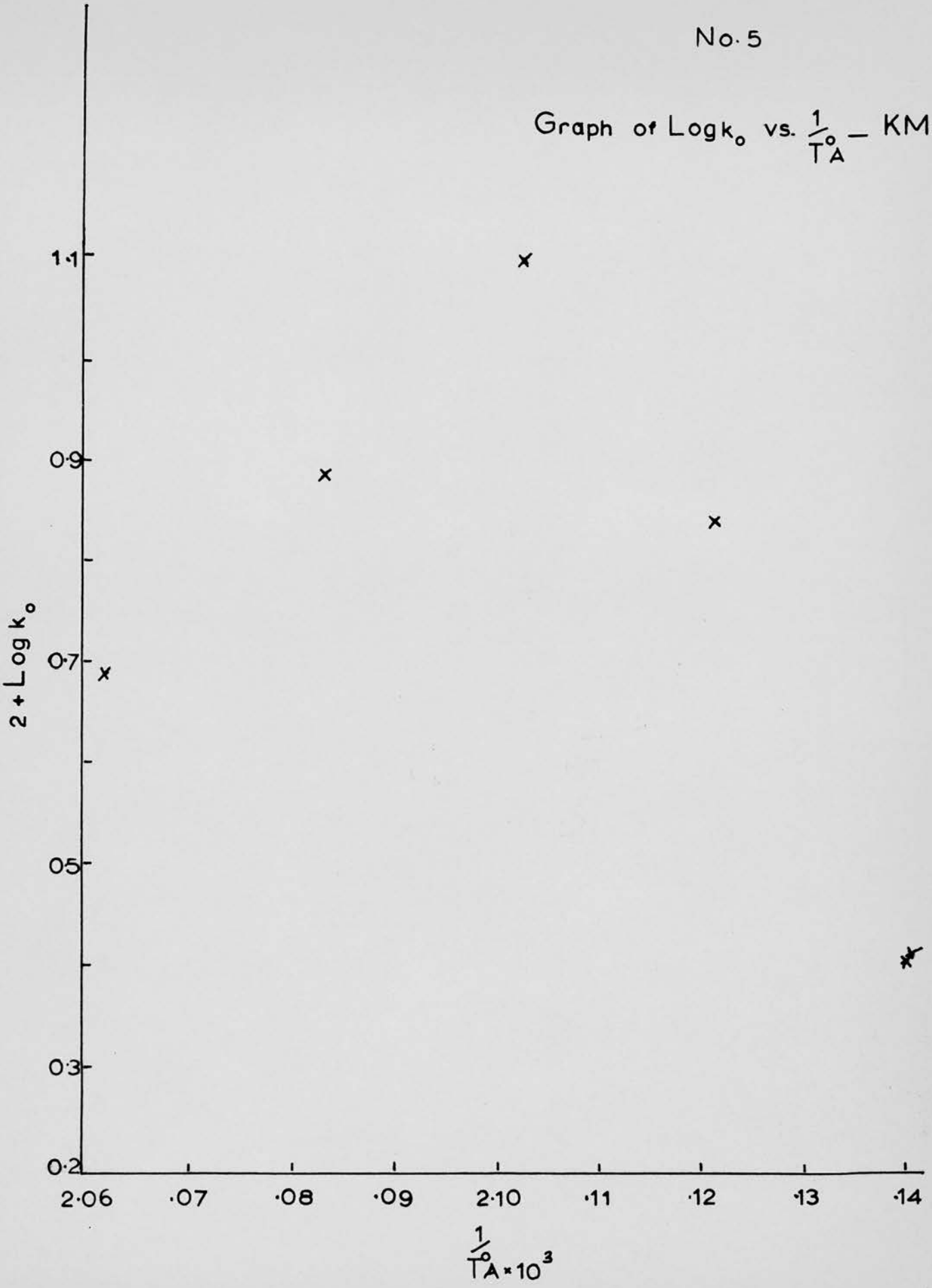

No. 6

Graph of $\text{Log } k_{\frac{1}{3}}$ vs. $\frac{1}{T_A^\circ}$ – $KMnO_4$

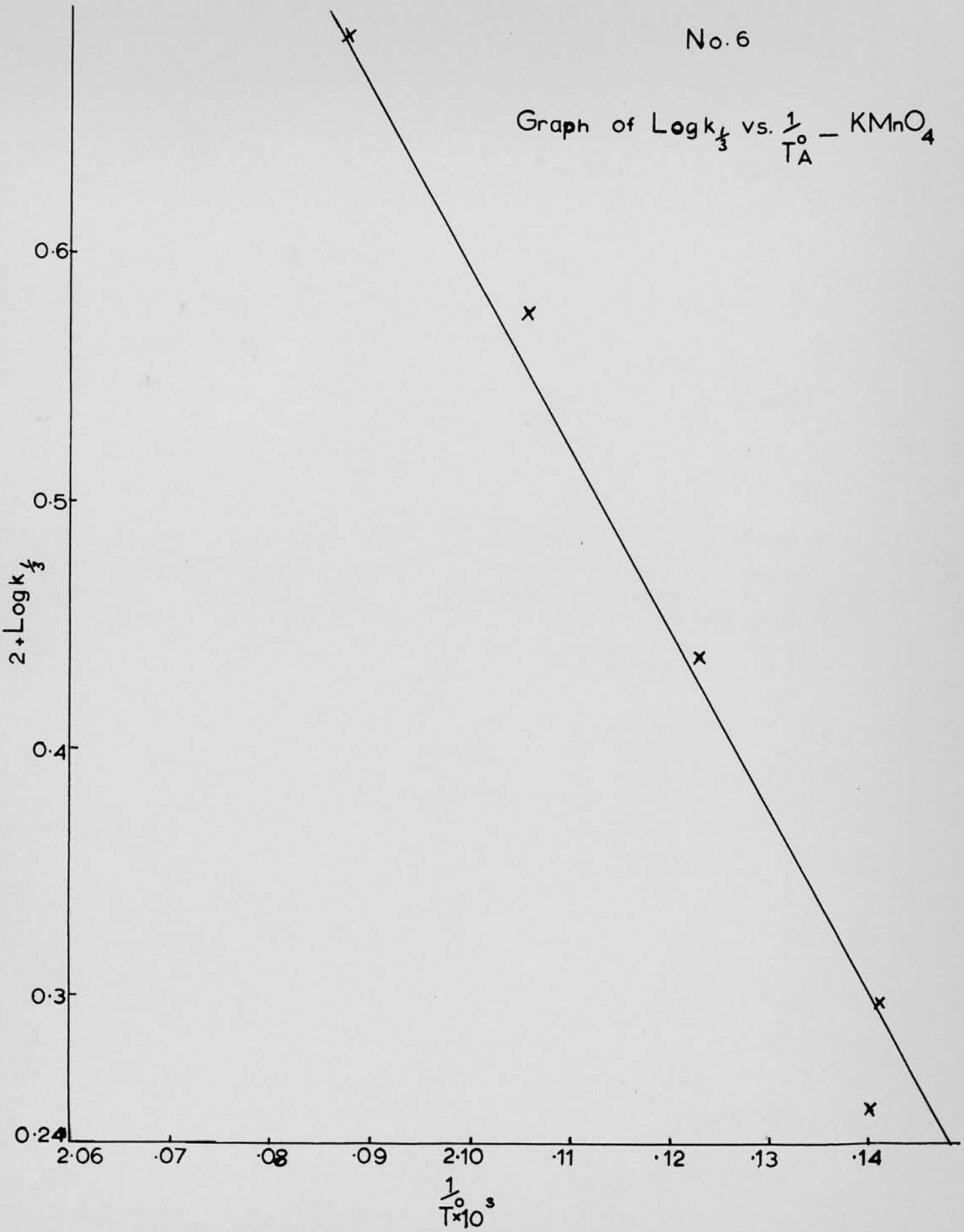

2.5.2. Kinetics of the decomposition for potassium permanganate/ Alumina (B)

Tables 5, 6, 7 and 8 and graphs 7, 8, 9 and 10 illustrate the effect of adding Alumina. The induction period has been reduced but the curves are still acceleratory. The initial decomposition in now fitted, in the region $\alpha = 0.01 - 0.1$ by the power law

$$\alpha = kt^n \qquad \text{where } n = 2$$

The later stages of the reaction were fitted by the Prout-Tompkins equation, two values of "k" being required.

Tables 5, 6 and 7	Analysis of system (B).
Table 8	Rate constants for (B).
Graph 7	The initial stage of the "α" - time curves.
Graph 8	The initial reaction, a plot of $\alpha^{\frac{1}{2}}$ vs. Time.
Graph 9	Acceleration and decay stages, plot of $\log_{10} \alpha/1 - \alpha$ vs. Time.
Graph 10	Arrhenius diagram for initial reaction which gives an activation energy of E = 38±2 K cals./mole.

Table 5 System B $KMnO_4$ / Al_2O_3

Run		B1			B2	
Temp.		211.8°C			207.9°C	
Time Min.	x 10^2	$\frac{1}{2}$ x 10	P.T.	x 10^2	$\frac{1}{2}$ x 10	P.T.
5	0.70	0.86		0.32	0.56	
10	2.95	1.72		1.57	1.25	
15	6.37	2.52		3.68	1.92	
20	10.3	3.21		6.57	2.56	
25				9.62	3.10	
27	19.5		$\bar{1}$.39	14.3		$\bar{1}$.22
47	43.5		$\bar{1}$.89	43.1		$\bar{1}$.69
67	68.5		0.34	57.0		0.12
87	85.1		0.76	75.7		0.49
107	94.0		1.19	87.4		0.84
127	98.4		1.78	94.0		1.19
147	99.6			97.4		1.57
167				99.6		2.35

Table 6 System B $KMnO_4/\alpha Al_2O_3$

Run		B3			B4		B5	
Temp.		203.7°C			199.0°C		195.2°C	
Time Min	$\alpha \times 10^2$	$\alpha^{\frac{1}{2}} \times 10$	P.T.	$\alpha \times 10^2$	$\alpha^{\frac{1}{2}} \times 10$	$\alpha \times 10^2$	$\alpha^{\frac{1}{2}} \times 10$
5	0.47	0.69		0.36	0.60	0.32	0.57
10	1.78	1.33		1.06	1.03	1.07	1.04
15	3.49	1.87		1.97	1.41	1.77	1.33
20	5.63	2.37		2.93	1.71	2.61	1.62
25	8.16	2.86		4.23	2.06	3.58	1.89
30	10.7	3.25		5.61	2.37	4.58	2.14
35	12.9	3.59		6.98	2.64	5.79	2.41
40	19.3		$\bar{1}.38$	8.59	2.93	7.04	2.65
45				10.3	3.21	8.43	2.90
50				12.0	3.89	9.75	3.12
55						10.9	3.30
60	32.2		$\bar{1}.68$			12.1	3.48
80	49.8		$\bar{1}.99$				
100	65.9		0.29				
120	77.6		0.54				
140	85.7		0.78				
160	91.7		1.04				
180	95.6		1.33				
200	98.1		1.72				
220	99.4		2.22				

Table 7 System B $KMnO_4$/ Al_2O_3

Run	B6		B7	
Temp.	185.5°C		193.2°C	
Time Min.	x 10	$\frac{1}{2}$ x 10	x 10^2	$\frac{1}{2}$ x 10
10	0.43	0.65	0.39	0.62
20	0.91	0.95	0.76	0.87
30	1.35	1.16	1.14	1.07
40	1.88	1.37	1.56	1.25
50	2.52	1.59	1.97	1.40
60	3.26	1.80	2.42	1.56
70	3.98	2.00	2.96	1.72
80	4.84	2.20	3.48	1.86
90	5.76	2.40	4.04	2.01
100	6.73	2.59	4.63	2.15
110	7.69	2.77	5.27	2.30
120	8.70	2.95	5.90	2.43
130	9.63	3.10	6.59	2.57
140	10.6	3.25	7.28	2.70
150	11.5	3.39	7.89	2.81
160	12.4	3.52	8.54	2.92
170			9.19	3.03
180			9.82	3.13
190			10.4	3.23

Table 8 Rate constants for System B $KMnO_4/\alpha Al_2O_3$

Run	$1/T°A \times 10^3$	$k_{\frac{1}{2}} \times 10^2$	$k_x \times 10^2$	$k_2 \times 10^2$
B1	2.063	16.5	10.1	2.22
B2	2.080	13.02	7.33	1.70
B3	2.098	10.33	7.33	1.50
B4	2.118	6.36	4.98	
B5	2.136	5.23	4.48	
B6	2.181	2.05	1.77	
B7	2.192	1.52	1.41	

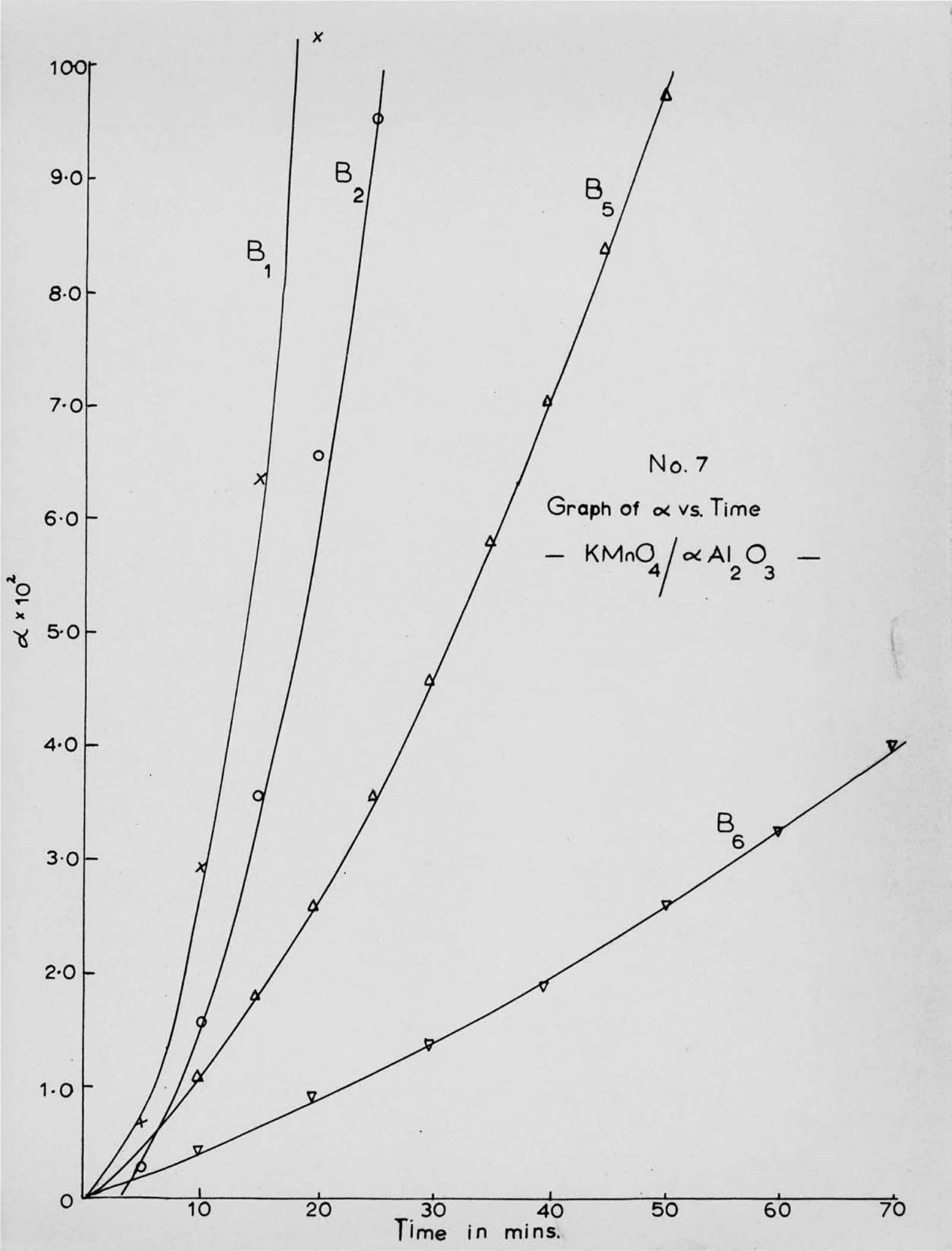
No. 7
Graph of α vs. Time
— KMnO4 / α Al2O3 —
B1
B2
B5
B6
α x 10²
Time in mins.
0
1·0
2·0
3·0
4·0
5·0
6·0
7·0
8·0
9·0
100
10
20
30
40
50
60
70

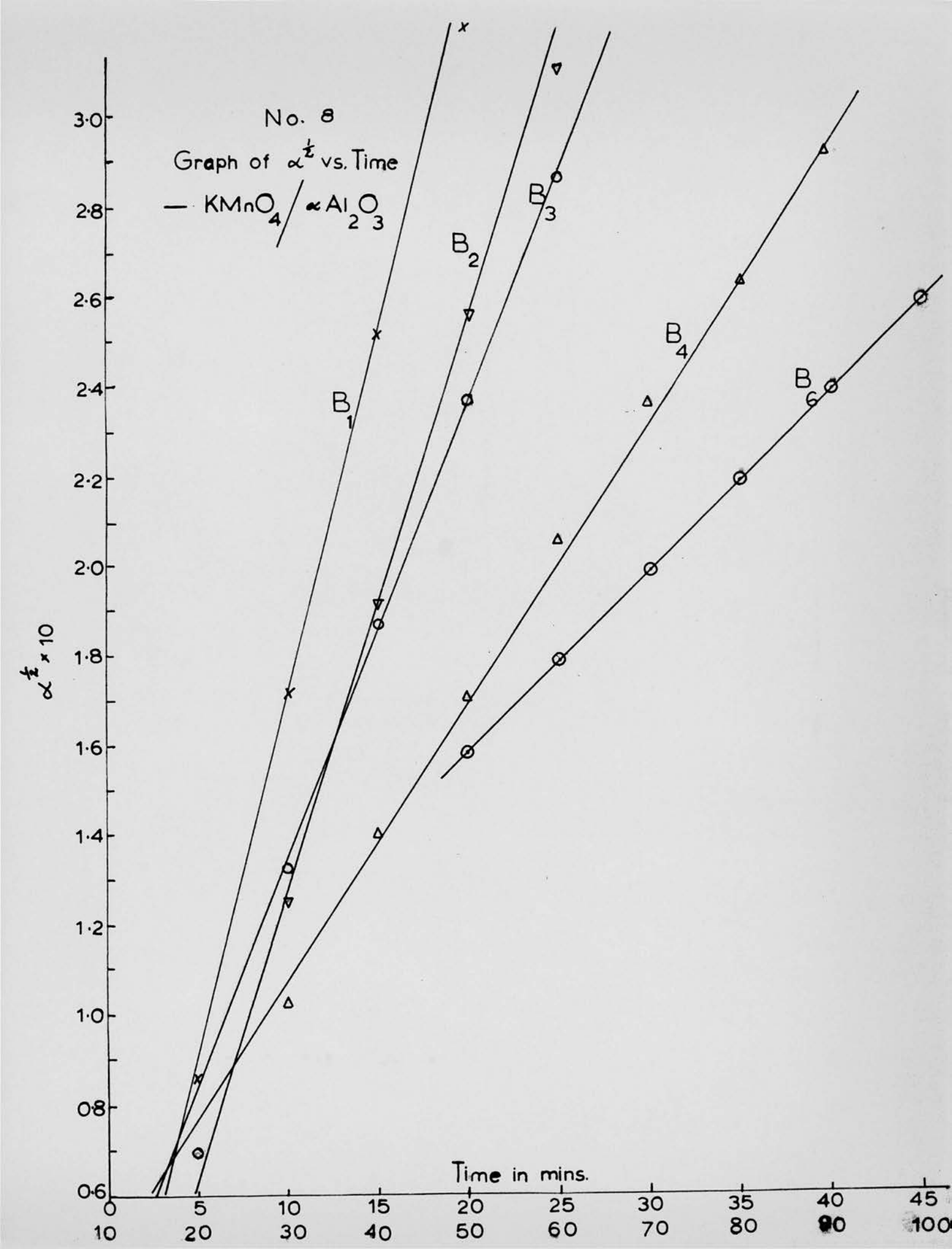
No. 8
Graph of $\alpha^{\frac{1}{t}}$ vs. Time
— $KMnO_4$ / ∝ Al_2O_3
B_1
B_2
B_3
B_4
B_6
$\alpha^{\frac{1}{t}} \times 10$
3·0
2·8
2·6
2·4
2·2
2·0
1·8
1·6
1·4
1·2
1·0
0·8
0·6
Time in mins.
0 5 10 15 20 25 30 35 40 45
10 20 30 40 50 60 70 80 90 100

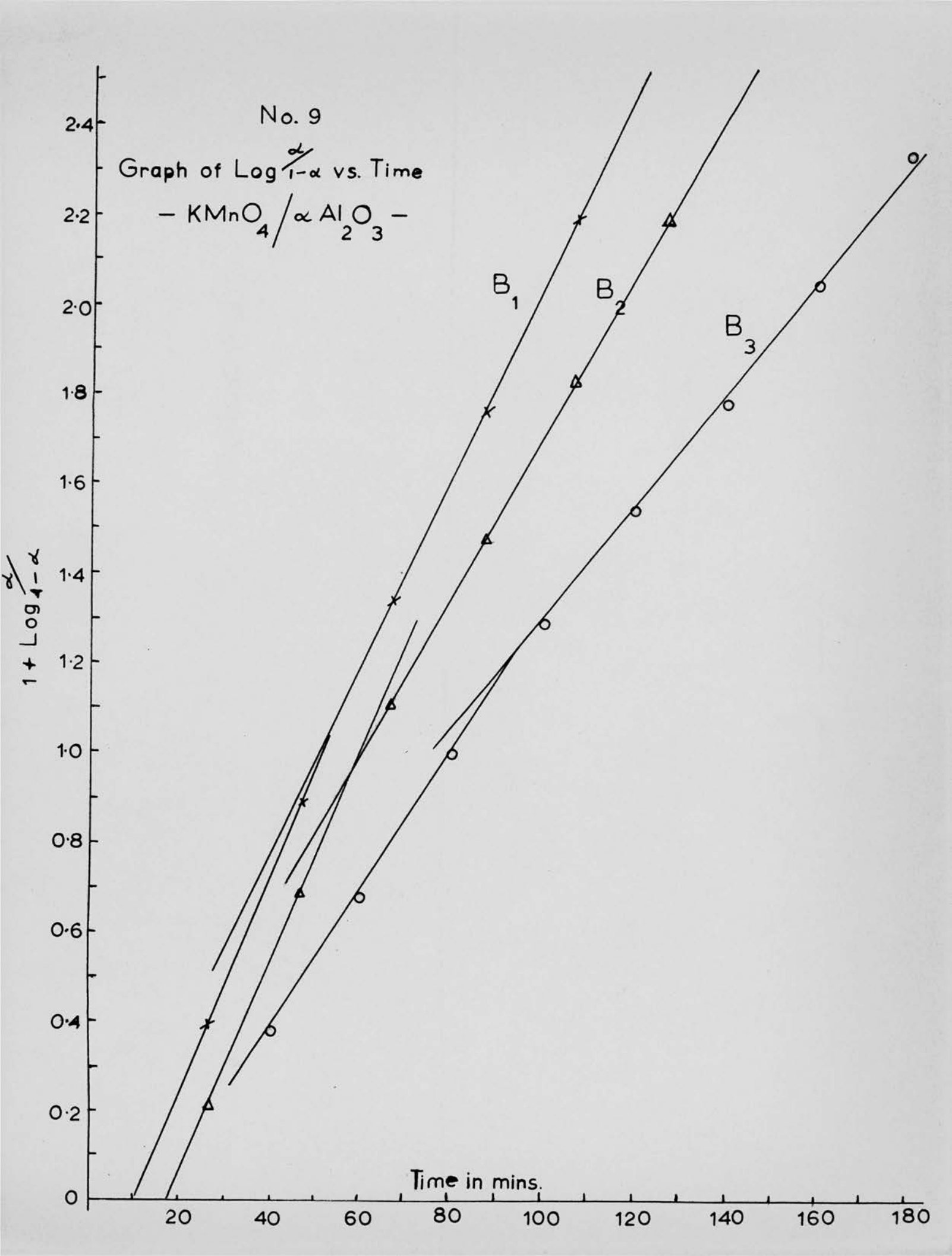
No. 9
Graph of Log α/1-α vs. Time
– KMnO4 / α Al2O3 –
B1
B2
B3
1 + Log α/4-α
Time in mins.
0
0·2
0·4
0·6
0·8
1·0
1·2
1·4
1·6
1·8
2·0
2·2
2·4
20
40
60
80
100
120
140
160
180

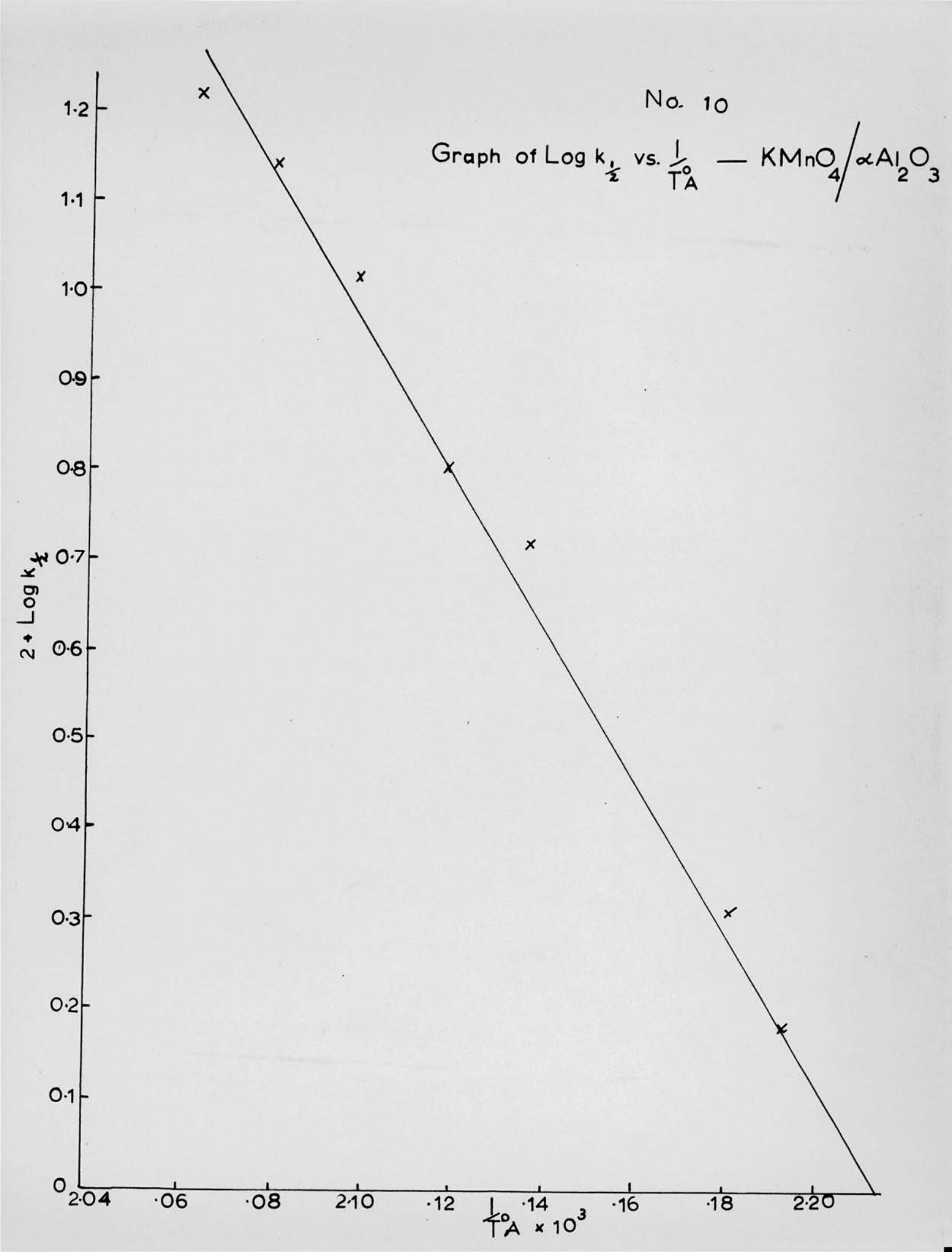
No. 10
Graph of Log $k_{\frac{1}{2}}$ vs. $\frac{1}{T^{\circ}A}$ — $KMnO_4/\alpha Al_2O_3$
1·2
1·1
1·0
0·9
0·8
0·7
0·6
0·5
0·4
0·3
0·2
0·1
0
2 + Log $k_{\frac{1}{2}}$
2·04
·06
·08
2·10
·12
·14
·16
·18
2·20
$\frac{1}{T^{\circ}A} \times 10^3$

2.5.3. Kinetics of the decomposition for potassium permanganate/ manganese dioxide (C)

Tables 9, 10, 11 and 12 and graphs 11, 12, 13 and 14 illustrate the effect of adding manganese dioxide. The induction period has been reduced but the curves still remain acceleratory. The initial decomposition is best fitted in the region $\alpha = 0.01 - 0.12$ by the power law

$$\alpha = kt^n \qquad \text{where } n = 2$$

The later stages of the decomposition were fitted by the Prout-Tompkins equation, two values of "k" being required.

Tables 9, 10 and 11	Analysis of system (C).
Table 12	Rate constants for system (C).
Graph 11	The initial stage of the "α" - time curves.
Graph 12	The initial reaction, a plot of $\alpha^{\frac{1}{2}}$ vs. Time.
Graph 13	Acceleration and decay stages; plot of $\log_{10} \alpha/1-\alpha$ vs. Time.
Graph 14	Arrhenius diagram for initial reaction which gives an activation energy of E = 34±4 K. cals./mole.

Table 9 System C $KMnO_4/MnO_2$

Run		C1			C3	
Temp		208.4°C			200.4°C	
Time Min	$\alpha \times 10^2$	$\alpha^{\frac{1}{2}} \times 10$	P.T.	$\alpha \times 10^2$	$\alpha^{\frac{1}{2}} \times 10$	P.T.
5	0.71	0.85		0.35	0.59	
10	1.83	1.35		1.01	1.0	
15	3.10	1.76		1.56	1.25	
20	4.64	2.16		2.12	1.46	
25	6.71	2.59		2.81	1.68	
30	9.05	3.01		3.54	1.88	
35	11.74	3.43		4.41	2.10	
40	14.72	3.84		5.24	2.29	
45	18.20	4.26		6.25	2.50	
50	21.80	4.67		7.43	2.73	
55	25.70	5.07		8.67	2.95	
60	30.48	5.52		10.09	3.18	
65	6			11.80	3.44	
70	36.80	6.07		13.53	3.68	
75				15.27	3.91	
80	54.50		0.08	17.10	4.13	
85				19.10	4.37	
90	61.6		0.21	20.8	4.56	
95				23.0	4.79	
100	68.6		0.34	25.3	5.03	
105				27.4	5.24	
110	74.9		0.47			
117				38.3		$\bar{1}.79$
120	81.4		0.64			
127				46.3		$\bar{1}.94$
130	87.2		0.83			
137				54.1		0.07
140	91.2		1.02			
147				60.5		0.19
150	94.4		1.22			
157				66.1		0.29
160	97.3		1.56			
167				71.0		0.39
170	98.9		1.95			
177				76.3		0.51
187				79.4		0.59
197				83.6		0.71
207				86.5		0.81
217				90.0		0.95
227				92.5		1.09
237				94.1		1.20

Table 10 System C $KMnO_4/MnO_2$

Run	C2		C4		C5	
Temp	204.0°C		195.8°C		191.8°C	
Time Min	$\alpha \times 10^2$	$\alpha^{\frac{1}{2}} \times 10$	$\alpha \times 10^2$	$\alpha^{\frac{1}{2}} \times 10$	$\alpha \times 10^2$	$\alpha^{\frac{1}{2}} \times 10$
5	0.37	0.61	0.56	0.75		
10	1.00	1.00	1.07	1.04	0.44	0.66
15	1.74	1.32	1.52	1.23		
20	2.55	1.60	1.98	1.41	0.94	0.97
25	3.40	1.84	2.44	1.56		
30	4.40	2.10	2.95	1.72	1.48	1.22
35	5.51	2.35	3.55	1.88		
40	6.66	2.58	4.12	2.03	2.14	1.46
45	8.24	2.87	481	2.19		
50	10.35	3.22	5.48	2.34	2.93	1.71
55	12.6	3.56	6.14	2.48		
60	15.5	3.94	6.83	2.61	3.82	1.95
65	18.9	4.34	7.62	2.76		
70	22.7	4.77	8.24	2.87	4.83	2.20
75			8.90	2.98		
80			9.45	3.08	5.82	2.41
85			10.1	3.17		
90					6.77	2.60
95						
100					7.69	2.77

Table 11 System C $KMnO_4//MnO_2$

Run	C6		C7		C8	
Temp	187.9°C		183.5°C		179.4°C	
Time Min	$\alpha \times 10^2$	$\alpha^{\frac{1}{2}} \times 10$	$\alpha \times 10^2$	$\alpha^{\frac{1}{2}} \times 10$	$\alpha \times 10^2$	$\alpha^{\frac{1}{2}} \times 10$
5	0.11	0.32				
10	0.34	0.58				
15	0.50	0.71				
20	0.62	0.79			0.32	0.56
25	0.78	0.89				
30	0.96	0.98				
40	1.37	1.17	1.06	1.03	0.53	0.73
50	1.89	1.38	1.37	1.17		
60	2.46	1.57	1.68	1.30	0.75	0.86
70	3.21	1.79	2.00	1.41		
80	4.01	2.00	2.31	1.52	0.99	1.00
90	4.86	2.21	2.63	1.62		
100	5.75	2.40	2.95	1.72	1.26	1.12
110	6.62	2.57	3.28	1.81		
120	7.43	2.73	3.66	1.91	1.58	1.26
130	8.23	2.87	3.99	2.00		
140			4.39	2.10	1.88	1.37
150			4.78	2.19		
160			5.17	2.28	2.24	1.50
170			5.59	2.36		
180			5.99	2.45	2.65	1.63
190			6.47	2.54		
200			6.88	2.62	3.02	1.74
210			7.32	2.71		
220			7.76	2.79	3.46	1.86
230			8.18	2.86		
240			8.62	2.94	3.91	1.98
250			9.03	3.00		
260					4.43	2.10
280					5.07	2.25
300					5.71	2.39
320					6.44	2.54
340					7.23	2.69

Table 12 Rate Constants for System C $KMnO_4/MnO_2$

Run	$1/T^{\circ}A \times 10^3$	$k_{\frac{1}{2}} \times 10^2$	$k_x \times 10^2$	$k_2 \times 10^2$
C1	2.077	8.32	6.67	1.31
C2	2.096	5.14	4.35	
C3	2.112	3.71	3.85	0.94
C4	2.133	3.15	3.30	
C5	2.140	2.48	1.97	
C6	2.155	2.02	2.40	
C7	2.191	1.11		
C8	2.211	0.63	0.51	

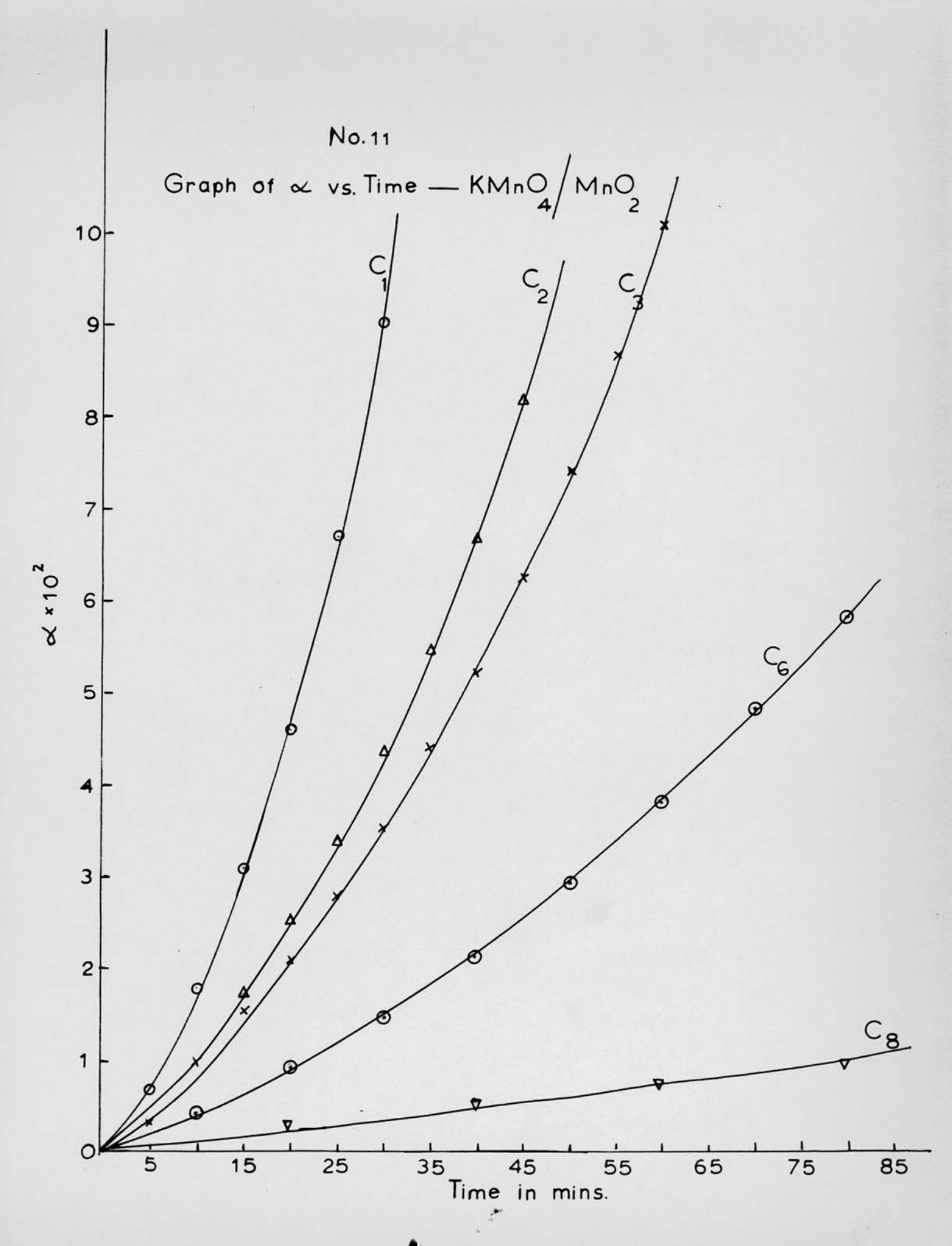
No. 11
Graph of α vs. Time — KMnO4 / MnO2
C1
C2
C3
C6
C8
α × 10²
Time in mins.
0
1
2
3
4
5
6
7
8
9
10
5
15
25
35
45
55
65
75
85

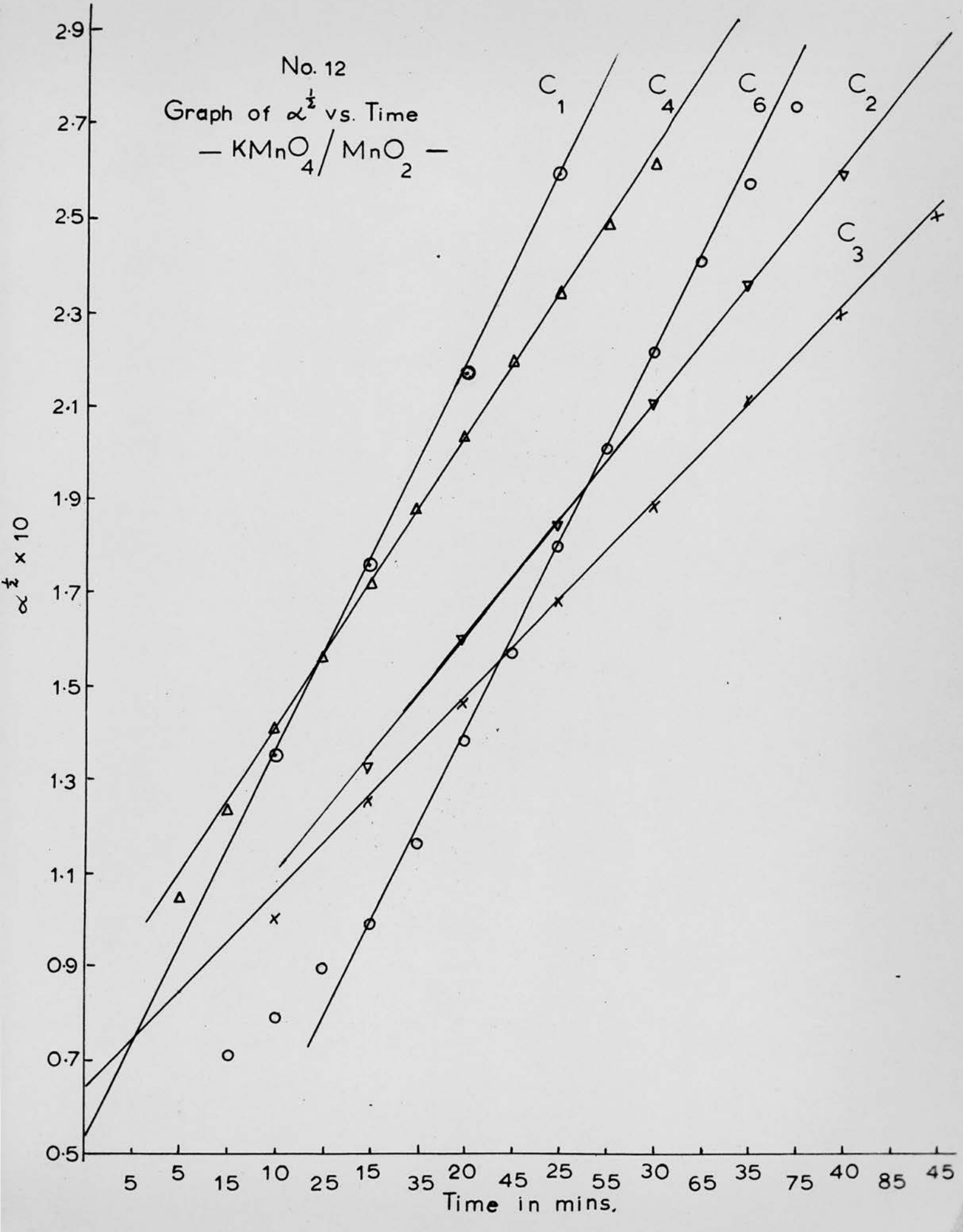
No. 12
Graph of $\alpha^{\frac{1}{2}}$ vs. Time
— $KMnO_4$ / MnO_2 —
C_1
C_4
C_6
C_2
C_3
$\alpha^{\frac{1}{2}} \times 10$
2·9
2·7
2·5
2·3
2·1
1·9
1·7
1·5
1·3
1·1
0·9
0·7
0·5
5
5
15
10
25
15
35
20
45
25
55
30
65
35
75
40
85
45
Time in mins.

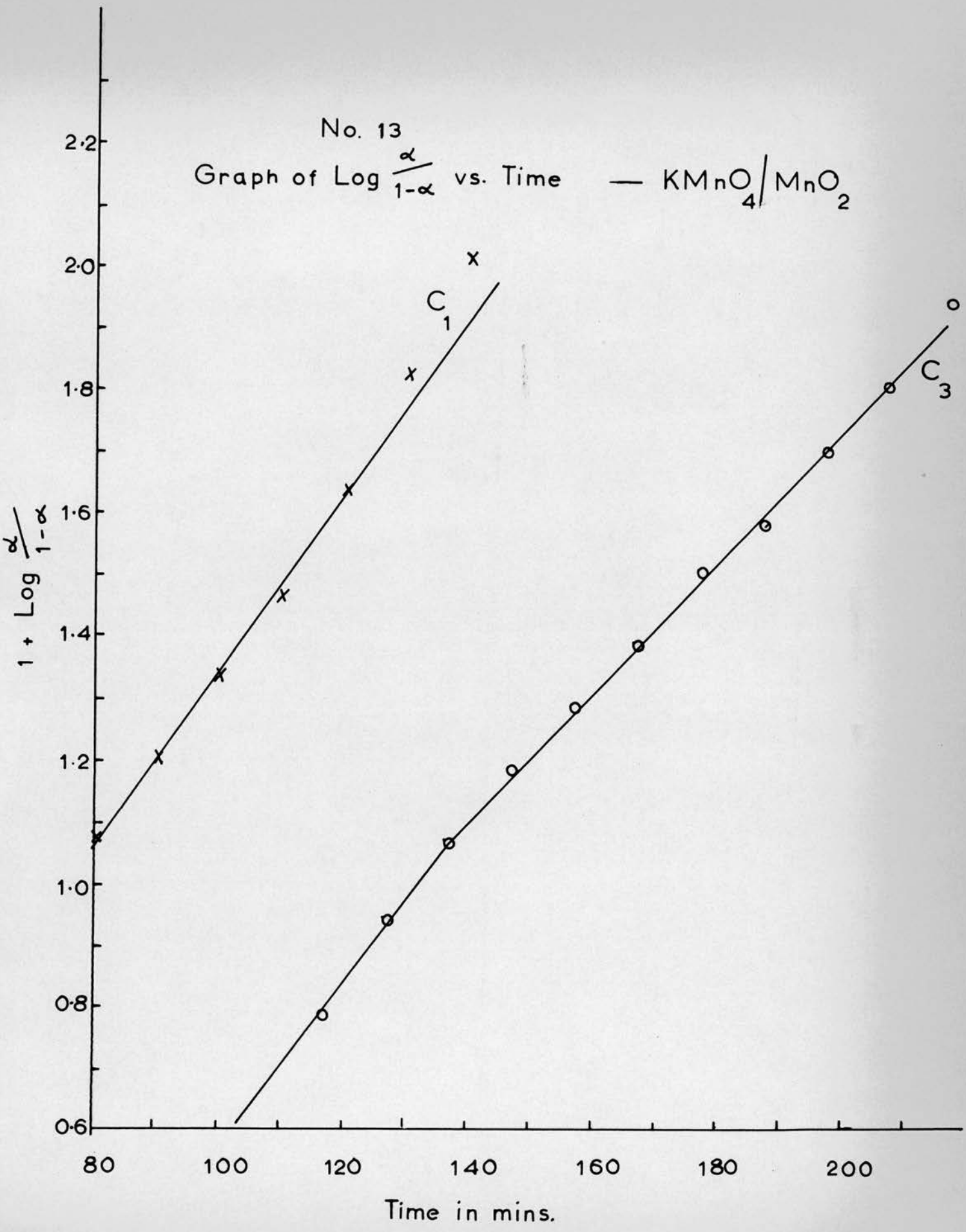
No. 13
Graph of Log α/1-α vs. Time — KMnO4/MnO2
C1
C3
1 + Log α/1-α
2·2
2·0
1·8
1·6
1·4
1·2
1·0
0·8
0·6
80
100
120
140
160
180
200
Time in mins.

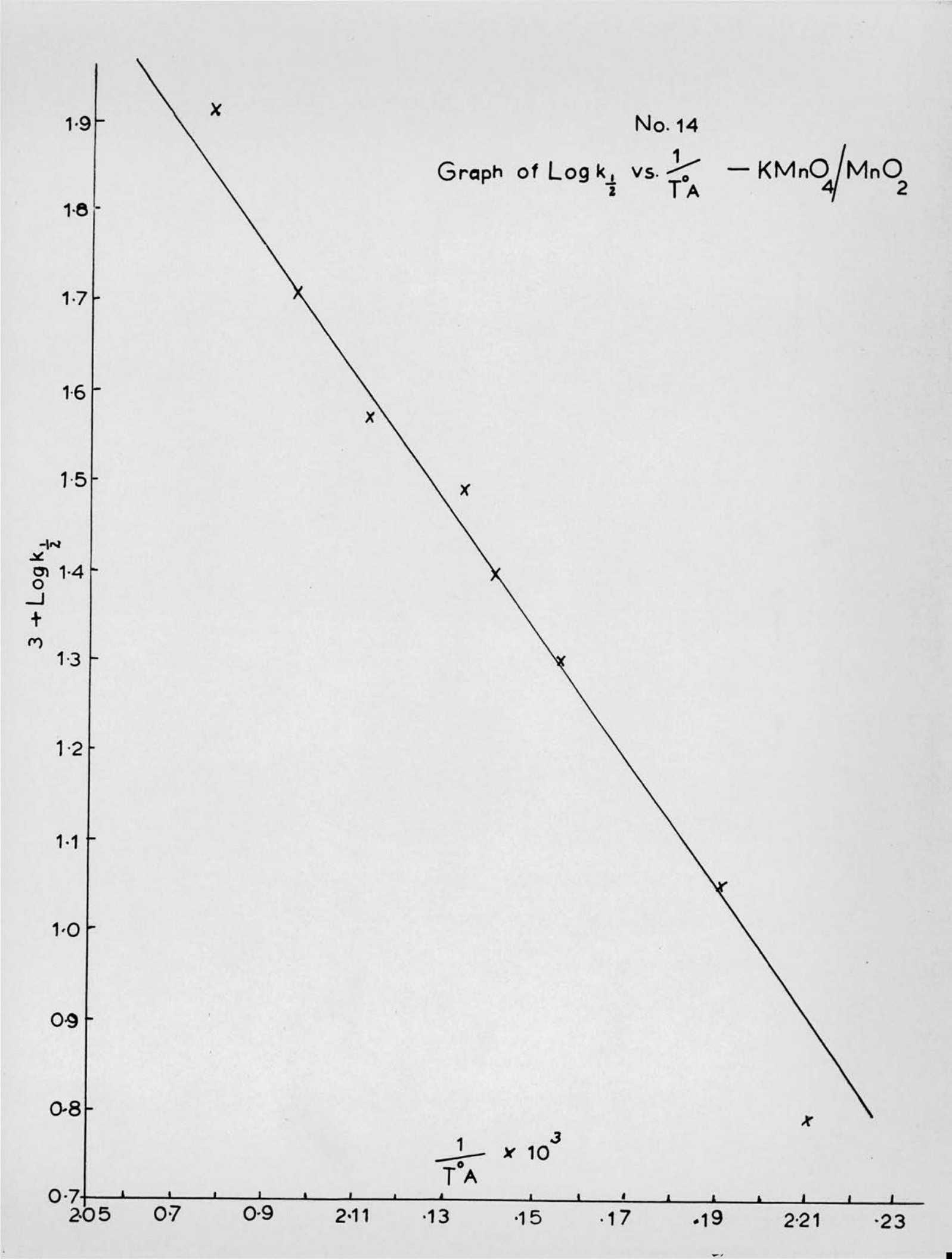
No. 14
Graph of Log $k_{\frac{1}{2}}$ vs. $\frac{1}{T°A}$ — $KMnO_4/MnO_2$
3 + Log $k_{\frac{1}{2}}$
1·9
1·8
1·7
1·6
1·5
1·4
1·3
1·2
1·1
1·0
0·9
0·8
0·7
$\frac{1}{T°A} \times 10^3$
2·05
0·7
0·9
2·11
·13
·15
·17
·19
2·21
·23

2.5.4. Kinetics for the decomposition for potassium permanganate/cupric oxide (D)

Tables 13, 14 and 15 and graphs 15, 16, 17 and 18 illustrate the effect of adding cupric oxide. The initial stage of the "α" - time curves now tend to show a slight deceleration and are best fitted in the region $\alpha = 0.02 - 0.09$ by the expression $\log {}^{1}/_{1-\alpha} = kt + c$.

The later stages of the decomposition were fitted by the Prout-Tompkins equation, two values of "k" being required.

Tables 13 and 14	Analysis of system (D).
Table 15	Rate constants for system (D).
Graph 15	The initial stage of the "α" - time curves.
Graph 16	The initial reaction, a plot of $\log_{10} (1-\alpha)$ vs. Time.
Graph 17	Acceleration and decay stages; plot of $\log_{10} \alpha/1-\alpha$ vs. Time.
Graph 18	Arrhenius diagram for initial reaction, which gives an activation energy of $E = 40 \pm 4$ K. cals./mole.

Table 13 System D $KMnO_4/CuO$

Run	D1		D2		D4	
Temp.	191.7°C		194.0°C		201.7°C	
Time Min.	$\alpha \times 10^2$	log (1 - α)	$\alpha \times 10^2$	log (1 - α)	$\alpha \times 10^2$	log (1 - α)
10	0.82	$\bar{1}$.996	0.92	$\bar{1}$.996	2.21	$\bar{1}$.990
15					3.34	$\bar{1}$.985
20	1.52	$\bar{1}$.993	1.96	$\bar{1}$.991	4.32	$\bar{1}$.981
25					5.40	$\bar{1}$.976
30	2.16	$\bar{1}$.991	2.88	$\bar{1}$.987	6.33	$\bar{1}$.972
35					7.23	$\bar{1}$.967
40	2.81	$\bar{1}$.988	3.71	$\bar{1}$.984	8.18	$\bar{1}$.963
45					9.05	$\bar{1}$.959
50	3.47	$\bar{1}$.985	4.63	$\bar{1}$.980	9.90	$\bar{1}$.955
55					10.7	$\bar{1}$.951
60	4.09	$\bar{1}$.982	5.43	$\bar{1}$.976	11.6	$\bar{1}$.946
65					12.5	$\bar{1}$.942
70	4.78	$\bar{1}$.979	6.30	$\bar{1}$.972		
80	5.39	$\bar{1}$.976	7.43	$\bar{1}$.968		
90	6.07	$\bar{1}$.973	7.87	$\bar{1}$.964		
100	6.67	$\bar{1}$.970	8.61	$\bar{1}$.961		
110	7.25	$\bar{1}$.967	9.38	$\bar{1}$.957		
120			10.2	$\bar{1}$.954		

Table 14 System D $KMnO_4/CuO$

Run		D3		D5	
Temp.		203.2°C		206.4°C	
Time Min.	$\alpha \times 10^2$	log (1 - α)	$\alpha \times 10^2$	log (1 - α)	P.T.
2			0.12	$\bar{1}$.999	
4			0.93	$\bar{1}$.996	
5	2.37	$\bar{1}$.999			
6			3.13	$\bar{1}$.986	
8			4.76	$\bar{1}$.979	
10	4.96	$\bar{1}$.980	6.18	$\bar{1}$.972	
12			7.54	$\bar{1}$.966	
14			8.70	$\bar{1}$.960	
15	6.65	$\bar{1}$.970			
16			9.75	$\bar{1}$.955	
18			10.7	$\bar{1}$.951	
20	8.12	$\bar{1}$.963	12.9		$\bar{1}$.77
25	9.45	$\bar{1}$.957			
30	10.7	$\bar{1}$.951			
40			24.6		$\bar{1}$.51
60			34.5		$\bar{1}$.72
80			46.0		$\bar{1}$.93
100			59.1		0.16
120			72.9		0.43
140			83.9		0.72
160			91.3		1.02
180			95.6		1.34
200			97.8		1.65

Table 14 (Contd.) System D $KMnO_4/CuO$

Run		D6			D7	
Temp		210.7°C			214.9°C	
Time Min	$\alpha \times 10^2$	log $(1-\alpha)$	P.T.	$\alpha \times 10^2$	log $(1-\alpha)$	P.T.
2	0.27	$\bar{1}.999$				
4	0.96	$\bar{1}.996$		0.89	$\bar{1}.996$	
6	2.05	$\bar{1}.991$		3.84	$\bar{1}.983$	
8	3.01	$\bar{1}.987$		6.01	$\bar{1}.973$	
10	3.77	$\bar{1}.983$		7.93	$\bar{1}.964$	
12	4.58	$\bar{1}.980$		9.72	$\bar{1}.956$	
14	5.43	$\bar{1}.976$		11.4	1.948	
16	6.24	$\bar{1}.972$				
18	7.11	$\bar{1}.968$				
20	7.84	$\bar{1}.965$		18.4		$\bar{1}.35$
22	8.56	$\bar{1}.961$				
24	9.28	$\bar{1}.958$				
26	9.95	$\bar{1}.954$				
28	10.6	1.951				
40				36.2		$\bar{1}.75$
60	30.5		$\bar{1}.64$	61.1		0.19
80	51.4		0.02	82.0		0.66
100	74.8		0.47	92.2		1.07
120	88.2		0.88	95.9		1.37
140	95.4		1.31	97.8		1.64
160	97.9		1.67	98.8		1.91

Table 15 Rate Constants for System D $KMnO_4/CuO$

Run	$1/T^\circ$ A x 10^3	$k_{(1-\alpha)} \times 10^4$	$k_x \times 10$	$k_2 \times 10^2$
D1	2.152	2.93	0.22	
D2	2.141	3.80	0.44	
D3	2.100	11.2	1.51	
D4	2.107	8.22	0.77	
D5	2.085	30.7	1.67	1.0
D6	2.067	17.6	1.24	2.08
D7	2.049	30.2	1.88	2.16

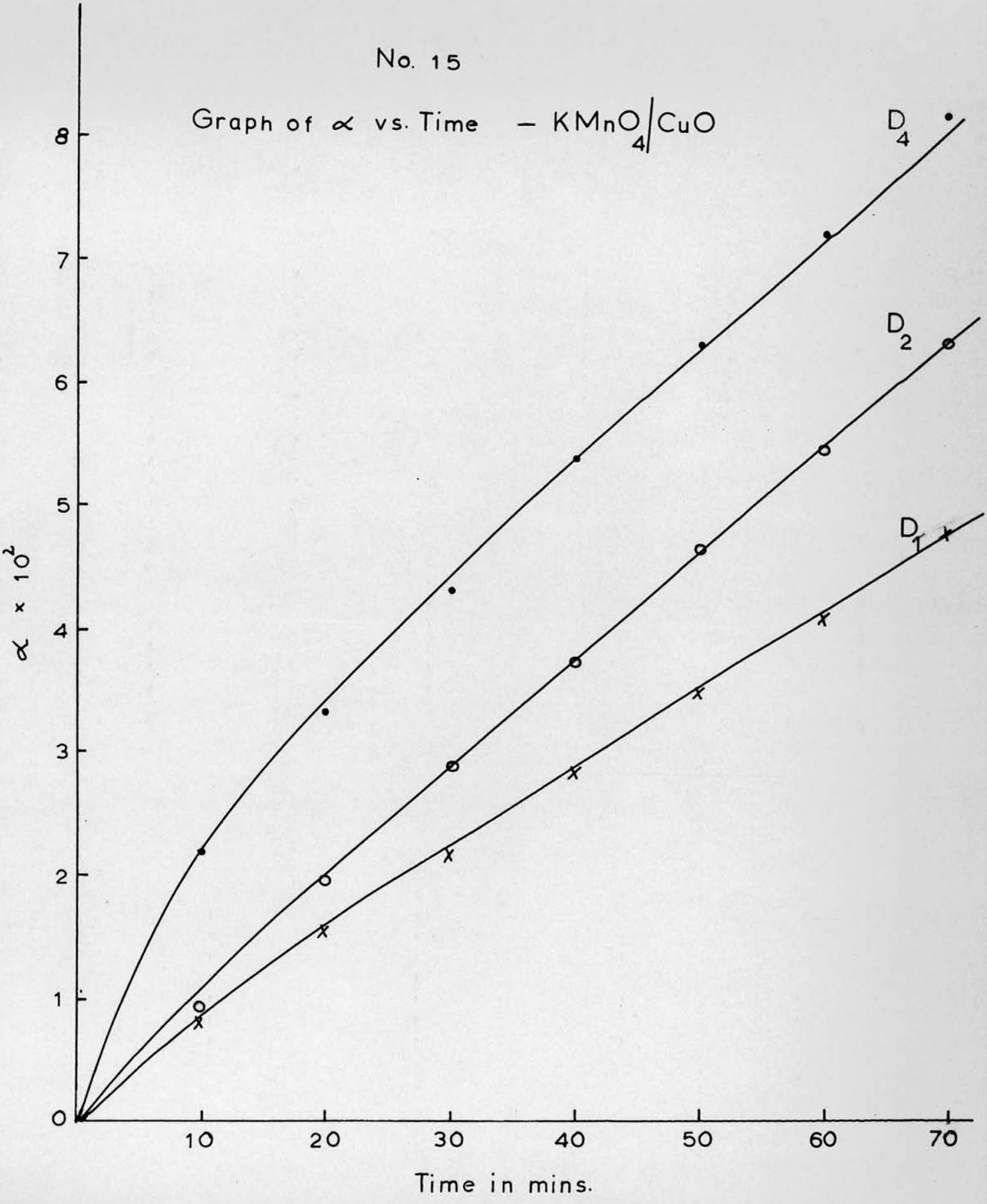
No. 15
Graph of α vs. Time – KMnO4/CuO
D4
D2
D1
α × 10²
0
1
2
3
4
5
6
7
8
10
20
30
40
50
60
70
Time in mins.

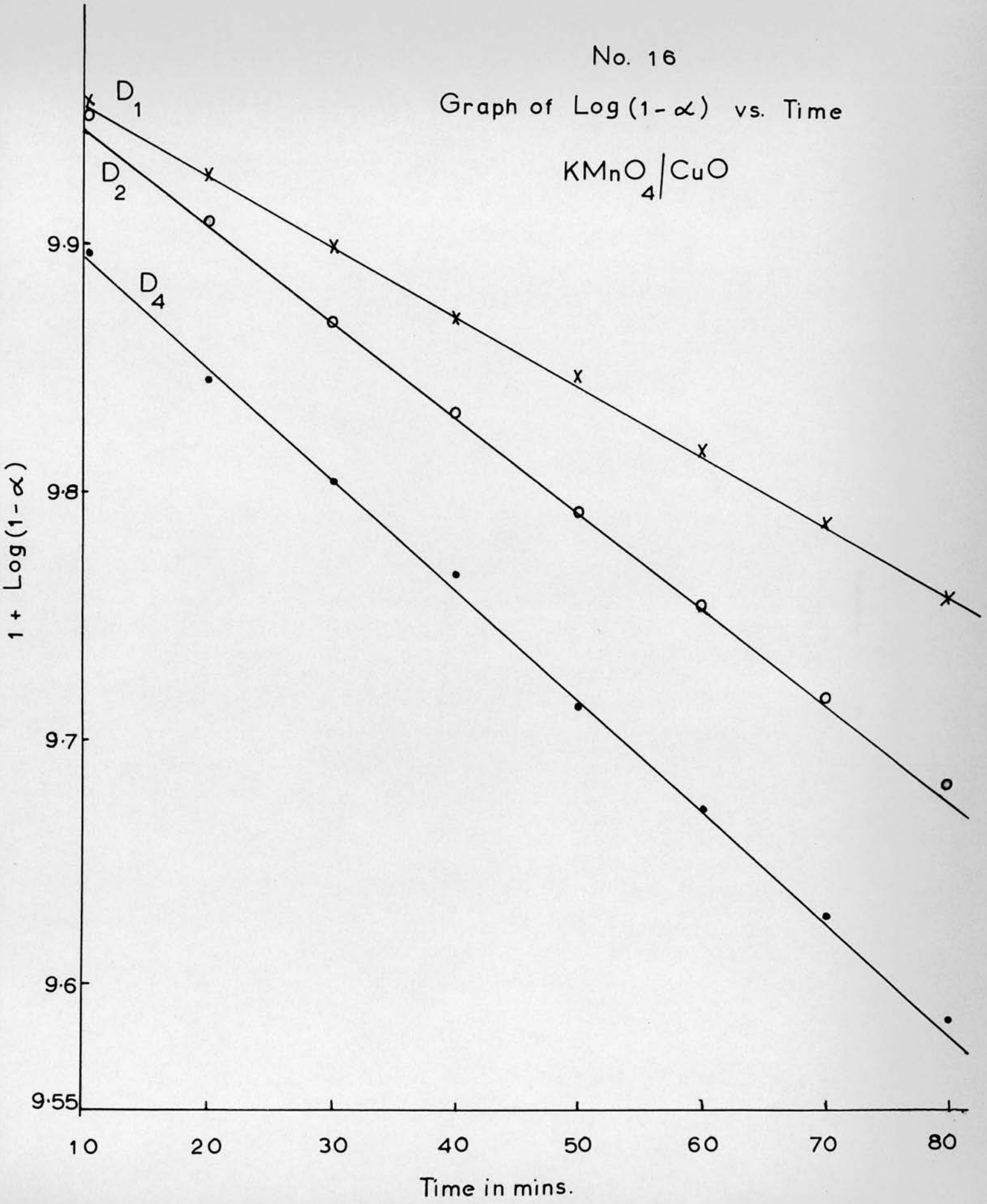
No. 16
Graph of Log (1-α) vs. Time
KMnO4/CuO
D1
D2
D4
9·9
9·8
9·7
9·6
9·55
1 + Log (1-α)
10
20
30
40
50
60
70
80
Time in mins.

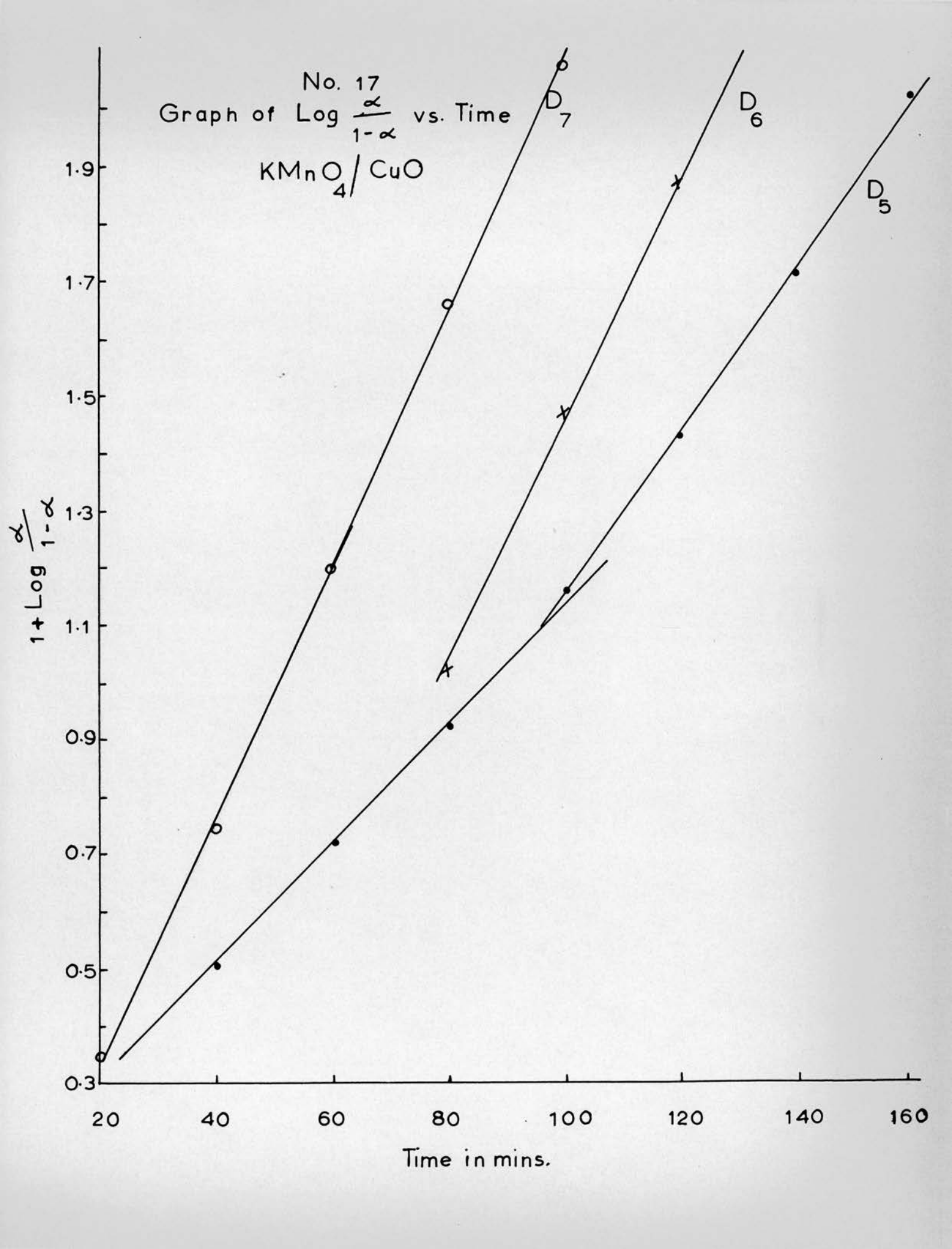
No. 17
Graph of Log $\frac{\alpha}{1-\alpha}$ vs. Time
$KMnO_4$ / CuO
D_7
D_6
D_5
1+Log $\frac{\alpha}{1-\alpha}$
1·9
1·7
1·5
1·3
1·1
0·9
0·7
0·5
0·3
20
40
60
80
100
120
140
160
Time in mins.

No. 18

Graph of $\text{Log}\, k_{(1-\alpha)}$ vs. $\frac{1}{T_A^\circ}$ — $KMnO_4/CuO$

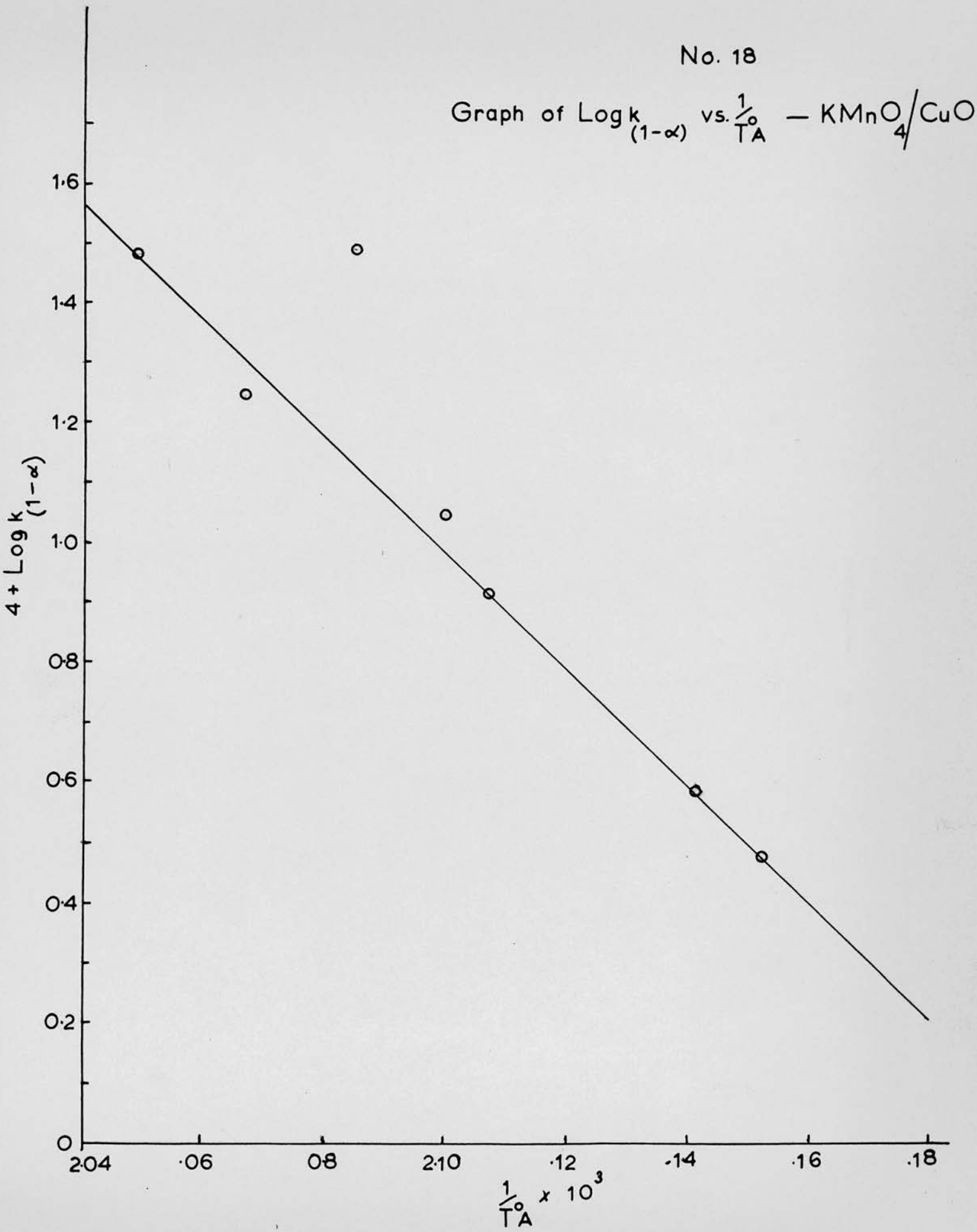

2.5.5. Kinetics for the decomposition potassium permanganate/ferric oxide (E).

Tables 16, 17 and 18 and graphs 19, 20, 21 and 22 illustrate the effect of adding ferric oxide. The initial stage of the "α" - time curve are best fitted in the region $\alpha = 0.02 - 0.10$ by the expression $^{1}/_{1-\alpha} = kt + c$.

The later stages of the decomposition were fitted by the Prout-Tompkins equation, two values of "k" being required.

Tables 16 and 17	Analysis of system (E).
Table 18	Rate constants for system (E).
Graph 19	The initial stage of the "α" - time curves.
Graph 20	The initial reaction, a plot of $\log_{10}(1-\alpha)$ vs. Time.
Graph 21	Acceleration and decay stages; plot of $\log_{10} \alpha/1-\alpha$ vs. Time.
Graph 22	Arrhenius diagram for initial reaction, which gives an activation energy of $E = 38 \pm 3$ K. cals./mole.

Table 16 System E $KMnO_4/Fe_2O_3$

Run	E1			E2		
Temp	208.4°C			201.8°C		
Time Min	$\alpha \times 10^2$	log $(1-\alpha)$	P.T.	$\alpha \times 10^2$	log $(1-\alpha)$	P.T.
5	2.02	$\bar{1}.991$		0.63	$\bar{1}.997$	
10	6.31	$\bar{1}.972$		2.65	$\bar{1}.988$	
15	11.6	$\bar{1}.947$		5.41	$\bar{1}.976$	
20	16.5	1.922		8.46	$\bar{1}.962$	
25	20.6			11.5	$\bar{1}.947$	
30	24.3			14.4	1.932	
35	27.1			17.2		
40	29.8			19.4		
45	32.2			21.9		
50				23.9		
55				25.9		
57	43.7		$\bar{1}.89$			
60				27.8		
65				29.4		
67	50.0		0.00			
70				31.0		
75				32.4		
80				33.9		
87	63.5		0.24			
100				46.3		$\bar{1}.94$
107	74.5		0.47			
120				54.6		0.20
127	83.0		0.69			
140				62.8		-0.23
147	91.0		1.00			
160				70.0		0.37
167	96.3		1.42			
180				76.3		0.51
187	98.8		1.90			
200				81.9		0.66
220				87.0		0.82
240				91.1		1.01
260				94.9		1.27
280				97.5		1.59

Table 17 System E $KMnO_4/Fe_2O_3$

Run	E3		E4		E5		E6	
Temp	195.4°C		189.9°C		181.6°C		178.4°C	
Time Min	$\alpha \times 10^2$	$\log(1-\alpha)$	$\alpha \times 10^2$	$\log(1-\alpha)$	$\alpha \times 10^2$	$\log(1-\alpha)$	$\alpha \times 10^2$	$\log(1-\alpha)$
5	0.33	$\bar{1}.999$	0.32	$\bar{1}.999$	0.69	$\bar{1}.997$	0.39	$\bar{1}.998$
10	1.05	$\bar{1}.995$	1.34	$\bar{1}.993$	1.14	$\bar{1}.995$	0.88	$\bar{1}.996$
15	1.88	$\bar{1}.992$	2.41	$\bar{1}.989$	1.66	$\bar{1}.993$	1.16	$\bar{1}.995$
20	2.75	$\bar{1}.988$	3.48	$\bar{1}.985$	2.11	$\bar{1}.991$	1.42	$\bar{1}.994$
25	3.65	$\bar{1}.984$	4.76	$\bar{1}.979$	2.60	$\bar{1}.989$	2.29	$\bar{1}.990$
30	4.52	$\bar{1}.980$	5.49	$\bar{1}.975$	3.15	$\bar{1}.986$	2.70	$\bar{1}.988$
35	5.29	$\bar{1}.976$	6.51	$\bar{1}.971$	3.74	$\bar{1}.984$	3.15	$\bar{1}.986$
40	6.04	$\bar{1}.973$	7.47	$\bar{1}.966$	4.23	$\bar{1}.981$	3.60	$\bar{1}.984$
45	6.91	$\bar{1}.969$	8.35	$\bar{1}.962$	4.88	$\bar{1}.978$	3.95	$\bar{1}.982$
50	7.63	$\bar{1}.966$	9.15	$\bar{1}.958$	5.54	$\bar{1}.975$	4.36	$\bar{1}.981$
55	8.43	$\bar{1}.962$	9.98	$\bar{1}.954$	6.20	$\bar{1}.972$	4.85	$\bar{1}.978$
60	9.18	$\bar{1}.958$	10.8	$\bar{1}.951$	6.89	$\bar{1}.969$	5.33	$\bar{1}.976$
65	9.99	$\bar{1}.954$	11.6	$\bar{1}.947$	7.52	$\bar{1}.966$		
70	11.13	$\bar{1}.949$			8.19	$\bar{1}.963$	6.51	$\bar{1}.971$
75					8.97	$\bar{1}.959$		
80					9.52	$\bar{1}.957$	7.14	$\bar{1}.968$
85					10.3	$\bar{1}.953$		
90					10.9	$\bar{1}.950$	8.21	$\bar{1}.963$
100							9.21	$\bar{1}.958$
110							10.3	$\bar{1}.953$
120							11.4	$\bar{1}.947$

Table 18 Rate Constants for System E $KMnO_4/Fe_2O_3$

Run	$1/T^\circ$ A x 10^3	$k_{(1-\alpha)}$ x 10^4	k_x x 10^2	k_2 x 10^2
E1	2.077	46.0	15.0	1.12
E2	2.106	27.7	8.96	0.72
E3	2.135	7.55	4.72	
E4	2.161	9.18	4.55	
E5	2.200	4.88	3.55	
E6	2.215	3.96	2.17	

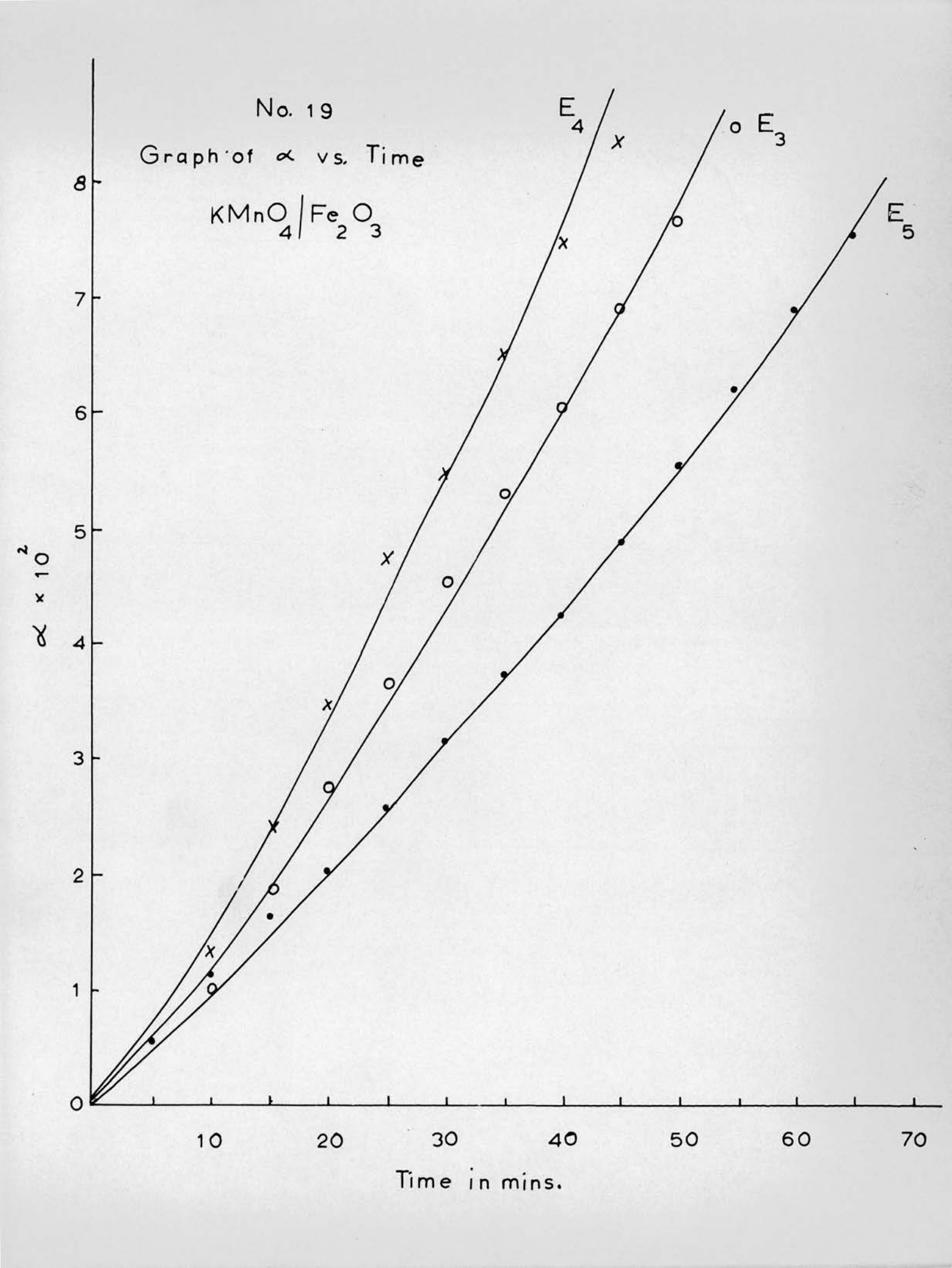
No. 19
Graph of α vs. Time
KMnO4 / Fe2O3
E4
E3
E5
α x 10²
Time in mins.
0
1
2
3
4
5
6
7
8
10
20
30
40
50
60
70

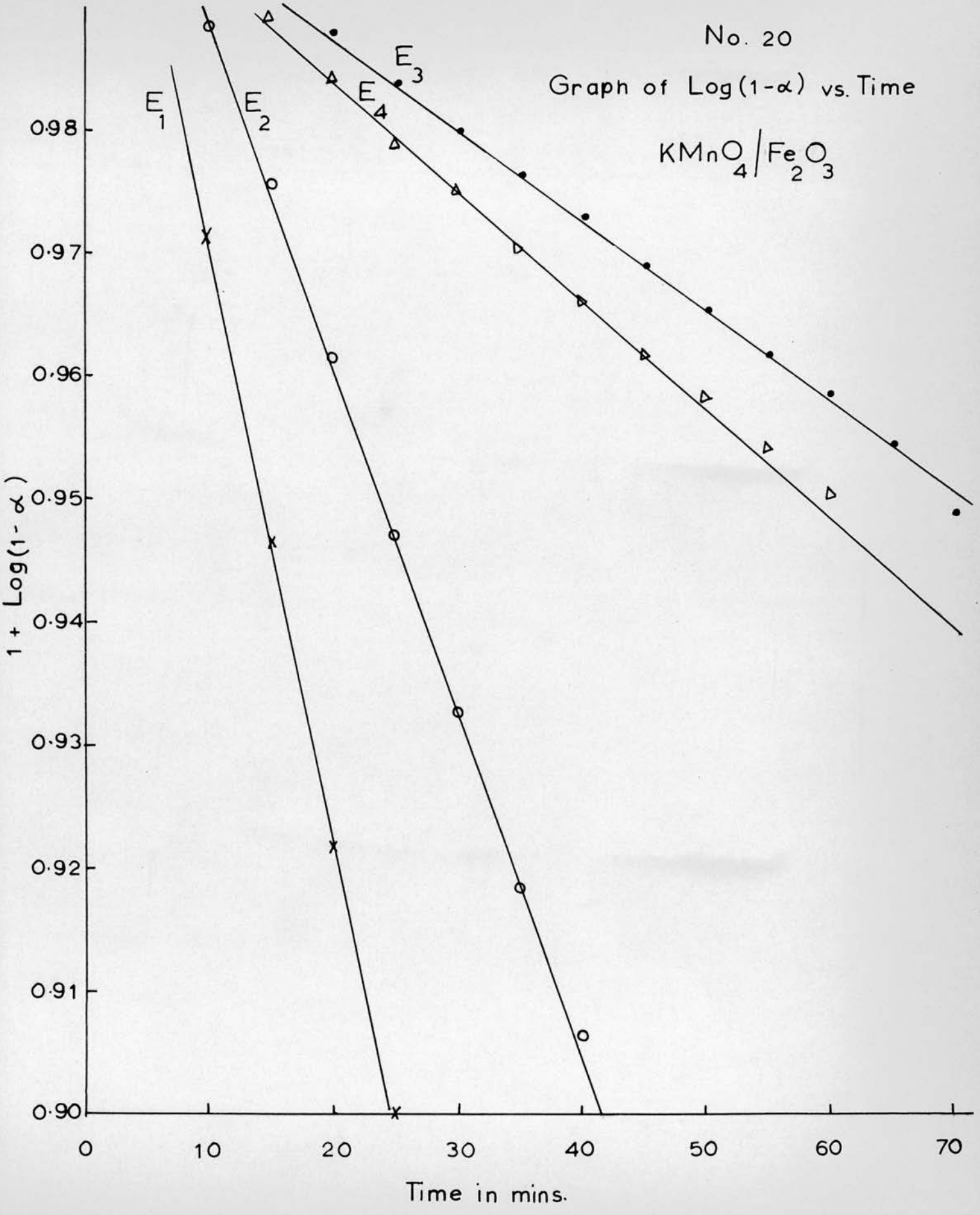
No. 20
Graph of Log(1-α) vs. Time
KMnO4/Fe2O3
E1
E2
E3
E4
1 + Log(1- α)
0·98
0·97
0·96
0·95
0·94
0·93
0·92
0·91
0·90
0
10
20
30
40
50
60
70
Time in mins.

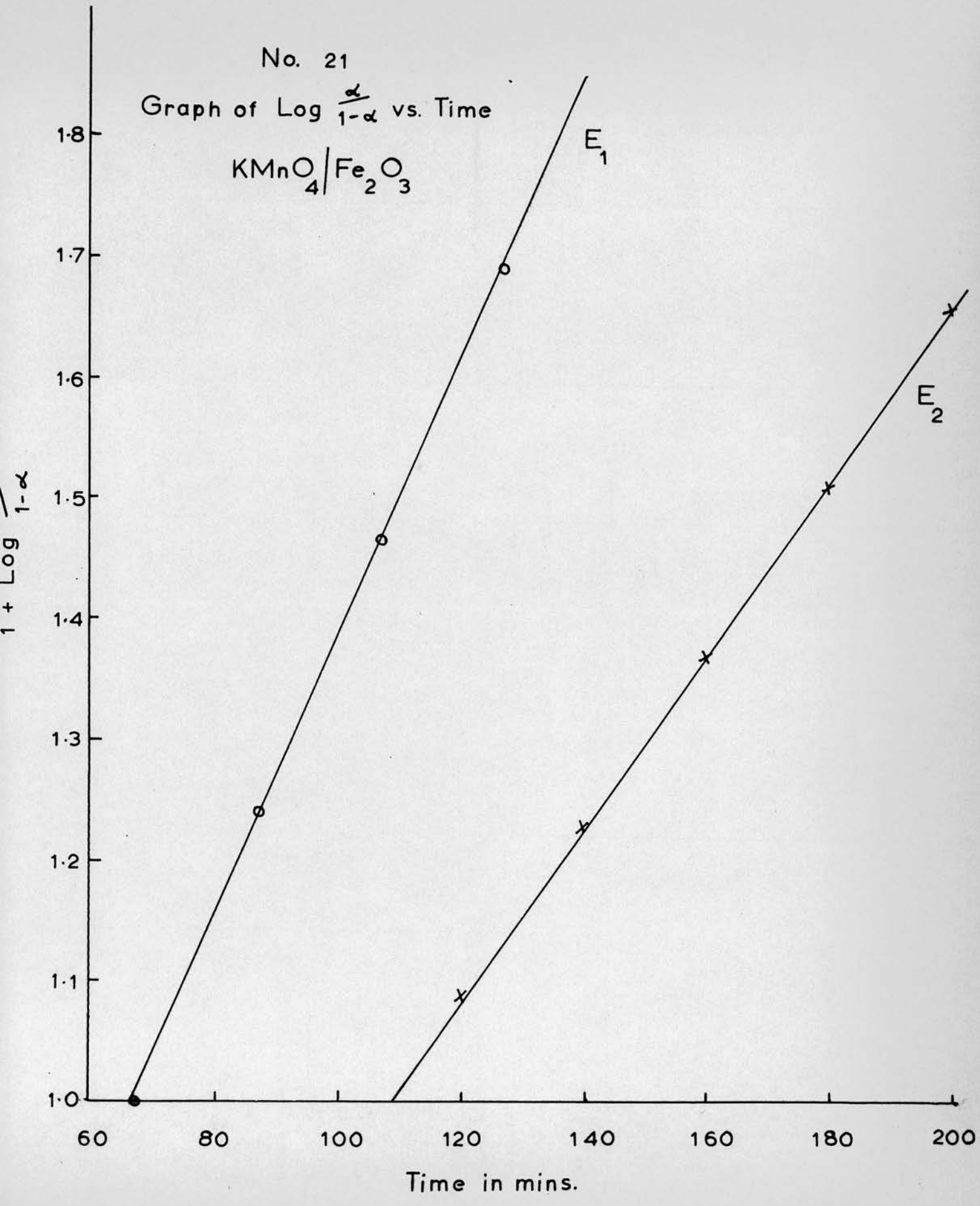
No. 21
Graph of Log α/1-α vs. Time
KMnO4/Fe2O3
E1
E2
1·8
1·7
1·6
1·5
1·4
1·3
1·2
1·1
1·0
1 + Log α/1-α
60
80
100
120
140
160
180
200
Time in mins.

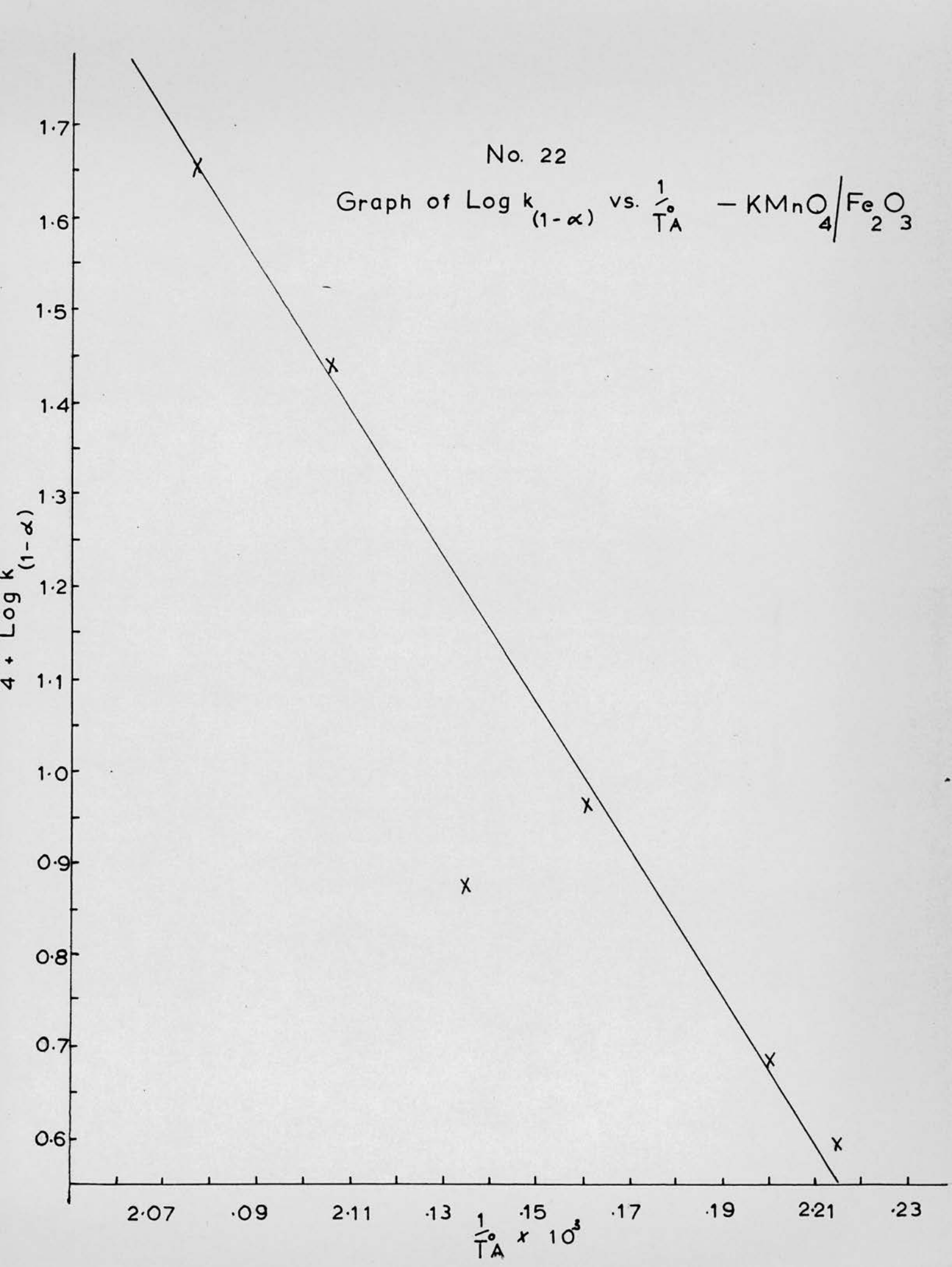
No. 22
Graph of Log k(1-α) vs. 1/To TA — KMnO4/Fe2O3
4 + Log k(1-α)
1·7
1·6
1·5
1·4
1·3
1·2
1·1
1·0
0·9
0·8
0·7
0·6
2·07
·09
2·11
·13
·15
·17
·19
2·21
·23
1/To TA x 10³

2.5.6. Kinetics for the decomposition for potassium permanganate/Zinc oxide (F)

Tables 19, 20 and 21 and graphs 23, 24 and 25 illustrate the effect of adding zinc oxide. The initial stage of the "α" - time curves are now linear and tend to break into two sections (1) $\alpha = 0 - 0.05$ and (2) $\alpha = 0.05 - 0.12$.

The later stages of the decomposition were fitted by the Prout-Tompkins equation, two values of "k" being required.

Tables 19 and 20	Analysis of system (F).
Table 21	Rate constants for system (F).
Graph 23	Initial stage of the "α" - time curves.
Graph 24	Acceleration and decay stages; plot of $\log_{10} \frac{\alpha}{1-\alpha}$ vs. Time.
Graph 25	Arrhenius diagram for initial reaction, which gives an activation energy of E = 36±3 K. cals./mole.

Table 19 System F $KMnO_4/ZnO$

Run	F1		F2		F3	
Temp	214.7°C		210.2°C		206.5°C	
Time Min	$\alpha \times 10^2$	P.T.	$\alpha \times 10^2$	P.T.	$\alpha \times 10^2$	P.T.
2	0.28					
4	1.21	$\bar{2}.09$				
5			1.61	$\bar{2}.21$	1.04	$\bar{2}.02$
6	2.16	$\bar{2}.34$				
8	3.22	$\bar{2}.52$				
10	4.18	$\bar{2}.64$	2.30	$\bar{2}.37$	2.49	$\bar{2}.41$
12	5.39	$\bar{2}.76$				
14	6.61	$\bar{2}.85$				
15			5.98	$\bar{2}.80$	4.01	$\bar{2}.63$
16	7.78	$\bar{2}.93$				
18	9.06	$\bar{1}.00$				
20	10.3	$\bar{1}.06$	8.13	$\bar{2}.95$	5.73	$\bar{2}.78$
22	11.5	$\bar{1}.11$				
24	12.5	$\bar{1}.16$				
25			10.5	$\bar{1}.07$	7.59	$\bar{2}.91$
27	15.0	$\bar{1}.31$				
30			12.7	$\bar{1}.16$	9.54	$\bar{1}.02$
37	24.9	$\bar{1}.52$				
40			20.7	$\bar{1}.42$	13.1	$\bar{1}.18$
47	37.5	$\bar{1}.78$			16.7	$\bar{1}.30$
50			26.6	$\bar{1}.56$		
57	57.9	0.14			20.6	$\bar{1}.41$
60			34.6	$\bar{1}.72$		
67	78.6	0.56			25.5	$\bar{1}.53$
70			44.2	$\bar{1}.90$		
77	90.7	0.99			32.0	$\bar{1}.67$
80			55.4	0.09		
87	96.5	1.44			38.7	$\bar{1}.80$
90			66.5	0.30		
97	98.2	1.75			47.0	$\bar{1}.95$
100			75.3	0.48		
107	98.7	1.89			55.5	0.09
110			84.0	0.72		
117	99.2				64.0	0.25
120			90.2	0.97		
127					71.1	0.39
130			95.1	1.29		
137					77.9	0.55
140			97.4	1.57		
147					83.3	0.70
150						
157					88.3	0.88
160			99.3			
167					92.1	1.07
187					97.2	1.55
207					98.8	

Table 20 System F $KMnO_4/ZnO$

Run	F4	F5	F6	F7
Temp	202.4°C	194.0°C	189.8°C	197.6°C
Time Min	$\alpha \times 10^2$	$\alpha \times 10^2$	$\alpha \times 10^2$	$\alpha \times 10^2$
5	0.9	0.3		0.4
10	2.49	1.03	0.6	1.07
15	3.77	1.48		1.77
20	5.06	2.02	1.37	2.41
25	6.31	2.51		3.13
30	7.60	2.99	2.12	3.88
35	8.88	3.60		4.68
40	10.2	4.13	2.93	5.53
45	11.4	4.76		6.40
50		5.35	3.92	7.30
55		6.01		8.25
60		6.62	4.98	9.11
65		7.25		10.1
70		7.98	6.13	10.9
75		8.63		11.9
80		9.23	7.35	
85		9.85		
90		10.5	8.70	
95		11.1		
100		11.6	10.0	
110			11.3	

Table 21 Rate Constants for System F $KMnO_4/ZnO$

Run	$1/T^\circ$ A x 10^3	α range	k_{α_1} x 10^3	α range	k_{α_2} x 10^3	k_x x 10^2	k_1 x 10^2	k_2 x 10^2
F1	2.050	0–0.05	4.79	0.05–0.11	6.17	12.5	2.45	3.87
F2	2.069			0–0.18	4.44	12.5	1.76	2.23
F3	2.085	0–0.05	2.94	0.05–0.15	3.77	8.44	1.48	
F4	2.103			0–0.12	2.54	8.83		
F5	2.141	0–0.04	1.03	0.04–0.12	1.29	3.42		
F6	2.161	0–0.05	0.77	0.05–0.12	1.28	2.47		
F7	2.126	0–0.05	1.35	0.05–0.15	1.85	4.17		

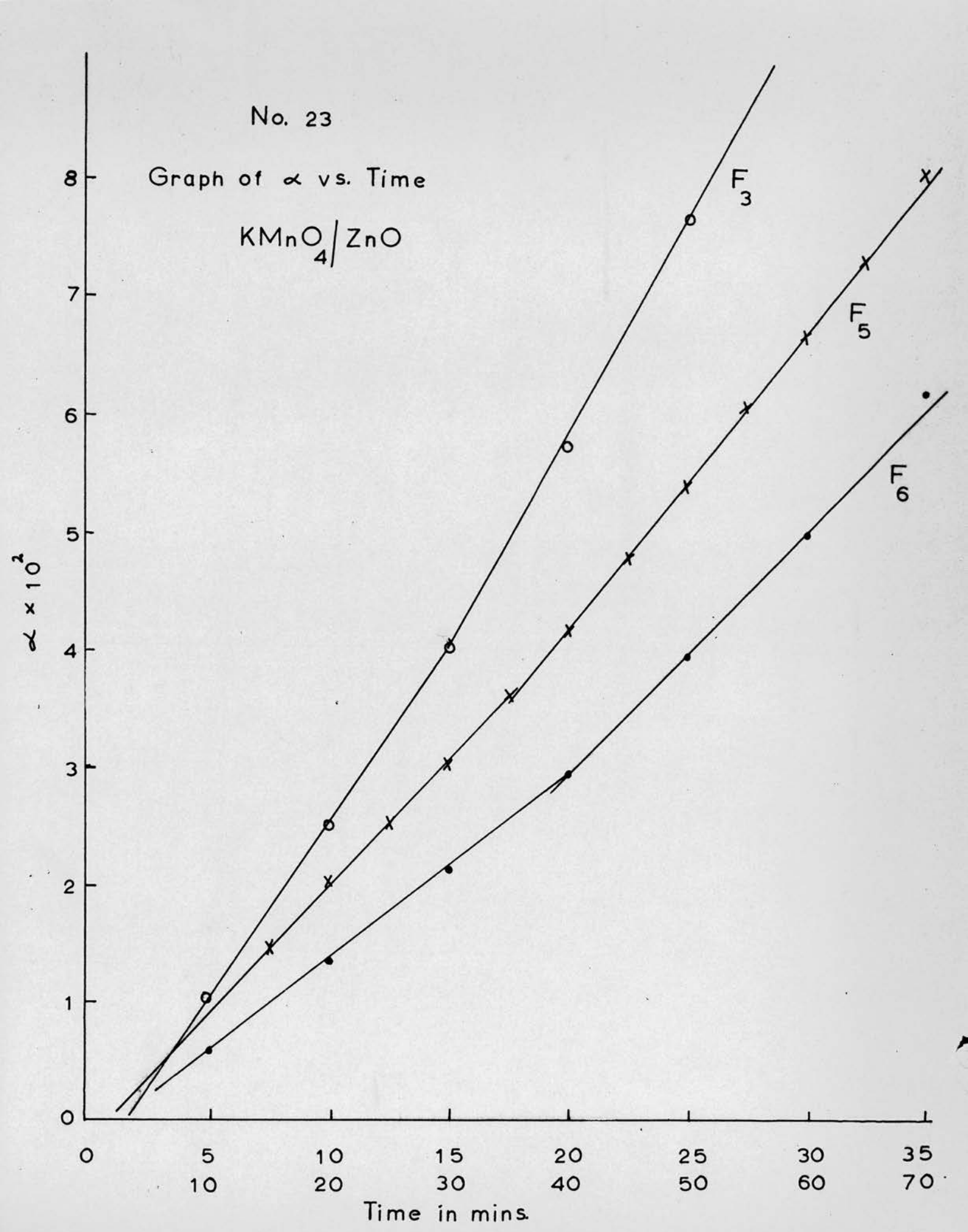
No. 23
Graph of α vs. Time
KMnO4/ZnO
F3
F5
F6
α x 10²
0
1
2
3
4
5
6
7
8
0
5
10
15
20
25
30
35
10
20
30
40
50
60
70
Time in mins.

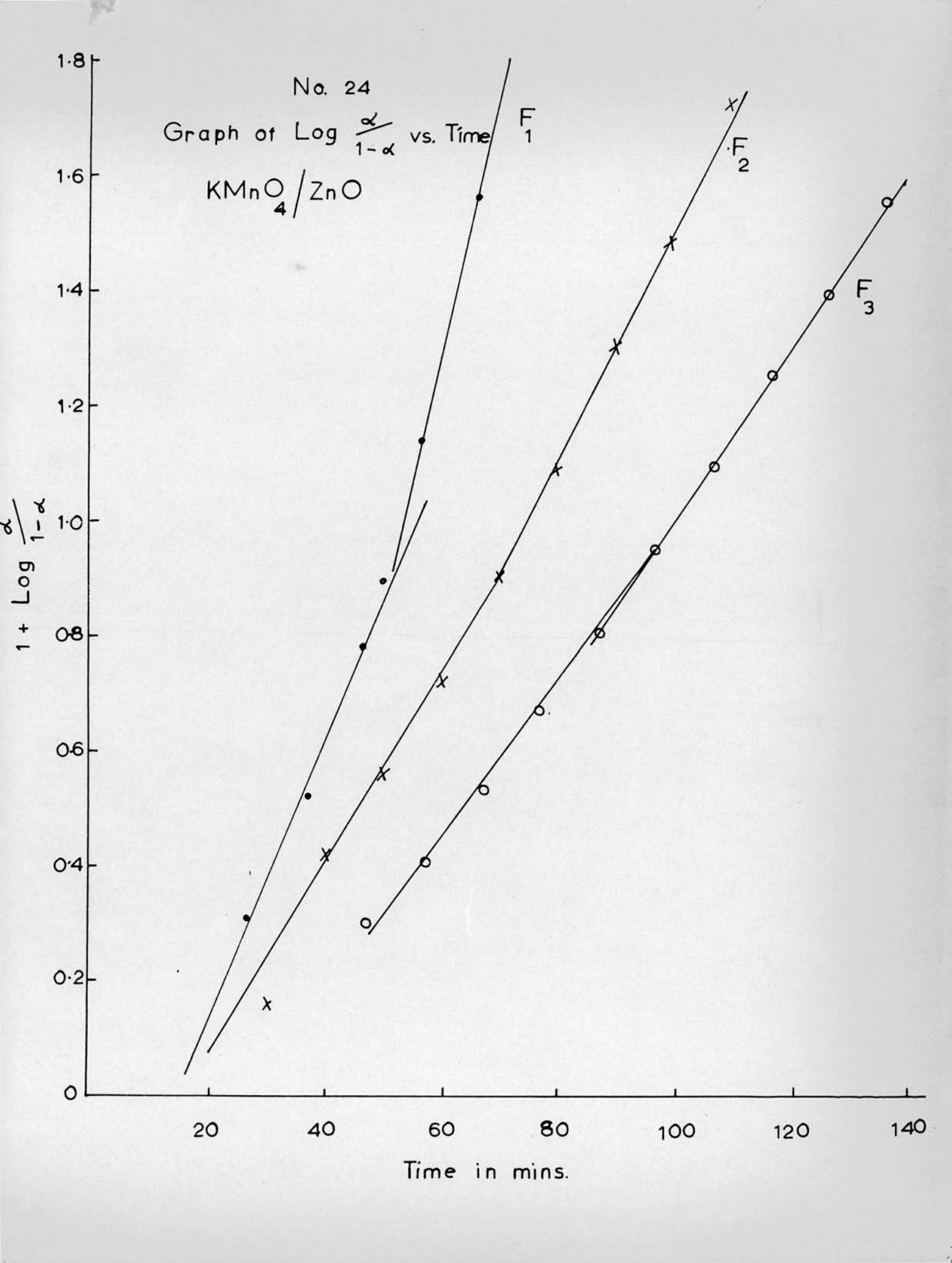
No. 24
Graph of Log α/1-α vs. Time
KMnO4/ZnO
F1
F2
F3
1·8
1·6
1·4
1·2
1·0
0·8
0·6
0·4
0·2
0
1 + Log α/1-α
20
40
60
80
100
120
140
Time in mins.

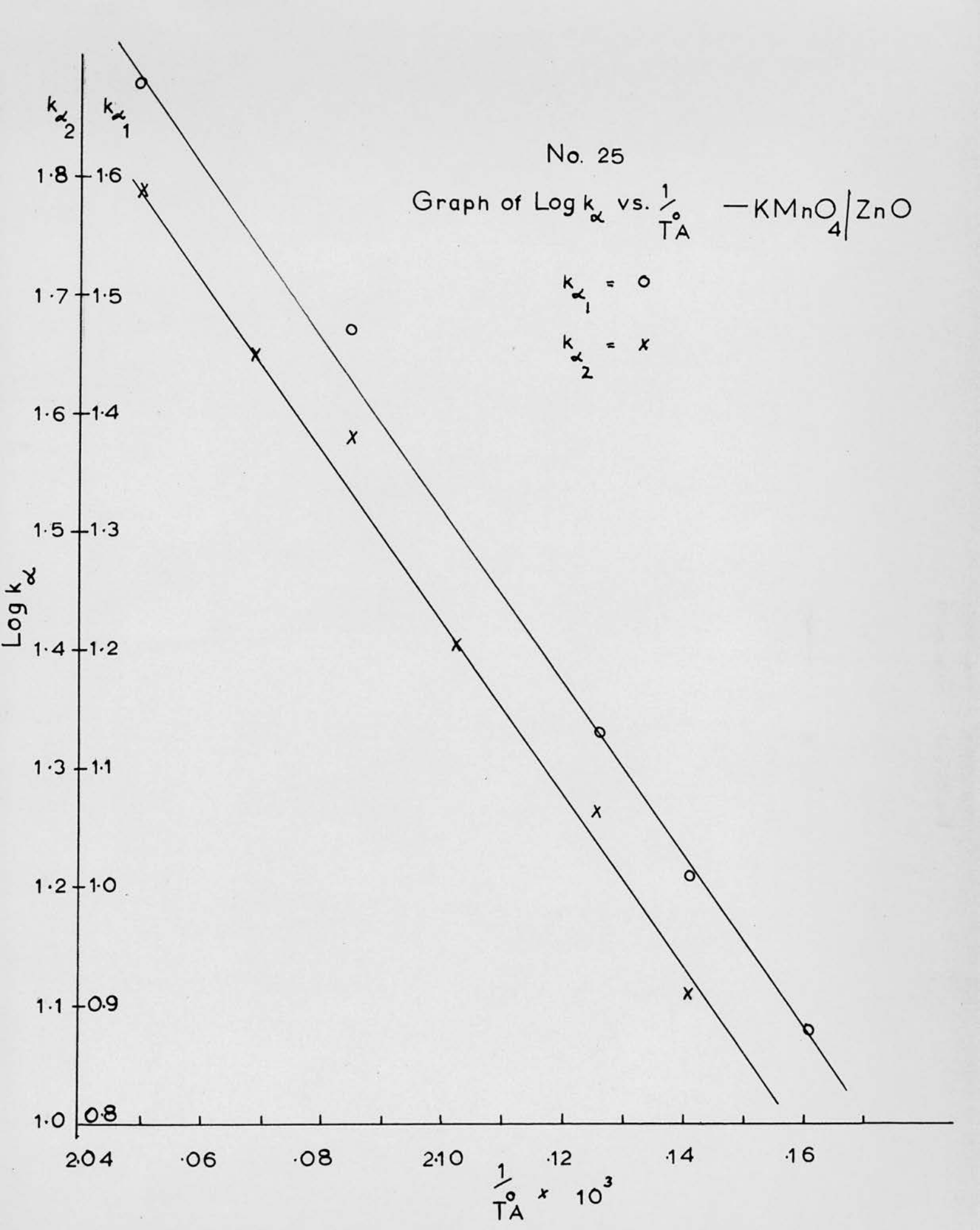
No. 25
Graph of Log k_α vs. $\frac{1}{T_A^\circ}$ — $KMnO_4$ / ZnO
k_{α_1} = o
k_{α_2} = x
k_{α_2}
k_{α_1}
1·8 1·6
1·7 1·5
1·6 1·4
1·5 1·3
1·4 1·2
1·3 1·1
1·2 1·0
1·1 0·9
1·0 0·8
Log k_α
2·04 ·06 ·08 2·10 ·12 ·14 ·16
$\frac{1}{T_A^\circ} \times 10^3$

2.5.7. Kinetics for the decomposition for potassium permanganate/zinc oxide (1000°) (G) and zinc oxide + 1 mole % chromic oxide (H)

Tables 22, 23 and 24 and graphs 26, 27, 28 and 29 illustrate the effect of adding zinc oxide (1000°) and zinc oxide + 1 mole % chromic oxide. The initial stage of the "α" - time curves are once again acceleratory and are best fitted in the region $\alpha = 0.01 - 0.1$ by the power law

$$\alpha = kt^{n} \quad \text{where } n = 2$$

The later stages of the decomposition are fitted by the Prout-Tompkins equation, two values of "k" being required.

Tables 22 and 23	Analysis of systems (G) and (H).
Table24	Rate constants for systems (G) and (H).
Graph 26	Initial stage of the "α" - time curves.
Graph 27	Initial reaction, plot of $\alpha^{\frac{1}{2}}$ vs. Time.
Graph 28	Acceleration and decay stages, plot of $\log_{10} \alpha/1-\alpha$ vs. Time.
Graph 29	Arrhenius diagram for initial reaction, which gives an activation energy of E = 43±5 K. cals./mole.

Table 22 System H and G $KMnO_4/ZnO$ (1000°) and $KMnO_4/ZnO + Cr_2O_3$

Run	H2			G2		
Temp	204.6°C			204.6°C		
Time Min	$\alpha \times 10^2$	$\alpha^{\frac{1}{2}} \times 10$	P.T.	$\alpha \times 10^2$	$\alpha^{\frac{1}{2}} \times 10$	P.T.
5	0.48	0.69		0.60	0.78	
10	1.41	1.19		1.68	1.30	
15	2.55	1.60		2.97	1.72	
20	4.06	2.02		4.50	2.12	
25	5.98	2.44		6.36	2.52	
30	8.04	2.84		8.28	2.88	
35	10.1	3.18		10.2	3.19	
40	12.1	3.48		14.6		1.23
60	26.3		1.55	24.7		1.52
80	44.0		1.90	42.6		1.87
100	63.5		0.24	62.8		0.23
120	77.3		0.53	76.2		0.51
140	87.5		0.85	86.0		0.79
160	94.3		1.22	93.2		1.13
180	96.9		1.49	97.5		1.59
200	99.8		1.68	99.5		

Run	H5		G5		H6		G6	
Temp	190.2°C		190.0°C		187.9°C		187.7°C	
Time Min	$\alpha \times 10^2$	$\alpha^{\frac{1}{2}} \times 10$	$\alpha \times 10^2$	$\alpha^{\frac{1}{2}} \times 10$	$\alpha \times 10^2$	$\alpha^{\frac{1}{2}} \times 10$	$\alpha \times 10^2$	$\alpha^{\frac{1}{2}} \times 10$
10	0.24	0.49	0.19	0.43	0.45	0.67	0.13	0.36
20	0.30	0.55	0.29	0.54	0.59	0.77	0.17	0.41
30	0.51	0.71	0.43	0.66	0.87	0.93	0.23	0.48
40	0.76	0.87	0.62	0.79	1.07	1.03	0.27	0.52
50	1.10	1.05	0.93	0.96	1.36	1.15	0.36	0.60
60	1.67	1.29	1.41	1.19	1.74	1.32	0.48	0.70
70	2.35	1.53	2.03	1.43	2.20	1.48	0.64	0.80
80	3.27	1.81	2.79	1.67	2.76	1.66	0.87	0.93
90	4.31	2.08	3.72	1.93	3.39	1.84	1.13	1.06
100	5.51	2.35	4.67	2.16	4.11	2.03	1.48	1.22
110	6.86	2.62	5.72	2.39	4.94	2.22	1.84	1.36
120	8.24	2.87	6.84	2.61	5.85	2.42	2.25	1.50
130	9.66	3.11	7.90	2.81	6.76	2.60	2.77	1.66
140			9.05	3.01	7.77	2.79	3.29	1.81
150			1.02	3.19	8.75	2.96	3.93	1.98
160							4.65	2.16

Table 23 System G and H $KMnO_4/ZnO$ (1000°) and $KMnO_4/ZnO + Cr_2O_3$

Run	H3		G3		H4		G4	
Temp	198.0°C		198.1°C		103.9°C		194.0°C	
Time Min	$\alpha \times 10^2$	$\alpha^{\frac{1}{2}} \times 10$	$\alpha \times 10^2$	$\alpha^{\frac{1}{2}} \times 10$	$\alpha \times 10^2$	$\alpha^{\frac{1}{2}} \times 10$	$\alpha \times 10^2$	$\alpha^{\frac{1}{2}} \times 10$
5	0.14	0.37	0.20	0.45				
10	0.48	0.69	0.45	0.67	0.22	0.47	0.42	0.64
15	0.82	0.91	0.69	0.83				
20	1.28	1.13	0.99	0.99	0.51	0.71	0.55	0.74
25	1.86	1.37	1.30	1.13				
30	2.52	1.59	1.70	1.30	0.83	0.91	0.84	0.92
35	3.28	1.81	2.15	1.47				
40	4.20	2.05	2.72	1.65	1.34	1.16	1.40	1.19
45	5.22	2.28	3.36	1.83				
50	6.26	2.50	4.05	2.01	1.97	1.40	2.34	1.53
55	7.36	2.71	4.77	2.18				
60	8.44	2.91	5.55	2.36	2.74	1.66	3.63	1.90
65	9.50	3.08	6.40	2.53				
70	10.6	3.25	7.25	2.69	3.57	1.89	5.21	2.28
75			8.10	2.85				
80			8.98	3.00	4.54	2.13	6.91	2.63
85			9.85	3.14				
90					5.61	2.37	8.57	2.93
100					7.39	2.72	10.1	3.18
110					9.47	3.08		

Table 24 Rate Constants for System G and H $KMnO_4/ZnO$ (1000°) and $KMnO_4/ZnO + Cr_2O_3$

Run	$1/T^\circ$ A x 10^3	$k_{\frac{1}{2}}$ x 10^2	k_x x 10^2	k_1 x 10^2	k_2 x 10^2
H1	2.076		11.4		
G1	2.076		8.07		
H2	2.094	8.56	6.05	1.20	1.59
G2	2.094	7.86	6.58	1.78	1.42
H3	2.123	4.46	3.10		
G3	2.122	3.53	2.36		
H4	2.142	2.42	1.61		
G4	2.141	3.58	1.79		
H5	2.159	2.66	1.30		
G5	2.160	2.38	1.22		
H6	2.170	1.86	1.19		
G6	2.170	1.16	0.75		
G7	2.046		4.17		
G8	2.045	4.68			

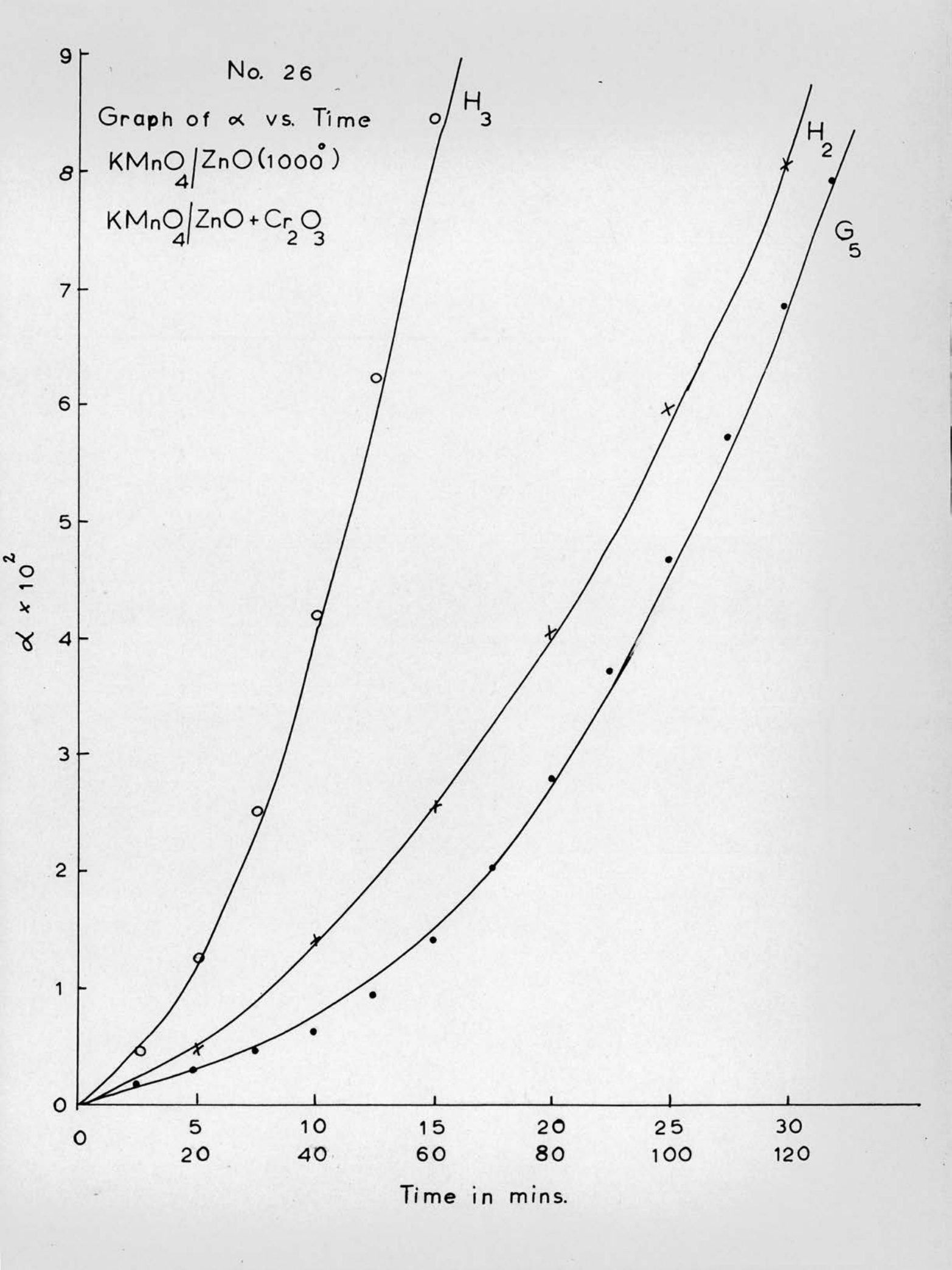
No. 26
Graph of α vs. Time
KMnO4/ZnO(1000°)
KMnO4/ZnO + Cr2O3
H3
H2
G5
α x 10²
Time in mins.
0
1
2
3
4
5
6
7
8
9
0
5
10
15
20
25
30
20
40
60
80
100
120

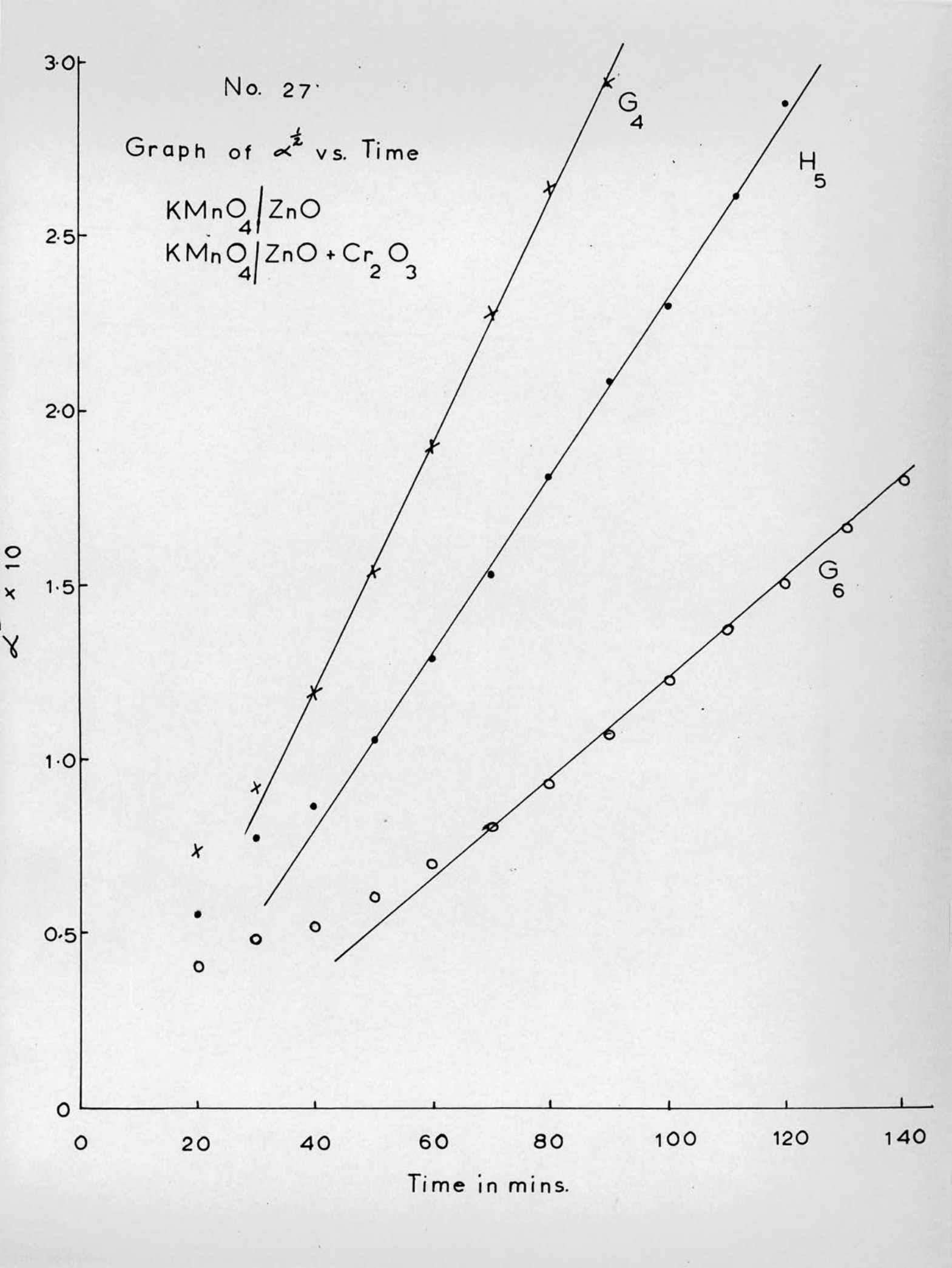
No. 27
Graph of $\alpha^{\frac{1}{2}}$ vs. Time
$KMnO_4$ / ZnO
$KMnO_4$ / ZnO + Cr_2O_3
G_4
H_5
G_6
α x 10
3·0
2·5
2·0
1·5
1·0
0·5
0
0
20
40
60
80
100
120
140
Time in mins.

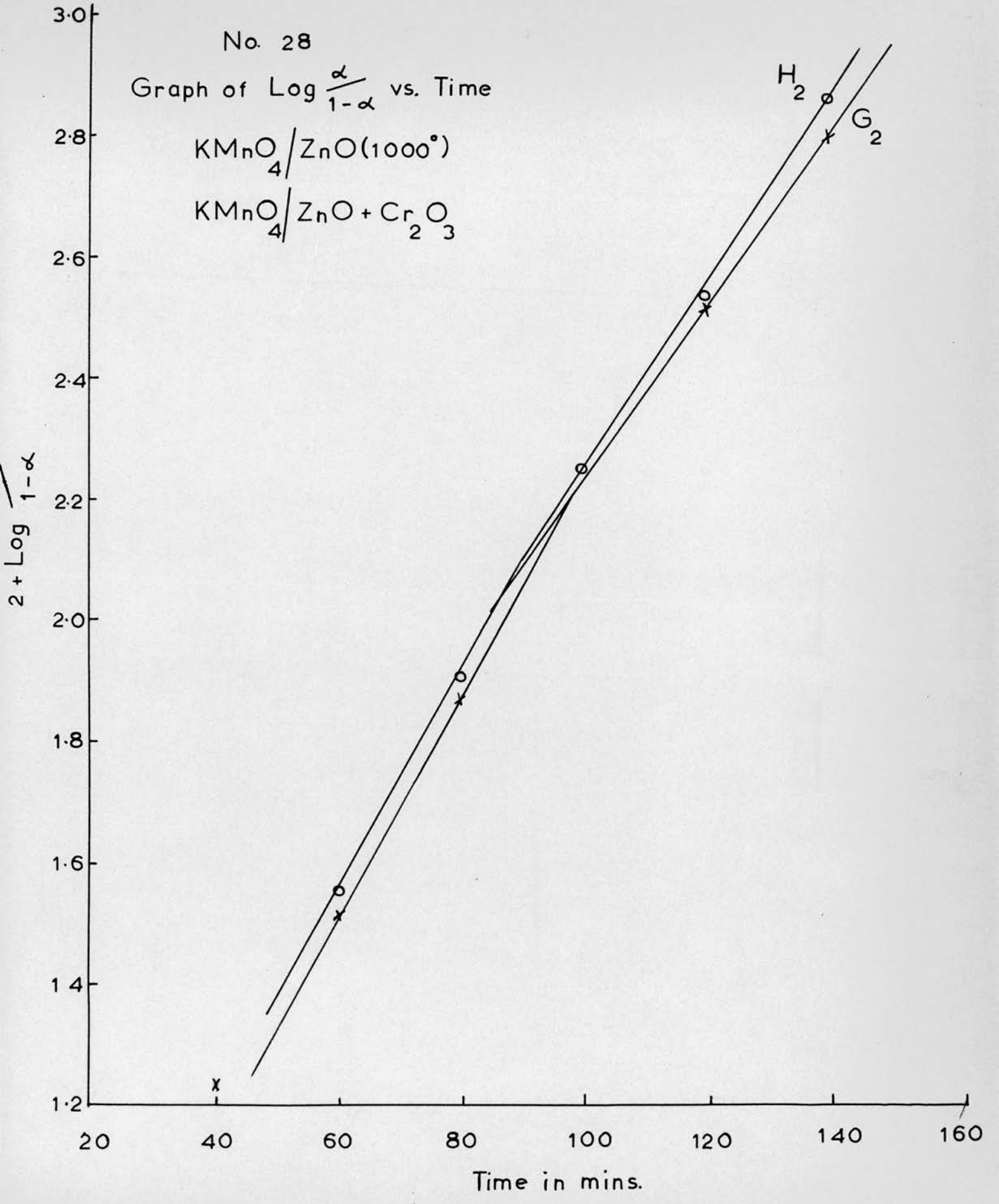
No. 28
Graph of Log α/1-α vs. Time
KMnO4/ZnO(1000°)
KMnO4/ZnO + Cr2O3
H2
G2
3·0
2·8
2·6
2·4
2·2
2·0
1·8
1·6
1 4
1·2
2 + Log α/1-α
20
40
60
80
100
120
140
160
Time in mins.

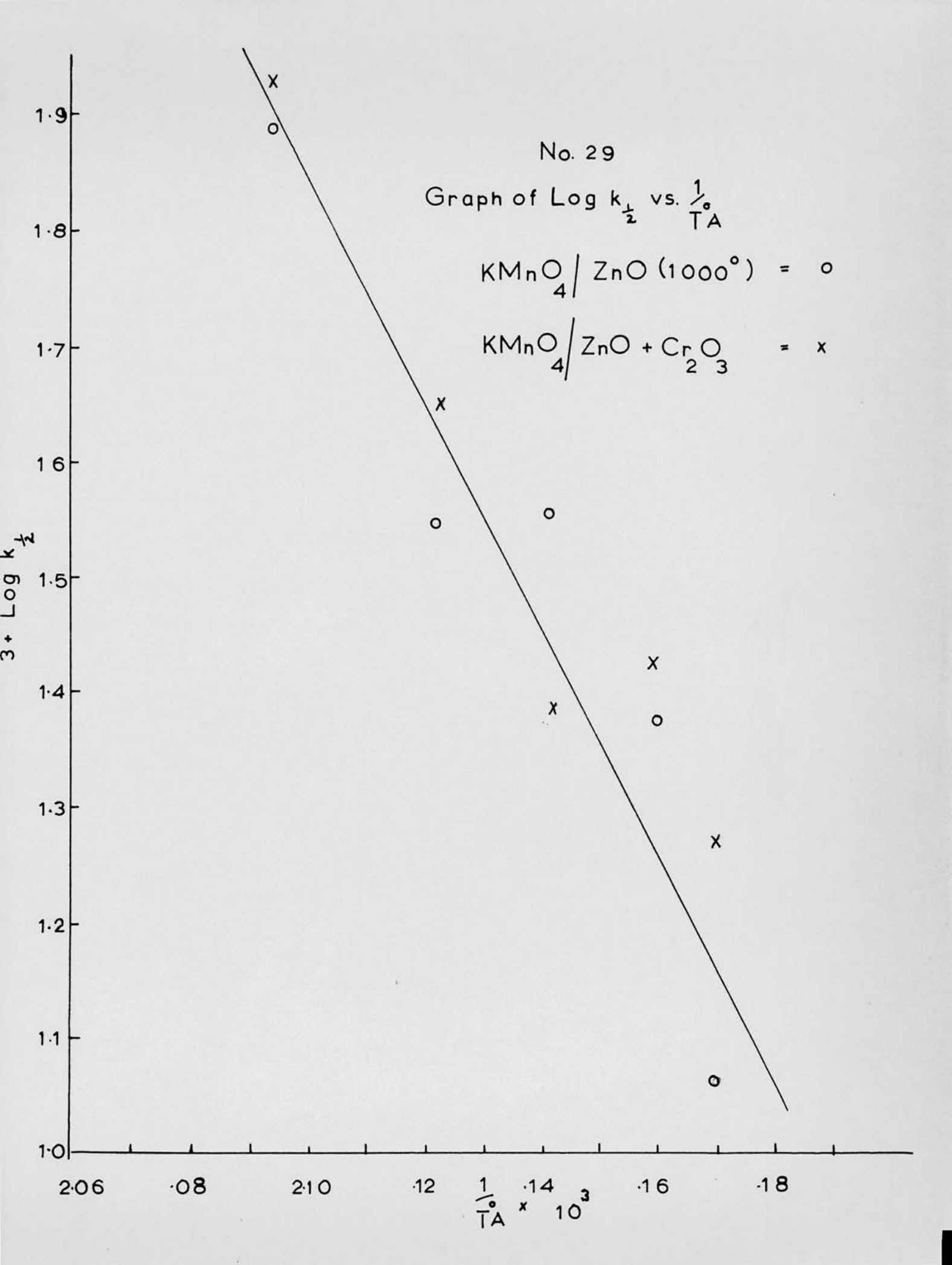
No. 29
Graph of Log $k_{\frac{1}{2}}$ vs. $\frac{1}{°TA}$
$KMnO_4$ / ZnO (1000°) = o
$KMnO_4$ / ZnO + Cr_2O_3 = x
3+ Log $k_{\frac{1}{2}}$
1·9
1·8
1·7
1 6
1·5
1·4
1·3
1·2
1·1
1·0
2·06
·08
2·10
·12
·14
·16
·18
$\frac{1}{°TA} \times 10^3$

2.5.8. Kinetics for the decomposition for potassium permanganate/nickel oxide (I)

Tables 25, 26 and 27 and graphs 30, 31, 32 and 33 illustrate the effect of adding nickel oxide. The reaction now commences at maximum rate and the traces are deceleratory throughout, they are best fitted in the region $\alpha = 0 - 0.09$ by the "contracting sphere" expression

$$\alpha = 1 - \left[c - k (t - t_o) \right]^3$$

The later stages of the decomposition are fitted by the Prout-Tompkins equation, two values of "k" being required.

Tables 25 and 26	Analysis of system (I).
Table 27	Rate constants for system (I).
Graph 30	Initial stage of the "α" - time curves.
Graph 31	Initial reaction, plot of $(1 - \alpha)^{\frac{1}{3}}$ vs. Time.
Graph 32	Acceleration and decay stages; plot of $\log_{10} \alpha/1 - \alpha$ vs. Time.
Graph 33	Arrhenius diagram for initial reaction, which gives an activation of E = 35±3 K. cals./mole.

EX LIBRIS UNIV. EDINBURGEN

Table 25 System I $KMnO_4/NiO$

Run	I1		I2		I3	
Temp	203.8°C		198.8°C		167.3°C	
Time Min	$\alpha \times 10^2$	$(1-\alpha)^{\frac{1}{3}}$	$\alpha \times 10^2$	$(1-\alpha)^{\frac{1}{3}}$	$\alpha \times 10^2$	$(1-\alpha)^{\frac{1}{3}}$
2	0.37	0.999	1.52	0.995		
4	3.22	0.989	4.56	0.985		
5					0.80	0.997
6	6.31	0.979	6.38	0.978		
8	7.67	0.974	7.65	0.974		
10	8.79	0.970	8.51	0.971	2.03	0.993
12	9.72	0.967	9.23	0.968		
14	10.5		9.81	0.966		
15					2.83	0.990
16	11.0		10.4	0.964		
20					3.36	0.989
25					3.80	0.987
30					4.24	0.986
35					4.58	0.985
40					4.90	0.983
45					5.21	0.982
50					5.46	0.981
55					5.74	0.980
60					5.87	
65					6.27	

Table 26 System I $KMnO_4/NiO$

Run	I4		I7		I6		I5	
Temp	211.0°C		180.9°C		218.4°C		213.3°C	
Time Min	$\alpha \times 10^2$	$(1-\alpha)^{\frac{1}{3}}$	$\alpha \times 10^2$	$(1-\alpha)^{\frac{1}{3}}$	$\alpha \times 10$	P.T.	$\alpha \times 10$	P.T.
2	1.31	0.996						
3	3.68	0.988						
4	5.81	0.980						
5	7.30	0.975	3.27	0.989	1.56	$\bar{1}.27$		
6	8.62	0.971						
7	9.14	0.968					2.1	$\bar{1}.43$
8	10.2							
10			6.03	0.980	2.56	$\bar{1}.54$		
12							2.57	$\bar{1}.54$
15			7.75	0.973	3.21	$\bar{1}.67$		
17							3.14	$\bar{1}.66$
20			8.96	0.969	3.66	$\bar{1}.76$		
22							3.58	$\bar{1}.75$
25			10.1	0.965	4.10	$\bar{1}.84$		
27							3.91	$\bar{1}.81$
30			11.1	0.961	4.47	$\bar{1}.91$		
32							4.24	$\bar{1}.87$
35					4.92	$\bar{1}.99$		
37							4.56	$\bar{1}.92$
40					5.31	0.05		
42							4.90	$\bar{1}.98$
45					5.70	0.12		
47							5.21	0.04
50					6.13	0.20		
52							5.54	0.09
55					6.53	0.27		
57							5.84	0.15
60					6.96	0.36		
62							6.17	0.21
65					7.39	0.45		
67							6.45	0.26
70					7.84	0.56		
75					8.27	0.68		
77							7.09	0.39
80					8.67	0.81		
85					9.03	0.97		
87							7.71	0.53
90					9.29	1.12		
95							8.29	0.69
107							8.88	0.90

Table 27 Rate Constants for System I $KMnO_4/NiO$

Run	$1/T^\circ$ A x 10^3	$k_{(1-\alpha)^{\frac{1}{3}}} \times 10^3$	$k_x \times 10$	$k_2 \times 10^2$
I1	2.097	4.8	2.60	
I2	2.120	2.7	3.75	
I3	2.271	0.21	0.61	
I4	2.066	7.56	3.75	
I5	2.056		4.5	1.4
I6	2.035		5.0	1.6
I7	2.203	0.69		

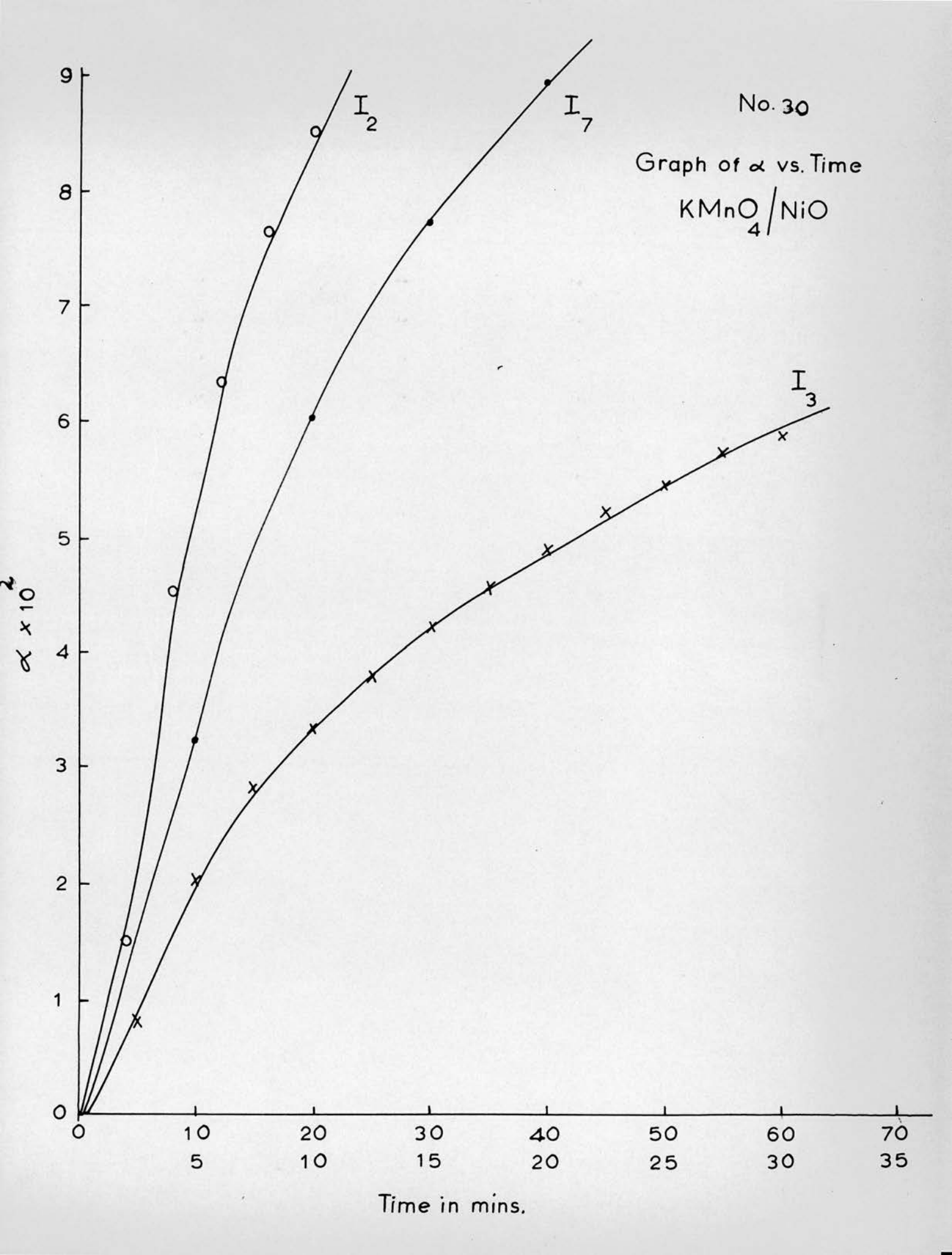
No. 30
Graph of α vs. Time
KMnO4/NiO
I2
I7
I3
α x 10²
0
1
2
3
4
5
6
7
8
9
0
10
5
20
10
30
15
40
20
50
25
60
30
70
35
Time in mins.

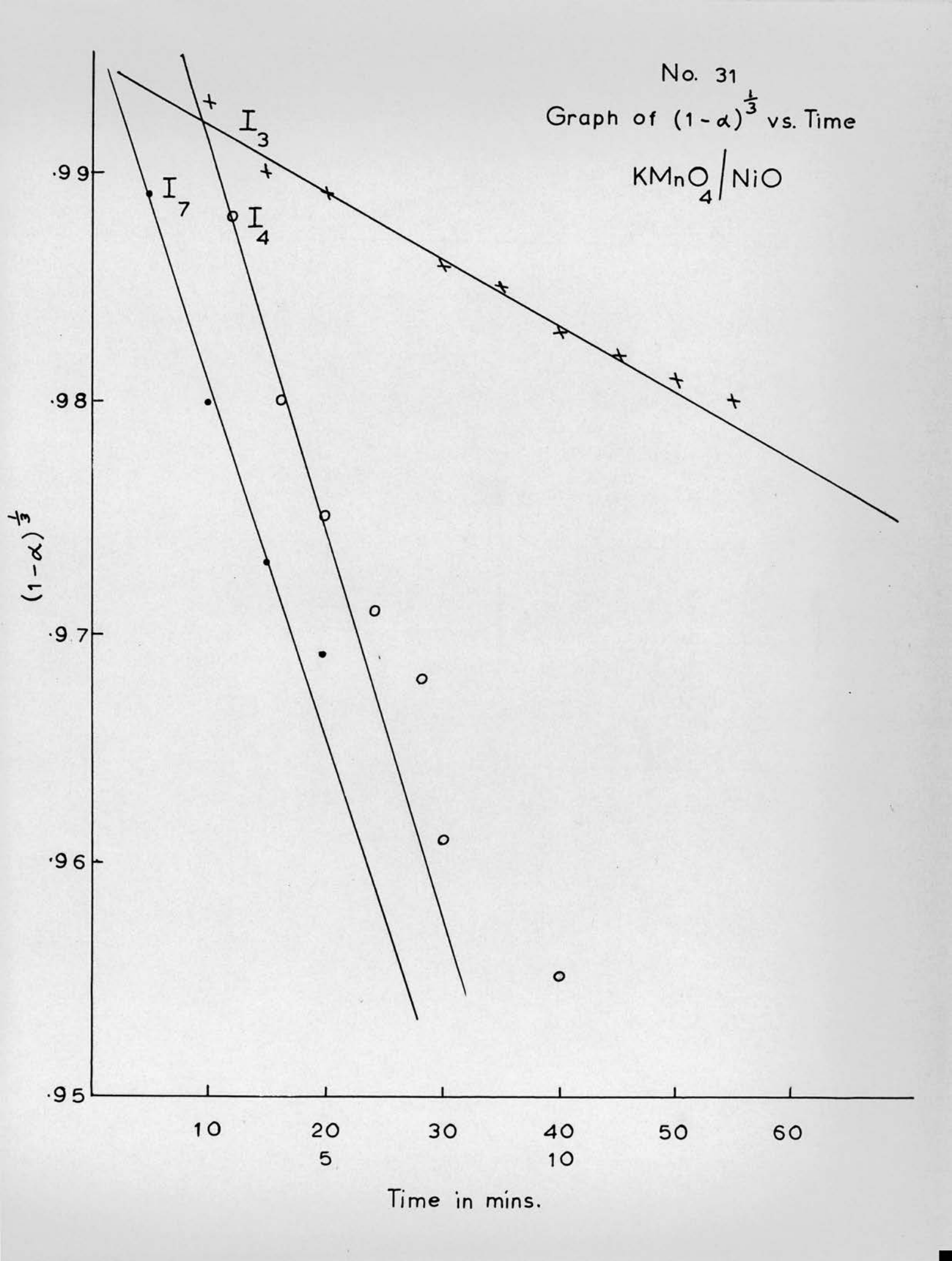
No. 31
Graph of $(1-\alpha)^{\frac{1}{3}}$ vs. Time
$KMnO_4$ / NiO
I_3
I_7
I_4
.99
.98
.97
.96
.95
$(1-\alpha)^{\frac{1}{3}}$
10
20
30
40
50
60
5
10
Time in mins.

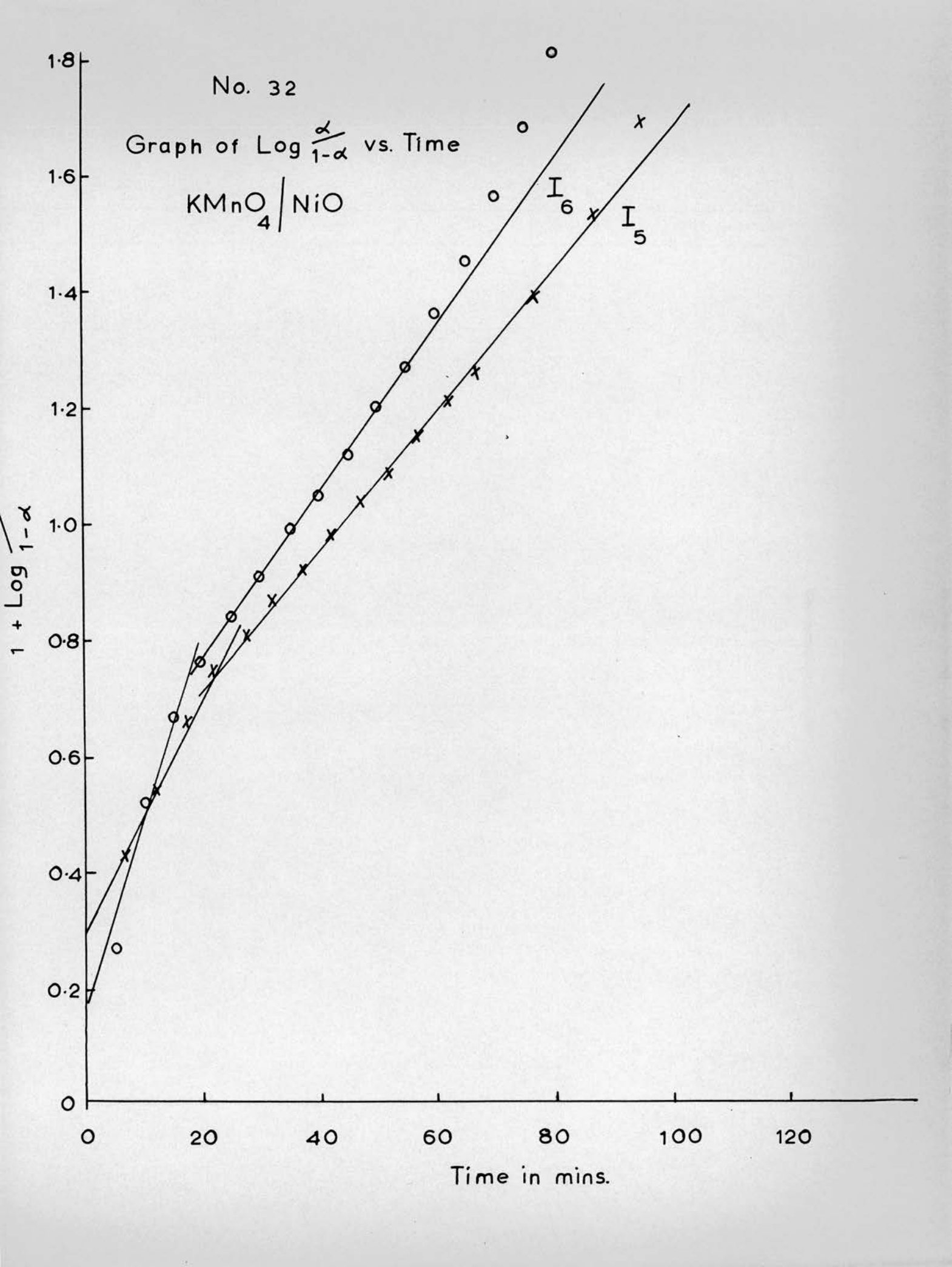
No. 32
Graph of Log α/1-α vs. Time
KMnO4 / NiO
I6
I5
1·8
1·6
1·4
1·2
1·0
0·8
0·6
0·4
0·2
0
1 + Log α/1-α
0
20
40
60
80
100
120
Time in mins.

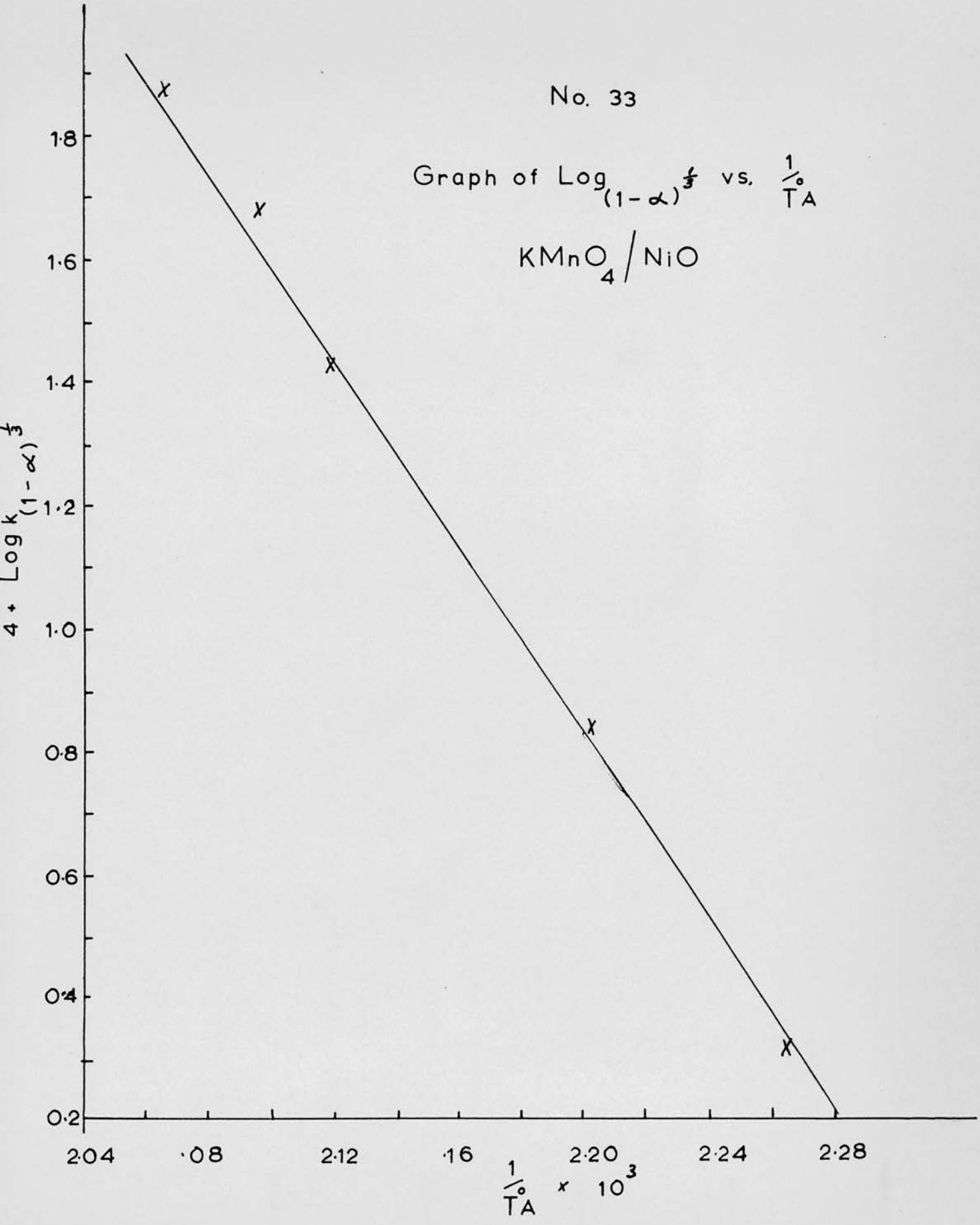
No. 33
Graph of $\text{Log}_{(1-\alpha)^{\frac{1}{3}}}$ vs. $\frac{1}{T_A^\circ}$
$KMnO_4 / NiO$
$4 + \text{Log}\, k_{(1-\alpha)^{\frac{1}{3}}}$
1·8
1·6
1·4
1·2
1·0
0·8
0·6
0·4
0·2
2·04
·08
2·12
·16
2·20
2·24
2·28
$\frac{1}{T_A^\circ} \times 10^3$

2.5.9. Kinetics for the decomposition for potassium permanganate/nickel oxide (1000°) (J) and nickel oxide + 1 mole % lithium oxide (K).

Tables 28, 29, 30 and 31 and graphs 34, 35, 36 and 37 illustrate the effect of adding nickel oxide (1000°) and nickel oxide + 1 mole % lithium oxide. The main features in this case are that the traces show an initial sigmoid section to $\alpha = 0.02$ followed by a smooth acceleration. They are best fitted in the region $\alpha = 0.02 - 0.1$ by the exponential law

$$\alpha = A \exp(kt)$$

The later stages of the decomposition are fitted by the Prout-Tompkins equation, two values of "k" being required.

Tables 28, 29 and 30	Analysis of system (J) and (K).
Table 31	Ratecconstants for systems (J) and (K).
Graph 34	Initial stage of the "α" - time curves.
Graph 35	Initial reaction, plot of $\log_{10}\alpha$ vs. Time.
Graph 36	Acceleration and decay stages; plot of $\log_{10} \alpha/1-\alpha$ vs. Time.
Graph 37	Arrhenius diagram for initial reaction, which gives an activation energy of E = 38±3 K. cals./mole.

Table 28 Systems J and K $KMnO_4/NiO$ (1000°) and $KMnO_4/NiO + Li_2O$

Run	J1		K1		J2		K2	
Temp	192.5°C		192.4°C		206.8°C		206.8°C	
Time Min	$\alpha \times 10^2$	$\log\alpha$	$\alpha \times 10^2$	$\log\alpha$	$\alpha \times 10^2$	$\log\alpha$	$\alpha \times 10^2$	$\log\alpha$
5	0.57	$\bar{3}.76$	0.13	$\bar{3}.10$	0.40	$\bar{3}.60$	0.58	$\bar{3}.77$
10	1.03	$\bar{2}.01$	0.24	$\bar{3}.38$	0.83	$\bar{3}.92$	1.23	$\bar{2}.09$
15	1.16	$\bar{2}.06$	0.29	$\bar{3}.46$	0.88	$\bar{3}.95$	1.59	$\bar{2}.20$
20	1.28	$\bar{2}.11$	0.32	$\bar{3}.50$	0.90	$\bar{3}.95$	2.02	$\bar{2}.30$
25	1.44	$\bar{2}.16$	0.45	$\bar{3}.65$	1.02	$\bar{2}.01$	2.47	$\bar{2}.39$
30	1.57	$\bar{2}.20$	0.54	$\bar{3}.73$	1.20	$\bar{2}.08$	3.15	$\bar{2}.50$
35	1.68	$\bar{2}.22$	0.62	$\bar{3}.79$	1.60	$\bar{2}.20$	4.16	$\bar{2}.62$
40	1.76	$\bar{2}.25$	0.76	$\bar{3}.88$	2.19	$\bar{2}.34$	5.48	$\bar{2}.74$
45	1.90	$\bar{2}.28$			3.04	$\bar{2}.48$	7.24	$\bar{2}.86$
50	2.0	$\bar{2}.30$	1.05	$\bar{2}.02$	4.22	$\bar{2}.63$	9.24	$\bar{2}.97$
55					6.20	$\bar{2}.79$	11.4	$\bar{2}.05$
60	2.19	$\bar{2}.34$	1.26	$\bar{2}.10$	8.84	$\bar{2}.95$		
70	2.48	$\bar{2}.40$	1.57	$\bar{2}.20$				
80	2.90	$\bar{2}.46$	1.91	$\bar{2}.28$				
90	3.37	$\bar{2}.53$	2.35	$\bar{2}.37$				
100	3.96	$\bar{2}.60$	2.83	$\bar{2}.45$				
110	4.66	$\bar{2}.67$	3.47	$\bar{2}.54$				
120	5.42	$\bar{2}.73$	4.10	$\bar{2}.61$				
130	6.38	$\bar{2}.80$	4.90	$\bar{2}.69$				
140	7.47	$\bar{2}.87$	5.74	$\bar{2}.76$				
150	8.64	$\bar{2}.94$	6.79	$\bar{2}.83$				
160	9.94	$\bar{2}.99$	7.90	$\bar{2}.90$				
170	11.3	$\bar{1}.05$	9.16	$\bar{2}.96$				
180			10.5	$\bar{1}.02$				
190			11.9	$\bar{1}.07$				

Table 29 System J and K $KMnO_4/NiO$ (1000°) and $KMnO_4/NiO + Li_2O$

Run	J3			K3		
Temp	212.8°C			212.8°C		
Time Min	$\alpha \times 10^2$	log α	P.T.	$\alpha \times 10^2$	log α	P.T.
5	0.41	$\bar{3}.61$		0.56	$\bar{3}.75$	
10	0.79	$\bar{3}.89$		0.73	$\bar{3}.86$	
15	0.95	$\bar{3}.98$		0.87	$\bar{3}.94$	
20	1.16	$\bar{2}.06$		1.26	$\bar{2}.10$	
25	1.72	$\bar{2}.24$		2.20	$\bar{2}.34$	
30	2.82	$\bar{2}.45$		3.96	$\bar{2}.60$	
35	6.02	$\bar{2}.78$		6.81	$\bar{2}.83$	
40	15.2	$\bar{1}.18$		10.9	$\bar{1}.04$	
50	38.9		1.80	27.7		$\bar{1}.58$
60	56.3		0.11	43.4		$\bar{1}.88$
70	70.2		0.37	55.5		0.09
80	80.9		0.63	65.5		0.28
90	89.5		0.93	75.6		0.49
100	95.6		1.34	84.4		0.73
110	98.8		1.90	92.5		1.09
120				97.5		1.59
130				99.2		

Table 30 System J and K $KMnO_4/NiO$ (1000°) and $KMnO_4/NiO + li_2O$

Run	J4			K4	
Temp..	208.4°C			208.4°C	
Time Min.	x 10^2	log	P.T.	x 10^2	log
5	0.27	$\bar{3}.42$		0.34	$\bar{3}.53$
10	0.32	$\bar{3}.51$		0.37	$\bar{3}.57$
15	0.32			0.37	
20	0.32			0.48	$\bar{3}.68$
25	0.32			0.63	$\bar{3}.80$
30	0.44	$\bar{3}.65$		0.94	$\bar{3}.97$
35	0.63	$\bar{3}.80$		1.72	$\bar{2}.23$
40	1.09	$\bar{2}.04$		3.23	$\bar{2}.51$
45	2.21	$\bar{2}.34$		5.69	$\bar{2}.76$
50	4.38	$\bar{2}.64$		8.74	$\bar{2}.94$
55	7.59	$\bar{2}.88$		14.1	$\bar{1}.15$
60	14.2	$\bar{1}.15$			
70	31.5		$\bar{1}.66$		
80	45.9		$\bar{1}.93$		
90	57.5		0.13		
100	67.1		0.31		
110	75.4		0.49		
120	82.2		0.66		
130	87.7		0.85		
140	92.9		1.11		
150	96.5		1.43		
160	98.9				

Table 31 Rate Constants for Systems J and K $KMnO_4/NiO$ (1000°) and $KMnO_4/NiO + Li_2O$

Run	$1/T°A \times 10^3$	$k_{log} \times 10^2$	$k_x \times 10^2$	$k_2 \times 10^2$
J1	2.148	0.71	1.16	
K1	2.148	0.84	0.97	
J2	2.084	2.72	2.75	
K2	2.084	2.40	3.43	
J3	2.059	4.20	3.22	2.07
K3	2.059	6.45	3.59	1.65
J4	2.077	5.62	2.11	1.80
K4	2.077	5.16	2.54	
J5	2.044	5.60	1.41	
K5	2.044	6.05	1.54	

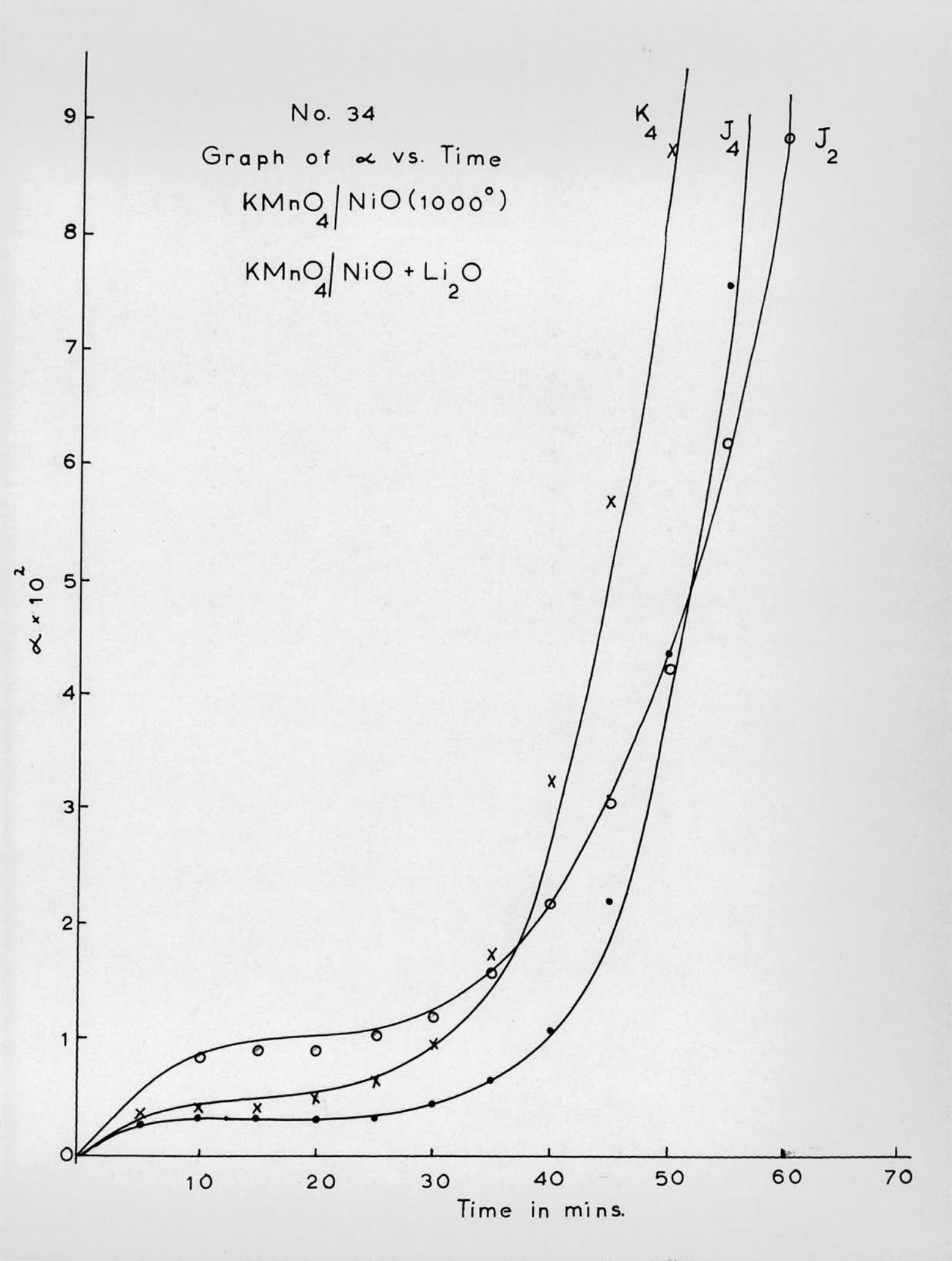
No. 34
Graph of ∝ vs. Time
KMnO4 / NiO (1000°)
KMnO4 / NiO + Li2O
K4
J4
J2
∝ x 10²
Time in mins.
0
1
2
3
4
5
6
7
8
9
10
20
30
40
50
60
70

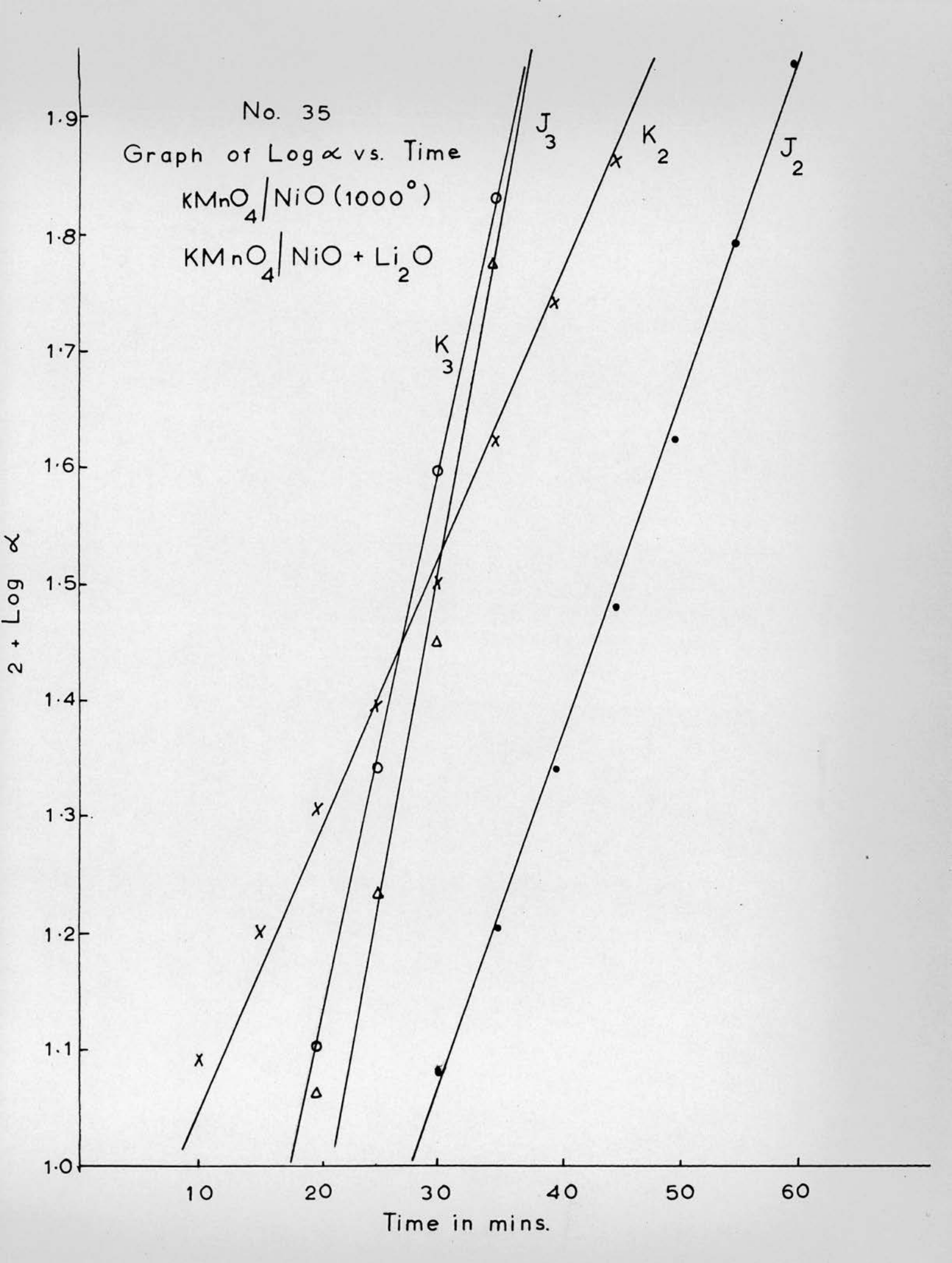
No. 35
Graph of Log α vs. Time
KMnO4/NiO (1000°)
KMnO4/NiO + Li2O
J3
K2
J2
K3
2 + Log α
1·9
1·8
1·7
1·6
1·5
1·4
1·3
1·2
1·1
1·0
10
20
30
40
50
60
Time in mins.

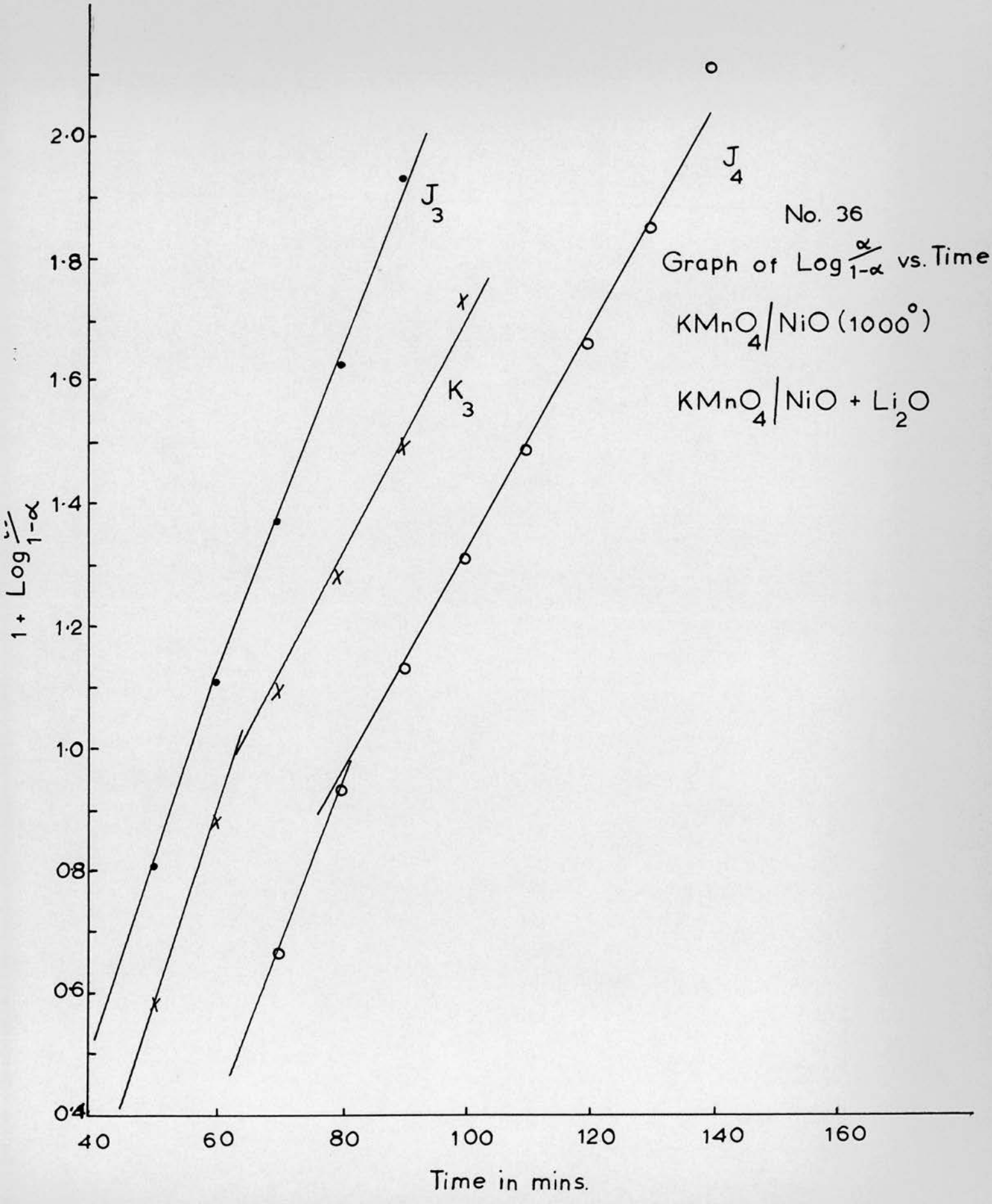
No. 36
Graph of Log α/1-α vs. Time
KMnO4/NiO (1000°)
KMnO4/NiO + Li2O
J3
J4
K3
1 + Log α/1-α
Time in mins.
2·0
1·8
1·6
1·4
1·2
1·0
08
06
04
40
60
80
100
120
140
160

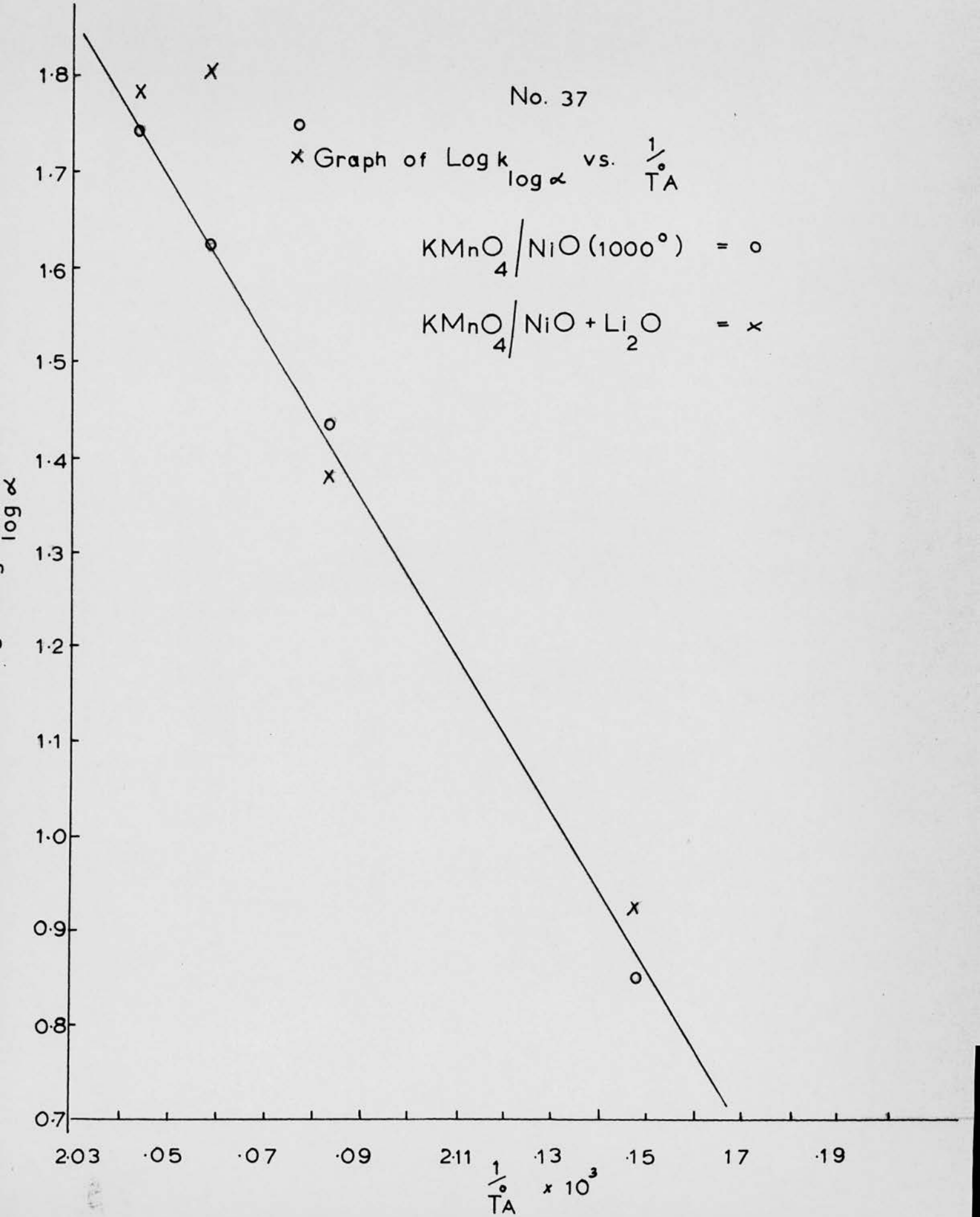
No. 37
o
× Graph of Log k log α vs. 1/T°A
KMnO4 / NiO (1000°) = o
KMnO4 / NiO + Li2O = ×
log α
1·8
1·7
1·6
1·5
1·4
1·3
1·2
1·1
1·0
0·9
0·8
0·7
2·03
·05
·07
·09
2·11
·13
·15
17
·19
1/T°A × 10³

2.5.10. Kinetics for the decomposition for potassium permanganate/10 - 80% nickel oxide (L)

Tables 32, 33, 34, 35 and 36 and graphs 38, 39, 40, 41 and 42 illustrate the effect of adding various proportions of nickel oxide. The decomposition commences at maximum rate and the traces are deceleratory throughout. They are best fitted in the region $\alpha = 0 - 0.1$ by the contracting sphere expression

$$= 1 - \left[c - k\ (t - t_o)\right]^3$$

The later stages of the reaction are fitted by the Prout-Tompkins equation, two values of "k" being required.

Tables 32, 33, 34 and 35	Analysis of system (L).
Table 36	Rate constants for system (L).
Graph 38	Initial stage of the "α" - time curves.
Graph 39	Initial reaction, plot of $(1 - \alpha)^{\frac{1}{3}}$ vs. Time.
Graph 40	Acceleration and decay stages; plot of $\log_{10} \alpha/1 - \alpha$ vs. Time.
Graph 41	Plot of initial reaction rates vs. % nickel oxide.
Graph 42	Plot of Prout-Tompkins reaction rates vs. % nickel oxide.

Table 32 System L $KMnO_4$/ (10 - 80%) NiO

Run	L1			L2		
Temp	188.1°C			188.1°C		
Time Min	$\alpha \times 10^2$	$(1-\alpha)^{\frac{1}{3}}$	P.T.	$\alpha \times 10^2$	$(1-\alpha)^{\frac{1}{3}}$	P.T.
5	0.69	0.998	$\bar{3}.84$	1.13	0.996	$\bar{2}.06$
10	1.14	0.996		2.26	0.992	
15	1.45	0.995	$\bar{2}.17$	2.82	0.991	$\bar{2}.46$
20	1.81	0.994		3.35	0.989	
25	2.10	0.993	$\bar{2}.33$	3.88	0.987	$\bar{2}.61$
30	2.40	0.992		4.35	0.985	
35	2.71	0.991	$\bar{2}.45$	4.82	0.984	$\bar{2}.70$
40	3.07	0.990	2.50	4.28	0.982	2.75
45	3.36	0.989		5.72	0.981	
50	3.67	0.988	$\bar{2}.58$	6.15	0.979	$\bar{2}.82$
55	3.98	0.987		6.57	0.977	
60	4.35	0.985		6.94	0.976	
65	4.83	0.984		7.40	0.975	$\bar{2}.90$
70	5.06	0.983	$\bar{2}.73$	7.75	0.973	$\bar{2}.92$
75	5.37	0.982		8.18		$\bar{2}.95$
80	5.76	0.980	$\bar{2}.79$	8.57		2.97
85	6.12	0.98				
90				9.32		$\bar{1}.01$
97	7.42		$\bar{2}.90$			
100				10.0		$\bar{1}.05$
107	7.77		$\bar{2}.93$			
110				10.7		$\bar{1}.08$
117	8.49		$\bar{2}.97$			
120				11.4		$\bar{1}.11$
127	9.19		$\bar{1}.00$			
130				11.9		$\bar{1}.13$
140				12.5		1.16
147	10.6		$\bar{1}.07$			
167	11.9		$\bar{1}.13$			
187	12.0		1.13			
200				15.8		$\bar{1}.27$
207	13.5		$\bar{1}.19$			
260				22.3		$\bar{1}.46$
267	19.7		$\bar{1}.39$			
320				28.5		$\bar{1}.60$
327	26.4		$\bar{1}.55$			
380				36.4		$\bar{1}.76$
387	34.2		$\bar{1}.72$			
440				44.9		$\bar{1}.91$
447	43.4		$\bar{1}.88$			
500				54.0		0.07
507	52.9		0.05			
560				63.5		0.24
567	64.8		0.26			
620				70.5		0.38
627	72.6		0.42			
680				76.3		0.51
687	79.2		0.58			
740				81.7		0.65
747	84.4		0.73			
800				86.0		0.79
807	89.4		0.93			
860				90.3		1.07
867	93.4		1.15			
920				94.1		1.20
980				97.1		1.52

Table 33 System L $KMnO_4$/(10 - 80%) NiO

Run		L3			L4	
Temp		188.1°C			188.1°C	
Time Min	$\alpha \times 10^2$	$(1-\alpha)^{\frac{1}{3}}$	P.T.	$\alpha \times 10^2$	$(1-\alpha)^{\frac{1}{3}}$	P.T.
2	0.23					
4	3.29	0.989	$\bar{2}.53$	1.77	0.994	$\bar{2}.26$
6	4.88	0.984		3.41	0.989	
8	5.76	0.980	$\bar{2}.78$	4.55	0.985	$\bar{2}.68$
10	6.39	0.978		5.33	0.982	
12	7.02	0.976	$\bar{2}.88$	6.04	0.980	$\bar{2}.81$
14	7.51	0.974		6.56	0.978	
16	7.98	0.973	$\bar{2}.94$	7.08	0.976	$\bar{2}.88$
18	8.45	0.971		7.60	0.974	
20	8.90	0.969	$\bar{2}.990$	8.01	0.972	$\bar{2}.94$
22	9.27	0.968		8.48	0.971	
24	9.64	0.967	$\bar{1}.03$	8.93	0.969	$\bar{2}.99$
26	10.0	0.965		9.34	0.968	
28	10.4		$\bar{1}.06$	9.73	0.966	$\bar{1}.03$
30	10.7			10.1	0.965	
32	11.0		$\bar{1}.09$	10.5	0.964	$\bar{1}.07$
34	11.3			10.8	0.963	
36	11.5			11.1		
40	12.1		$\bar{1}.14$	11.7		$\bar{1}.12$
60	14.4		$\bar{1}.22$	15.1		$\bar{1}.25$
80	17.5		$\bar{1}.33$	18.2		$\bar{1}.35$
100	20.3		$\bar{1}.41$	21.3		$\bar{1}.43$
160	28.0		$\bar{1}.59$	28.2		$\bar{1}.59$
220	34.5		$\bar{1}.72$	34.0		$\bar{1}.71$
280	41.7		$\bar{1}.85$	40.0		$\bar{1}.82$
340	48.6		1.98	45.7		1.92
400	55.3		0.09	51.8		0.03
460	61.2		0.20	57.9		0.14
520	67.0		0.31	63.9		0.25
580	72.2		0.41	69.7		0.36
640	76.8		0.52	74.4		0.46
700	79.9		0.60	79.1		0.58
760	83.6		0.71	82.9		0.68
820	87.3		0.84	86.9		0.82
880	90.8		0.99	90.6		0.98
940	93.5		1.16	93.5		1.16
1000	96.1		1.39	96.7		1.47
1060				98.2		1.74

Table 34 System L $KMnO_4$/(10 - 80%) NiO

Run	L5			L6		
Temp	188.1°C			188.1°C		
Time Min	$\alpha \times 10^2$	$(1-\alpha)^{\frac{1}{3}}$	P.T.	$\alpha \times 10^2$	$(1-\alpha)^{\frac{1}{3}}$	P.T.
1				0.15	0.999	
2	0.45			0.18	0.999	
3				3.38	0.988	
4	3.30	0.989		6.12	0.79	
5				8.57	0.971	$\bar{2}.97$
6	6.22	0.981		10.3	0.965	
7				11.3	0.961	
8	7.87	0.973		12.7	0.956	
10	9.11	0.969	$\bar{1}.00$	13.5		$\bar{1}.19$
12	10.2	0.965		14.4		
14	11.0	0.962				
16	11.8	0.959				
18	12.5	0.957				
20	13.1	0.954	$\bar{1}.18$			
33				24.1		$\bar{1}.50$
40	18.7		$\bar{1}.36$			
53				28.8		$\bar{1}.61$
60	24.1		$\bar{1}.50$			
73				34.1		$\bar{1}.71$
93				37.2		$\bar{1}.77$
120	35.1		$\bar{1}.73$			
153				47.1		$\bar{1}.95$
180	42.7		$\bar{1}.87$			
213				51.5		0.03
240	49.2		1.99			
273				55.9		0.10
300	54.7		0.08			
333				60.3		0.18
360	60.1		0.18			
393				64.3		0.26
420	64.9		0.27			
453				68.2		0.33
480	69.0		0.35			
513				71.5		0.40
540	73.2		0.44			
573				75.0		0.48
600	76.9		0.52			
633				78.6		0.57
660	80.8		0.62			
693				81.8		0.65
720	84.0		0.72			
753				85.7		0.78
780	86.7		0.81			
813				88.9		0.90
840	89.6		0.94			
873				92.9		1.11
900	92.1		1.07			
933				95.9		1.36
960	94.7		1.25			
993				98.2		
1020	96.7					
1080	98.5					

Table 35 System L $KMnO_4$/(10 - 80%) NiO

Run	L7			L8		
Temp	188.1°C			188.1°C		
Time Min	$\alpha \times 10^2$	$(1-\alpha)^{\frac{1}{3}}$	P.T.	$\alpha \times 10^2$	$(1-\alpha)^{\frac{1}{3}}$	P.T.
1	0.20	0.999				
2	5.97	0.80		0.32	0.999	
3	16.3	0.943	$\bar{1}$.29	3.95	0.987	
4				7.38	0.975	
5				9.82	0.966	$\bar{1}$.04
6				11.9	0.959	
7				13.0	0.954	
13	37.2		$\bar{1}$.77			
20				21.3		$\bar{1}$.43
23	40.6		$\bar{1}$.83			
30				26.0		$\bar{1}$.54
33	46.4		$\bar{1}$.94			
40				29.1		$\bar{1}$.61
43	49.5		$\bar{1}$.99			
50				32.7		$\bar{1}$.69
53	51.3		0.02			
60				34.8		$\bar{1}$.73
63	53.8		0.07			
70				37.1		$\bar{1}$.77
73	54.9		0.09			
80				39.0		$\bar{1}$.81
83	57.5		0.13			
90				41.1		$\bar{1}$.84
93	58.9		0.16			
100				42.8		$\bar{1}$.87
103	59.4		0.16			
160				49.0		$\bar{1}$.98
163	64.2		0.25			
220				53.6		0.06
223	67.9		0.32			
280				57.8		0.14
283	70.2		0.37			
340				60.5		0.19
343	72.9		0.43			
400				65.2		0.27
403	74.7		0.47			
460				69.2		0.39
463	77.4		0.53			
520				73.4		0.44
523	79.1		0.58			
580				78.1		0.55
583	81.1		0.67			
640				81.2		0.64
643	83.7		0.71			
700				85.2		0.76
703	86.0		0.79			
760				87.8		0.85
763.	88.4		0.88			
820				91.4		1.02
823	89.9		0.95			
880				93.9		1.19
883	91.6		1.04			
940				95.8		
1000				97.5		

Table 36 Rate Constants for System L $KMnO_4$/(10-80%) NiO

Run	% NiO	$1/T^{\circ}$ A x 10^3	$k_{(1-\alpha)^{\frac{1}{3}}}$ x 10^3	k_x x 10	k_1 x 10^3	k_2 x 10^3
L1	10	2.169	0.2	0.26	2.7	2.75
L2	20	2.169	0.35	0.60	2.6	2.44
L3	30	2.169	0.91	2.58	2.12	1.79
L4	40	2.169	1.0	1.87	1.82	1.82
L5	50	2.169	4.2	2.73	2.1	1.46
L6	60	2.169	10.0	3.57	3.04	1.23
L7	70	2.169	28.3	6.0	3.33	0.82
L8	80	2.169	10.0	3.75	3.96	1.19

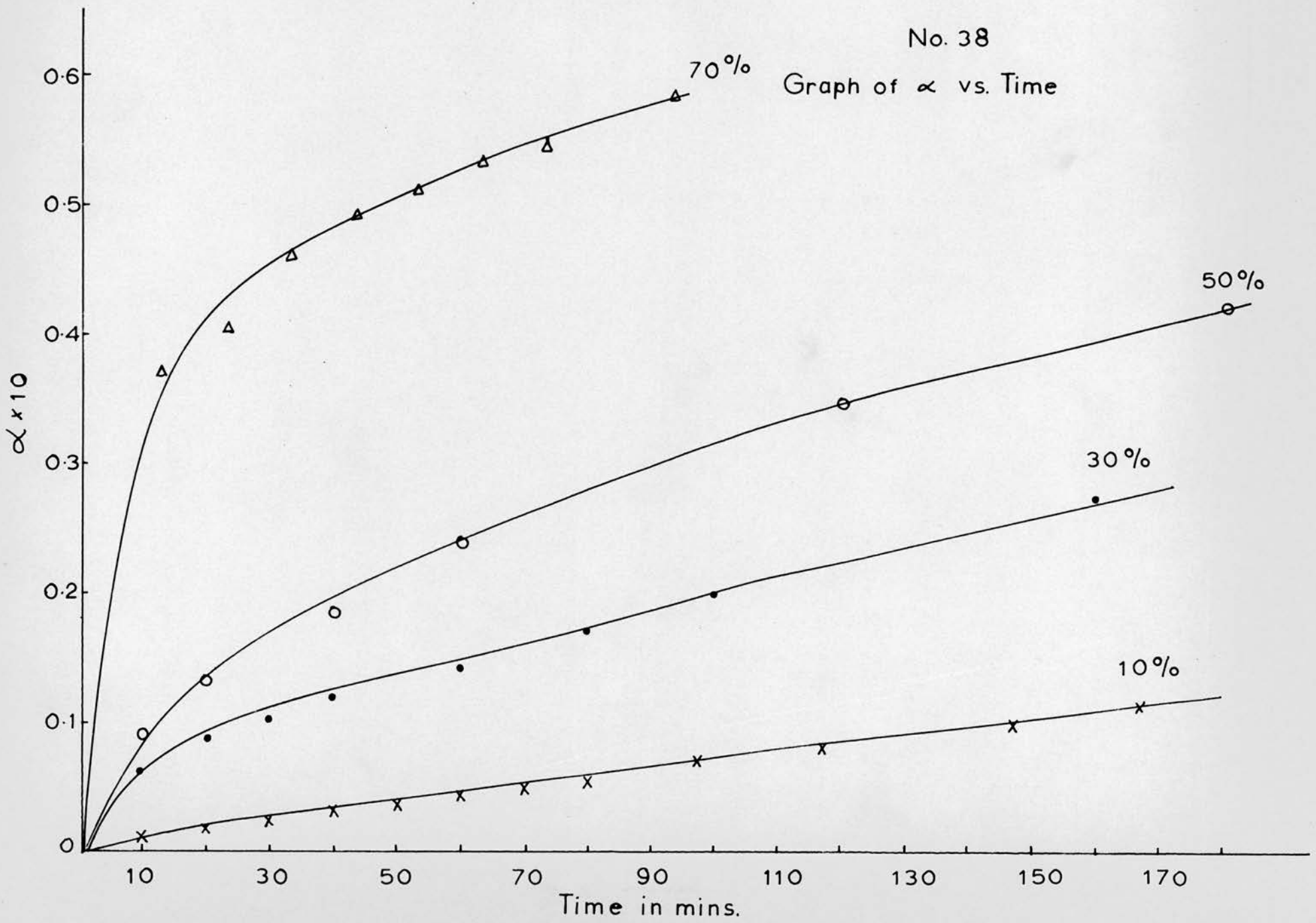
No. 38
Graph of ∝ vs. Time
70%
50%
30%
10%
0·6
0·5
0·4
0·3
0·2
0·1
0
∝ x 10
10
30
50
70
90
110
130
150
170
Time in mins.

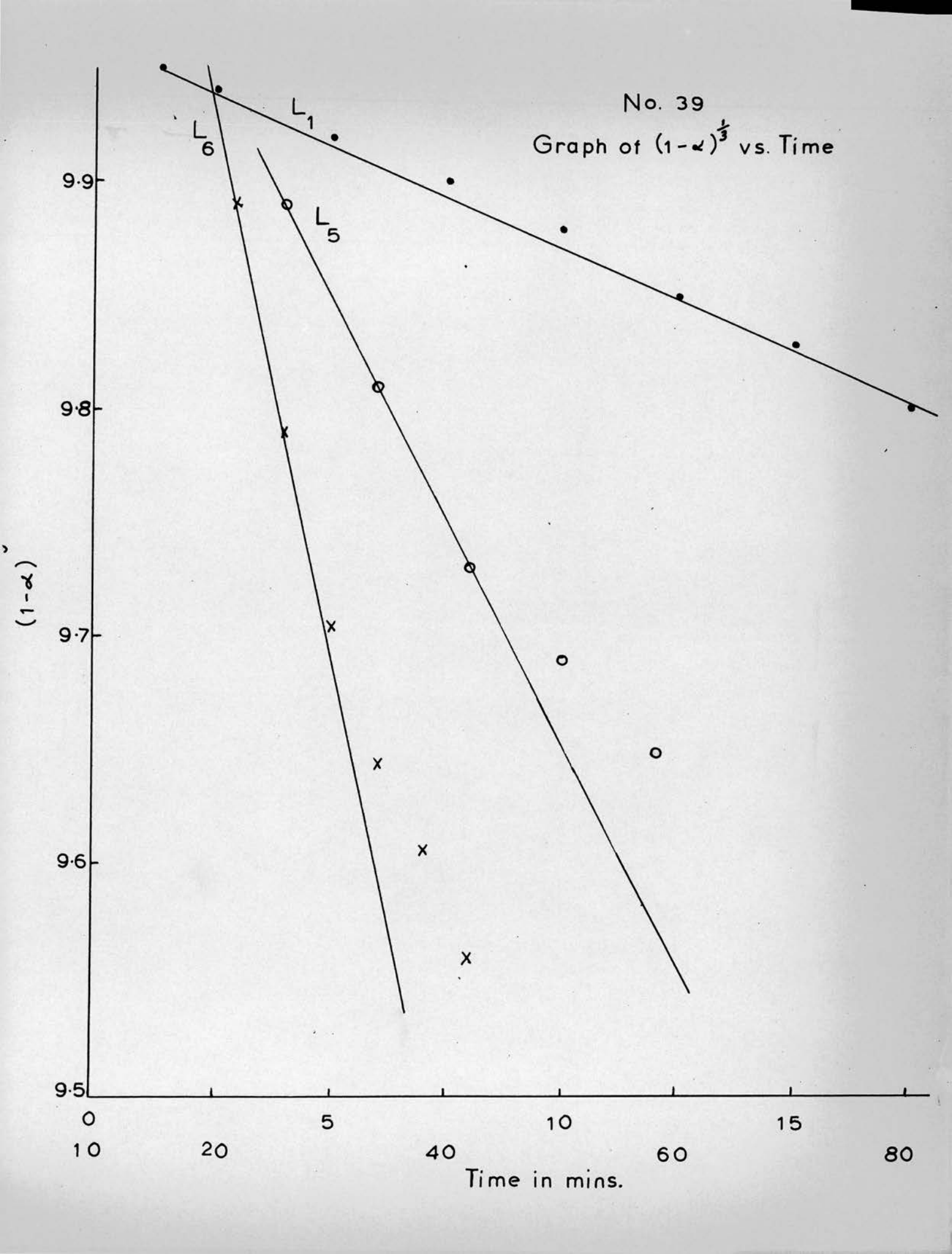
No. 39
Graph of $(1-\alpha)^{\frac{1}{3}}$ vs. Time
L_1
L_5
L_6
9·9
9·8
9·7
9·6
9·5
$(1-\alpha)$
0
5
10
15
10
20
40
60
80
Time in mins.

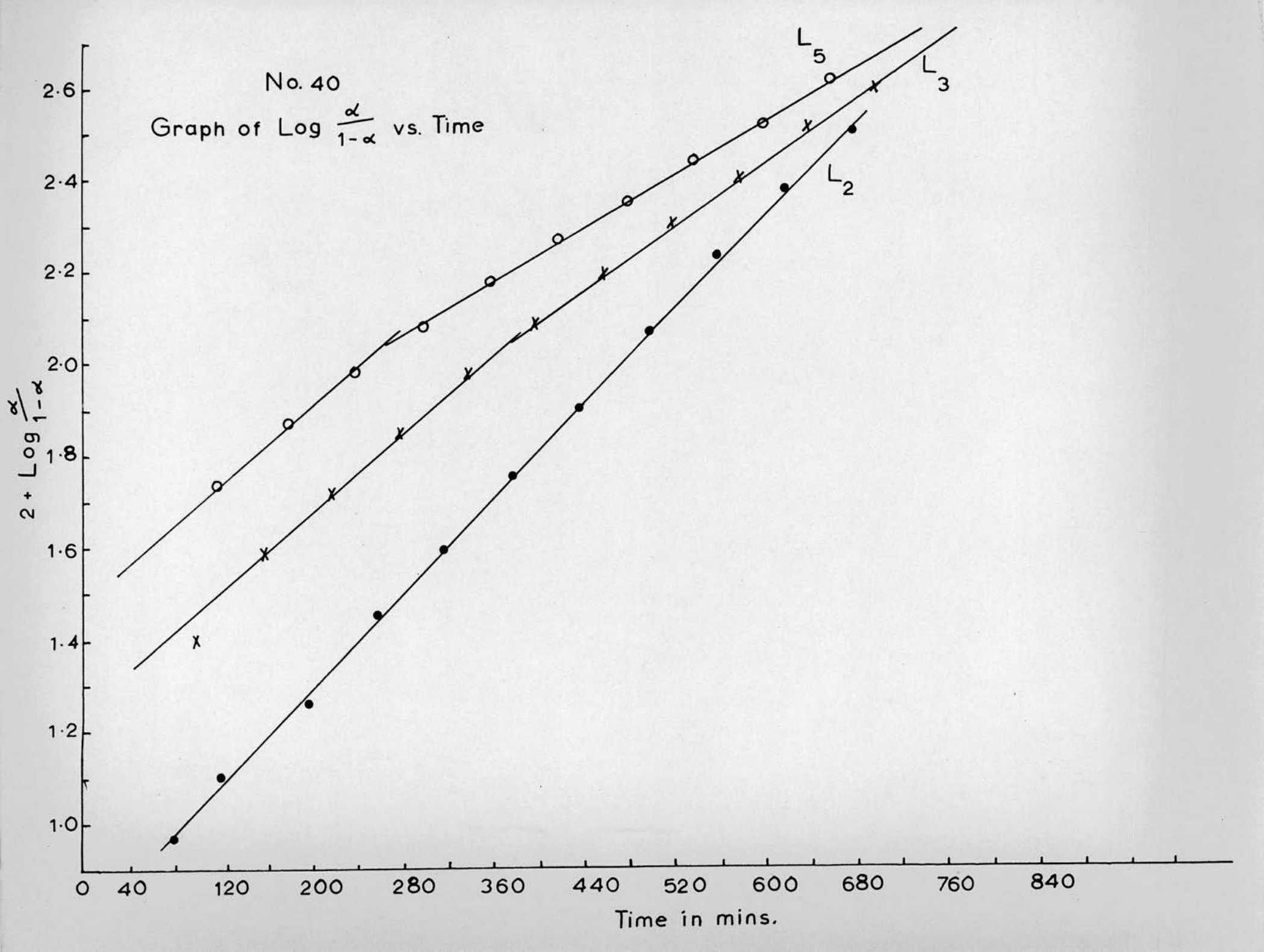
No. 40
Graph of Log $\frac{\alpha}{1-\alpha}$ vs. Time
L_5
L_3
L_2
2·6
2·4
2·2
2·0
1·8
1·6
1·4
1·2
1·0
$2 + \text{Log}\frac{\alpha}{1-\alpha}$
0
40
120
200
280
360
440
520
600
680
760
840
Time in mins.

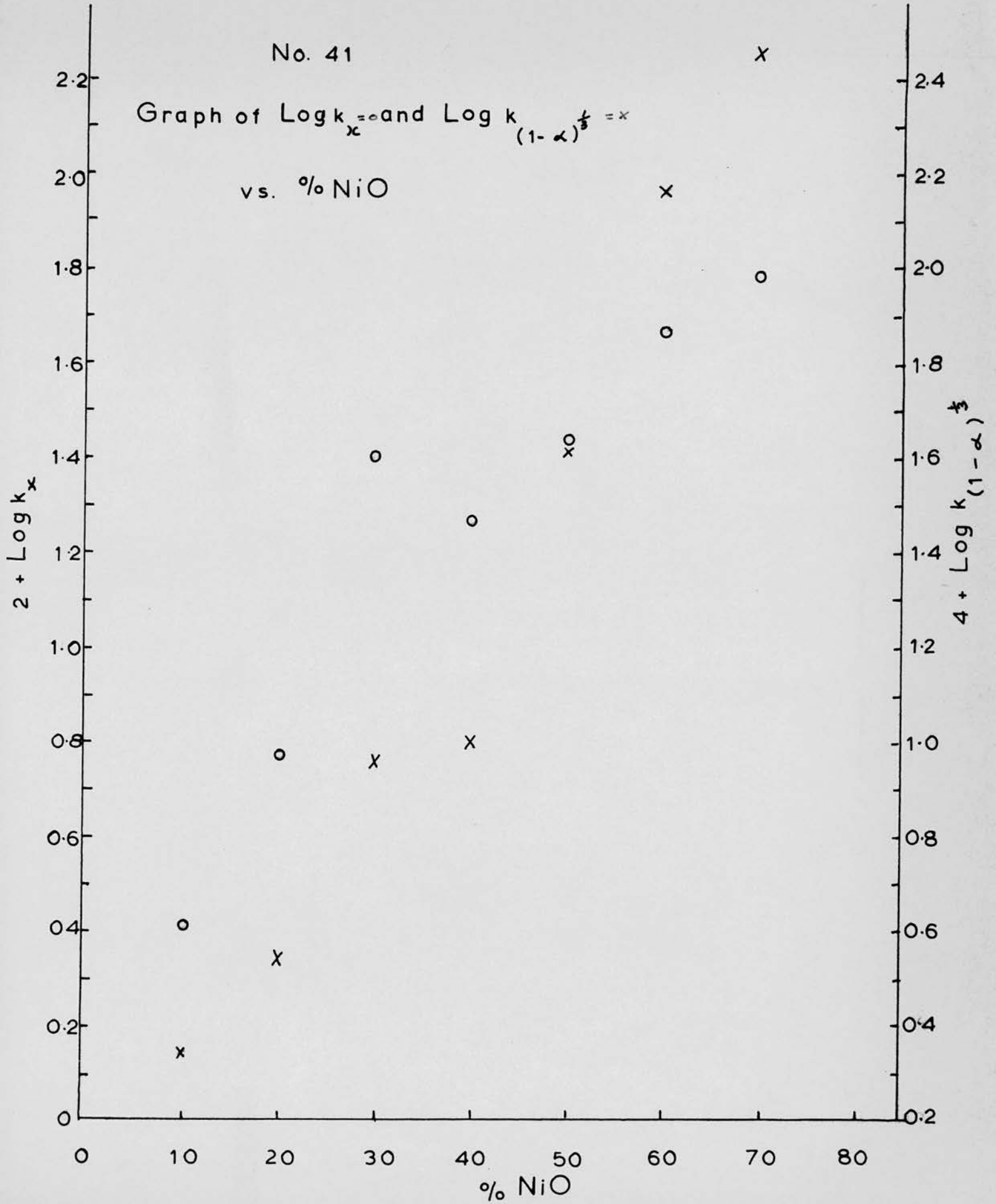
No. 41
Graph of Log $k_{x=o}$ and Log $k_{(1-\alpha)^{\frac{1}{3}}=x}$
vs. % NiO
2 + Log k_x
4 + Log $k_{(1-\alpha)^{\frac{1}{3}}}$
% NiO
0
10
20
30
40
50
60
70
80
0
0.2
0.4
0.6
0.8
1.0
1.2
1.4
1.6
1.8
2.0
2.2
2.4

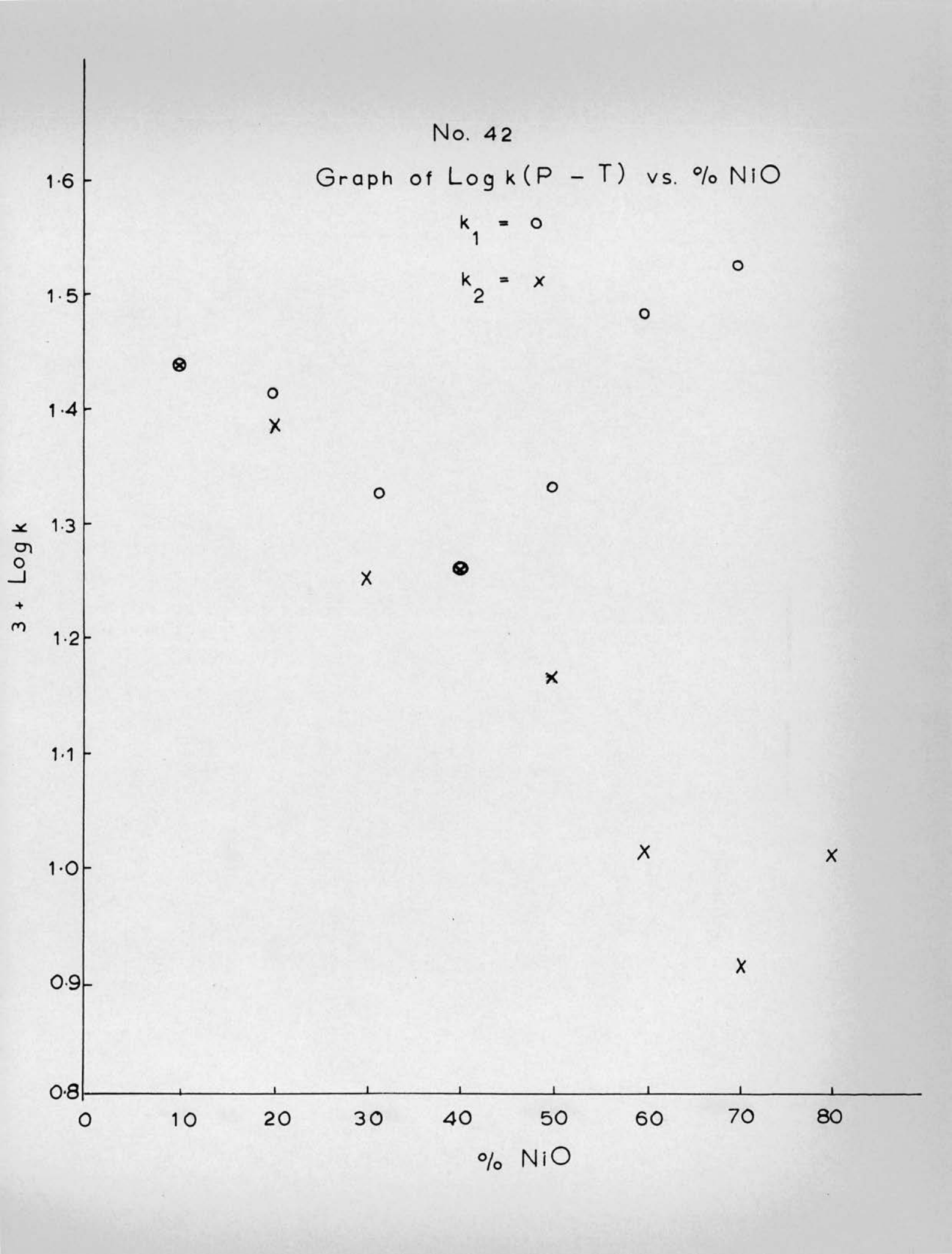
No. 42
Graph of Log k(P – T) vs. % NiO
k_1 = o
k_2 = x
1·6
1·5
1·4
1·3
1·2
1·1
1·0
0·9
0·8
3 + Log k
0
10
20
30
40
50
60
70
80
% NiO

2.5.11. Kinetics for the decomposition for powder samples

Table 37 and graph 43 illustrate the results obtained, from a series of runs at a fixed temperature, using uncompressed powder moxtures of potassium permanganate and oxide. The main features are that all the systems with the exception of potassium permanganate/nickel oxide show catalysis and the enhanced activity of potassium permanganate/ferric oxide system relative to the others.

Table 37 Analysis of powder runs.

Graph 43 Initial stage of the "α" - time curves.

Table 37 Analysis of Runs using powdered samples

Run	$KMnO_4$	$KMnO_4/NiO$	$KMnO_4/Fe_2O_3$	$KMnO_4/Al_2O_3$	$KMnO_4/CuO$	$KMnO_4/ZnO$
Time	$\alpha \times 10^2$	$\alpha \times 10^2$	$\alpha \times 10^2$	$\alpha \times 10^2$	$\alpha \times 10^2$	$\alpha \times 10^2$
2			1.70			
4			4.72			
5				0.8	1.0	0.6
6			7.23			
8			8.86			
10			10.2	1.64	1.79	1.31
12			11.3			
14			12.3			
15				2.29	2.40	1.88
20	1.41	1.40		3.00	2.96	2.49
25				3.70	3.62	3.11
30				4.50	4.26	3.74
35				5.35	4.91	4.33
40	2.66	2.72		6.16	5.58	5.08
45				7.04	6.19	5.79
50				7.91	6.90	6.49
55				8.68	7.54	7.16
60	3.28	3.30		9.42	8.15	7.81
65				10.2	8.77	
70				10.8	9.40	9.31
75				11.5		
80	4.69	4.80				10.5
100	5.94	6.00				12.5

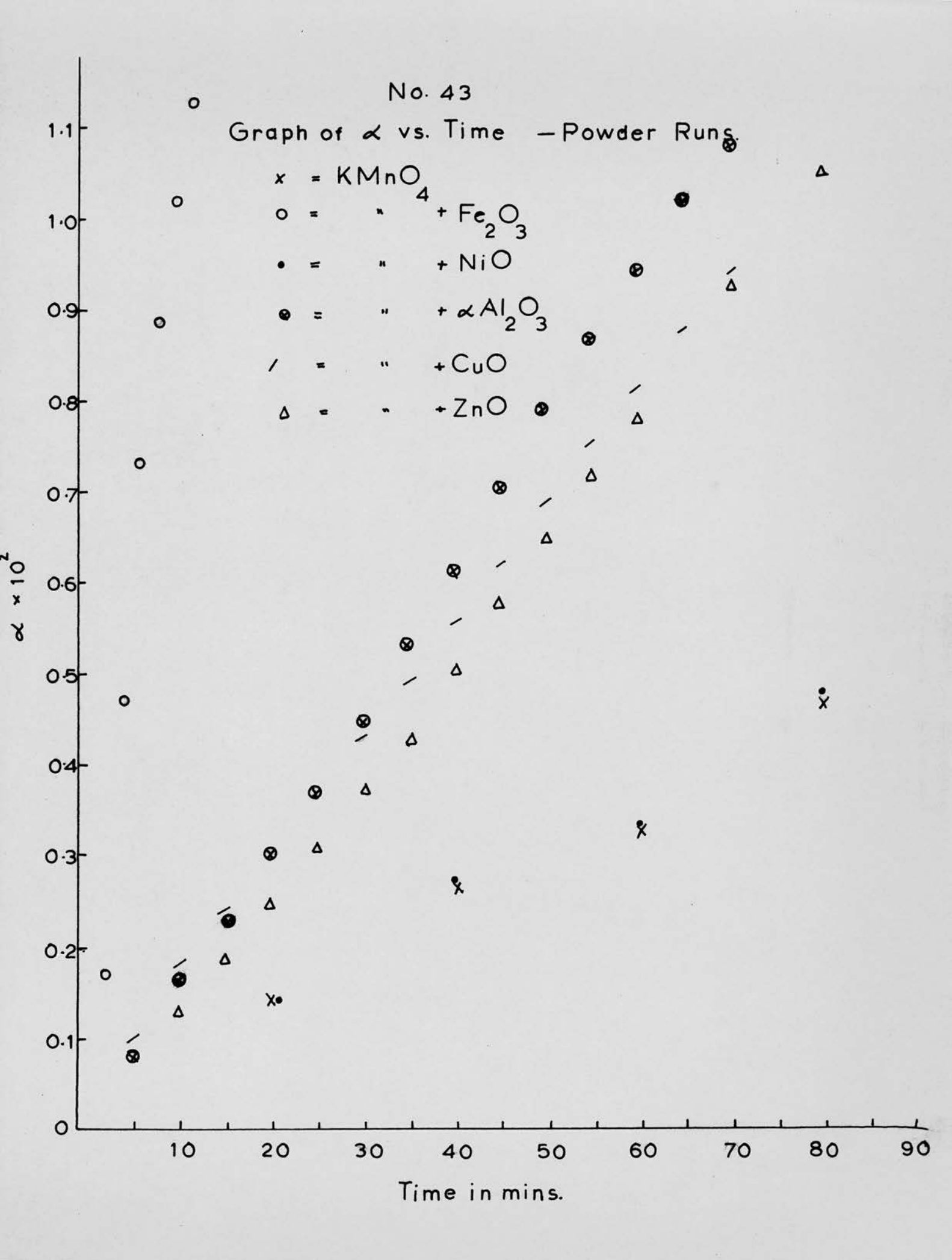
No. 43
Graph of α vs. Time — Powder Runs.
x = KMnO4
o = " + Fe2O3
• = " + NiO
⊗ = " + αAl2O3
/ = " + CuO
Δ = " + ZnO
α × 10²
0
0·1
0·2
0·3
0·4
0·5
0·6
0·7
0·8
0·9
1·0
1·1
10
20
30
40
50
60
70
80
90
Time in mins.

Table 38 Activation energies for the initial decomposition k cals/mole

System	Analysis used					
	$\alpha^{\frac{1}{3}}$	$\alpha^{\frac{1}{2}}$	α	$\log_{10}(1-\alpha)$	$\log_{10}\alpha$	$(1-\alpha)^{\frac{1}{3}}$
$KMnO_4$	37±2					
$KMnO_4/\alpha\text{-}Al_2O_3$		38±2				
$KMnO_4/MnO_2$		34±4				
$KMnO_4/CuO$				40±4		
$KMnO_4/Fe_2O_3$				38±3		
$KMnO_4/ZnO$			36±3			
$KMnO_4/Zno$ (1000°)		43±5				
$KMnO_4/ZnO + Cr_2O_3$		43±5				
$KMnO_4/NiO$						35±3
$KMnO_4/Nio$ (1000°)					38±3	
$KMnO_4/NiO + Li_2O$					38±3	

2.5.12. Kinetics for the system potassium permanganate/silica - alumina

The effect of a silica-alumina cracking catalyst, containing 13% alumina, on the decomposition of potassium permanganate was studied as in section 2, the catalyst in this case was first heated for four hours at 300°C. The preparation of the sample was carried out, however, as far as possible, in a "dry box" over P_2O_5 and the pellet was stored in this box.

Graph 43A illustrates a typical example of the results obtained; the initial fast oxygen evolution was finished within approximately one minute of the sample reaching the furnace temperature and corresponded to approximately 3% decomposition. Thereafter the behaviour was similar to that for pure permanganate, in graph 43Aa, the scales have been expanded to show more clearly the initial decomposition. This initial decomposition may therefore be associated with the Lewis and Bronsted sites present in silica/alumina catalysts. If this is the case such sites must be gradually neutralised or destroyed at room temperature since storage of the permanganate/silica-alumina pellet, for three days in the dry box, eliminated this fast initial decomposition.

There are two possible mechanisms by which Lewis and Bronsted sites could affect the initial decomposition of permanganate. The first concerns the Lewis sites which could be regarded as a sink or trap for the electrons removed from the permanganate ion, assuming the decomposition occurs by the mechanism proposed by Smirnova. The Bronsted sites, on the other hand, could facilitate the decomposition by an entirely different mechanism; but one similar to that proposed for the decomposition of the perchlorates: here the Bronsted site would act as a proton donor thus forming the intermediate $HMnO_4$ which then decomposes presumably at a faster rate.

No. 43A

Graph of α vs. Time – $KMnO_4/SiO_2 - Al_2O_3$

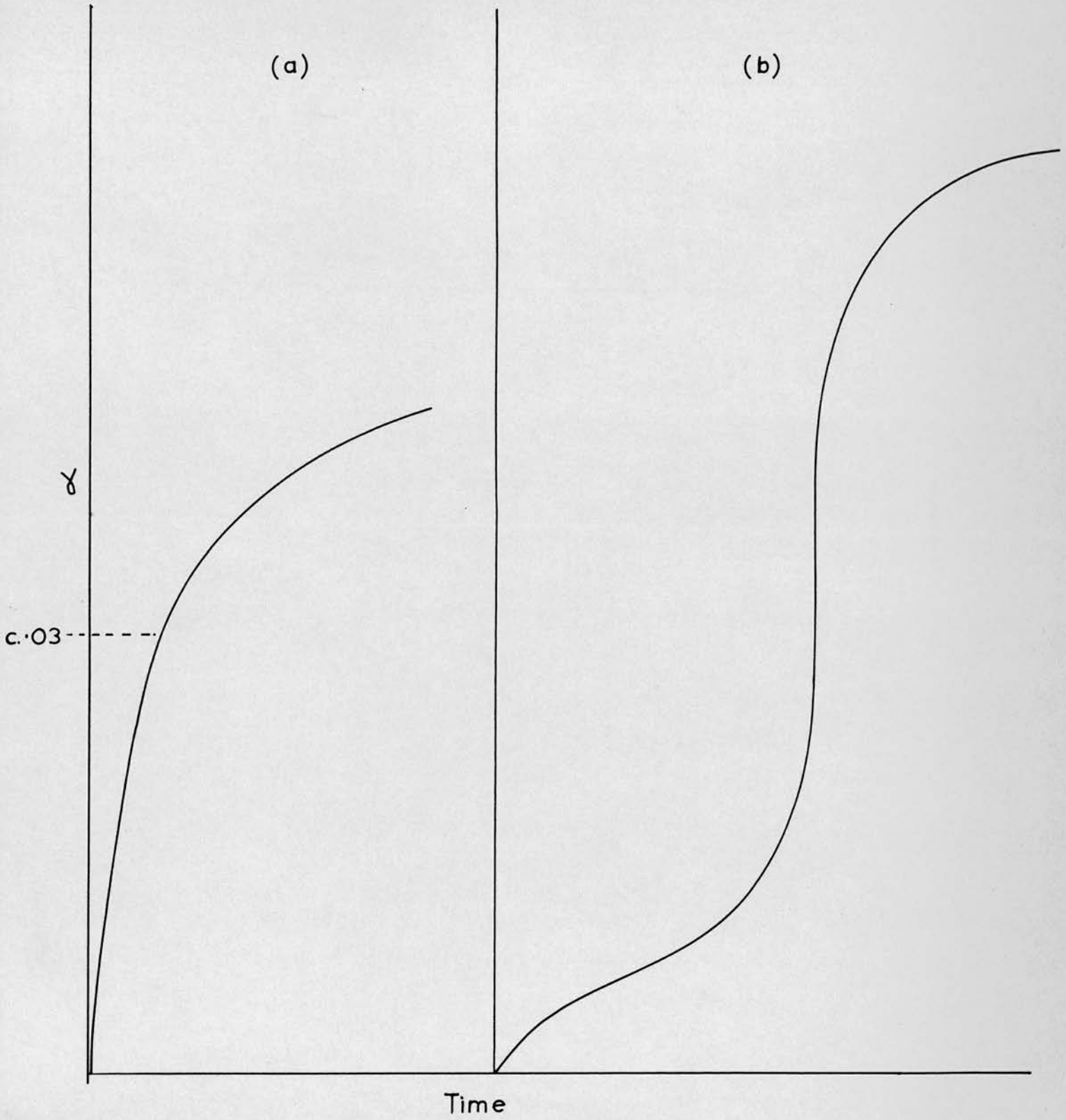

3. Electrical Conductivity Measurements

This section is primarily concerned with measuring the change in electrical conductivity of the various systems during the decomposition of the potassium permanganate. It was hoped that these results, in conjunction with the studies using doped nickel and zinc oxide, would allow some insight into the mechanism of the decomposition.

3.1 Apparatus

The apparatus used was basically the same as in section 2.1. The winch, at the top of the reaction vessel was replaced by a B24 cone through which were sealed two tungsten leads. These leads were used to connect the conductivity cell to the electrical circuit shown in fig. 3A. The voltage drop across the precision resistors was measured on an E.I.L. Vibron Electrometer model 33B. This circuit measured resistances from $10^{13}\Omega$ to $10^{7}\Omega$ When the resistance dropped below the last figure it was measured directly on a Model 8 Avometer. The conductivity cell is shown in fig. 3B, the overall size being kept to a minimum, to reduce the heat capacity. It consists essentially of a screwing device, made of brass, which ensures a good contact between the electrodes and the "pellet sample" surface. The lower electrode consisted of a piece of platinum foil insulated from the cell by means of a thin plate of vitreous silica. The upper electrode was basically a "pyrex glass plunger" the stem of which was plated with platinum and which could just slip into the quartz sleeve S. The sample sat inside this sleeve on the platinum electrode and by tightening the screw the plunger was firmly pressed down on to the sample surface thus completing the circuit. The locking nut was then adjusted to maintain this position.

Fig. 3a

Electrical Circuit

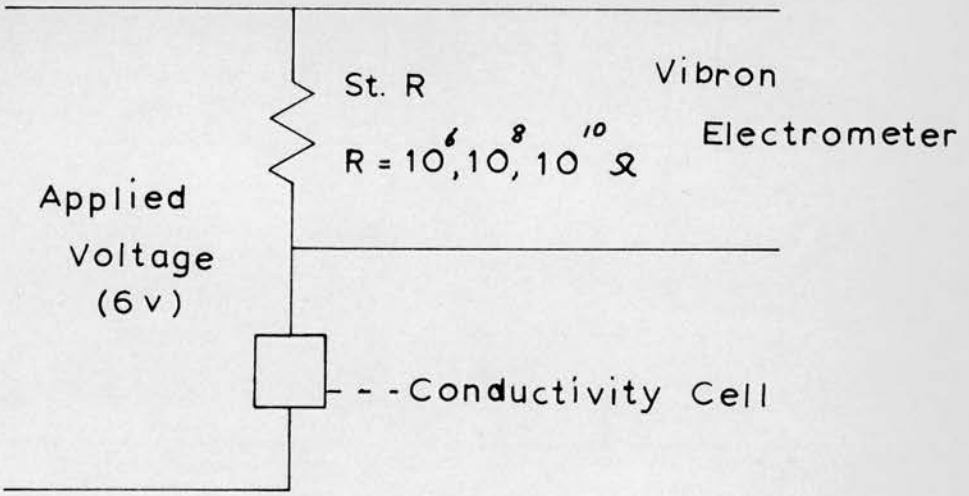

Fig. 3b

Conductivity Cell

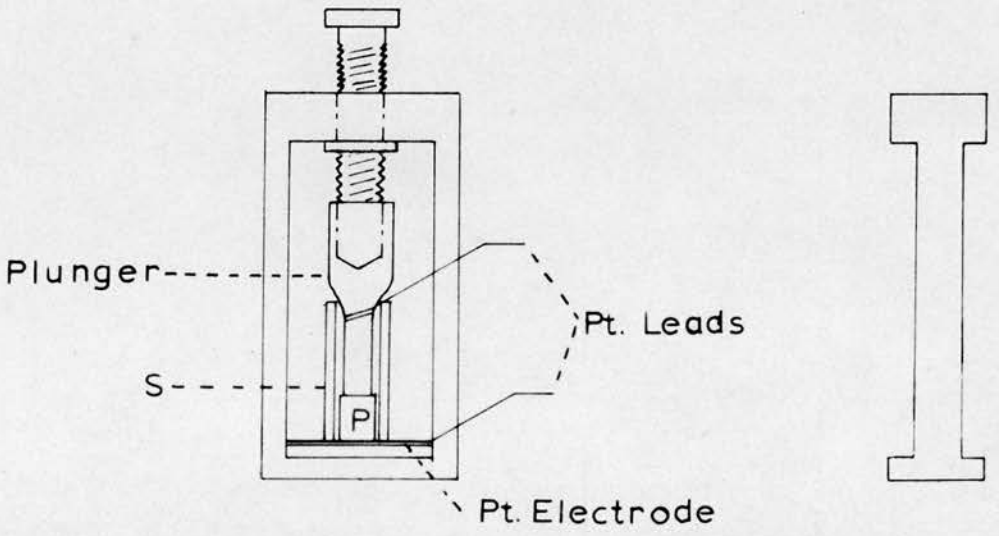

3.2 Procedure

As has already been stated it is necessary in conductivity measurements to use pellet samples, as this ensures that the spurious electrical effects due to poor contact between the individual particles[49] are minimised. The pellets were made in exactly the same manner as described in section 2.3.

Small pieces of such pellets, approx. 20 mg., were loaded into the conductivity cell and the electrodes assembled. The cell was then lowered to the foot of the reaction vessel and the whole system evacuated overnight.

The heating procedure adopted was designed to enable a study of the temperature dependence of the conductivity to be made and also to minimise the effect of the "heating up" period of the cell. The furnace temperature was therefore gradually raised from room temperature to the working temperature at which it was stabilised. While this was being carried out the resistance of the sample was measured at 10°C intervals.

Graph 44 shows a typical example of the results obtained for all the systems studied, with the exception of $KMnO_4$/NiO which will be dealt with in the appropriate sub-section. The plot breaks into two sections, the break occurring at approx. 130°C. The section 20 - 130°C gives an activation energy of 20±5 K. cals./mole which is much higher than would be expected if it was surface conduction. It would therefore appear to be ionic conductance although the energy value is slightly less than that normally associated with ionic conductance e.g. 30 k. cals as suggested by Jacobs and Tompkins for solid azides[50] and the alkali metal halides[51] but is similar to the figure reported by Simpson[52] for ammonium dichromate using a similar apparatus.

It was not possible to obtain an activation energy for the second

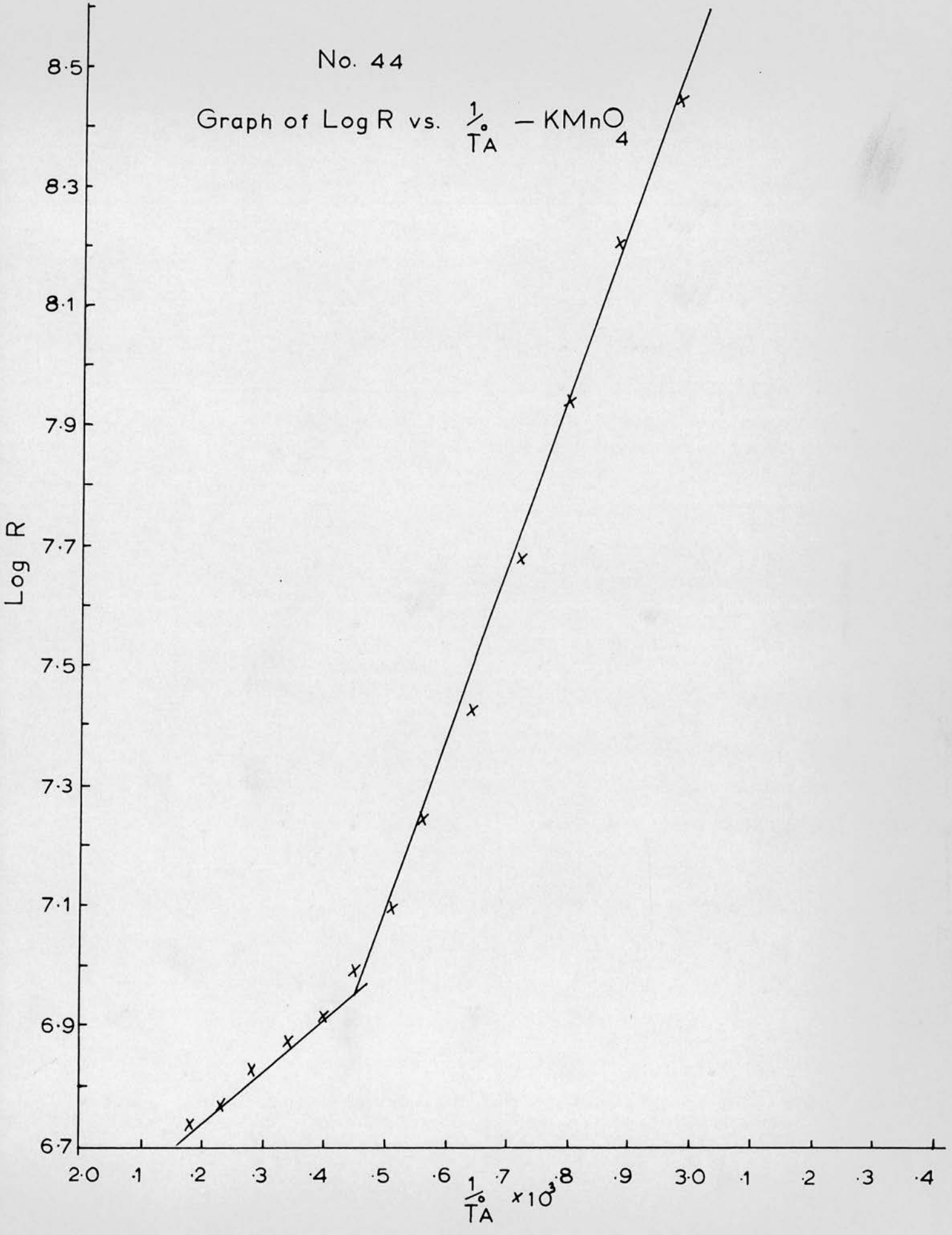
No. 44
Graph of Log R vs. 1/°TA — KMnO4
Log R
8·5
8·3
8·1
7·9
7·7
7·5
7·3
7·1
6·9
6·7
2·0
·1
·2
·3
·4
·5
·6
·7
·8
·9
3·0
·1
·2
·3
·4
1/°TA x 10³

section due to the scatter of results, even amongst the one system, which may infer that in this temperature region initial decomposition occurs and therefore the resistance measurements become to some extent time dependent.

On reaching the working temperature the resistance measurements were taken at fixed time intervals. Throughout the whole of the heating procedure the evolved oxygen pressure was continuously monitored using the Pirani gauge as in section 2.3. Thus a correlation between electrical resistance and fraction decomposed "α" was obtained.

In this section every run was studied to completion and "α" calculated from the final pressure.

3.3 Analysis of the Resistance Measurements

Such a procedure as outlined in section 3.2 cannot be used to determine specific conductivities, it can however be used to obtain a measure of the relative rate of change of conduction, since this is independent of the size of the sample and of the area of contact.

An exponential relationship was found to hold between the resistance and time. The exact range over which this was valid depended on the "system" being used. The slope of the graph $\log_{10}R$ vs Time therefore provided a convenient measure for the rate of change of conduction. By carrying out this procedure, therefore, over a temperature range, it was possible to obtain a value for the activation energy required for the production of the "charge carriers".

This procedure was carried out with the following systems

A* pure $KMnO_4$

B* $KMnO_4/\alpha Al_2O_3$

E* $KMnO_4/Fe_2O_3$

F* $KMnO_4/ZnO$

G* $KMnO_4/ZnO$ (1000^o)

H* $KMnO_4/ZnO$ + 1 mole % Cr_2O_3

I* $KMnO_4/NiO$

J* $KMnO_4/NiO$ (1000^o)

K* $KMnO_4/NiO$ + 1 mole % Li_2O

The following tables and graphs show the majority of the runs performed, at various temperatures in the range 177 - 212°C. The tables give the respective functions of "α" as required for the analysis used and the graphs show the plots of the different functions.

In addition to the abbreviations already listed the following have also been used - k_c = rate constant derived from the slope of the plot $\log_{10}R$ vs Time; log R = $\log_{10}$ of the resistance.

3.3.1. Resistance Measurements for pure Potassium Permanganate (A*)

Tables 39, 40, 41 and 42 and graphs 45, 46, 47 and 48 illustrate the change in resistance during the decomposition and also the fit of the Prout-Tompkins equation over the later stages of the reaction.

The most notable feature in the resistance measurements is that the exponential decrease holds to approx. $\alpha = 0.5$ after which they exhibit a minimum before rising slightly again, but there is little change after $\alpha = 0.6$.

The Prout-Tompkins equation holds over the region $\alpha = 0.1 - 0.9$, two values of k being required, one for the acceleratory stage, $\alpha = 0.1 - 0.5$, the other for the decay stage, $\alpha = 0.5 - 0.9$.

Tables 39, 40 and 41	Analysis of system A*.
Table 42	Rate constants for system A*.
Graph 45	Plot of $\log_{10} R$ vs. Time.
Graph 46	Plot of $\log_{10} \frac{\alpha}{1-\alpha}$ vs. Time.
Graph 47	Arrhenius plot for "rate of change of conduction" which gives an activation energy of $E_{c_1} = 27 \pm 2$ K. cals./mole. and $E_{c_2} = 38 \pm 2$ K. cals./mole.
Graph 48	Arrhenius plot for acceleratory and decay stages which gives an activation energy of $E_1 = 26 \pm 2$ K. cals./mole. and $E_2 = 28 \pm 2$ K. cals./mole.

Table 39 System A* pure $KMnO_4$

Run	A*4			A*5			A*2
Temp.	209.3°C			204.6°C			202.1°C
Time Min.	α x 10	P.T.	log R	α x 10	P.T.	log R	log R
5			6.60			6.25	5.94
10	0.10	$\bar{2}$.01	6.59			6.34	5.88
15			6.58			6.40	5.81
20	0.22	$\bar{2}$.34	6.40	0.11	$\bar{2}$.05	6.30	5.74
25			6.14			6.23	5.67
30	0.44	$\bar{2}$.67	5.92	0.20	$\bar{2}$.31	6.15	5.60
35			5.79			6.07	5.53
40	1.14	$\bar{1}$.11	5.74	0.30	$\bar{2}$.49	5.97	5.45
45			5.58			5.88	5.36
50	2.67	$\bar{1}$.56	5.36	0.46	$\bar{2}$.68	5.77	5.29
55			5.17			5.66	5.20
60	4.82	$\bar{1}$.97	5.03	0.89	$\bar{2}$.99	5.55	5.14
65						5.43	5.08
70	6.49	0.27	5.83	1.52	$\bar{1}$.25	5.32	4.98
75						5.21	4.87
80	7.58	0.49		2.50	$\bar{1}$.52	5.11	4.79
85							4.70
90	8.39	0.71	4.78	3.66	$\bar{1}$.76	4.89	4.63
95							4.56
100	8.89	0.90	4.81	4.72	$\bar{1}$.95	4.71	4.48
110	9.37	1.17	4.85	5.74	0.13	4.56	4.35
120	9.67	1.47	5.09	6.79	0.33	4.42	4.23
130	9.86	1.86	5.08	7.58	0.50	4.30	
140	9.91	2.03	5.04	8.21	0.66	4.20	
150				8.67	0.81	4.15	
170				9.34	1.41	4.04	
190				9.77		4.11	
210				9.98			
215						4.18	4.04
225						4.23	4.10
235						4.28	4.11
255						4.30	4.18

Table 40 System A* pure $KMnO_4$

Run	A*9			A*8			A*1
Temp.	213.1°C			192.6°C			200.1°C
Time Min.	α x 10	P.T.	log R	α x 10	P.T.	log R	log R
5			5.85			6.52	5.46
10	0.36	$\bar{2}$.57	5.69			6.48	5.40
15			5.54				5.32
20	0.75	$\bar{2}$.91	5.26				5.26
25			4.98				5.18
30	1.76	$\bar{1}$.33	4.74			6.40	5.11
32.5			4.66				
35			4.58			6.45	5.04
37.5			4.49				
40	4.10	$\bar{1}$.84	4.38			6.42	4.96
42.5			4.30				
45			4.16			6.46	4.88
47.5			4.08				
50	6.06	0.19	3.99			6.43	4.81
52.5			3.93				
55			3.89				4.70
57.5			3.85				
60	7.29	0.43	3.82			6.40	4.60
62.5			3.80				
65			3.78				4.49
67.5			3.77				
70	8.35	0.70	3.77			6.38	4.40
72.5			3.77				
75			3.78				4.30
80	9.19	1.05	3.80	0.17	$\bar{2}$.25	6.32	4.18
90	9.68	1.48	3.81			6.24	4.23
100	9.90		3.80	0.20	$\bar{2}$.31	6.18	3.89
110			3.79			6.09	3.76
120			3.76	0.28	$\bar{2}$.46	6.00	3.65
140			3.72	0.35	$\bar{2}$.56	5.81	3.54
160				0.56	$\bar{2}$.77	5.53	3.54
180				0.86	$\bar{2}$.97	5.31	3.60
200				1.36	$\bar{1}$.20	5.11	3.65
220				2.05	$\bar{1}$.41	4.92	
240				2.92	$\bar{1}$.61	4.77	
260				3.92	$\bar{1}$.81	4.63	
280				4.96	1.99	4.52	
300				5.92	0.16	4.43	
320				6.86	0.34		
340				7.39	0.45		
360				7.98	0.60	4.25	
380				8.38	0.71	4.25	
400				8.70	0.83	4.30	
420				9.00	0.95	4.32	
440				9.26	1.10	4.34	
460				9.49	1.27	4.38	

Table 41 System A* pure $KMnO_4$

Run	A*3			A*7	A*10			A*6
Temp.	185.6°C			189.9°C	199.6°C			203.2°C
Time Min.	α x 10	P.T.	log R	log R	α x 10	P.T.	log R	P.T.
5			5.93	8.03				
10			5.90	7.00				$\bar{2}.04$
15			5.88					
20			5.86		0.01		6.57	$\bar{2}.27$
25			5.84				6.54	
30			5.82	7.84			6.46	$\bar{2}.38$
35			5.81	7.80			6.42	
40			5.79	7.78	0.06		6.36	$\bar{2}.53$
45			5.77	7.75			6.32	
50			5.75	7.72			6.24	$\bar{2}.66$
55			5.72	7.70			6.18	
60			5.70	7.66	0.16	$\bar{2}.21$	6.26	$\bar{2}.80$
65			5.68					
70			5.66	7.62			6.00	$\bar{1}.02$
80				7.58	0.32	$\bar{2}.52$	5.80	$\bar{1}.31$
90				7.54			5.49	$\bar{1}.66$
100			5.56	7.53	0.86	$\bar{2}.97$	5.36	1.91
110				7.50			5.05	0.13
120	0.14	$\bar{2}.16$	5.47	7.48	2.17	$\bar{1}.44$	4.83	0.29
130			5.43		3.22	$\bar{1}.68$	4.65	0.42
140	0.18	$\bar{2}.27$	5.40		4.22	$\bar{1}.86$	4.53	0.55
150			5.35		5.22	0.04	4.43	0.68
160	0.24	$\bar{2}.39$			5.94	0.17	4.35	0.81
170			5.25		6.52	0.27	4.30	0.96
180	0.27	$\bar{2}.44$	5.19		7.06	0.38	4.28	1.12
190			5.14				4.28	1.39
200	0.34	$\bar{2}.54$	5.01		7.86	0.56	4.28	
220	0.43	$\bar{2}.66$	4.92		8.55	0.77	4.30	
240	0.55	$\bar{2}.77$	4.83		9.13	1.02	4.34	
260	0.74	$\bar{2}.92$	4.97		9.57	1.34	4.40	
280	1.08	$\bar{1}.08$	4.91					
300	1.50	$\bar{1}.24$	4.79					
340	2.95	$\bar{1}.62$	4.57					
380	4.82	$\bar{1}.97$						
420	6.39	0.25	4.11					
460	7.39	0.45	4.11					
500	8.07	0.62	4.11					
540	8.62	0.80						
580	9.07	0.99						
620	9.43	1.22						
660	9.69	1.49						

Table 42 Rate Constants for System A* $KMnO_4$

Run	$1/T^{\circ}A \times 10^3$	α- range	$k_{c_1} \times 10^2$	α- range	$k_{c_2} \times 10^2$	α- range	$k_1 \times 10^2$	α- range	$k_2 \times 10^2$
A*1	2.114	-	-	0-0.5	1.41	-	-	-	-
A*2	2.105	-	-	0-0.53	1.56	-	-	-	-
A*3	2.180	0-0.04	0.40	-	-	0.08-0.56	0.89	0.56-0.9	0.45
A*4	2.073	-	-	0.01-0.6	3.08	0.09-0.51	4.33	0.51-0.9	2.31
A*5	2.094	-	-	0.02-0.4	2.10	0.1 -0.4	2.77	0.4 -0.9	1.71
A*6	2.100	-	-	-	-	0.08-0.56	2.90	0.56-0.9	1.31
A*7	2.160	0-0.02	0.52	-	-	-	-	-	-
A*8	2.148	0.01-0.06	1.25	0.06-0.4	0.87	0.1 -0.57	1.02	0.57-0.9	0.62
A*9	2.057	-	-	0.15-0.6	4.22	0.1 -0.5	4.60	0.5 -0.9	2.73
A*10	2.116	0.0 -0.09	0.95	0.09-0.4	2.35	0.08-0.46	2.29	0.46-019	1.03

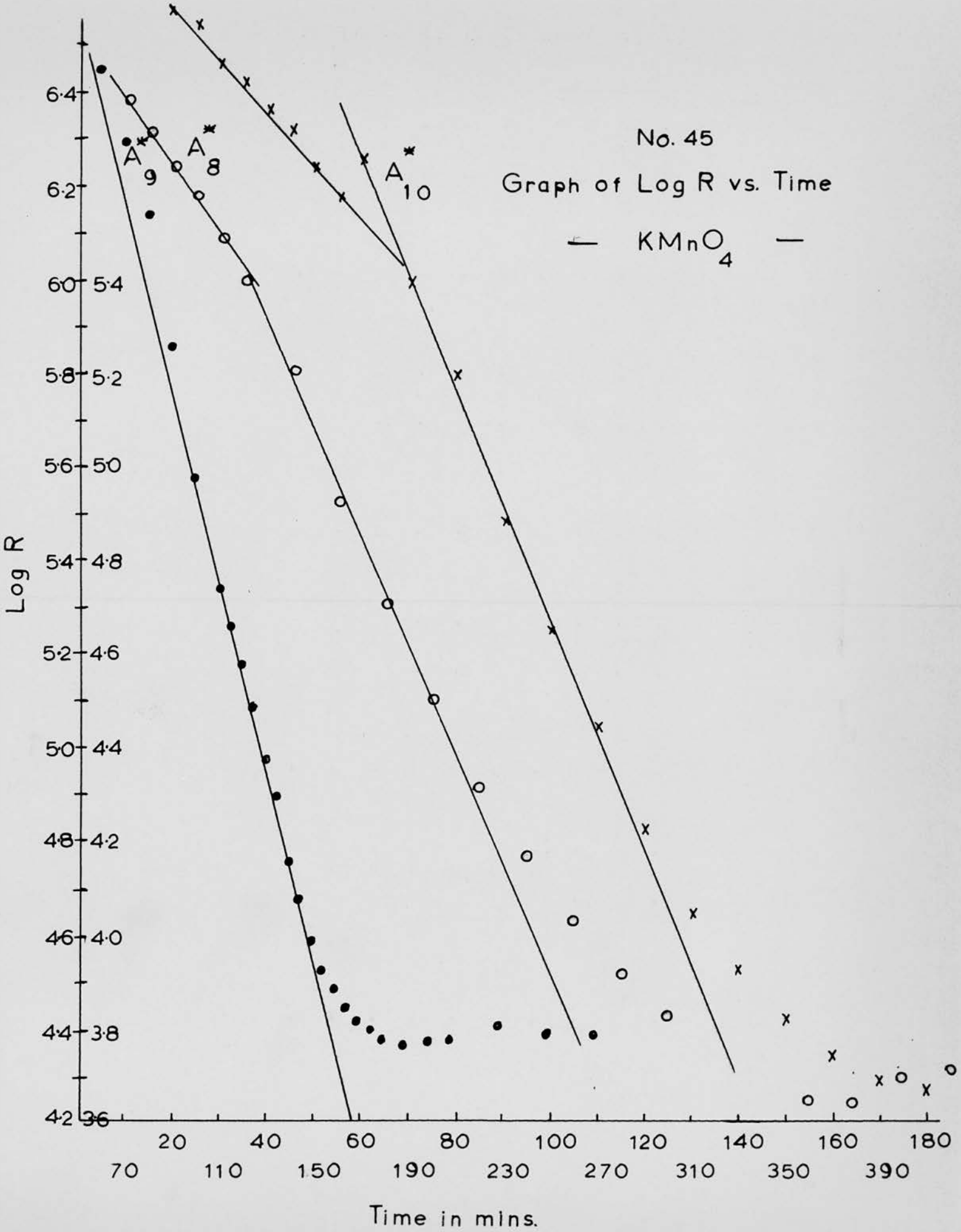
No. 45
Graph of Log R vs. Time
— KMnO4 —
A*9
A*8
A*10
Log R
6·4
6·2
6·0
5·8
5·6
5·4
5·2
5·0
4·8
4·6
4·4
4·2
5·4
5·2
5·0
4·8
4·6
4·4
4·2
4·0
3·8
3·6
20
40
60
80
100
120
140
160
180
70
110
150
190
230
270
310
350
390
Time in mins.

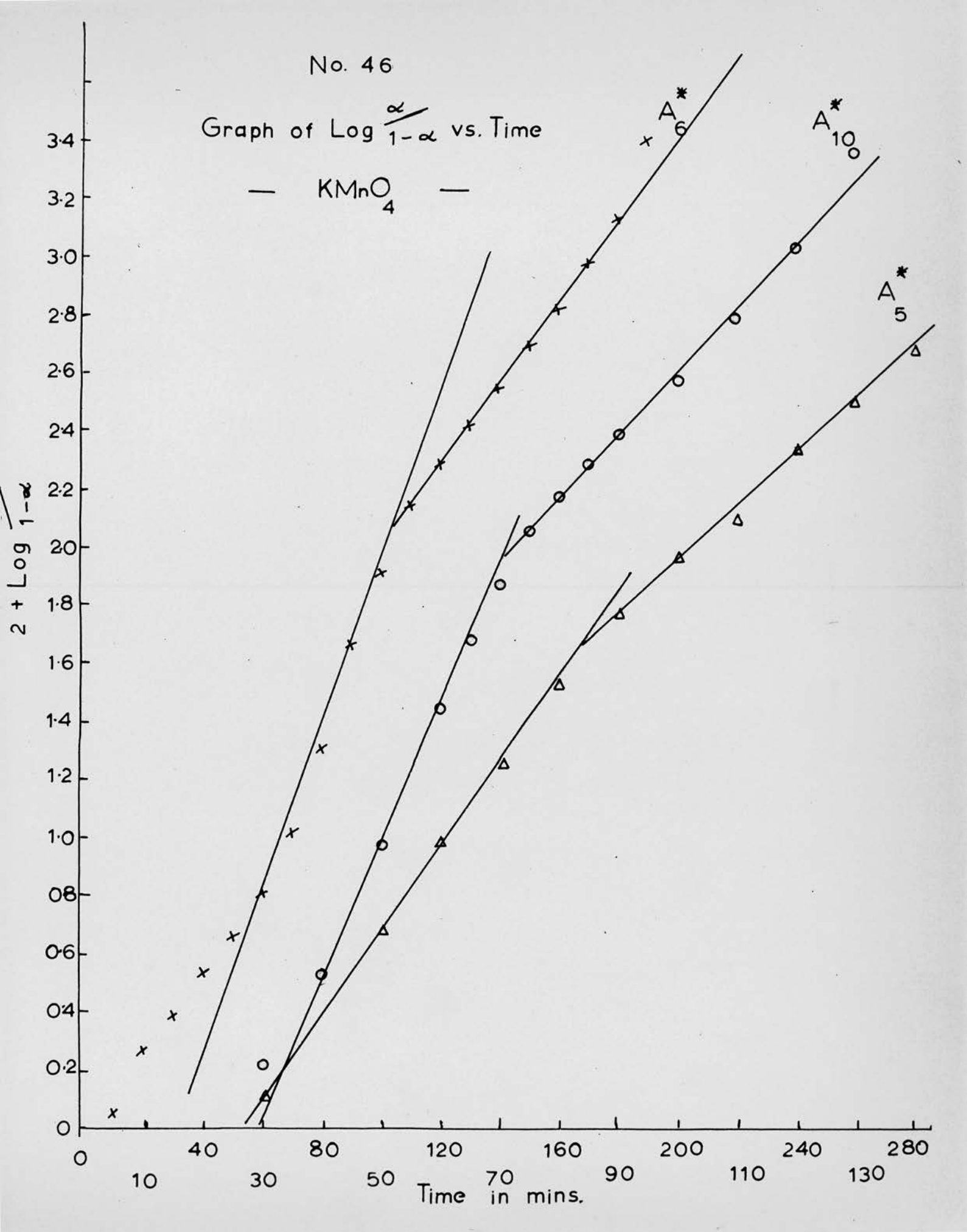
No. 46
Graph of Log α/1−α vs. Time
— KMnO4 —
A*6
A*10
A*5
2 + Log 1−α
3·4
3·2
3·0
2·8
2·6
2·4
2·2
2·0
1·8
1·6
1·4
1·2
1·0
0·8
0·6
0·4
0·2
0
0
40
80
120
160
200
240
280
10
30
50
70
90
110
130
Time in mins.

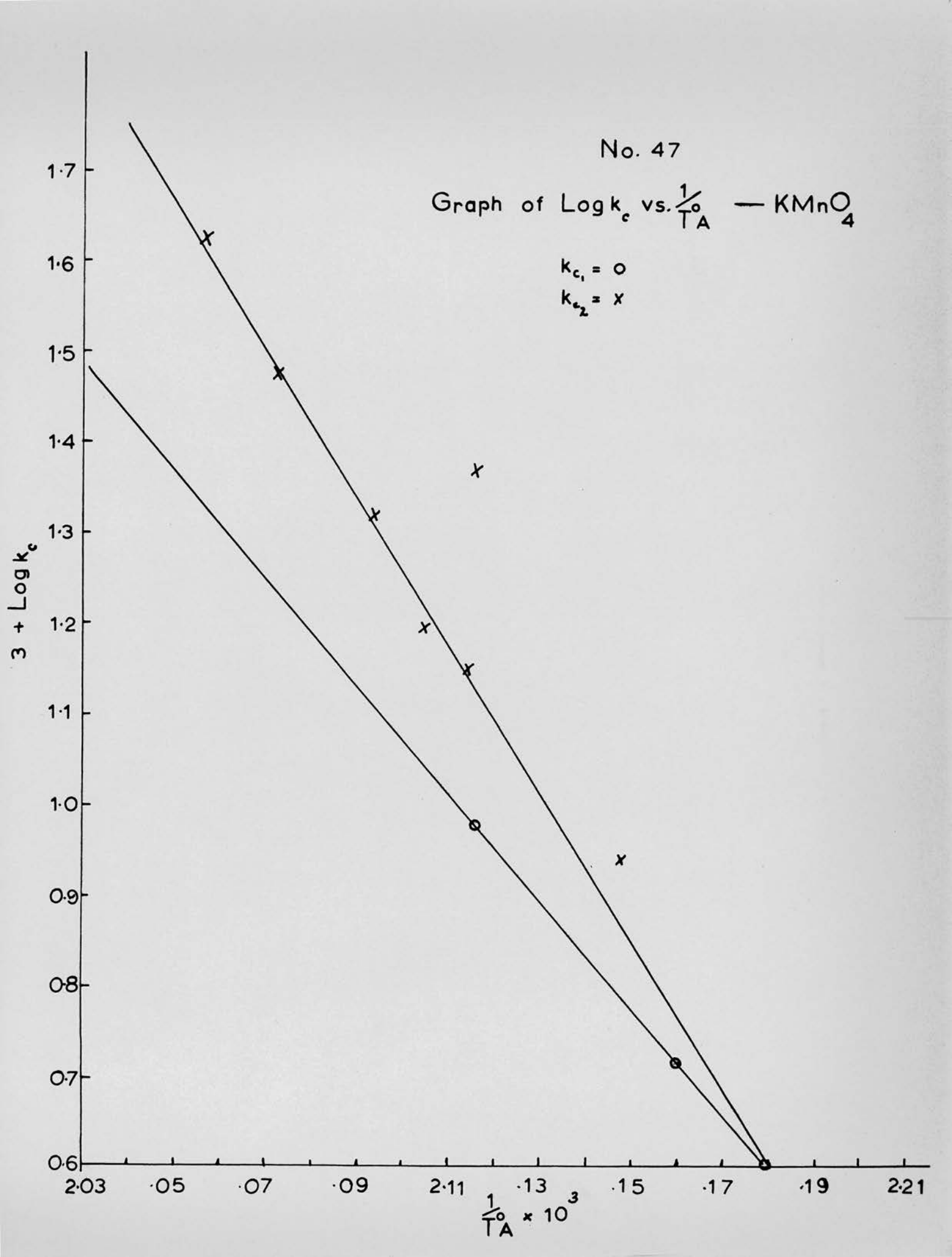
No. 47
Graph of Log k_c vs. $\frac{1}{T_A^o}$ — $KMnO_4$
k_{c_1} = o
k_{c_2} = x
3 + Log k_c
1·7
1·6
1·5
1·4
1·3
1·2
1·1
1·0
0·9
0·8
0·7
0·6
2·03
·05
·07
·09
2·11
·13
·15
·17
·19
2·21
$\frac{1}{T_A^o} \times 10^3$

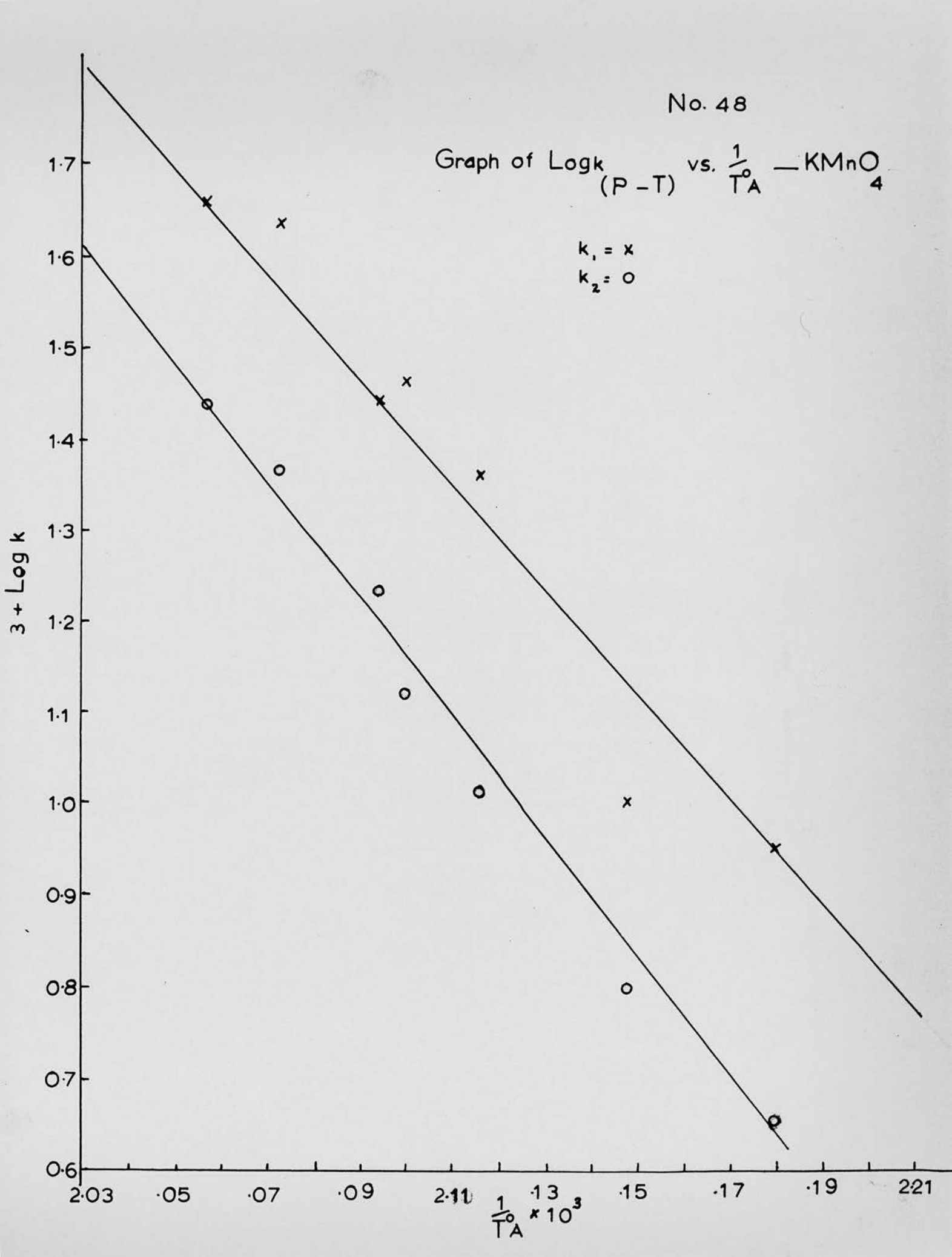
No. 48
Graph of Log k (P – T) vs. 1/T°A — KMnO4
k1 = x
k2 = o
3 + Log k
1·7
1·6
1·5
1·4
1·3
1·2
1·1
1·0
0·9
0·8
0·7
0·6
2·03
·05
·07
·09
2·11
·13
·15
·17
·19
2·21
1/T°A × 10³

3.3.2. Resistance Measurements for Potassium Permanganate/α-Alumina (B*)

Tables 43, 44 and 45 and graphs 49, 50, 51 and 52 illustrate, for the system potassium permanganate/α-Alumina, the change in resistance during the decomposition and also the fit of the Prout-Tompkins equation over the later stages of the reaction.

In this system the resistance measurements again show an exponential decrease over the range $\alpha = 0 - 0.2$, after which they continue to decrease, again there is little change after $\alpha = 0.6$.

The Prout-Tompkins equation holds over the region $\alpha = 0.2 - 0.9$ two values of k being required, one for the acceleratory stage $\alpha = 0.2 - 0.5$, the other for the decay stage, $\alpha = 0.5 - 0.9$.

Tables 43 and 44	Analysis of system B*.
Table 45	Rate constants for system B*.
Graph 49	Plot of $\log_{10} R$ vs. Time.
Graph 50	Plot of $\log_{10} \frac{\alpha}{1-\alpha}$ vs. Time.
Graph 51	Arrhenius plot for "rate of change of conduction" which gives an activation energy of $E_{c_2} = 32 \pm 3$ K. cals./mole.
Graph 52	Arrhenius plot for acceleratory and decay stages which gives an activation energy of $E_1 = 43 \pm 2$ K. cals./mole. and $E_2 = 38 \pm 2$ K. cals./mole.

Table 43 System B* $KMnO_4/\alpha\text{-}Al_2O_3$

Run	B*1			B*3			B*4	
Temp.	209.3°C			199.2°C			204.6°C	
Time Min.	α x 10	P.T.	log R	α x 10	P.T.	log R	P.T.	log R
5	0.12	$\bar{2}$.08	6.48			6.40	$\bar{2}$.59	6.16
10	0.22	$\bar{2}$.36	6.32	0.16	$\bar{2}$.22	6.32	$\bar{2}$.73	5.98
15	0.34	$\bar{2}$.55	6.15			6.24	$\bar{2}$.90	5.81
20	0.49	$\bar{2}$.71	5.95	0.20	$\bar{2}$.32	6.15	$\bar{1}$.00	5.66
25	0.66	$\bar{2}$.85	5.76			6.08	$\bar{1}$.12	5.53
30	0.92	$\bar{1}$.01	5.57	0.33	$\bar{2}$.53	5.98	$\bar{1}$.22	5.39
35	1.28	$\bar{1}$.17	5.39			5.90		5.26
40	1.74	$\bar{1}$.32	5.22	0.41	$\bar{2}$.63	5.83	$\bar{1}$.39	5.17
45	2.50	$\bar{1}$.52	5.07			5.74	$\bar{1}$.47	5.07
50	3.55	$\bar{1}$.74	4.93	0.59	$\bar{2}$.80	5.65	$\bar{1}$.54	4.98
55	4.63	$\bar{1}$.93	4.85			5.56	$\bar{1}$.62	4.90
60	5.51	0.09	4.79	0.78	$\bar{2}$.94	5.48	$\bar{1}$.70	4.82
65	6.20	0.21	4.77			5.41	$\bar{1}$.77	4.76
70	6.84	0.33	4.76	0.98	$\bar{1}$.04	5.32	$\bar{1}$.87	4.85
75	7.38	0.45	4.76			5.25	$\bar{1}$.96	4.64
80	7.88	0.57	4.76	1.23	$\bar{1}$.15	5.18	0.06	4.59
85	8.29	0.69	4.76			5.11	0.15	4.56
90	8.68	0.82		1.56	$\bar{1}$.27	5.04	0.23	4.53
95	8.97	0.94	4.77				0.29	4.52
100	9.24	1.08		2.03	$\bar{1}$.41	4.92	0.35	4.52
105	9.47	1.25	4.77				0.43	4.52
110	9.63	1.42		2.69	$\bar{1}$.56	4.81	0.48	4.53
115	9.76		4.75				0.55	4.54
120	9.87			3.65	$\bar{1}$.76	4.73	0.62	4.54
125	9.96		4.72			4.69	0.68	
130	9.99			4.61	$\bar{1}$.93	4.65	0.74	4.56
135			4.70			4.64	0.83	
140			4.69	5.37	0.06	4.64	0.89	4.58
150				6.05	0.18	4.61	1.07	4.59
160				6.58	0.28	4.61	1.27	4.60
170				7.15	0.40	4.64	1.55	4.60
180				7.68	0.51	4.65	1.89	4.59
190				7.99	0.60	4.67		4.58
200				8.40	0.72	4.69		
210				8.77	0.85	4.70		
220				9.02	0.96	4.71		
230				9.26	1.10	4.71		
240				9.47	1.25	4.72		
250				9.65	1.44	4.71		
260				9.84	1.78	4.71		
270				9.98		4.70		

Table 44 System B* $KMnO_4$ /α- Al_2O_3

Run	B*2			B*5		
Temp.	188.8°C			194.9°C		
Time Min.	α x 10	P.T.	log R	α x 10	P.T.	log R
5			6.61			6.42
10	0.11	$\bar{2}$.06	6.57	0.19	$\bar{2}$.30	6.34
20	0.17		6.45	0.32		6.01
30	0.24	$\bar{2}$.39	6.35	0.49	$\bar{2}$.71	6.04
40	0.34		6.26	0.65		5.91
50	0.44	$\bar{2}$.67	6.15	0.87	$\bar{2}$.98	5.79
60	0.56		6.06	1.12		5.65
70	0.68	$\bar{2}$.86	5.96	1.33	$\bar{1}$.18	5.56
80	0.81		5.88	1.60		5.51
90	0.99	$\bar{1}$.04	5.80	1.88	$\bar{1}$.36	5.48
100	1.13		5.71	2.14		5.43
110	1.28	$\bar{1}$.17	5.64	2.54	$\bar{1}$.53	5.36
120	1.47		5.58	2.91		5.28
130	1.63	$\bar{1}$.29	5.51	3.40	$\bar{1}$.71	5.20
140	1.82		5.44	4.03		5.13
150	2.02	$\bar{1}$.40	5.38	4.69	$\bar{1}$.95	5.07
160	2.21		5.33	5.36		5.01
170	2.41	$\bar{1}$.50	5.27	5.97	0.17	4.98
180	2.63		5.22	6.44		4.95
190	2.86	$\bar{1}$.60	5.18	6.88	0.34	4.93
200	3.09		5.12	7.26		4.92
210	3.38	$\bar{1}$.71	5.08	7.61	0.50	4.91
220	3.64		5.04	7.93		4.90
230	3.94	$\bar{1}$.81	5.00	8.25	0.67	4.89
240	4.22		4.95	8.46	0.74	4.88
260	4.93	$\bar{1}$.99	4.69	8.95	0.93	4.87
280	5.67		4.84	9.29	1.11	4.86
300	6.27	0.23	4.79	9.60	1.38	
320	6.78			9.85		
340	7.16	0.40		9.92		
360	7.52					
380	7.85	0.56				
400	8.17					
420	8.41	0.72				
440	8.64					
460	8.86	0.89				
480	9.07					
500	9.23	1.08				
520	9.41					
540	9.55	1.32				
560	9.66					
580	9.77	1.63				
600	9.87					

Table 45 Rate Constants for System B* $KMnO_4/\alpha\text{-}Al_2O_3$

Run	$1/T^oA \times 10^3$	α-range	$k_c \times 10^2$	α-range	$k_1 \times 10^2$	α-range	$k_2 \times 10^2$
B*1	2.073	0.01-0.5	3.68	0.17-0.5	4.02	0.5-0.9	2.46
B*2	2.165	0.01-0.15	1.09	0.11-0.5	0.51	0.5-0.9	0.41
B*3	2.118	0.01-0.2	1.65	0.2-0.5	1.45	0.5-0.9	1.10
B*4	2.094	0.02-0.2	3.07	0.16-0.5	1.71	0.5-0.9	1.31
B*5	2.137	0.01-0.2	1.36	0.18-0.5	1.09	0.5-0.9	0.83

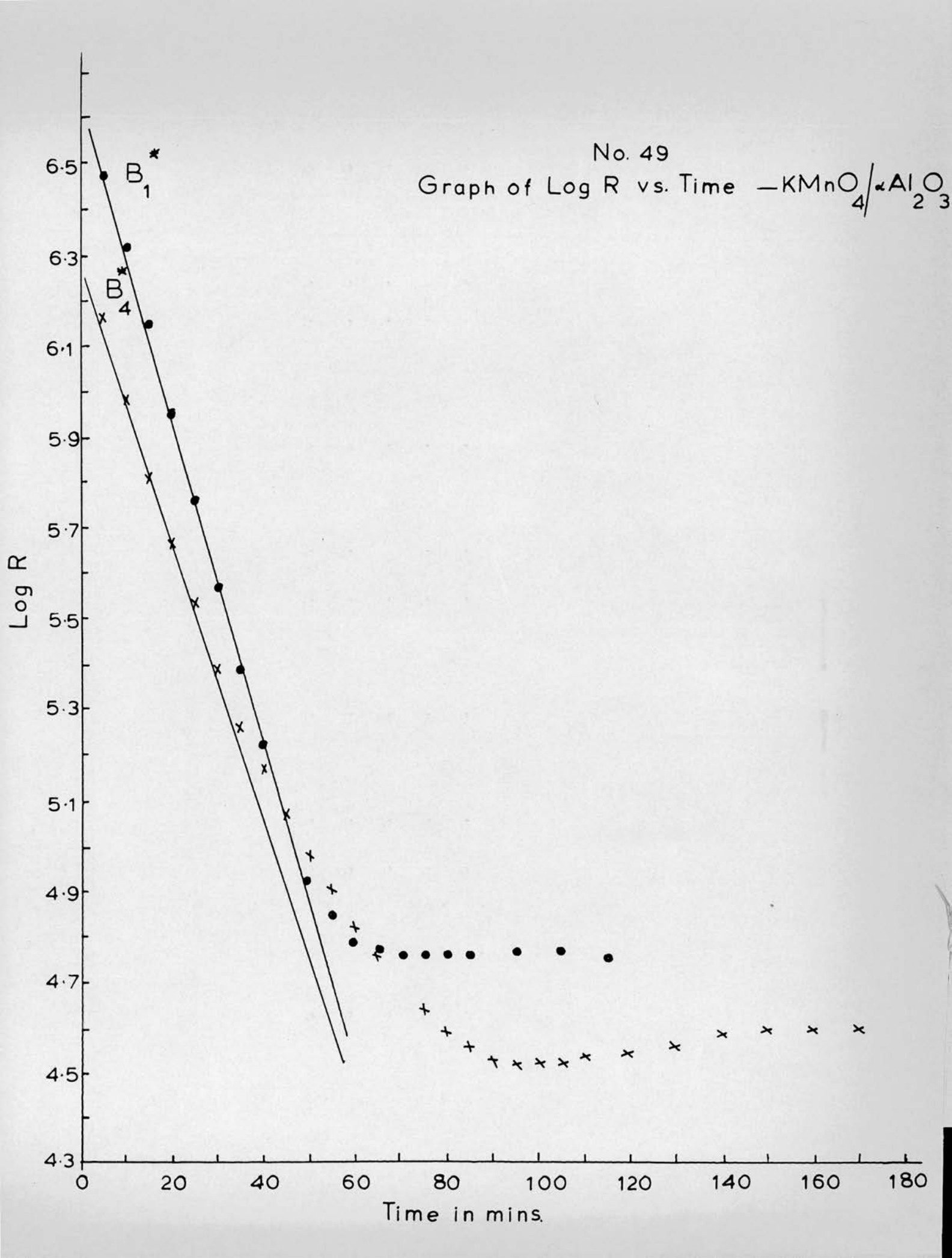
No. 49
Graph of Log R vs. Time —KMnO4/αAl2O3
B1
B4
Log R
6·5
6·3
6·1
5·9
5·7
5·5
5·3
5·1
4·9
4·7
4·5
4·3
0
20
40
60
80
100
120
140
160
180
Time in mins.

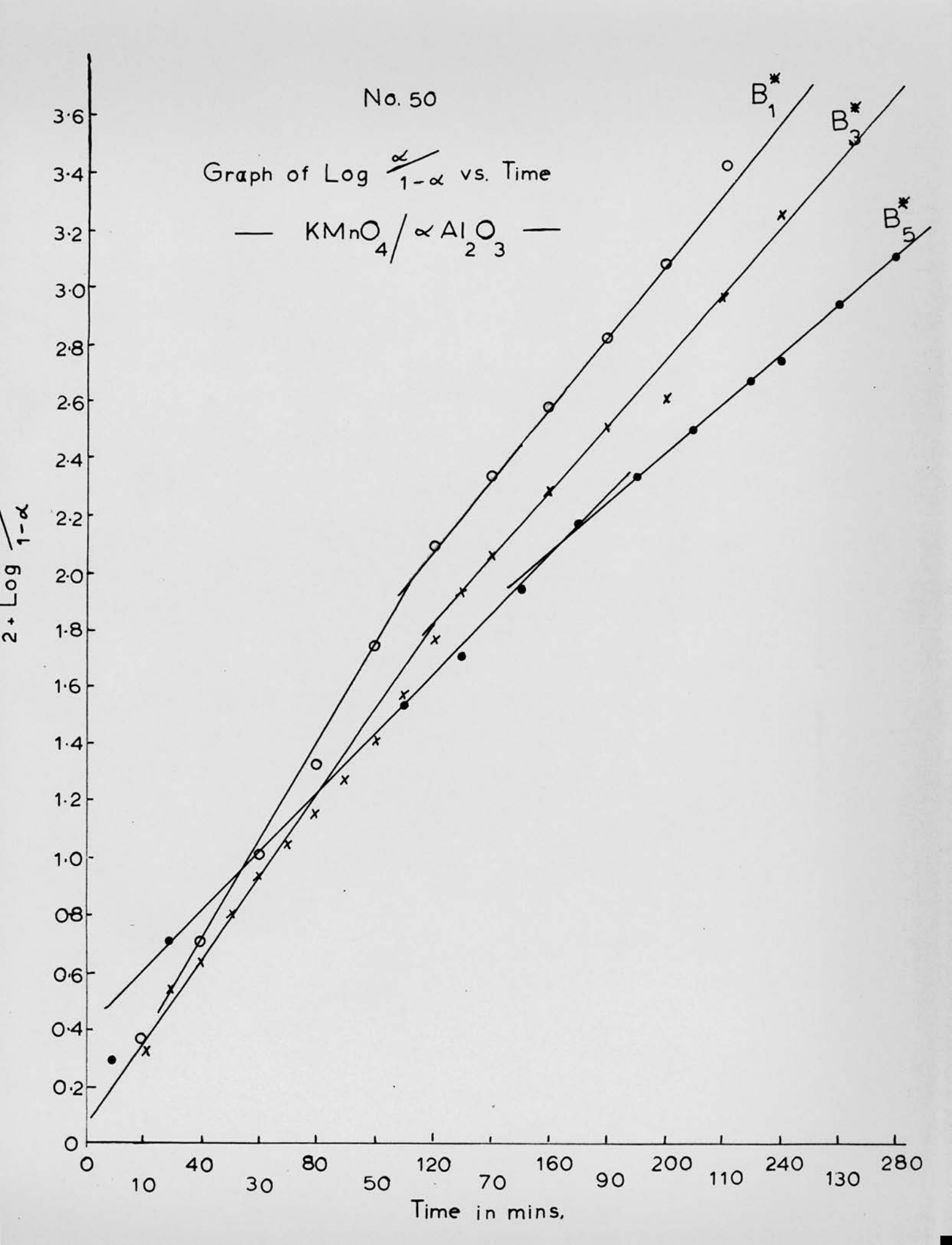
No. 50
Graph of Log α/1-α vs. Time
— KMnO4/∝Al2O3 —
B*1
B*3
B*5
2+ Log α/1-α
3·6
3·4
3·2
3·0
2·8
2·6
2·4
2·2
2·0
1·8
1·6
1·4
1·2
1·0
0·8
0·6
0·4
0·2
0
0
10
40
30
80
50
120
70
160
90
200
110
240
130
280
Time in mins.

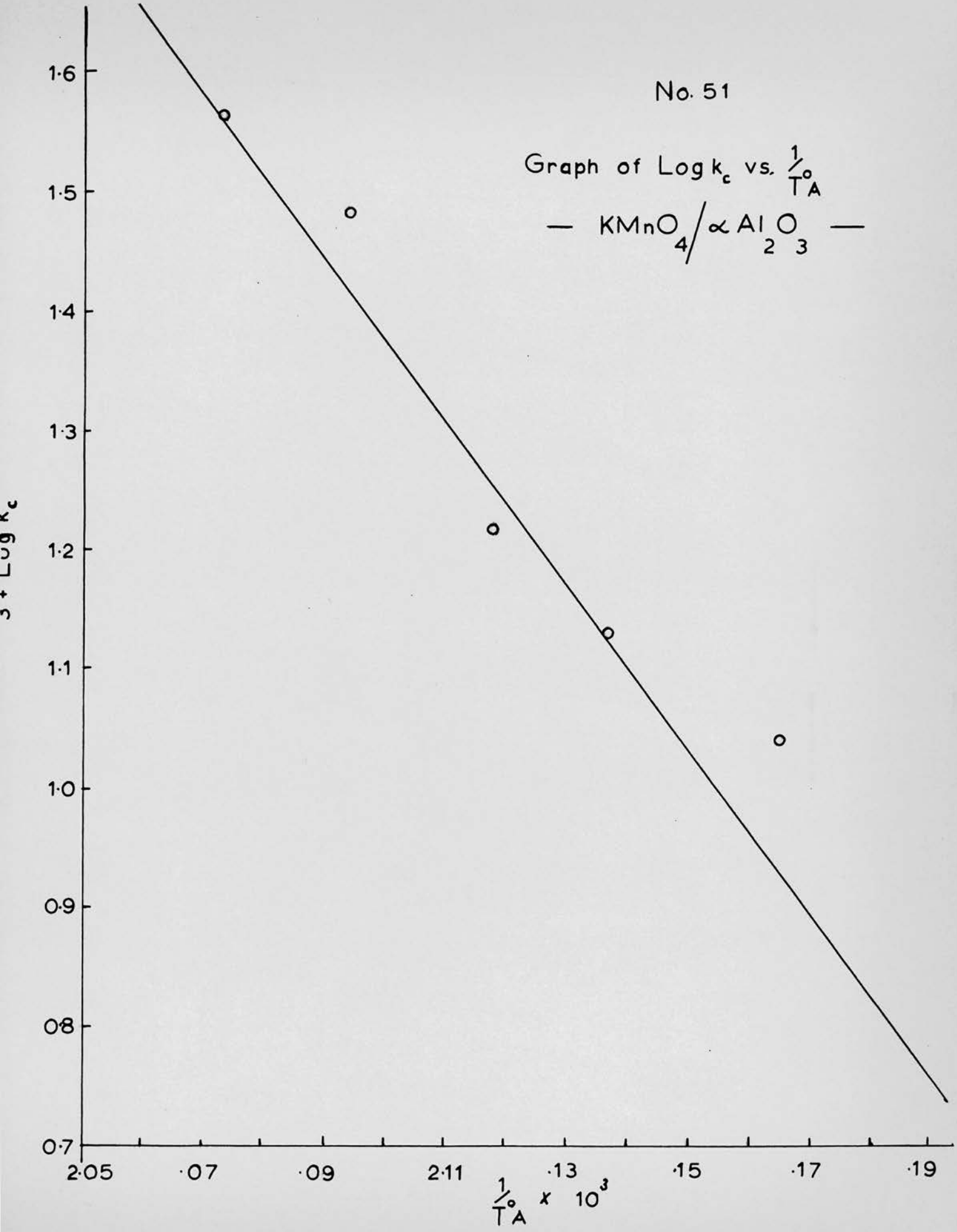
No. 51
Graph of Log k_c vs. $\frac{1}{T_A^\circ}$
— $KMnO_4/\alpha Al_2O_3$ —
3 + Log k_c
1·6
1·5
1·4
1·3
1·2
1·1
1·0
0·9
0·8
0·7
2·05
·07
·09
2·11
·13
·15
·17
·19
$\frac{1}{T_A^\circ} \times 10^3$

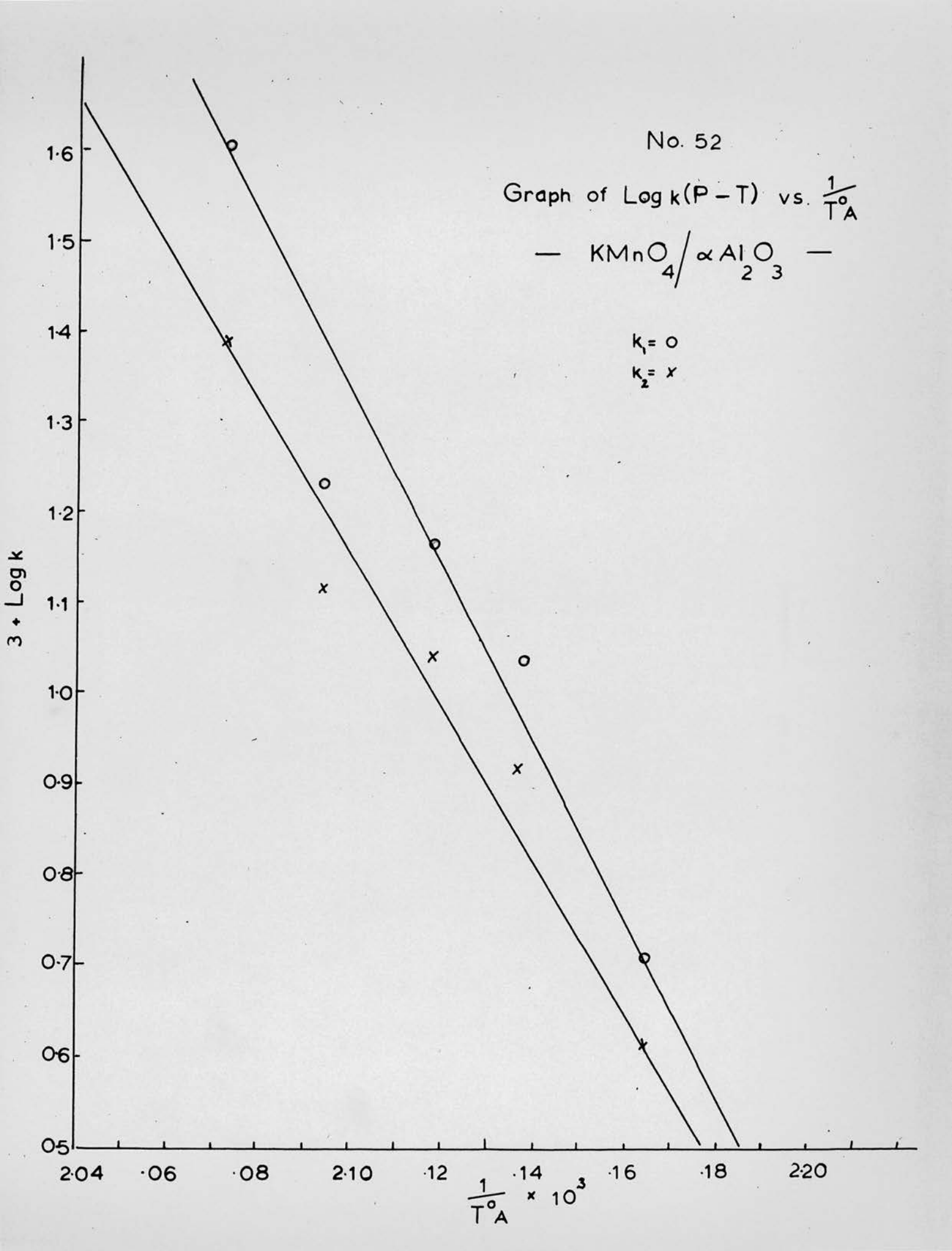
No. 52
Graph of Log k(P – T) vs. 1/T°A
— KMnO4/αAl2O3 —
k1 = o
k2 = x
3 + Log k
1·6
1·5
1·4
1·3
1·2
1·1
1·0
0·9
0·8
0·7
0·6
0·5
2·04
·06
·08
2·10
·12
·14
·16
·18
2·20
1/T°A × 10³

3.3.3. Resistance Measurements for Potassium Permanganate/Ferric Oxide (E*)

Tables 46, 47, 48 and 49 and graphs 53, 54, 55 and 56 illustrate, for the system potassium permanganate/ferric oxide, the change in resistance during the decomposition and also the fit of the Prout-Tompkins equation over the later stages of the reaction.

In this system the resistance measurements again show an exponential decrease over the range $\alpha = 0 - 0.5$, after which there is a continued decrease until $\alpha = 0.6$ after which there is little change.

The Prout-Tompkins equation holds over the region $\alpha = 0.1 - 0.9$, two values of k being required, one for the acceleratory stage $\alpha = 0.1 - 0.5$, the other for the decay stage, $\alpha = 0.5 - 0.9$.

Tables 46, 47 and 48	Analysis of system E*.
Table 49	Rate constants for system E*.
Graph 53	Plot of $\log_{10} R$ vs. Time.
Graph 54	Plot of $\log_{10} \frac{\alpha}{1-\alpha}$ vs. Time.
Graph 55	Arrhenius plot for "rate of change of conduction" which gives an activation energy of $E_{c_2} = 40$ K. cals./mole.
Graph 56	Arrhenius plot for acceleratory and decay stages which gives an activation energy of $E_2 = 30 \pm 2$ K. cals./mole.

Table 46 System E* $KMnO_4$ / Fe_2O_3

Run		E*1			E*2	
Temp.		209.1°C			205.0°C	
Time Min.	λ x 10	P.T.	log R	λ x 10	P.T.	log R
5	2.65	$\bar{1}$.56	6.15			6.36
10	3.08	$\bar{1}$.65	5.96	0.12	$\bar{2}$.06	6.26
15	3.41	$\bar{1}$.71	5.81			6.20
20	3.79	$\bar{1}$.79	5.68	0.13	$\bar{2}$.12	6.15
25	4.05	$\bar{1}$.83	5.56			6.11
30	4.34	$\bar{1}$.88	5.45	0.13	$\bar{2}$.12	6.07
35	4.72	1.95	5.35			6.01
40	5.00	0.00	5.26	0.15	$\bar{2}$.17	5.97
45	5.38	0.06	5.20			5.93
50	5.69	0.12	5.14	0.21	$\bar{2}$.34	5.89
55	6.16	0.21	5.08			5.85
60	6.40	0.25	5.06	0.34	$\bar{2}$.55	5.81
65	6.68	0.30	5.01			
70	7.06	0.38	4.99	0.49	$\bar{2}$.71	5.72
75	7.37	0.45	4.97			
80	7.65	0.51	4.95	0.67	$\bar{2}$.86	5.64
85	8.03	0.61	4.93			
90	8.29	0.69	4.91	0.92	$\bar{1}$.00	5.56
95	8.60	0.79	4.90			
100	8.96	0.93	4.88	1.15	$\bar{1}$.11	5.48
105	9.22	1.07				
110	9.43	1.22	4.85	1.48	$\bar{1}$.24	5.42
115	9.67	1.47				
120	9.76	1.24	4.81	1.84	$\bar{1}$.35	5.36
125	9.93	1.99				
130			4.77	2.30	$\bar{1}$.47	5.32
140				2.82	$\bar{1}$.59	5.46
150				3.43	$\bar{1}$.72	5.42
160				3.97	$\bar{1}$.82	5.38
170				4.57	$\bar{1}$.93	5.33
180				5.08	0.01	5.28
190				5.59	0.10	5.25
200				6.08	0.19	5.22
210				6.56	0.28	5.20
220				7.02	0.37	5.19
230				7.41	0.46	5.18
240				7.84	0.56	5.17
250				8.21	0.66	5.17
260				8.57	0.78	5.17
270				8.89	0.90	5.17
280				9.20	1.06	5.17
290				9.48	1.26	
300				9.67	1.47	

Table 47 System E* $KMnO_4$ / Fe_2O_3

Run		E*3			E*4	
Temp.		203.2°C			194.7°C	
Time Min.	α x 10	P.T.	log R	α x 10	P.T.	log R
5	1.44	$\bar{1}$.22	6.65			6.54
10	1.79	$\bar{1}$.34	6.56	1.39	$\bar{1}$.21	6.46
15	2.07	$\bar{1}$.42	6.48			6.48
20	2.36	$\bar{1}$.49	6.40	1.88	$\bar{1}$.36	6.40
25	2.69	$\bar{1}$.57	6.32			
30	3.00	$\bar{1}$.63	6.29	2.29	$\bar{1}$.47	6.28
35	3.32	$\bar{1}$.70	6.23			
40	3.62	$\bar{1}$.75	6.15	2.60	$\bar{1}$.55	6.16
45	3.95	$\bar{1}$.81	6.05			
50	4.23	$\bar{1}$.87	5.88	2.89	$\bar{1}$.61	6.08
55	4.51	$\bar{1}$.92	5.70			
60	4.79	$\bar{1}$.96	5.64	3.11	$\bar{1}$.65	5.98
65	5.06	0.01	5.57			
70	5.30	0.05	5.51	3.39	$\bar{1}$.71	5.92
75	5.59	0.10	5.48			
80	5.85	0.15	5.43	3.69	$\bar{1}$.77	5.85
85	6.12	0.20	5.40			
90	6.46	0.26	5.37	4.00	$\bar{1}$.82	5.78
95	6.62	0.29				
100	6.86	0.34	5.32	4.31	$\bar{1}$.88	5.72
105	7.10	0.39				
110	7.35	0.44	5.30	4.62	$\bar{1}$.93	5.66
115	7.58	0.50				
120	7.83	0.56	5.26	4.91	$\bar{1}$.98	5.60
125	8.02	0.61				
130	8.24	0.67		5.20	0.03	5.58
135	8.43	0.73				
140	8.65	0.81	5.20	5.42	0.07	5.53
145	8.84	0.88				
150	9.04	0.97	5.18	5.69	0.12	5.48
160	9.35	1.16	5.11	5.97	0.17	5.45
170	9.66	1.46		6.18	0.21	5.42
180	9.85	1.80		6.45	0.26	5.40
190						5.36
200				6.88	0.34	5.34
220				7.25	0.42	5.31
240				7.68	0.52	5.28
260				7.99	0.60	5.25
280				8.31	0.69	5.23
300				8.62	0.79	5.20
320				8.92	0.92	5.18
340				9.23	1.08	5.16
360				9.51	1.29	5.14
380				9.69	1.50	5.11
400				9.86	1.86	5.08

Table 48 System E* $KMnO_4/Fe_2O_3$

Run	E*5	
Temp.	186.9°C	
Time Min.	α x 10	P.T.
20	1.15	$\bar{1}$.11
40	1.61	$\bar{1}$.28
60	2.05	$\bar{1}$.41
80	2.40	$\bar{1}$.50
100	2.74	$\bar{1}$.58
120	3.08	$\bar{1}$.65
140	3.42	$\bar{1}$.72
160	3.84	$\bar{1}$.79
180	4.19	$\bar{1}$.86
200	4.52	$\bar{1}$.92
220	4.84	$\bar{1}$.97
240	5.16	0.03
260	5.45	0.08
280	5.68	0.12
300	5.97	0.17
320	6.16	0.21
340	6.45	0.26
360	6.69	0.31
380	6.94	0.35
400	7.13	0.39
420	7.40	0.45
440	7.58	0.50
460	7.82	0.56
480	8.05	0.62
500	8.23	0.67
520	8.42	0.73
540	8.65	0.81
560	8.82	0.87
580	9.02	0.96
600	9.19	1.06
620	9.35	1.16
640	9.52	1.29
660	9.66	1.45
680	9.81	1.70
700	9.87	1.89

	E*6		
	185.6°C		
Time Min.	α x 10	P.T.	log R
5			6.94
10			6.89
15			6.83
20	0.14	$\bar{2}$.15	6.79
30			6.65
40	0.23	$\bar{2}$.37	6.60
50			6.56
60	0.35	$\bar{2}$.57	6.48
70			6.42
80	0.46	$\bar{2}$.68	6.38
90			6.32
100	0.63	$\bar{2}$.83	6.26
110			6.22
120	0.87	$\bar{2}$.98	6.18
140	1.13	$\bar{1}$.10	6.09
150			6.05
160	1.41	$\bar{1}$.21	6.00
170			5.97
180	1.73	$\bar{1}$.32	5.93
190			5.91
200	2.04	$\bar{1}$.41	5.88
210			5.85
220	2.39	$\bar{1}$.50	5.82
230			5.80
240	2.70	$\bar{1}$.57	5.77
250			5.74
260	3.06	$\bar{1}$.65	5.69
270			5.66
280	3.42	$\bar{1}$.72	5.64
290			5.62
300	3.77	$\bar{1}$.78	5.59
340	4.37	$\bar{1}$.89	
380	4.96	$\bar{1}$.99	
420	5.58	0.10	
460	6.11	0.20	
500	6.61	0.29	
540	7.08	0.38	
580	7.51	0.48	
620	7.95	0.59	
660	8.33	0.70	
700	8.66	0.81	
740	8.99	0.95	
780	9.27	1.10	
820	9.52	1.30	
860	9.75	1.59	
900	9.87	1.89	

Table 49 Rate Constants for System E* $KMnO_4/Fe_2O_3$

Run	$1/T^oA \times 10^3$	α- range	$k_{c_1} \times 10^2$	α- range	$k_{c_2} \times 10^2$	α- range	$k_1 \times 10^2$	α- range	$k_2 \times 10^2$
E*1	2.074	-	-	0.02-0.5	2.7	-	-	0.3 -0.75	1.16
E*2	2.092	-	-	0.01-0.4	0.83	0.08-0.35	1.27	0.35-0.9	0.93
E*3	2.100	-	-	0.1 -0.5	1.6	0.15-0.42	1.34	0.42-0.85	0.94
E*4	2.138	0.1 -0.3	1.3	0.3 -0.57	0.70	0.1 -0.54	0.86	0.54-0.87	0.43
E*5	2.174	-	-	-	-	0.1 -0.5	0.35	0.5 -0.82	0.23
E*6	2.180	0.01-0.11	0.53	0.11-0.4	0.31	-	-	0.4 -0.9	0.24

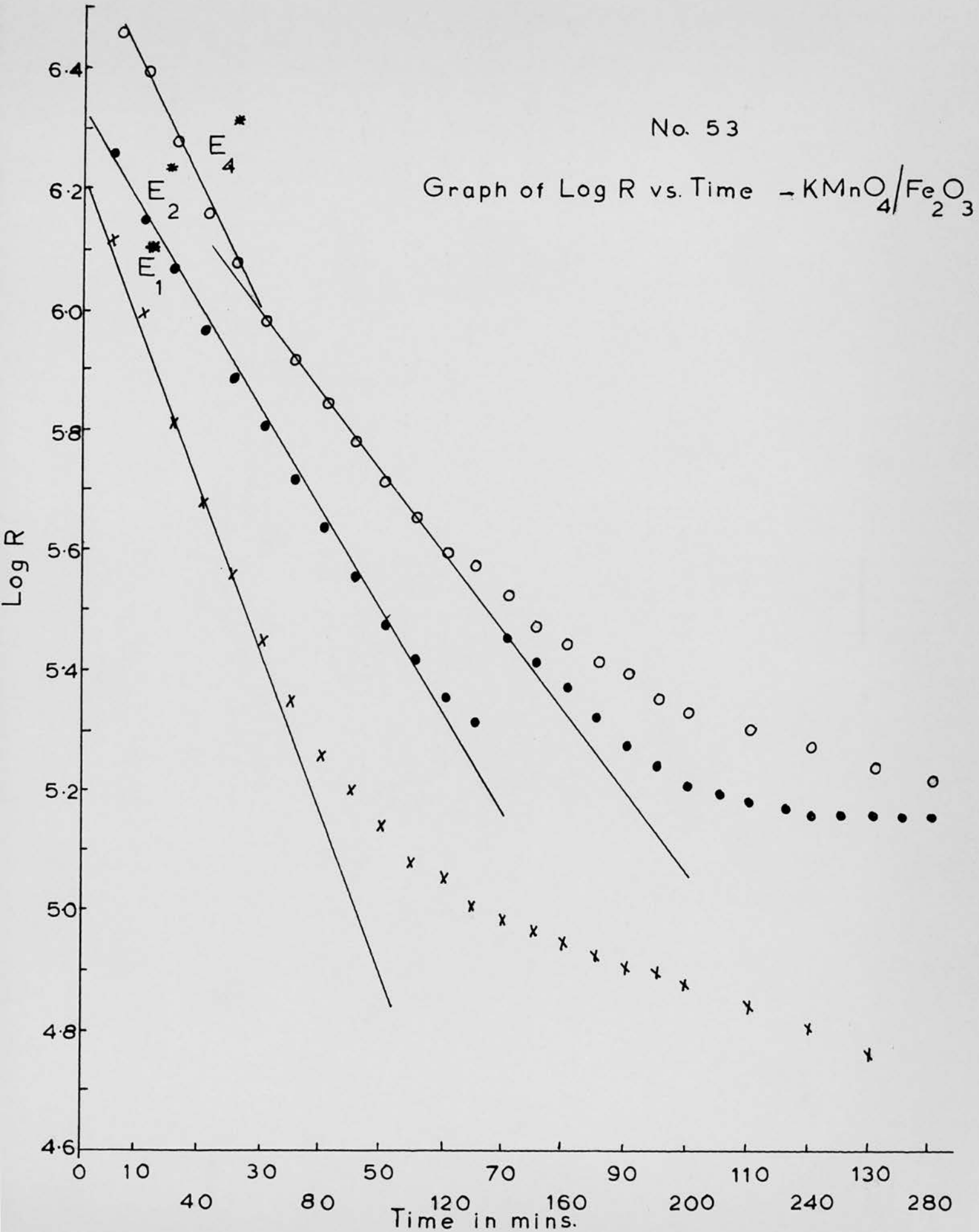
No. 53
Graph of Log R vs. Time – $KMnO_4/Fe_2O_3$
E_4
E_2
E_1
Log R
6·4
6·2
6·0
5·8
5·6
5·4
5·2
5·0
4·8
4·6
0
10
30
50
70
90
110
130
40
80
120
160
200
240
280
Time in mins.

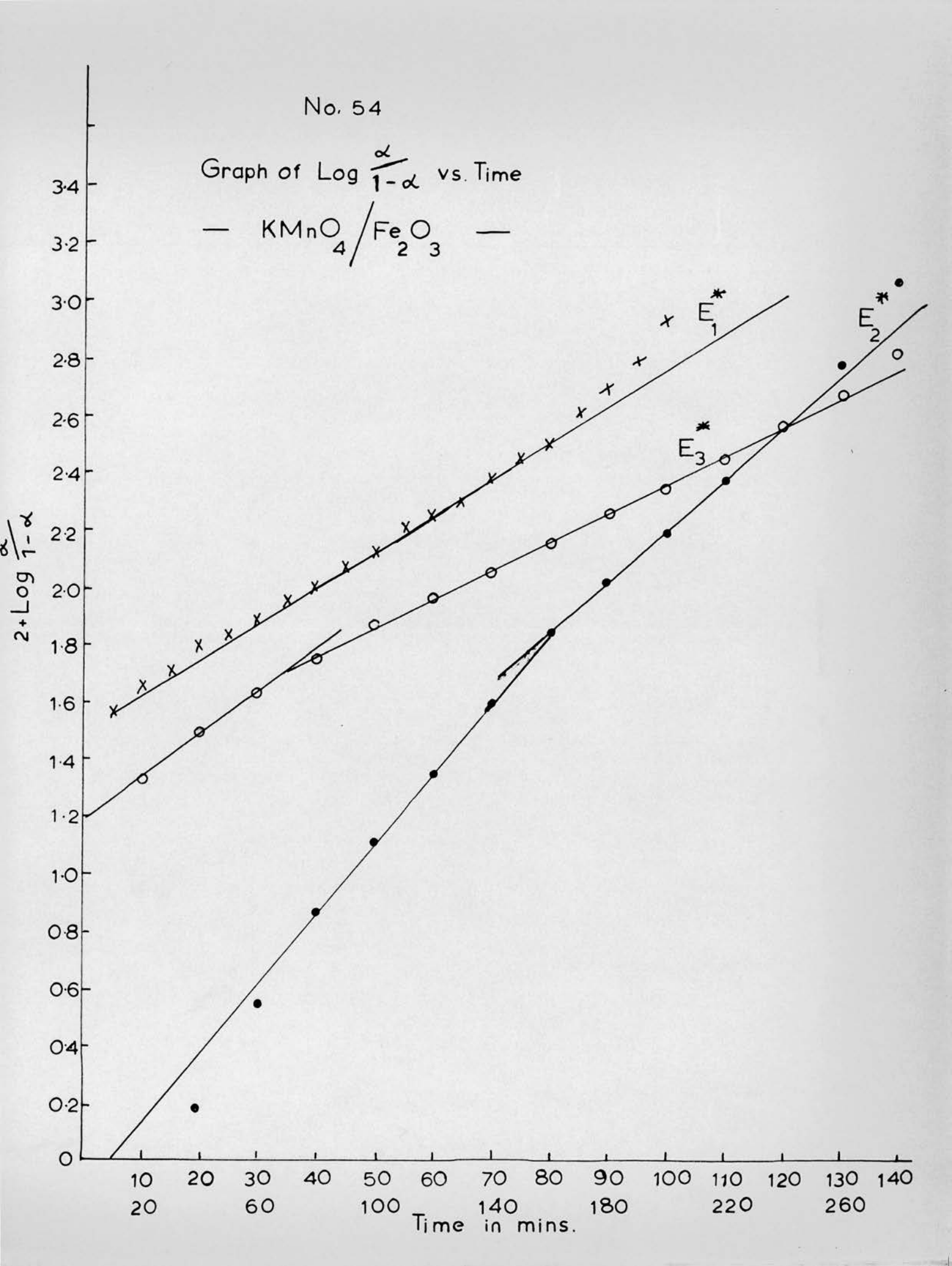
No. 54
Graph of Log α/1-α vs. Time
— KMnO4/Fe2O3 —
E1*
E2*
E3*
2+Log α/1-α
3·4
3·2
3·0
2·8
2·6
2·4
2·2
2·0
1·8
1·6
1·4
1·2
1·0
0·8
0·6
0·4
0·2
0
10 20 30 40 50 60 70 80 90 100 110 120 130 140
20 60 100 140 180 220 260
Time in mins.

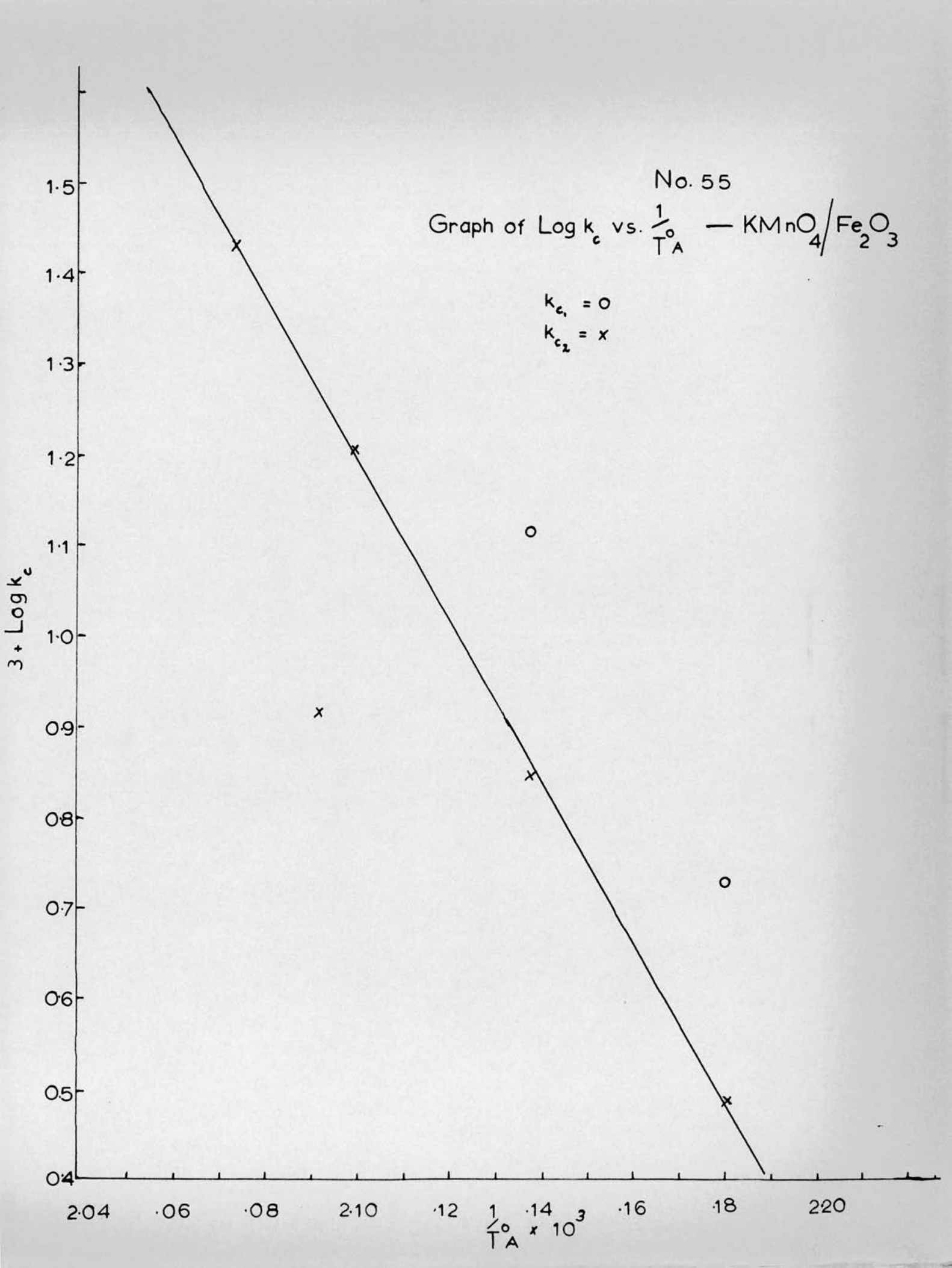
No. 55
Graph of Log k_c vs. $\frac{1}{T^o_A}$ — $KMnO_4/Fe_2O_3$
k_{c_1} = o
k_{c_2} = x
3 + Log k_c
1·5
1·4
1·3
1·2
1·1
1·0
0·9
0·8
0·7
0·6
0·5
0·4
2·04
·06
·08
2·10
·12
·14
·16
·18
220
$\frac{1}{T^o_A} \times 10^3$

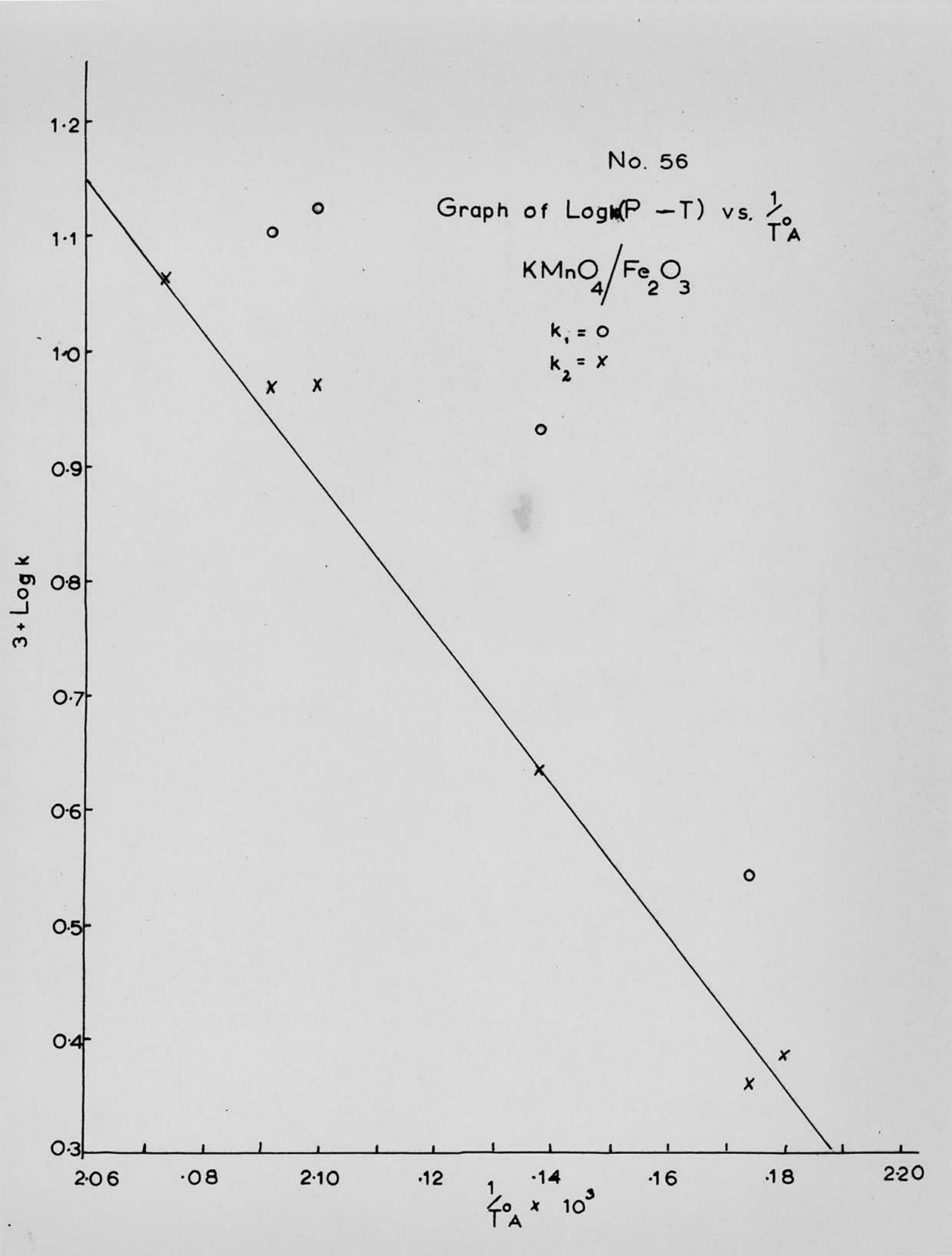
No. 56
Graph of Log k (P − T) vs. 1/T°A
KMnO4/Fe2O3
k1 = o
k2 = x
3 + Log k
1·2
1·1
1·0
0·9
0·8
0·7
0·6
0·5
0·4
0·3
2·06
·08
2·10
·12
·14
·16
·18
2·20
1/T°A x 10³

3.3.4. Resistance Measurements for Potassium Permanganate/Zinc Oxide (F*)

Tables 50, 51, 52 and 53 and graphs 57, 58, 59 and 60 illustrate, for the system potassium permanganate/zinc oxide, the change in resistance during the decomposition and also the fit of the Prout-Tompkins equation over the later stages of the reaction.

In this system the resistance measurements again show an exponential decrease over the range $\alpha = 0 - 0.6$, after which there is little change in resistance.

The Prout-Tompkins equation holds over the region $\alpha = 0.15 - 0.9$, two values of k being required, one for the acceleratory stage, $\alpha = 0.15 - 0.5$, the other for the decay stage, $\alpha = 0.5 - 0.9$.

Tables 50, 51 and 52	Analysis of system F*.
Table 53	Rate constants for system F*.
Graph 57	Plot of $\log_{10} R$ vs. Time.
Graph 58	Plot of $\log_{10} \frac{\alpha}{1-\alpha}$ vs. Time.
Graph 59	Arrhenius plot for "rate of conduction" which gives an activation energy of $E_{c_2} = 40 \pm 3$ K. cals./mole.
Graph 60	Arrhenius plot for acceleratory and decay stages which gives an activation energy of $E_1 = 30 \pm 2$ K. cals./mole. and $E_2 = 33 \pm 2$ K. cals./mole.

Table 50 System F* $KMnO_4$ / ZnO

Run	F*1			F*5		
Temp.	210.5°C			199.0°C		
Time Min.	α x 10	P.T.	log R	α x 10	P.T.	log R
5	0.72	$\bar{2}$.89	6.31			
10	1.13	$\bar{1}$.11	6.16	0.18	$\bar{2}$.27	6.89
15	1.61	$\bar{1}$.28	5.95			6.81
20	2.03	$\bar{1}$.41	5.79	0.40	$\bar{2}$.62	6.59
25	2.49	$\bar{1}$.52	5.61			6.53
30	2.89	$\bar{1}$.61	5.46	0.57	$\bar{2}$.78	6.43
35	3.32	$\bar{1}$.70	5.32			6.38
40	3.77	$\bar{1}$.78	5.17	0.74	$\bar{2}$.90	6.30
45	4.38	$\bar{1}$.89	5.03			6.24
50	5.19	0.03	4.91	1.01	$\bar{1}$.05	6.19
55	6.03	0.18	4.79			6.14
60	6.86	0.34	4.76	1.21	$\bar{1}$.14	6.08
65	7.48	0.47	4.67			6.02
70	7.98	0.60	4.66	1.49	$\bar{1}$.24	5.98
75	8.44	0.73	4.64			5.93
80	8.83	0.88	4.60	1.78	$\bar{1}$.33	5.89
85	9.13	1.02	4.56			5.84
90	9.44	1.23	4.49	1.07	$\bar{1}$.42	5.80
95	9.69	1.49	4.42			5.73
100	9.85	1.81	4.38	2.42	$\bar{1}$.50	5.68
105			4.36			5.61
110			4.32	2.74	$\bar{1}$.58	5.56
115						5.51
120				3.20	$\bar{1}$.67	5.48
130				3.75	$\bar{1}$.78	5.42
140				4.35	$\bar{1}$.89	
150				5.02	0.00	5.25
160				5.77	0.14	5.17
170				6.42	0.25	5.09
180				7.03	0.37	5.02
190				7.60	0.50	4.96
200				7.98	0.60	4.93
210				8.39	0.72	4.91
220				8.70	0.82	4.90
230				9.00	0.96	4.88
240				9.31	1.13	4.85
250				9.48	1.26	4.84
260				9.73	1.55	4.81
270				9.77		4.79

Table 51 System F* $KMnO_4/ZnO$

Run	F*3			F*2		
Temp.	185.6°C			188.3°C		
Time Min.	α x 10	P.T.	log R	α x 10	P.T.	log R
5			6.87			6.95
10			6.87			6.87
15			6.84			6.81
20	0.17	$\bar{2}$.25	6.82	0.30	$\bar{2}$.50	6.69
25			6.79			6.65
30			6.70			6.60
40	0.29	$\bar{2}$.47	6.65	0.57	$\bar{2}$.78	6.51
50			6.59			6.40
60	0.38	$\bar{2}$.60	6.58	1.02	$\bar{1}$.05	6.32
70			6.54			6.24
80	0.48	$\bar{2}$.70	6.48	1.43	$\bar{1}$.22	6.15
90			6.44			6.08
100	0.73	$\bar{2}$.90	6.40	1.86	$\bar{1}$.36	6.00
110			6.37			5.94
120	0.77	$\bar{2}$.92	6.32	2.32	$\bar{1}$.48	5.89
130			6.29			5.83
140	0.96	$\bar{1}$.03	6.25	2.84	$\bar{1}$.60	5.77
150			6.21			5.71
160	1.12	$\bar{1}$.10	6.16	3.23	$\bar{1}$.68	5.66
170			6.15			5.60
180	1.35	$\bar{1}$.19	6.11	3.72	$\bar{1}$.77	5.56
190			6.08			5.51
200	1.50	$\bar{1}$.25	6.06	4.11	$\bar{1}$.84	5.47
210			6.00			5.43
220	1.71	$\bar{1}$.32	5.98	4.57	$\bar{1}$.93	5.40
230			5.96			5.36
240	1.77		5.93	5.00	0.00	5.34
250			5.90			5.32
260	2.08	$\bar{1}$.42	5.88	5.54	0.09	5.26
270			5.85			5.23
280	2.31	$\bar{1}$.48	5.76	6.07	0.19	
290			5.70			5.17
300	2.63	$\bar{1}$.55	5.68	6.61	0.29	5.14
320	2.89	$\bar{1}$.61	5.59	7.27	0.42	5.08
340	3.31	$\bar{1}$.69	5.51	7.70	0.52	5.02
360	3.79	$\bar{1}$.78	5.46	8.07	0.62	4.97
380	4.23	$\bar{1}$.86		8.41	0.72	4.94
400	4.83	$\bar{1}$.97		8.70	0.82	4.93
420	5.40	0.07		8.93	0.92	
440	5.98	0.17		9.14	1.03	
460	6.54	0.28		9.43	1.22	
480	7.02	0.37		9.61	1.39	
500	7.40	0.46		9.77	1.62	
520	7.73	0.53		9.84	1.79	
540	8.06	0.62		9.93		
580	8.60	0.79				
620	9.02	0.96				
660	9.33	1.14				
700	9.62	1.40				

Table 52 System F* $KMnO_4/ZnO$

Run		F*4		F*6
Temp.		194.9°C		205.6°C
Time Min.	α x 10	P.T.	log R	log R
5			6.60	6.32
10	0.25	$\bar{2}.41$	6.54	6.20
15			6.48	6.09
20	0.46	$\bar{2}.69$	6.42	5.97
25			6.36	5.88
30	0.68	$\bar{2}.86$	6.30	5.79
35			6.23	5.68
40	0.95	$\bar{1}.02$	6.18	5.60
45				5.51
50	1.30	$\bar{1}.17$	6.04	5.43
60	1.59	$\bar{1}.28$	5.93	5.28
65				5.18
70	1.95	$\bar{1}.38$	5.82	5.05
75				4.95
80	2.28	$\bar{1}.47$	5.70	4.88
85				4.81
90	2.62	$\bar{1}.55$	5.56	4.74
95				4.68
100	2.93	$\bar{1}.62$	5.45	4.65
105				4.63
110	3.31	$\bar{1}.69$	5.34	4.63
120	3.74	$\bar{1}.78$	5.22	4.60
130	4.24	$\bar{1}.87$	5.12	4.60
140	4.77	$\bar{1}.96$	5.04	4.59
150	5.31	0.05	4.95	4.58
160	5.93	0.16	4.90	4.57
170	6.45	0.26	4.85	
180	6.89	0.35	4.81	
190	7.29	0.43	4.77	
200	7.59	0.50	4.75	
210	7.92	0.58	4.75	
220	8.21	0.66		
230	8.45	0.74	4.74	
240	8.65	0.81		
250	8.90	0.91	4.72	
260	9.07	0.99		
270	9.27	1.11	4.70	
280	9.41	1.20		
290	9.54	1.31	4.68	
300	9.67	1.47		

Table 53 Rate Constants for System F* $KMnO_4$/ZnO

Run	$1/T^{\circ}A \times 10^3$	α- range	$k_c \times 10^2$	α- range	$k_1 \times 10^2$	α- range	$K_2 \times 10^2$
F*1	2.068	0.05-0.66	3.00	0.11-0.5	1.96	0.5-0.9	2.84
F*2	2.168	0.03-0.8	0.34	0.10-0.5	0.41	0.5-0.9	0.53
F*3	2.180	0.02-0.5	0.35	0.08-0.5	0.43	0.5-0.94	0.48
F*4	2.137	0.01-0.4	1.20	0.11-0.5	0.82	0.5-0.9	0.84
F*5	2.119	0.02-0.6	1.05	0.1 -0.5	0.93	0.5-0.9	1.19
F*6	2.089	0.02-0.6	1.86	-	-	-	-

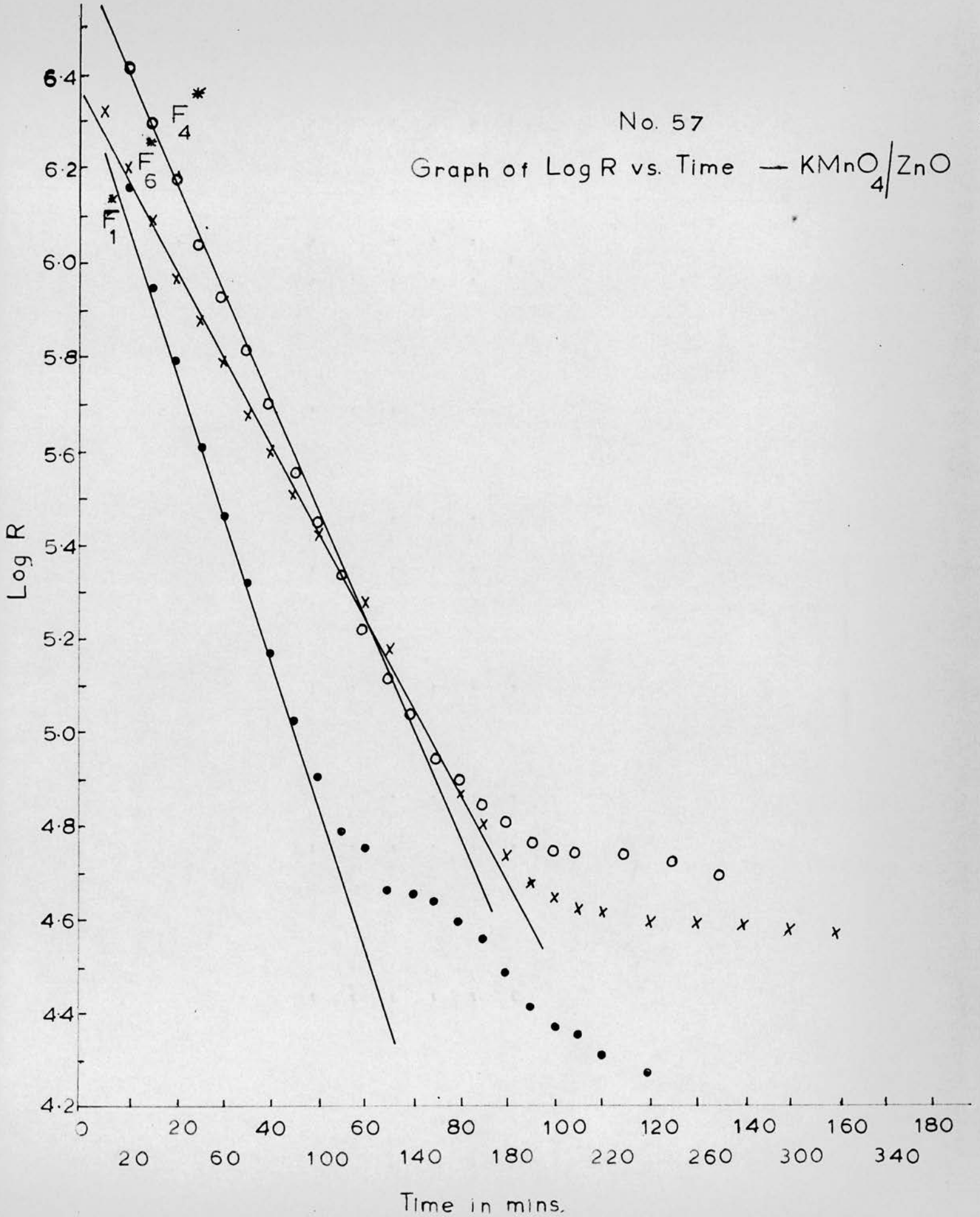
No. 57
Graph of Log R vs. Time — KMnO4/ZnO
F1
F4
F6
Log R
6·4
6·2
6·0
5·8
5·6
5·4
5·2
5·0
4·8
4·6
4·4
4·2
0 20 40 60 80 100 120 140 160 180
20 60 100 140 180 220 260 300 340
Time in mins.

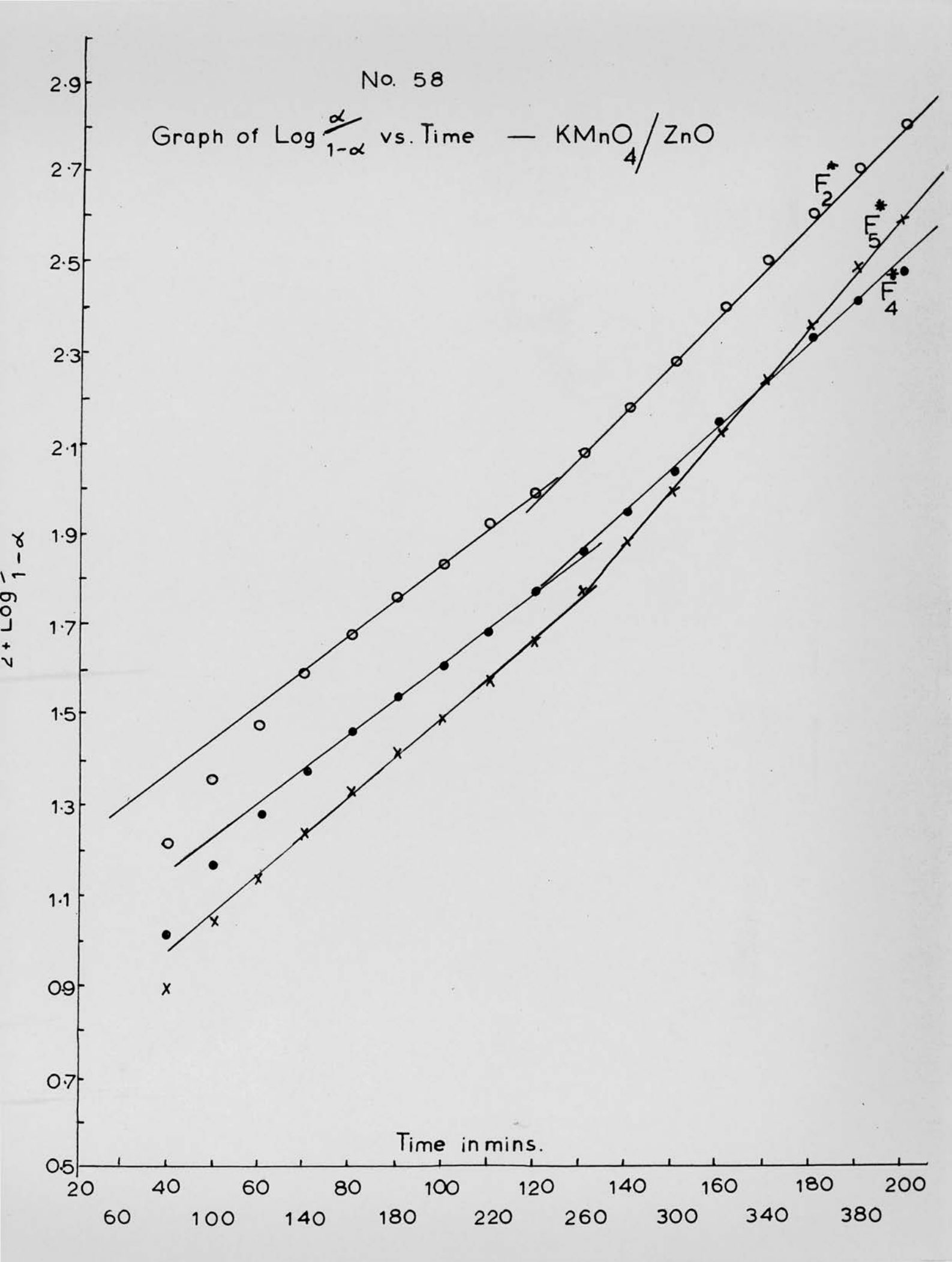
No. 58
Graph of Log α/1-α vs. Time — KMnO4/ZnO
F2*
F5*
F4*
2 + Log α/1-α
Time in mins.
2·9
2·7
2·5
2·3
2·1
1·9
1·7
1·5
1·3
1·1
0·9
0·7
0·5
20 40 60 80 100 120 140 160 180 200
60 100 140 180 220 260 300 340 380

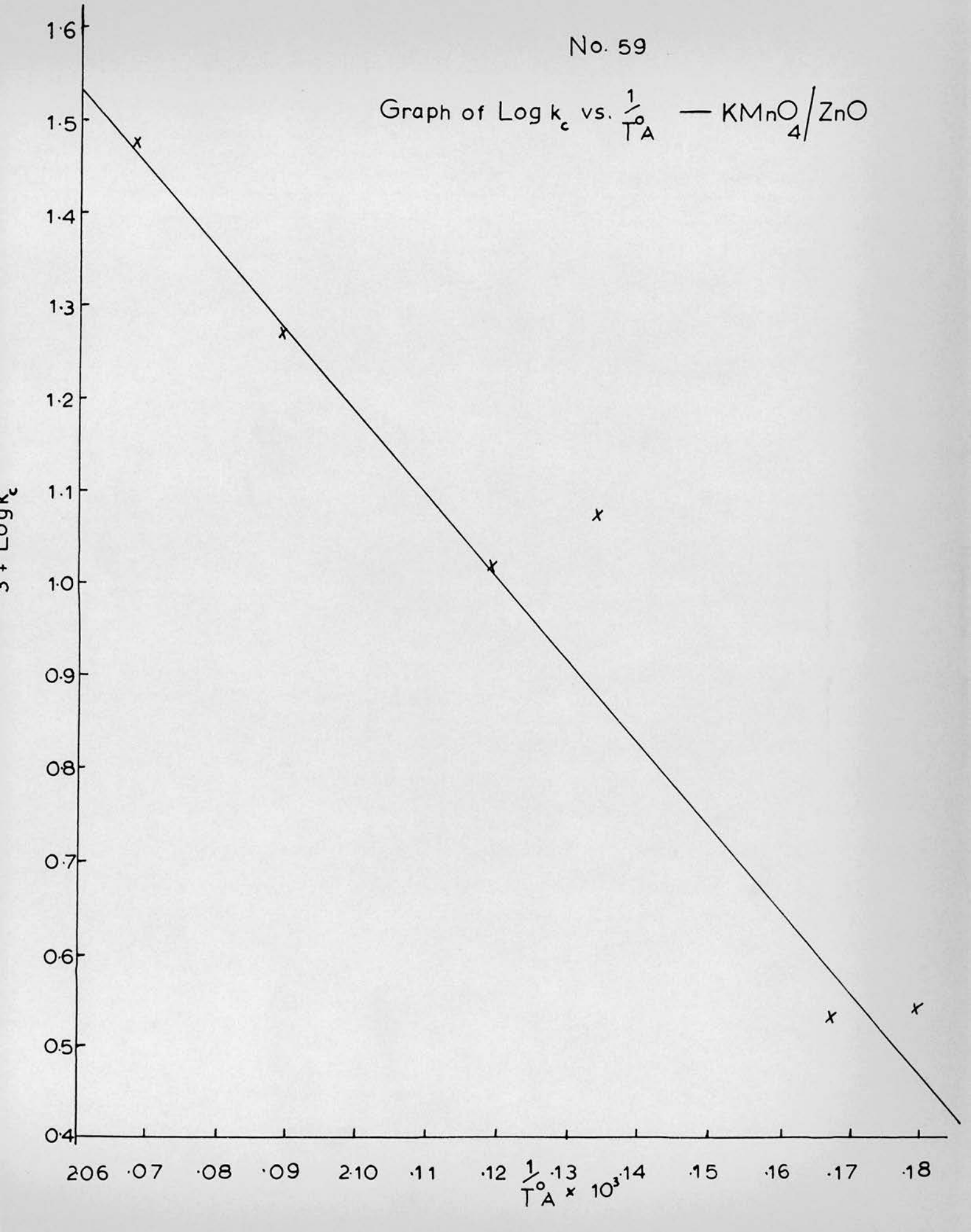
No. 59
Graph of Log k_c vs. $\frac{1}{T^\circ_A}$ — $KMnO_4/ZnO$
1·6
1·5
1·4
1·3
1·2
1·1
1·0
0·9
0·8
0·7
0·6
0·5
0·4
3 + Log k_c
206 ·07 ·08 ·09 2·10 ·11 ·12 ·13 ·14 ·15 ·16 ·17 ·18
$\frac{1}{T^\circ_A} \times 10^3$

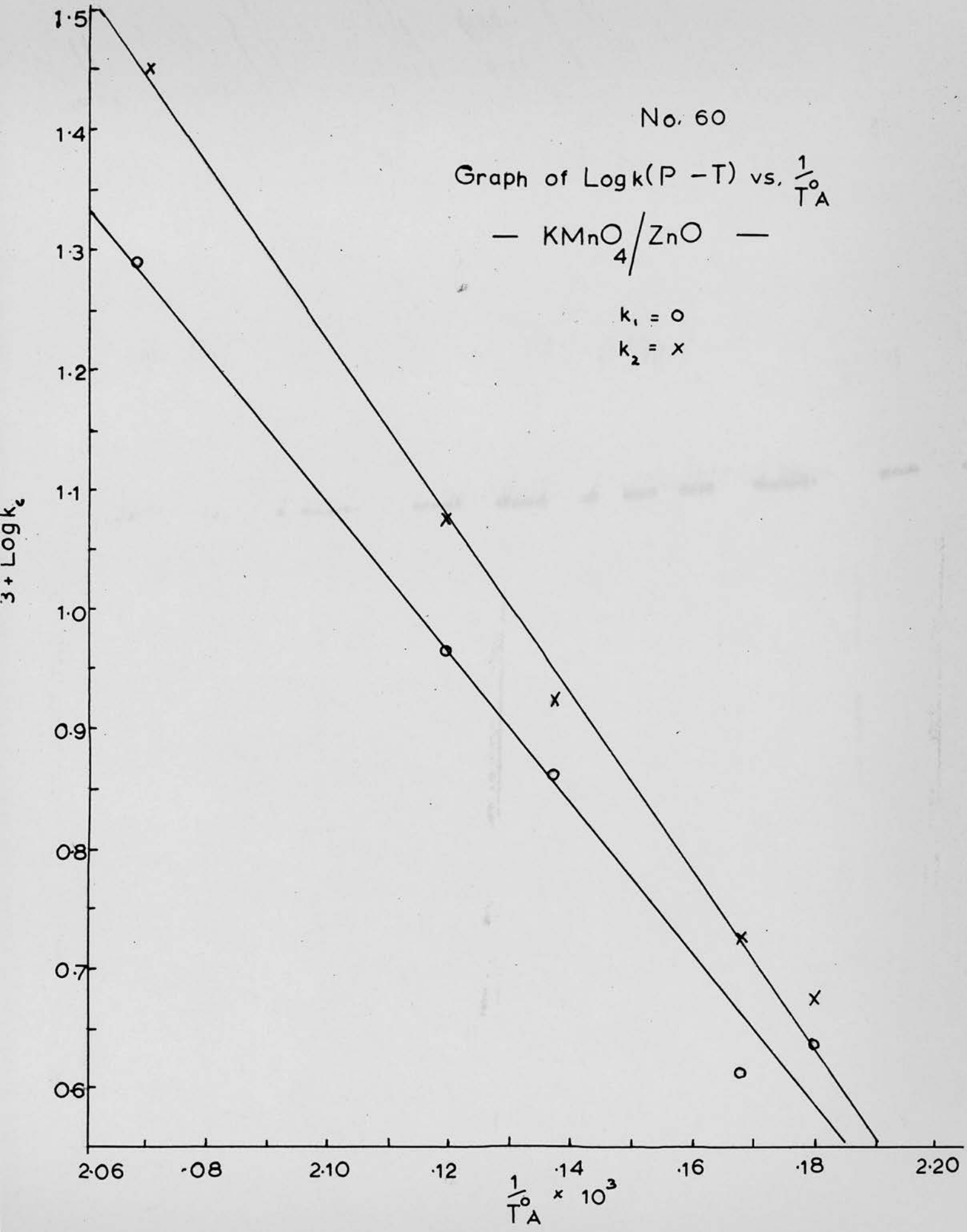
No. 60
Graph of Log k(P − T) vs. 1/T°A
— KMnO4/ZnO —
k1 = o
k2 = x
3 + Log k2
1·5
1·4
1·3
1·2
1·1
1·0
0·9
0·8
0·7
0·6
2·06
·08
2·10
·12
·14
·16
·18
2·20
1/T°A × 10³

3.3.5. Resistance Measurements for Potassium Permanganate/Zinc Oxide, 1000°C (G*)

Tables 54, 55, 56 and 57 and graphs 61, 62, 63 and 64 illustrate, for the system potassium permanganate/Zinc oxide (1000°C), the change in resistance during the decomposition and also the fit of the Prout-Tompkins equation over the later stages of the reaction.

In this system the resistance measurements again show an exponential decrease, over the range α = - 0 0.3, after α = 0.6 there is again little change in resistance.

The Prout-Tompkins equations holds over the region α = 0.2 - 0.9, two values of k being required, one for the acceleratory stage α = 0.2 - 0.5, the other for the decay stage α = 0.5 - 0.9.

Tables 54, 55 and 56	Analysis of system G*.
Table 57	Rate constants for system G*.
Graph 61	Plot of $\log_{10} R$ vs. Time.
Graph 62	Plot of $\log_{10} \frac{\alpha}{1-\alpha}$ vs. Time.
Graph 63	Arrhenius plot for "rate of conduction" which gives an activation energy of $E_{c_2} = 26 \pm 2$ K. cals./mole.
Graph 64	Arrhenius plot for acceleratory and decay stages which gives an activation energy of $E_1 = 29 \pm 2$ K. cals./mole. and $E_2 = 30 \pm 2$ K. cals./mole.

Table 54 System G* $KMnO_4/ZnO$ (1000°)

Run	G*1			G*2	
Temp.	203.6°C			199.2°C	
Time Min.	α x 10	P.T.	log R	α x 10	P.T.
5			6.24		
10	0.31	$\bar{2}$.51	6.13	0.16	$\bar{2}$.21
15			6.00		
20	0.50	$\bar{2}$.72	5.90	0.19	$\bar{2}$.30
25			5.81		
30	0.81	$\bar{2}$.95	5.70	0.32	$\bar{2}$.52
35			5.60		
40	1.13	$\bar{1}$.10	5.52	0.45	$\bar{2}$.68
45			5.44		
50	1.57	$\bar{1}$.27	5.39	0.63	$\bar{2}$.83
60	2.05	$\bar{1}$.41	5.25	0.86	$\bar{2}$.97
70	2.94	$\bar{1}$.62	5.05	1.29	$\bar{1}$.17
80	3.93	$\bar{1}$.81	4.87	1.79	$\bar{1}$.34
90	5.02	0.00	4.75	2.44	$\bar{1}$.51
100	5.88	0.16	4.65	3.25	$\bar{1}$.68
110	6.53	0.27	4.59	4.20	$\bar{1}$.86
120	7.06	0.38		5.12	0.02
130	7.56	0.49	4.57	5.98	0.17
140	8.00	0.60		6.64	0.30
150	8.45	0.74	4.51	7.27	0.43
160	8.78	0.86		7.72	0.53
170	9.10	1.00	4.45	7.98	0.60
180	9.39	1.19		8.51	0.76
190	9.59	1.37	4.43	9.01	0.96
200	9.73	1.56		9.06	0.99
210	9.86	1.84		9.32	1.14
220	9.97		4.38	9.53	1.31

Table 55 System C* $KMnO_4/ZnO$ (1000°)

Run		C*3			C*6	
Temp.		189.3°C			194.9°C	
Time Min.	α x 10	P.T.	log R	α x 10	P.T.	log R
5			6.56			6.34
10			6.54			6.28
15			6.53			6.21
20	0.03		6.49	0.03		6.15
25			6.46			
30			6.46			6.02
40	0.11	$\bar{2}$.06	6.40	0.28	$\bar{2}$.46	5.90
50			6.36			5.78
60	0.13	$\bar{2}$.11	6.32	0.51	$\bar{2}$.73	5.67
70			6.28			5.54
80	0.14	$\bar{2}$.16	6.25	0.72	$\bar{2}$.89	5.45
90			6.19			5.36
100	0.26	$\bar{2}$.42	6.00	1.10	$\bar{1}$.09	5.26
110			5.84			5.12
120	0.53	$\bar{2}$.75	5.71	1.48	$\bar{1}$.24	4.99
130			5.60			4.88
140	0.79	$\bar{2}$.93	5.50	2.13	$\bar{1}$.43	4.78
150			5.40			
160	1.13	$\bar{1}$.10	5.23	3.26	$\bar{1}$.68	4.60
180	1.64	$\bar{1}$.29	5.15	4.61	$\bar{1}$.93	4.53
200	2.20	$\bar{1}$.45	4.99	5.64	0.11	4.45
220	2.86	$\bar{1}$.60	4.88	6.36	0.24	4.43
240	3.83	$\bar{1}$.79	4.81	7.05	0.38	4.42
260	4.74	$\bar{1}$.96	4.70	7.62	0.50	4.42
280	5.54	0.09	4.65	8.05	0.62	4.42
300	6.40	0.25	4.62	8.54	0.77	
320	7.07	0.38		8.92	0.91	4.42
340	7.54	0.49		9.28	1.11	
360	7.97	0.59		9.51	1.29	
380	8.37	0.71		9.73	1.56	
400	8.69	0.82		9.87	1.89	
420	8.97	0.94		9.91		
440	9.19	1.05				
460	9.40	1.19				
480	9.56					
540	9.96					

Table 56 System G* $KMnO_4/ZnO$ (1000°)

Run	G*4			G*5		
Temp.	209.3°C			184.8°C		
Time Min.	α x 10	P.T.	log R	α x 10	P.T.	log R
5	0.35	$\bar{2}$.56	5.83			6.82
10	0.53	$\bar{2}$.74	5.65			6.79
15	0.70	$\bar{2}$.88	5.50			6.70
20	0.91	$\bar{1}$.00	5.34	0.03		6.69
25	1.19	$\bar{1}$.13	5.20			
30	1.42	$\bar{1}$.22	5.06			6.65
35	1.75	$\bar{1}$.33	4.93			
40	2.14	$\bar{1}$.43	4.80	0.12	$\bar{2}$.08	6.60
45	2.68	$\bar{1}$.56	4.68			
50	3.33	$\bar{1}$.70	4.57			6.55
60	4.74	$\bar{1}$.95	4.40	0.15	$\bar{2}$.17	6.51
70	5.89	0.16	4.30			6.46
80	6.70	0.31	4.25	0.24	$\bar{2}$.39	6.40
90	7.54	0.49	4.22			6.36
100	8.26	0.68	4.20	0.27	$\bar{2}$.44	6.30
110	8.93	0.92	4.20			6.25
120	9.42	1.21		0.37	$\bar{2}$.59	6.20
130	9.70	1.51	4.20			6.16
140	9.96			0.44	$\bar{2}$.66	6.11
150						6.06
160				0.55	$\bar{2}$.76	5.99
180				0.67	$\bar{2}$.85	5.87
220				0.93	$\bar{1}$.01	5.72
240				1.08	$\bar{1}$.08	5.62
260				1.31	$\bar{1}$.18	5.48
280				1.49	$\bar{1}$.24	5.36
300				1.83	$\bar{1}$.35	5.24
320				2.20	$\bar{1}$.45	5.15
340				2.69	$\bar{1}$.57	5.07
360				3.36	$\bar{1}$.72	4.99
400				4.80	1.97	
440				5.99	0.17	
480				6.71	0.31	
520				7.33	0.44	
560				8.12	0.64	
600				8.53	0.76	
640				8.92	0.92	
680				9.21		
700				9.36		

Table 57 Rate Constants for System G* $KMnO_4/ZnO$ (1000°)

Run	$1/T°A \times 10^3$	α-range	$k_c \times 10^2$	α-range	$k_1 \times 10^2$	α-range	$k_2 \times 10^2$
G*1	2.098	0.01-0.15	2.11	0.16-0.55	2.88	0.55-0.9	1.16
G*2	2.118	-	-	0.18-0.51	1.67	0.51-0.9	1.23
G*3	2.163	0.03-0.3	0.88	0.15-0.55	0.72	0.55-0.9	0.59
G*4	2.073	0.03-0.4	2.80	0.2 -0.52	2.40	0.52-0.9	1.75
G*5	2.184	0.01-0.2	0.49	0.18-0.54	0.63	0.54-0.9	0.38
G*6	2.137	0-0.3	1.16	0.21-0.52	1.24	0.52-0.9	0.64

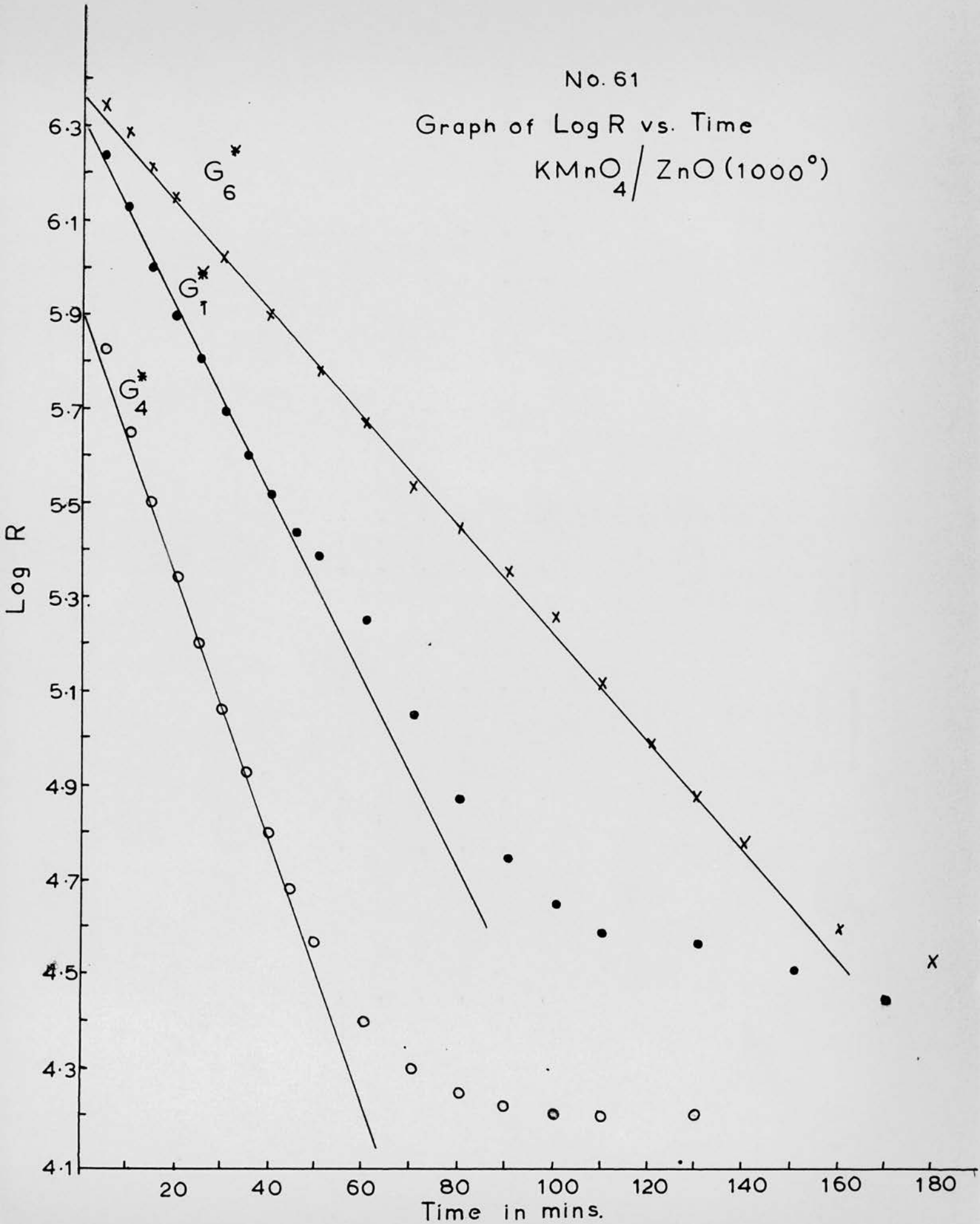
No. 61
Graph of Log R vs. Time
KMnO4 / ZnO (1000°)
G6
G1
G4
Log R
6·3
6·1
5·9
5·7
5·5
5·3
5·1
4·9
4·7
4·5
4·3
4·1
20
40
60
80
100
120
140
160
180
Time in mins.

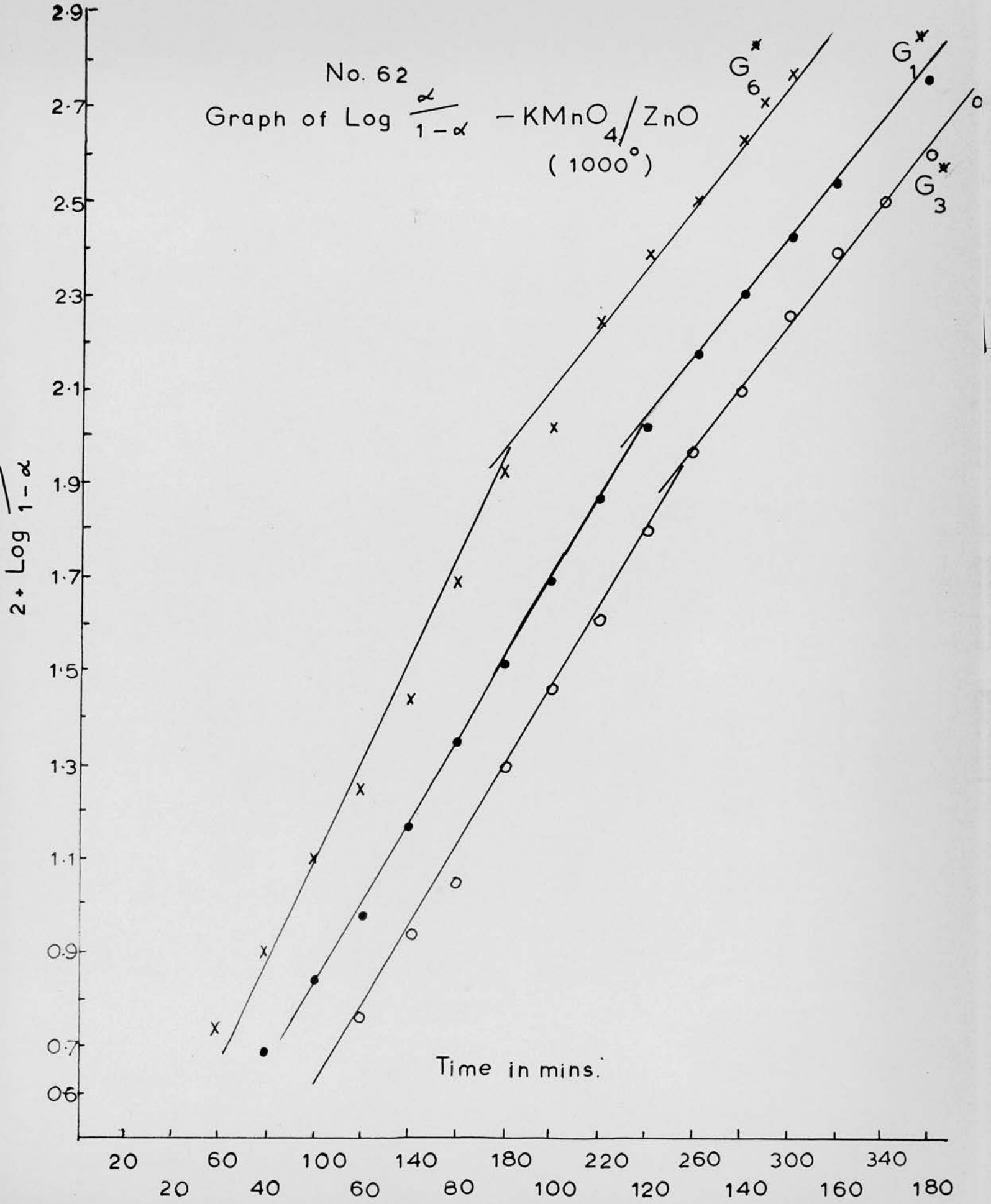
No. 62
Graph of Log α/1−α − KMnO4/ZnO
(1000°)
G6
G1
G3
2+ Log 1−α
Time in mins.
2·9
2·7
2·5
2·3
2·1
1·9
1·7
1·5
1·3
1·1
0·9
0·7
0·6
20 60 100 140 180 220 260 300 340
20 40 60 80 100 120 140 160 180

No. 63

Graph of Log k_c vs. $\frac{1}{T°_A}$ — $KMnO_4/ZnO$

(1000°)

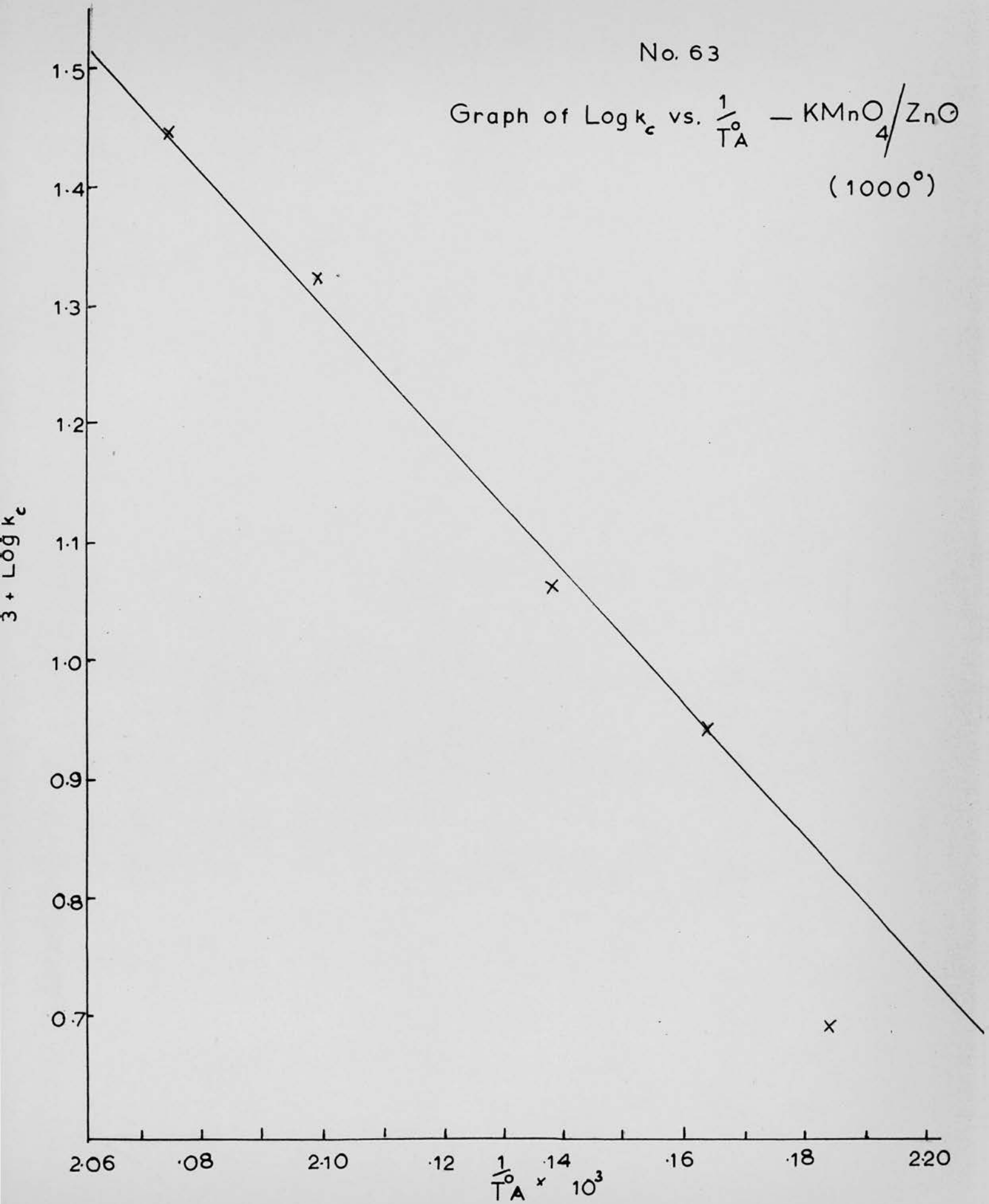

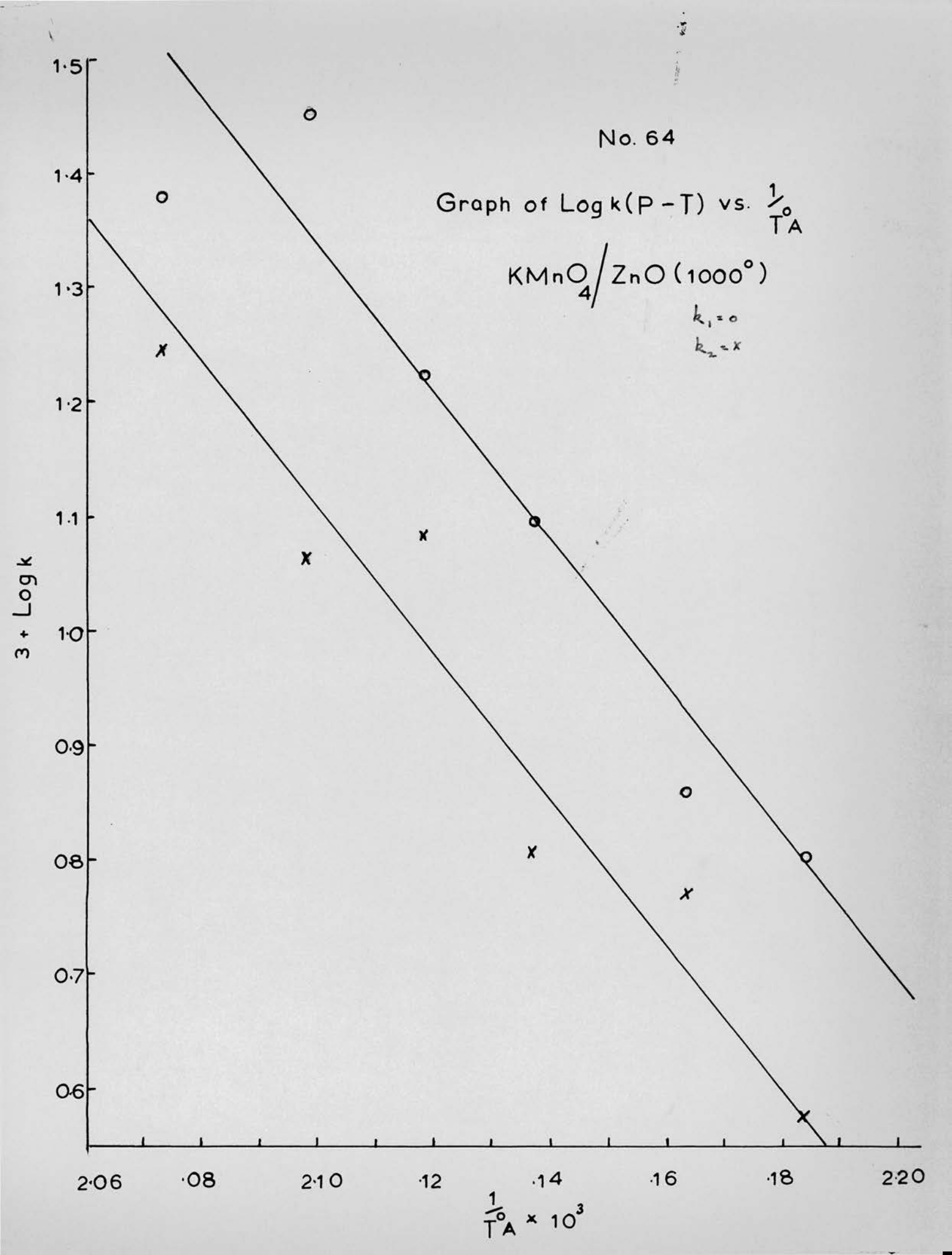
No. 64
Graph of Log k(P - T) vs. 1/T°A
KMnO4/ZnO (1000°)
k1 = o
k2 = x
3 + Log k
1·5
1·4
1·3
1·2
1·1
1·0
0·9
0·8
0·7
0·6
2·06
·08
2·10
·12
·14
·16
·18
2·20
1/T°A × 10³

3.3.6. Resistance Measurements for Potassium Permanganate/Zinc Oxide + 1 mole % Chromic Oxide (H*)

Tables 58, 59, 60 and 61 and graphs 65, 66, 67 and 68 illustrate, for the system potassium permanganate/zinc oxide + 1 mole % chromic oxide, the change in resistance during the decomposition and also the fit of the Prout-Tompkins equation over the later stages of the reaction.

In this system the resistance measurements again show an exponential decrease over the range $\alpha = 0 - 0.2$, after which there is a continued decrease until $\alpha = 0.6$ after which there is little change.

The Prout-Tompkins equation holds over the region $\alpha = 0.2 - 0.9$, two values of k being required, one for the acceleratory stage $\alpha = 0.2 - 0.54$, the other for the decay stage $\alpha = 0.54 - 0.9$.

Tables 58, 59 and 60	Analysis of system H*.
Table 61	Rate constants for system H*.
Graph 65	Plot of $\log_{10} R$ vs. Time.
Graph 66	Plot of $\log_{10} \frac{\alpha}{1-\alpha}$ vs. Time.
Graph 67	Arrhenius plot for "rate of change of conduction" which gives an activation energy of $E_{c_2} = 30$ K. cals./mole.
Graph 68	Arrhenius plot for acceleratory and decay stages which gives an activation energy of $E_1 = 33 \pm 2$ K. cals./mole. and $E_2 = 35$ K. cals./mole.

Table 58 System H* $KMnO_4/ZnO + Cr_2O_3$

Run	H*1			H*3		
Temp.	209.6°C			197.9°C		
Time Min.	α x 10	P.T.	log R	α x 10	P.T.	log R
5	0.38	$\bar{2}$.60	6.59			6.77
10	0.53	$\bar{2}$.74	6.43	0.15	$\bar{2}$.17	6.71
15	0.70	$\bar{2}$.88	6.29			
20	0.88	$\bar{2}$.98	6.15	0.28	$\bar{2}$.46	
25	1.12	$\bar{1}$.10	6.03			
30	1.39	$\bar{1}$.21	5.87	0.44	$\bar{2}$.67	6.48
35	1.77	$\bar{1}$.33	5.67			6.40
40	2.28	$\bar{1}$.47	5.53	0.61	$\bar{2}$.81	6.34
45	3.16	$\bar{1}$.66	5.39			6.26
50	4.39	$\bar{1}$.89	5.27	0.84	$\bar{2}$.96	6.20
52.5			5.19			
55	5.35	0.06	5.12			6.16
57.5			5.08			
60	6.01	0.18	5.04	1.09	$\bar{1}$.09	6.08
65	6.63	0.29	4.93			5.97
70	7.24	0.42	4.81	1.33	$\bar{1}$.18	5.85
75	7.68	0.52	4.72			5.70
80	8.08	0.62	4.61	1.64	$\bar{1}$.29	5.60
85	8.50	0.75	4.53			5.50
90	8.87	0.89	4.48	2.07	$\bar{1}$.42	5.41
95	9.17	1.04	4.45			
100	9.39	1.19	4.45	2.64	$\bar{1}$.55	5.27
110	9.79	1.67	4.42	3.46	$\bar{1}$.72	
120	9.98		4.40	4.40	$\bar{1}$.89	5.06
130			4.36	5.27	0.05	
140				5.91	0.16	4.93
150				6.46	0.26	
160				6.91	0.35	4.85
170				7.30	0.43	
180				7.68	0.52	4.75
190				7.99	0.60	
200				8.32	0.69	4.61
210				8.67	0.81	
220				8.91	0.91	4.54
230				9.16	1.04	
240				9.19	1.05	4.52
250				9.55	1.33	
260				9.72	1.54	4.51
270				9.85		
280				9.91		

Table 59 System H* $KMnO_4$ / ZnO + Dr_2O_3

Run	H*4			H*5		
Temp.	202.3°C			193.2°C		
Time Min.	α x 10	P.T.	log R	α x 10	P.T.	log R
5	0.20	$\bar{2}$.31	6.43			6.56
10	0.27	$\bar{2}$.44	6.30			6.51
15	0.38	2.60	6.19			6.46
20	0.45	$\bar{2}$.68	6.11	0.17	$\bar{2}$.24	6.40
25	0.58	$\bar{2}$.79	5.96			6.34
30	0.72	$\bar{2}$.89	5.84			6.27
35	0.89	$\bar{2}$.99	5.74			6.23
40	1.05	$\bar{1}$.07	5.64	0.31	$\bar{2}$.51	6.19
45	1.28	$\bar{1}$.16	5.54			6.13
50	1.56	$\bar{1}$.27	5.45			6.08
55	1.86	$\bar{1}$.36	5.35			6.02
60	2.30	$\bar{1}$.47	5.26	0.47	$\bar{2}$.69	5.98
65	2.91	$\bar{1}$.61	5.17			5.93
70	3.72	$\bar{1}$.77	5.08			5.89
75	4.53	$\bar{1}$.92	5.00			5.85
80	5.25	0.04		0.72	$\bar{2}$.89	5.80
85	5.79	0.14	4.89			
90	6.24	0.22				5.70
95	6.67	0.30	4.81			
100	7.05	0.38		0.97	$\bar{1}$.03	5.61
105	7.38	0.45	4.74			
110	7.73	0.53				5.53
115	8.03	0.61	4.67			
120	8.24	0.67		1.41	$\bar{1}$.21	5.45
130	8.77	0.85	4.57			
140	9.16	1.04		2.03	$\bar{1}$.41	5.30
150	9.49	1.27				
160	9.70	1.51	4.48	3.17	$\bar{1}$.67	5.18
180			4.45	4.72	1.95	5.07
200				5.89	0.16	4.98
220				6.70	0.31	
240				7.34	0.44	4.87
260				7.86	0.56	
280				8.31	0.69	4.79
300				8.75	0.85	
320				9.16	1.04	4.74
340				9.42	1.21	
360				9.69	1.49	
380				9.84	1.79	
400				9.98		

Table 60 System H* $KMnO_4$ / $ZnO + Cr_2O_3$

Run		H*6			H*2	
Temp.		183.2°C			189.5°C	
Time Min.	α x 10	P.T.	log R	α x 10	P.T.	log R
5			7.08			6.32
10			7.02			6.26
15			6.98			6.21
20			6.95	0.18	$\bar{2}$.26	6.16
25			7.07			6.13
30			7.04			6.08
35			7.00			6.02
40	0.11	$\bar{2}$.05	6.98	0.22	$\bar{2}$.36	5.98
45			6.95			5.94
50			6.92			5.90
55						5.87
60	0.14	$\bar{2}$.16	6.88	0.27	$\bar{2}$.44	5.83
70			6.83			5.76
80	0.17	$\bar{2}$.25	6.77	0.42	$\bar{2}$.64	5.68
90			6.72			5.60
100	0.24	$\bar{2}$.39	6.68	0.53	$\bar{2}$.75	5.53
120	0.32	$\bar{2}$.52	6.66	0.71	$\bar{2}$.88	5.46
140	0.37	$\bar{2}$.58	6.60	0.89	$\bar{2}$.99	5.28
160	0.48	$\bar{2}$.70	6.53	1.11	$\bar{1}$.10	5.17
180	0.60	$\bar{2}$.81	6.43	1.38	$\bar{1}$.20	5.07
200	0.67	$\bar{2}$.85	6.36	1.76	$\bar{1}$.33	4.98
220	0.81	$\bar{2}$.94	6.28	2.22	$\bar{1}$.46	5.13
240	0.97	$\bar{1}$.03	6.20	2.91	$\bar{1}$.61	5.03
260	1.11	$\bar{1}$.10	6.13	3.80	$\bar{1}$.79	4.92
280	1.29	$\bar{1}$.17	6.04	4.76	$\bar{1}$.96	4.82
300	1.56	$\bar{1}$.26	5.93	5.56	0.10	4.76
320	1.75	$\bar{1}$.33	5.83	6.11	0.20	4.71
340	2.05	$\bar{1}$.41	5.73	6.62	0.29	4.67
360	2.38	$\bar{1}$.49	5.64	7.09	0.39	4.64
380	2.73	$\bar{1}$.57	5.56	7.51	0.48	4.62
400	3.29	$\bar{1}$.69	5.51	7.80	0.55	4.60
420	3.90	$\bar{1}$.81	5.43	8.22	0.67	4.60
440	4.59	$\bar{1}$.93		8.47	0.74	4.60
460	5.21	0.04		8.73	0.84	
480	5.72	0.13		9.07	0.99	
500	6.06	0.19		9.31	1.13	
540	6.70	0.31		9.71	1.53	
580	7.27	0.43		9.96		
640	7.92	0.58				
680	8.25	0.67				
720	8.57	0.78				
760	8.89	0.90				
840	9.40					

Table 61 Rate Constants for System H* $KMnO_4$/ZnO + Cr_2O_3

Run	$1/T^oA \times 10^3$	α- range	$k_{c_1} \times 10^3$	α- range	$k_{c_2} \times 10^2$	α- range	$k_1 \times 10^2$	α- range	$k_2 \times 10^2$
H*1	2.072	-	-	0-0.14	2.74	0.23-0.54	4.07	0.54-0.9	2.36
H*2	2.162	0-0.03	9.32	0.03-0.1	0.73	0.18-0.56	0.80	0.56-0.9	0.45
H*3	2.124	-	-	0.01-0.14	1.27	0.15-0.59	1.37	0.59-0.9	1.0
H*4	2.104	-	-	0.02-0.16	2.27	0.18-0.53	2.94	0.53-0.9	1.53
H*5	2.145	-	-	0-0.10	1.07	0.2 -0.54	1.36	0.54-0.9	0.69
H*6	2.192	0-0.02	5.29	0.02-0.24	0.41	0.2 -0.57	0.53	0.57-0.9	0.26

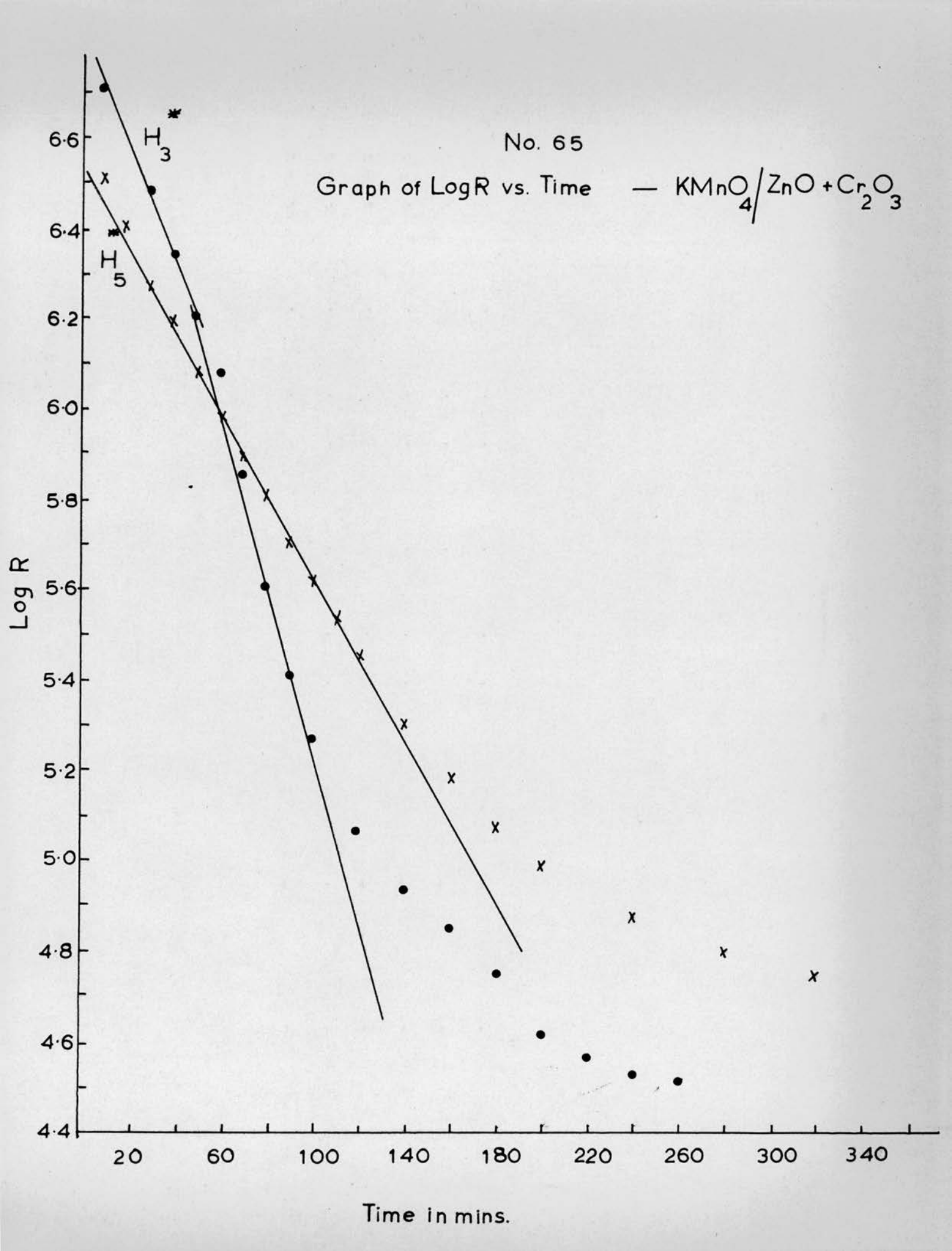
No. 65
Graph of LogR vs. Time — $KMnO_4/ZnO + Cr_2O_3$
H_3
H_5
Log R
6·6
6·4
6·2
6·0
5·8
5·6
5·4
5·2
5·0
4·8
4·6
4·4
20
60
100
140
180
220
260
300
340
Time in mins.

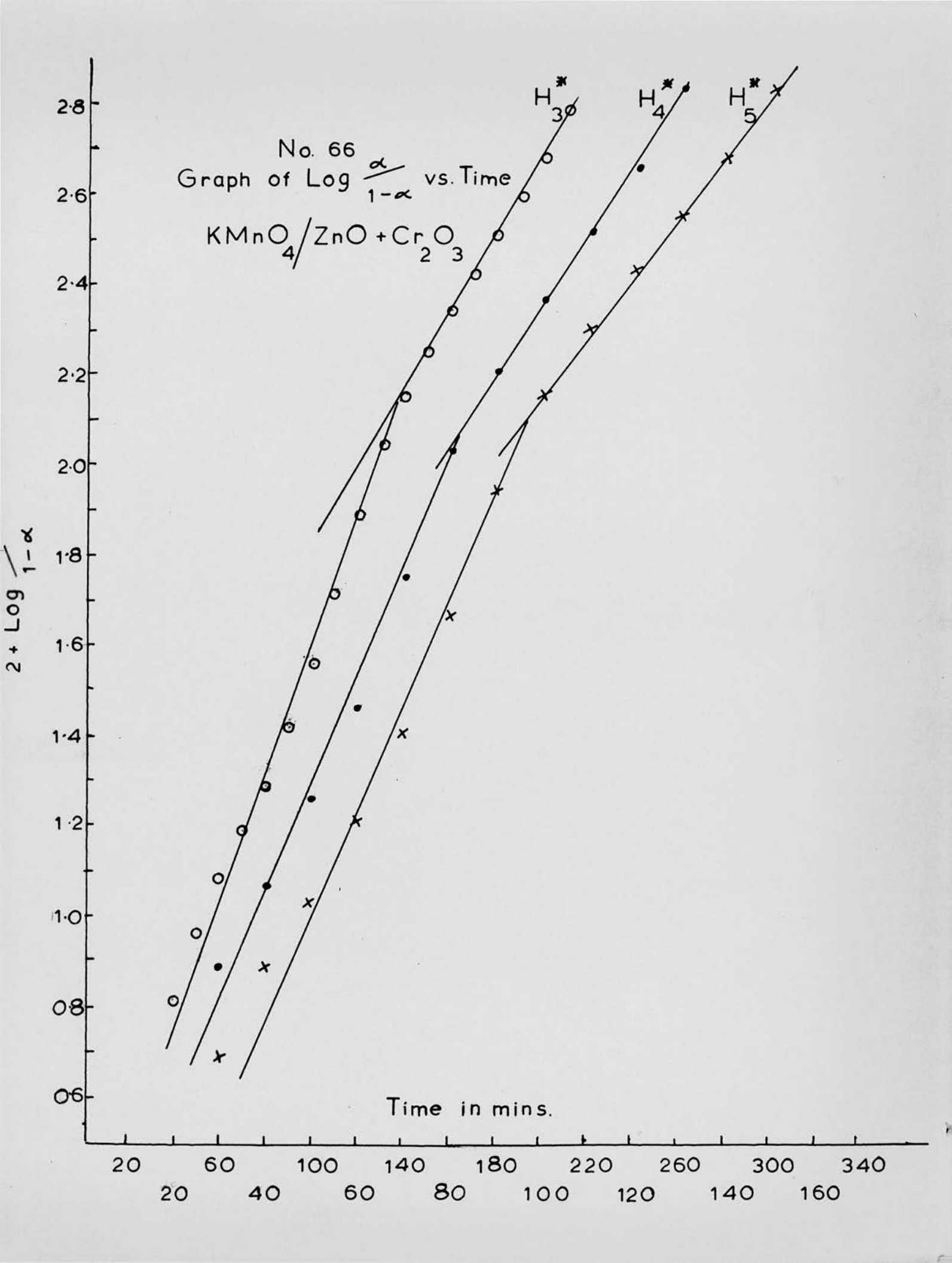
No. 66
Graph of Log α/1-α vs. Time
KMnO4/ZnO + Cr2O3
H*30
H*4
H*5
2 + Log α/1-α
2·8
2·6
2·4
2·2
2·0
1·8
1·6
1·4
1·2
1·0
0·8
0·6
Time in mins.
20 60 100 140 180 220 260 300 340
20 40 60 80 100 120 140 160

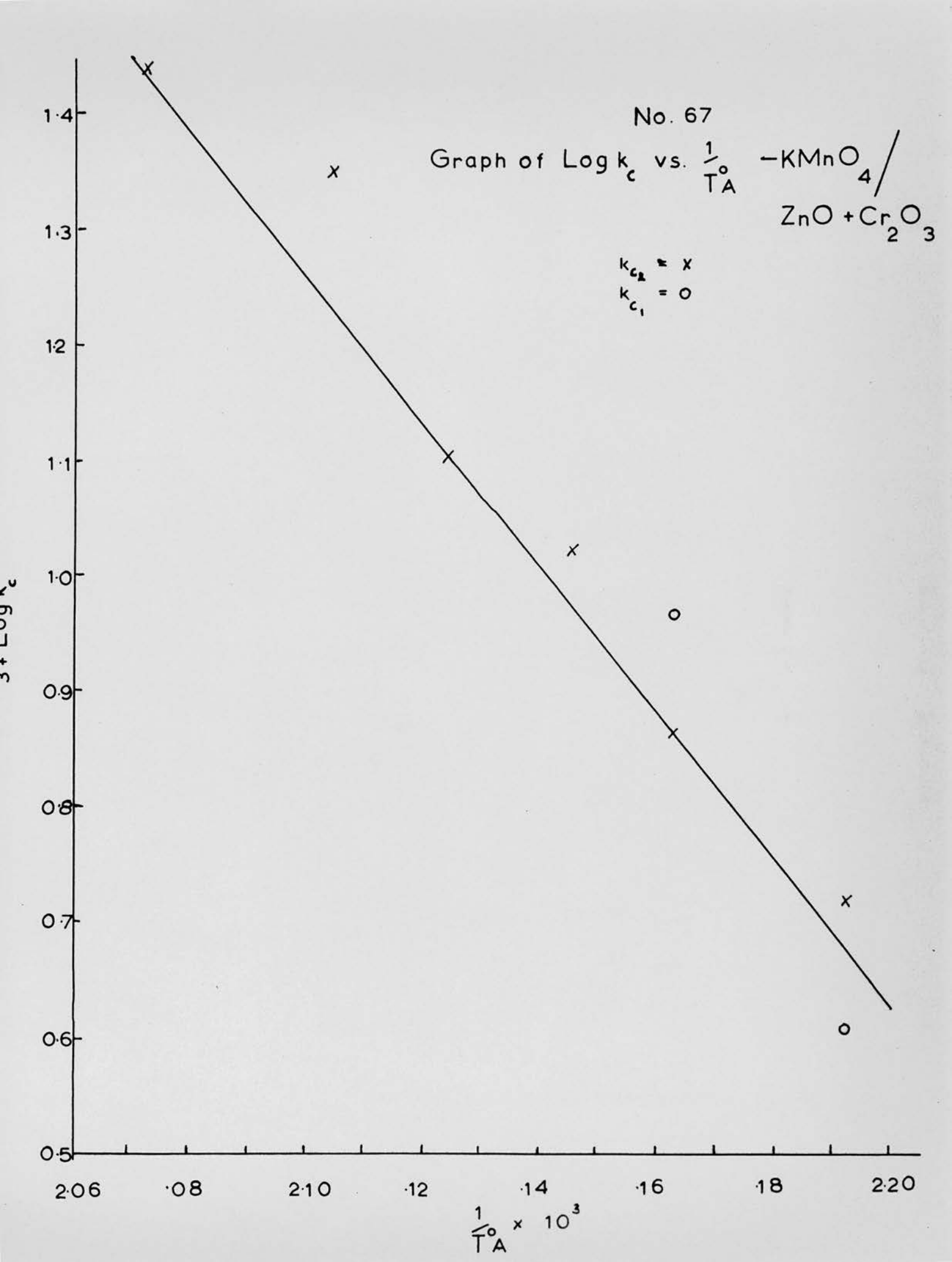
No. 67
Graph of Log k_c vs. $\frac{1}{T°_A}$ — $KMnO_4$ / $ZnO + Cr_2O_3$
k_{c_2} = X
k_{c_1} = O
3 + Log k_c
1·4
1·3
1·2
1·1
1·0
0·9
0·8
0·7
0·6
0·5
2·06
·08
2·10
·12
·14
·16
·18
2·20
$\frac{1}{T°_A} \times 10^3$

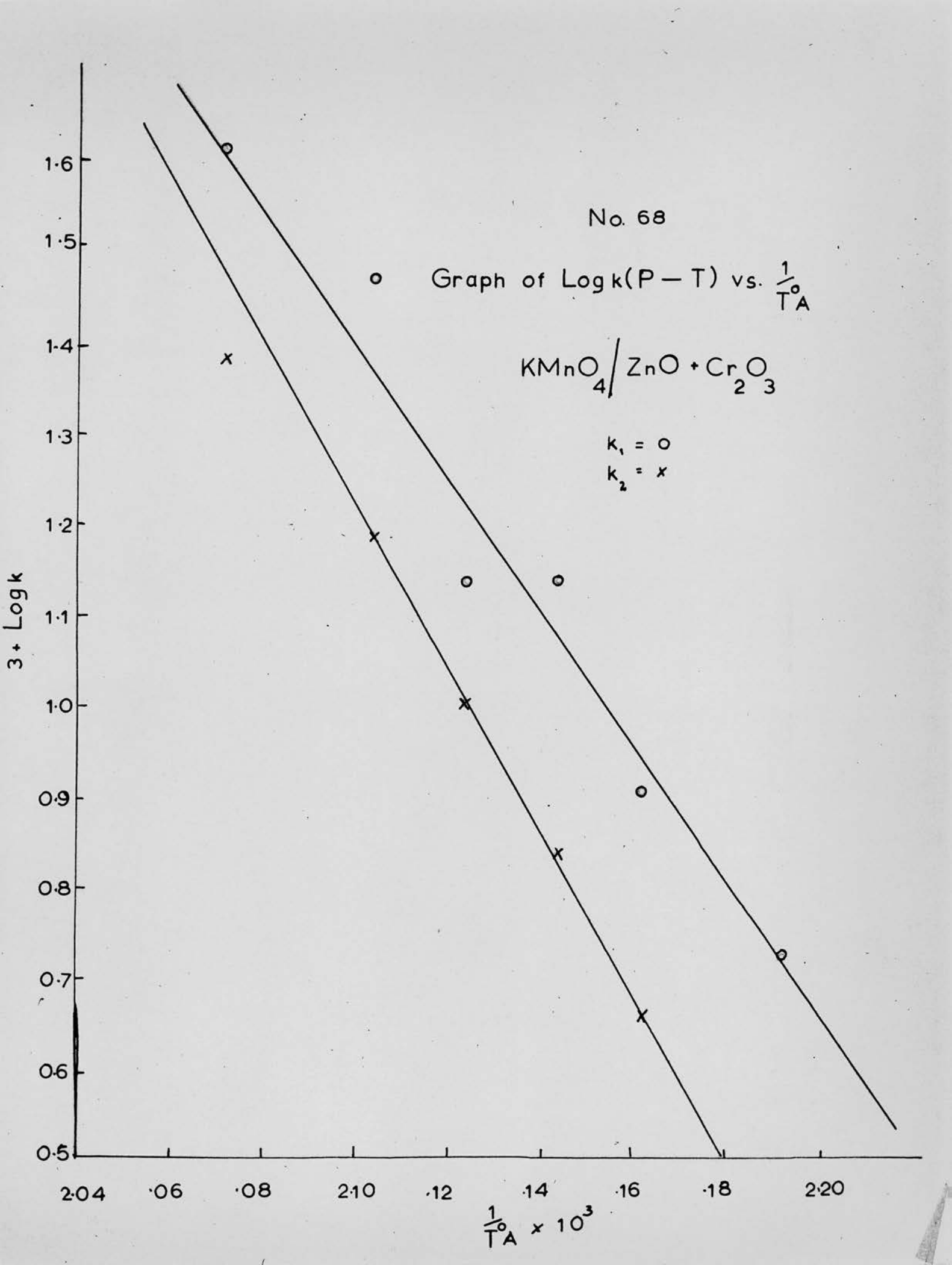
No. 68
o Graph of Log k(P — T) vs. 1/T°A
KMnO4 / ZnO + Cr2O3
k1 = o
k2 = x
3 + Log k
1·6
1·5
1·4
1·3
1·2
1·1
1·0
0·9
0·8
0·7
0·6
0·5
2·04
·06
·08
2·10
·12
·14
·16
·18
2·20
1/T°A x 10³

3.3.7 Resistance Measurements for Potassium Permanganate/Nickel Oxide (I*)

Graph 78 illustrates a typical example of the change in resistance with temperature for the system potassium permanganate/nickel oxide. This system was treated in exactly the same manner as the others but the results were strikingly different. Thus while initially the resistance dropped normally with increasing temperature at approximately 90°C the resistance commenced to rise quite sharply until the working temperature was reached, thereafter there was no change in resistance throughout the decomposition of the potassium permanganate. Such behaviour would tend to suggest that the initial fall in resistance with temperature is due to a surface species which is destroyed at higher temperatures. The temperature at which this destruction occurs suggesting that the species may be water although it is difficult to understand why only this system is so affected.

No. 78

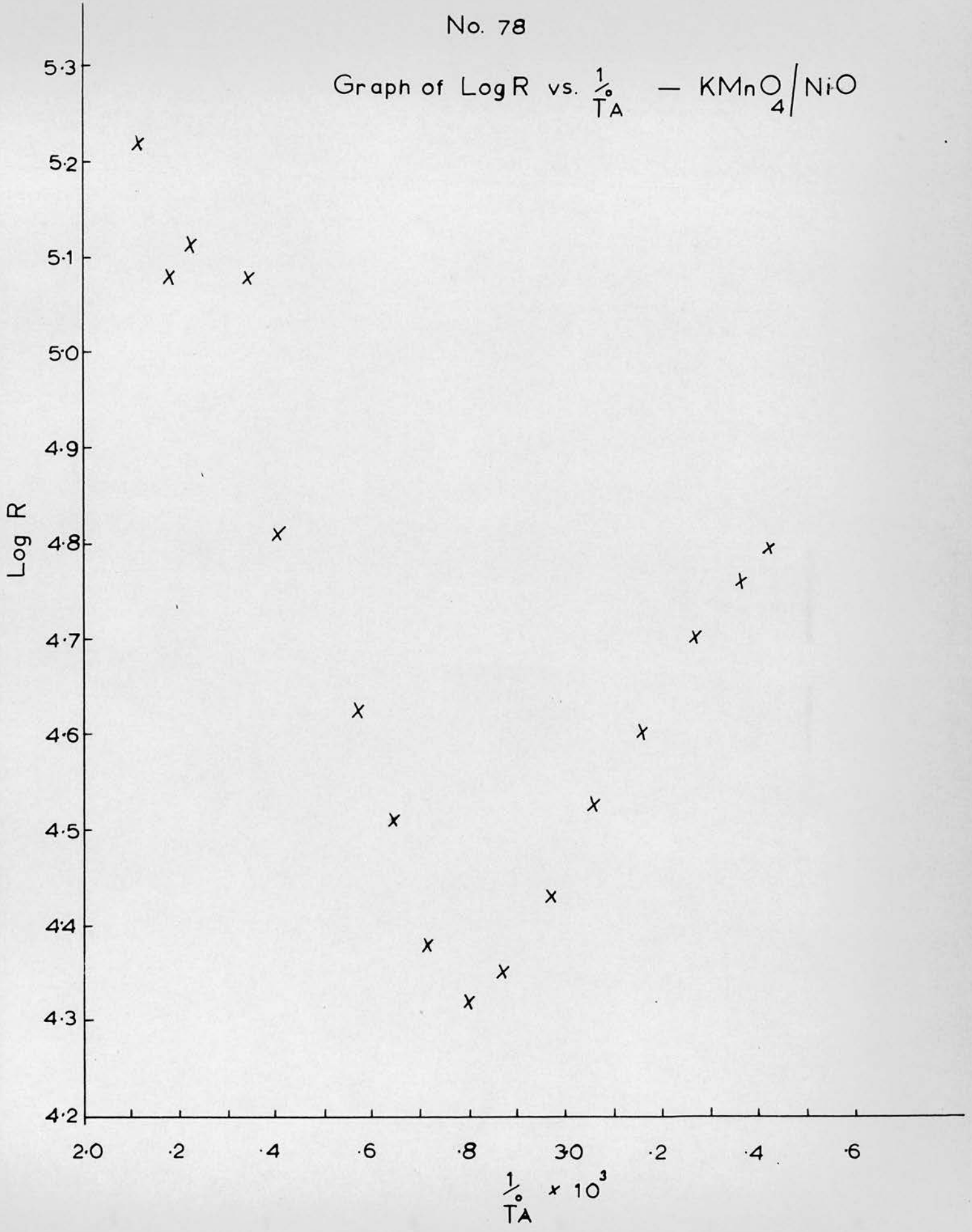
Graph of Log R vs. 1/TA — KMnO4/NiO
Log R
5·3
5·2
5·1
5·0
4·9
4·8
4·7
4·6
4·5
4·4
4·3
4·2
2·0
·2
·4
·6
·8
30
·2
·4
·6
1/TA × 10³

3.3.8. Resistance Measurements for Potassium Permanganate/Nickel Oxide (1000°C) (J*)

Tables 62, 63, 64 and 65 and graphs 69, 70, 71 and 72 illustrate, for the system potassium permanganate/nickel oxide (1000°C), the change in resistance during the decomposition and also the fit of the Prout-Tompkins equation over the later stages of the reaction.

In this system the resistance measurements again show an exponential decrease over the range $\alpha = 0 - 0.5$, after which there is little change in resistance.

The Prout-Tompkins equation holds over the region $\alpha = 0.1 - 0.9$, two values of k being required, one for the acceleratory stage $\alpha = 0.1 - 0.5$, the other for the decay stage $\alpha = 0.5 - 0.9$.

Tables 62, 63 and 64	Analysis of system J*.
Table 65	Rate constants for system J*.
Graph 69	Plot of $\log_{10} R$ vs. Time.
Graph 70	Plot of $\log_{10} \frac{\alpha}{1-\alpha}$ vs. Time.
Graph 71	Arrhenius plot for "rate of change of conduction" which gives an activation energy of $E_{c_2} = 33 \pm 2$ K. cals./mole.
Graph 72	Arrhenius plot for acceleratory and decay stages which gives an activation energy of $E_1 = 40 \pm 2$ K. cals./mole. and $E_2 = 25 \pm 2$ K. cals./mole.

Table 62 System J* $KMnO_4$ / NiO (1000°)

Run		J*2			J*6	
Temp.		188.0°C			184.4°C	
Time Min.	α x 10	P.T.	log R	α x 10	P.T.	log R
10			5.99			5.82
20			5.95	0.13	$\bar{2}$.13	5.81
30			5.93			5.80
40	0.19	$\bar{2}$.29	5.93	0.13	$\bar{2}$.13	5.78
50			5.90			5.77
60	0.22	$\bar{2}$.36	5.89	0.15	$\bar{2}$.19	5.76
70			5.88			5.74
80	0.37	$\bar{2}$.58	5.86	0.15	$\bar{2}$.19	5.73
90			5.84			5.72
100	0.40	$\bar{2}$.62	5.81			5.71
110			5.79			5.70
120	0.53	$\bar{2}$.75	5.75	0.19	$\bar{2}$.28	
130			5.70			5.68
140	0.64	$\bar{2}$.84	5.66			5.67
150			5.62			5.66
160	0.79	$\bar{2}$.93	5.55			5.64
170			5.47			5.62
180	1.01	$\bar{1}$.05	5.38	0.21	$\bar{2}$.33	5.61
200	1.41	$\bar{1}$.22	5.22	0.38	$\bar{2}$.59	
220	2.30	$\bar{1}$.47	5.45	0.72	$\bar{2}$.89	
240	3.10	$\bar{1}$.66	5.34	1.08	$\bar{1}$.08	
260	4.03	$\bar{1}$.83	5.21	1.48	$\bar{1}$.24	
280	4.88	$\bar{1}$.98	5.15	2.05	$\bar{1}$.41	
300	5.79	0.14		2.69	$\bar{1}$.56	
320	6.26	0.22	5.05	3.41	$\bar{1}$.71	
340	6.79	0.32	5.02	4.15	$\bar{1}$.85	
360	7.27	0.42	4.98	4.87	$\bar{1}$.98	
380	7.59	0.50	4.96	5.46	0.08	
400	7.93	0.58		5.99	0.17	
420	8.23	0.67		6.40	0.25	
440	8.52	0.76		6.80	0.33	
460	8.73	0.84		7.18	0.40	
480	8.99	0.95		7.54	0.49	
500	9.16	1.08		7.88	0.57	
520	9.23	1.17		8.13	0.64	
540	9.37	1.30		8.34	0.70	
560	9.52	1.42		8.60	0.79	
580	9.63	1.48		8.83		
600	9.68			9.02	0.96	
620	9.81			9.24		
640	9.84			9.32	1.14	
660	9.89			9.43		
680				9.60	1.38	
700				9.62		

Table 63 System J* $KMnO_4$ / NiO (1000°)

Run	J*1			J*3		
Temp.	209.3°C			204.6°C		
Time Min.	α x 10	P.T.	log R	α x 10	P.T.	log R
5	0.57	$\bar{2}$.78	5.81			5.49
10	0.74	$\bar{2}$.90	5.68			5.43
15	0.92	$\bar{1}$.00	5.53			5.36
20	1.21	$\bar{1}$.14	5.34			5.28
25	1.61	$\bar{1}$.28	5.18	0.19	$\bar{2}$.28	5.20
30	2.23	$\bar{1}$.46	5.03	0.21	$\bar{2}$.33	5.09
35	3.07	$\bar{1}$.65	4.90	0.34	$\bar{2}$.54	4.98
40	3.99	$\bar{1}$.82	4.78	0.49	$\bar{2}$.71	4.86
45	4.83	$\bar{1}$.97	4.67	0.83	$\bar{2}$.95	4.75
50	5.52	0.09	4.58	1.37	$\bar{1}$.20	4.63
55	5.06	0.19	4.50	2.09	$\bar{1}$.42	4.53
60	6.56	0.28	4.49	2.94	$\bar{1}$.62	4.43
65	7.03	0.37		3.84	$\bar{1}$.79	4.36
70	7.39	0.45	4.45	4.64	$\bar{1}$.94	4.30
75	7.79	0.55		5.27	0.05	
80	8.08	0.62	4.46	5.82	0.14	4.22
85	8.33	0.70		6.29	0.23	
90	8.59	0.78	4.45	6.71	0.31	4.16
95	8.85	0.89		7.08	0.38	
100	9.05	0.98	4.42	7.35	0.44	4.30
105	9.20	1.06		7.67		
110	9.43	1.22		7.91	0.58	4.30
120	9.71	1.52	4.40	8.37	0.71	4.30
130	9.95			8.70	0.82	
140			4.36	8.98	0.94	4.36
150				9.23	1.08	
160				9.46	1.25	4.49
170				9.65	1.44	
180				9.79		

Table 64 System J* $KMnO_4$ / NiO (1000°)

Run	J*4			J*5		
Temp.	198.8°C			193.7°C		
Time Min.	α x 10	P.T.	log R	α x 10	P.T.	log R
5			6.28			5.48
10			6.24			5.46
15			6.19			
20	0.14	$\bar{2}$.14	6.14			5.42
25			6.09			
30	0.22	$\bar{2}$.35	6.06			5.37
35			6.00			
40	0.23	$\bar{2}$.38	5.95	0.13	$\bar{2}$.11	5.33
45			5.89			
50	0.26	$\bar{2}$.43	5.84			5.30
55			5.77			
60	0.41	$\bar{2}$.63	5.70	0.19	$\bar{2}$.29	5.23
65			5.66			
70	0.69	$\bar{2}$.87	5.59			5.18
75			5.53			
80	1.23	$\bar{1}$.15	5.46	0.36	$\bar{2}$.57	5.11
85			5.40			
90	2.04	$\bar{1}$.41	5.34			5.01
95			5.28			
100	3.01	$\bar{1}$.63	5.23	0.54	$\bar{2}$.75	4.90
110	3.97	$\bar{1}$.82	5.15			
120	4.82	$\bar{1}$.85	5.07	1.24	$\bar{1}$.15	4.89
130	5.54	0.09	5.00	1.75	$\bar{1}$.33	4.77
140	6.07	0.19	4.95	2.42	$\bar{1}$.50	4.67
150	6.56	0.28	4.90	3.20	$\bar{1}$.67	4.58
160	6.99	0.36	4.87	3.97	$\bar{1}$.82	4.50
170	7.33	0.44		4.67	$\bar{1}$.94	4.43
180	7.67	0.52	4.81	5.24	0.04	4.38
190	7.95	0.59		5.74	0.13	
200	8.22	0.66	4.78	6.15	0.20	4.30
210	8.47	0.74		6.66	0.30	
220	8.63	0.80	4.75	6.89	0.35	4.30
230	8.79	0.86		7.19	0.41	
240	9.01	0.96	4.70	7.51	0.48	4.28
250	9.16	1.04		7.78	0.54	
260	9.32	1.33	4.64	7.95	0.59	4.29
270	9.45			8.19	0.65	
280	9.59	1.37	4.59	8.39	0.72	4.30
290	9.73			8.57	0.78	
300	9.84	1.77	4.54	8.70	0.82	4.32
320				8.98	0.94	4.34
340				9.23	1.08	
360				9.46	1.24	4.40
380				9.67	1.46	4.40
400				9.83		4.40

Table 65 Rate Constants for System J* $KMnO_4/NiO$ (1000°)

Run	$1/T^{\circ}A \times 10^3$	α- range	$k_{c_1} \times 10^3$	α- range	$k_{c_2} \times 10^2$	α- range	$k_1 \times 10^2$	α-range	$k_2 \times 10^2$
J*1	2.073	-	-	0-0.52	2.99	0.09-0.5	3.38	0.5 -0.9	1.77
J*2	2.169	0-0.05	1.70	0.05-0.48	0.67	0.08-0.5	0.92	0.5 -0.9	0.44
J*3	2.094	-	-	0-0.40	2.20	0.09-0.47	4.32	0.47-0.95	1.23
J*4	2.120	-	-	0-0.40	1.19	0.08-0.45	2.52	0.45-0.9	0.81
J*5	2.143	0-0.03	4.28	0.03-0.5	0.97	0.09-0.5	1.67	0.5 -0.9	0.66
J*6	2.186	0-0.02	1.24	-	-	0.07-0.45	0.56	0.45-0.9	0.39

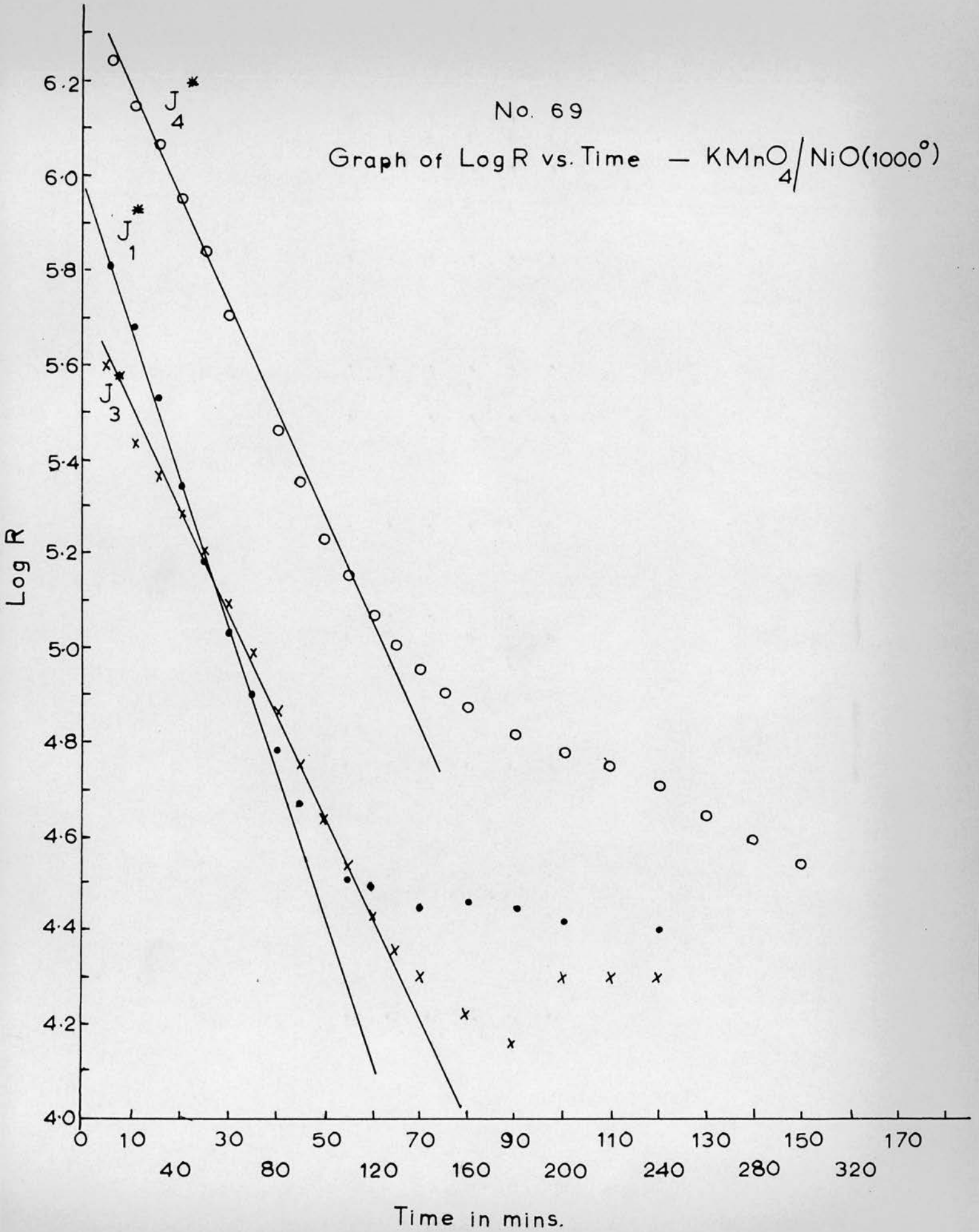
No. 69
Graph of Log R vs. Time — KMnO4/NiO(1000°)
J4
J1
J3
Log R
6·2
6·0
5·8
5·6
5·4
5·2
5·0
4·8
4·6
4·4
4·2
4·0
0
10
30
50
70
90
110
130
150
170
40
80
120
160
200
240
280
320
Time in mins.

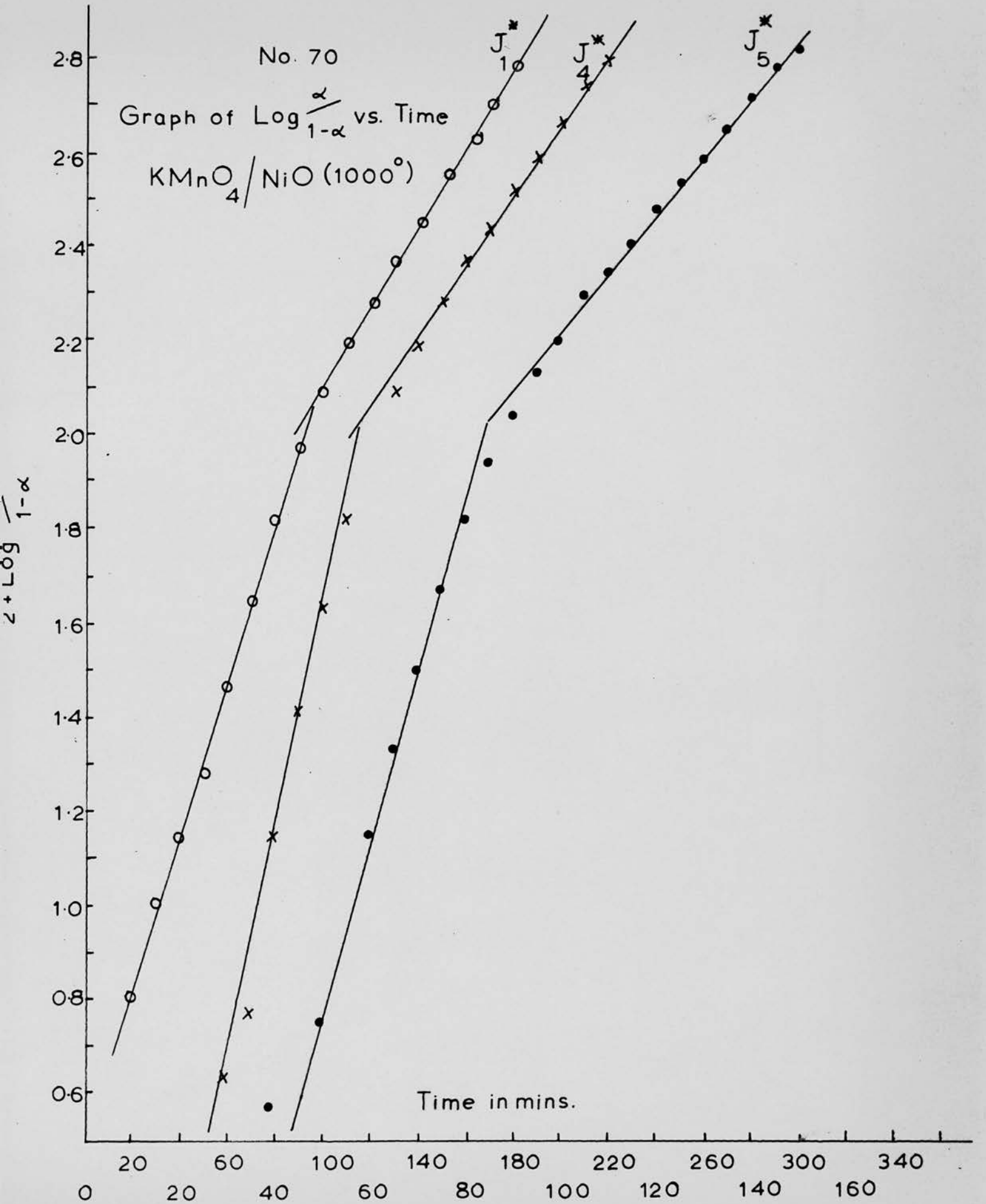
No. 70
Graph of Log α/1-α vs. Time
KMnO4/NiO (1000°)
J*1
J*4
J*5
2·8
2·6
2·4
2·2
2·0
1·8
1·6
1·4
1·2
1·0
0·8
0·6
2 + Log α/1-α
Time in mins.
20
60
100
140
180
220
260
300
340
0
20
40
60
80
100
120
140
160

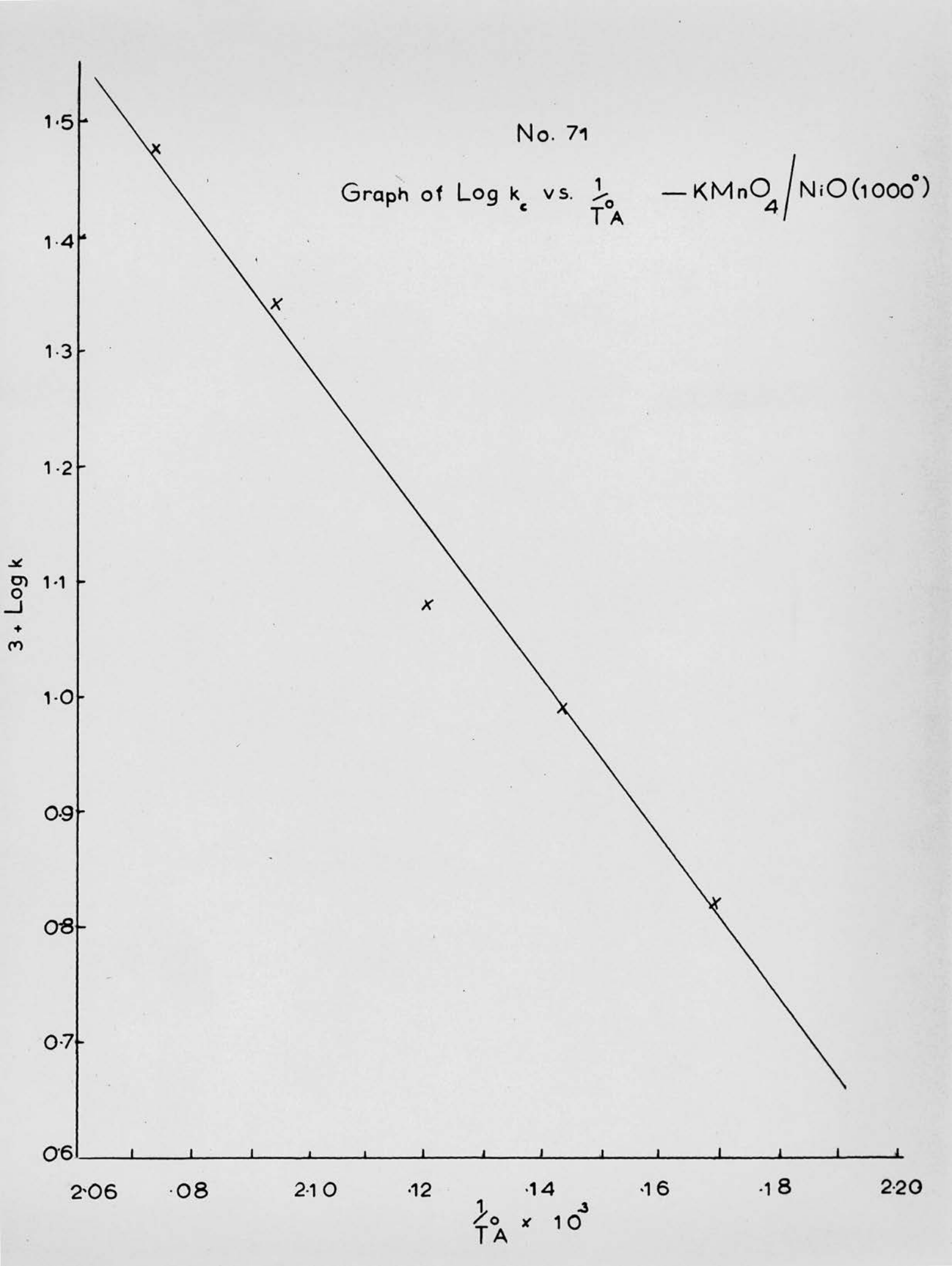
No. 71
Graph of Log k_c vs. $\frac{1}{T°A}$ — $KMnO_4$ / NiO (1000°)
1·5
1·4
1·3
1·2
1·1
1·0
0·9
0·8
0·7
0·6
3 + Log k
2·06
·08
2·10
·12
·14
·16
·18
2·20
$\frac{1}{T°A} \times 10^3$

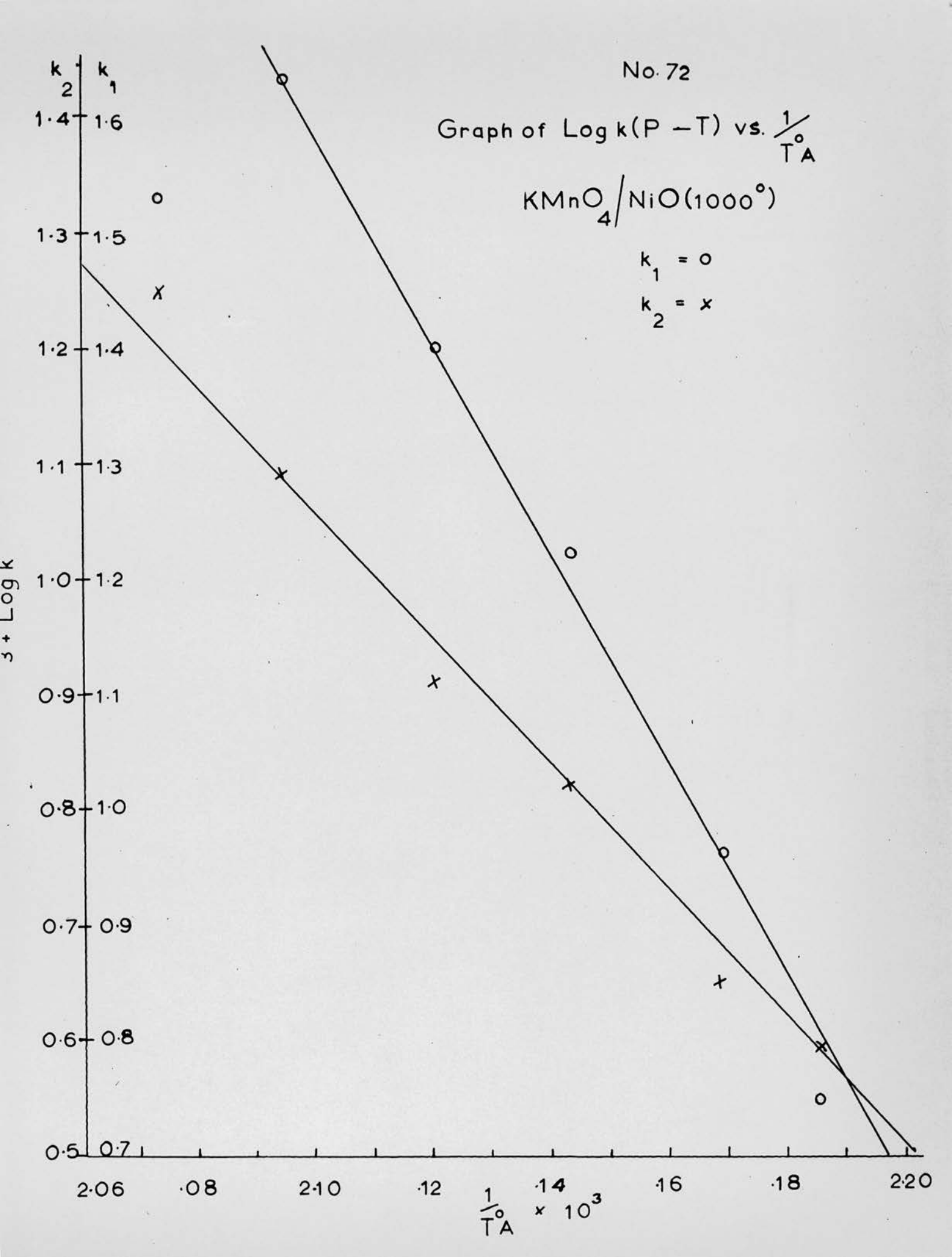
No. 72
Graph of Log k(P – T) vs. 1/T°A
KMnO4/NiO(1000°)
k1 = o
k2 = x
k2
k1
1·4
1·6
1·3
1·5
1·2
1·4
1·1
1·3
1·0
1·2
0·9
1·1
0·8
1·0
0·7
0·9
0·6
0·8
0·5
0·7
3 + Log k
2·06
·08
2·10
·12
·14
·16
·18
2·20
1/T°A x 10³

3.3.9. Resistance Measurements for Potassium Permanganate/Nickel Oxide + 1 mole % Lithium Oxide (K*)

Tables 66, 67, 68 and 69 and graphs 73, 74, 75, 76 and 77 illustrate, for the system potassium permanganate/nickel oxide + 1 mole % lithium oxide, the change in resistance during the decomposition and also the fit of the Prout-Tompkins equation over the later stages of the reaction.

In this system the resistance measurements again show an exponential decrease over the range $\alpha = 0 - 0.5$, after which there is a continued decrease until $\alpha = 0.6$ after which there is little change.

The Prout-Tompkins equation holds over the region $\alpha = 0.05 - 0.9$, two values of k being required, one for the acceleratory stage $\alpha = 0.05 - 0.5$, the other for the decay stage $\alpha = 0.5 - 0.9$.

Tables 66, 67 and 68	Analysis of system K*.
Table 69	Rate constants for system K*.
Graph 73	Plot of $\log_{10} R$ vs. Time.
Graph 74	Plot of $\log_{10} \frac{\alpha}{1-\alpha}$ vs. Time.
Graph 75	Arrhenius plot for "rate of conduction" which gives an activation energy of $E_{c_2} = 34 \pm 4$ K. cals./mole.
Graph 76	Arrhenius plot for acceleratory and decay stages which gives an activation energy of $E_1 = 28 \pm 3$ K. cals./mole. and $E_2 = 32 \pm 2$ K. cals./mole.
Graph 77	Arrhenius plot of initial "rate of conduction" for systems J* and K* which gives an activation energy of $E_{c_1} = 46 \pm 2$ K. cals./mole.

Table 66 System K* $KMnO_4$ / NiO + Li_2O

Run		K*7			K*1	
Temp.		199.0°C			199.2°C	
Time Min.	α x 10	P.T.	log R	α x 10	P.T.	log R
5			5.79			6.11
10	0.11	$\bar{2}$.04	5.75			6.08
15			5.72			6.05
20	0.13	$\bar{2}$.12	5.69	0.14	$\bar{2}$.14	6.00
25			5.66			5.96
30	0.14	$\bar{2}$.16	5.60	0.19	$\bar{2}$.29	5.92
35			5.57			5.88
40	0.22	$\bar{2}$.35		0.21	$\bar{2}$.35	5.84
45			5.54			5.79
50	0.33	$\bar{2}$.53	5.51	0.33	$\bar{2}$.53	5.74
55			5.47			5.69
60	0.44	$\bar{2}$.67	5.43	0.42	$\bar{2}$.65	5.64
65			5.40			5.60
70	0.65	$\bar{2}$.84	5.36	0.60	$\bar{2}$.80	5.55
75			5.31			
80			5.26	0.78	$\bar{2}$.93	5.45
90	1.71	$\bar{1}$.32	5.17	1.07	$\bar{1}$.08	5.36
100	2.39	$\bar{1}$.50	5.06	1.45	$\bar{1}$.23	5.34
110	3.23	$\bar{1}$.68	4.95	1.97	$\bar{1}$.39	5.22
120	4.01	$\bar{1}$.83	4.84	2.58	$\bar{1}$.54	5.12
130	4.78	1.96	4.75	3.30	$\bar{1}$.69	5.04
140	5.42	0.07	4.66	4.03	$\bar{1}$.83	4.96
150	5.97	0.17	4.60	4.67	1.94	4.89
160	6.40	0.25	4.54	5.25	0.04	4.84
170	6.77	0.32		5.74	0.13	4.78
180	7.09	0.39	4.48	6.23	0.22	4.73
190	7.40	0.45		6.63	0.29	
200	7.69	0.52	4.42	7.06	0.38	4.65
210	7.94	0.59		7.33	0.44	4.
220	8.22	0.66	4.40	7.66	0.51	4.59
230	8.43	0.73		7.95	0.59	
240	8.59	0.78	4.39	8.25	0.67	4.56
250	8.78	0.86		8.51	0.76	
260	8.99	0.95	4.39	8.71	0.83	4.52
270	9.11	1.01		8.97	0.94	
280	9.30	1.12	4.39	9.21	1.06	4.46
290	9.43	1.22		9.39	1.18	
300	9.55	1.32	4.39	9.55	1.32	4.43
310	9.65	1.45		9.70	1.51	
320	9.76	1.61		9.81	1.71	4.40
330	9.87	1.88		9.90	2.01	
340	9.96	2.35				4.36

Table 67 System K* $KMnO_4$ / NiO + Li_2O

Run	K*5			K*6		
Temp.	188.4°C			183.9°C		
Time Min.	α x 10	P.T.	log R	α x 10	P.T.	log R
10			5.50			5.81
20	0.10	$\bar{2}$.01	5.46	0.35	$\bar{2}$.57	5.78
30			5.43			5.75
40	0.10	$\bar{2}$.01	5.41	0.41	$\bar{2}$.63	5.77
50			5.40			5.73
60	0.11	$\bar{2}$.06	5.38	0.41	$\bar{2}$.63	5.71
70			5.36			5.69
80	0.14	$\bar{2}$.14	5.35	0.41	$\bar{2}$.63	5.69
90			5.33			5.69
100	0.15	$\bar{2}$.18	5.31	0.43	$\bar{2}$.65	5.69
110			5.28			5.68
120	0.20	$\bar{2}$.32	5.27	0.43	$\bar{2}$.65	5.67
130			5.24			5.66
140	0.23	$\bar{2}$.37	5.21	0.43	$\bar{2}$.65	5.65
150			5.18			5.64
160	0.28	$\bar{2}$.47	5.12	0.44	$\bar{2}$.66	5.63
170						5.62
180	0.36	$\bar{2}$.58		0.44	$\bar{2}$.66	5.60
190						5.59
200	0.49	$\bar{2}$.71		0.45	$\bar{2}$.67	5.57
210						5.55
220	0.69	$\bar{2}$.87	4.83	0.49	$\bar{2}$.72	5.53
230			4.78			5.51
240	1.08	$\bar{1}$.08	4.74	0.54	$\bar{2}$.75	5.49
250			4.70			5.47
260	1.70	$\bar{1}$.31	4.63	0.56	$\bar{2}$.77	5.44
270			4.57			5.42
280	2.41	$\bar{1}$.50	4.53	0.65	$\bar{2}$.84	5.40
290			4.50			5.37
300	3.20	$\bar{1}$.67	4.46	0.74	$\bar{2}$.90	5.34
320	4.03	$\bar{1}$.83	4.38	0.89	$\bar{2}$.99	5.28
340	4.64	$\bar{1}$.94	4.26	1.10	$\bar{1}$.09	5.20
360	5.21	0.04	4.20	2.04	$\bar{1}$.41	
380	5.68	0.12	4.18	2.46	$\bar{1}$.51	
400	6.11	0.20	4.15	2.93	$\bar{1}$.62	
440	6.82	0.33		4.10	$\bar{1}$.84	
480	7.50	0.48		5.17	0.03	
520	7.98	0.60		6.02	0.18	
560	8.41	0.72		6.69	0.31	
600	8.75	0.85		7.26	0.42	
640	8.98	0.94		7.74	0.53	
680	9.22	1.07		8.18	0.65	
720	9.44	1.23		8.54	0.77	
760	9.66	1.45		8.85	0.89	
800	9.82	1.73		9.13	1.02	
840	9.91			9.33	1.15	
880	9.95			9.47	1.25	
920				9.59		
960						
1000						

Table 68 System K* $KMnO_4/NiO + Li_2O$

Run	K*2			K*3			K*4	
Temp.	208.8°C			199.4°C			195.1°C	
Time Min.	α x 10	P.T.	log R	α x 10	P.T.	log R	α x 10	P.T.
5	0.18	$\bar{2}$.26	5.64					
10	0.25	$\bar{2}$.40	5.63	0.13	$\bar{2}$.12	5.48		
15	0.31	$\bar{2}$.51				5.45		
20	0.41	$\bar{2}$.63	5.45	0.25	$\bar{2}$.41	5.43	0.15	$\bar{2}$.18
25	0.64	$\bar{2}$.83	5.46			5.41		
30	0.82	$\bar{2}$.95	5.38	0.31	$\bar{2}$.51	5.40		
35	1.31	$\bar{1}$.18	5.34			5.40		
40	1.60	$\bar{1}$.28	5.32	0.39	$\bar{2}$.61	5.39	0.25	$\bar{2}$.41
45	2.18	$\bar{1}$.44	5.28			5.38		
50	2.93	$\bar{1}$.62	5.19	0.52	$\bar{2}$.74	5.37		
55	3.68	$\bar{1}$.77	5.08			5.34		
60	4.40	$\bar{1}$.90	4.94	0.64	$\bar{2}$.84	5.33		
65	5.07	0.01	4.86			5.27		
70	5.65	0.11	4.78	0.93	$\bar{1}$.01			
75	6.22	0.22	4.70					
80	6.71	0.31	4.65	1.36	$\bar{1}$.20		0.50	$\bar{2}$.72
85	7.20	0.41	4.61					
90	7.68	0.52	4.60	1.95	$\bar{1}$.38			
100	8.43	0.73	4.60	2.72	$\bar{1}$.57		0.75	$\bar{2}$.91
110	9.02	0.96	4.62	3.63	$\bar{1}$.76			
120	9.49	1.27	4.66	4.47	$\bar{1}$.91		1.63	$\bar{1}$.29
130	9.82	1.74	4.71	5.24	0.04			
140	9.98		4.73	5.88	0.15		2.95	$\bar{1}$.62
150			4.74	6.43	0.26			
160			4.72	6.95	0.36		4.28	$\bar{1}$.87
170			4.69	7.45	0.46			
180			4.65	7.84	0.56		5.45	0.08
190				8.23	0.67			
200				8.52	0.76		6.25	0.22
210				8.84	0.88			
220				9.11	1.01		6.92	0.35
230				9.32	1.14			
240				9.54	1.32		7.50	0.48
250				9.67	1.48			
260				9.80			8.10	0.63
270				9.91				
280							8.70	0.83
290								
300				9.55			9.07	0.99
320				9.76			9.47	1.25
340				9.96			9.75	1.59
360							9.95	

Table 69 Rate Constants for System K* $KMnO_4/NiO + Li_2O$

Run	$1/T^oA \times 10^3$	α-range	$k_{c_1} \times 10^3$	α-range	$k_{c_2} \times 10^2$	α-range	$k_1 \times 10^2$	α-range	$k_2 \times 10^2$
K*1	2.118	-	-	0-0.47	0.96	0.1 -0.48	1.53	0.48-0.9	0.77
K*2	2.075	-	-	0-0.6	1.53	0.08-0.46	3.14	0.46-0.9	2.04
K*3	2.117	0-0.05	5.60	-	-	0.01-0.5	1.79	0.5 -0.9	1.02
K*4	2.136	-	-	-	-	0.08-0.42	1.76	0.42-0.9	0.66
K*5	2.167	0-0.02	1.95	0.02-0.5	0.48	0.08-0.45	0.95	0.45-0.9	0.32
K*6	2.188	0-0.05	1.18	0.05-0.5	0.27	0.07-0.51	0.52	0.51-0.9	0.30
K*7	2.119	0-0.065	6.50	0.07-0.55	0.98	0.03-0.5	1.82	0.5 -0.9	0.68

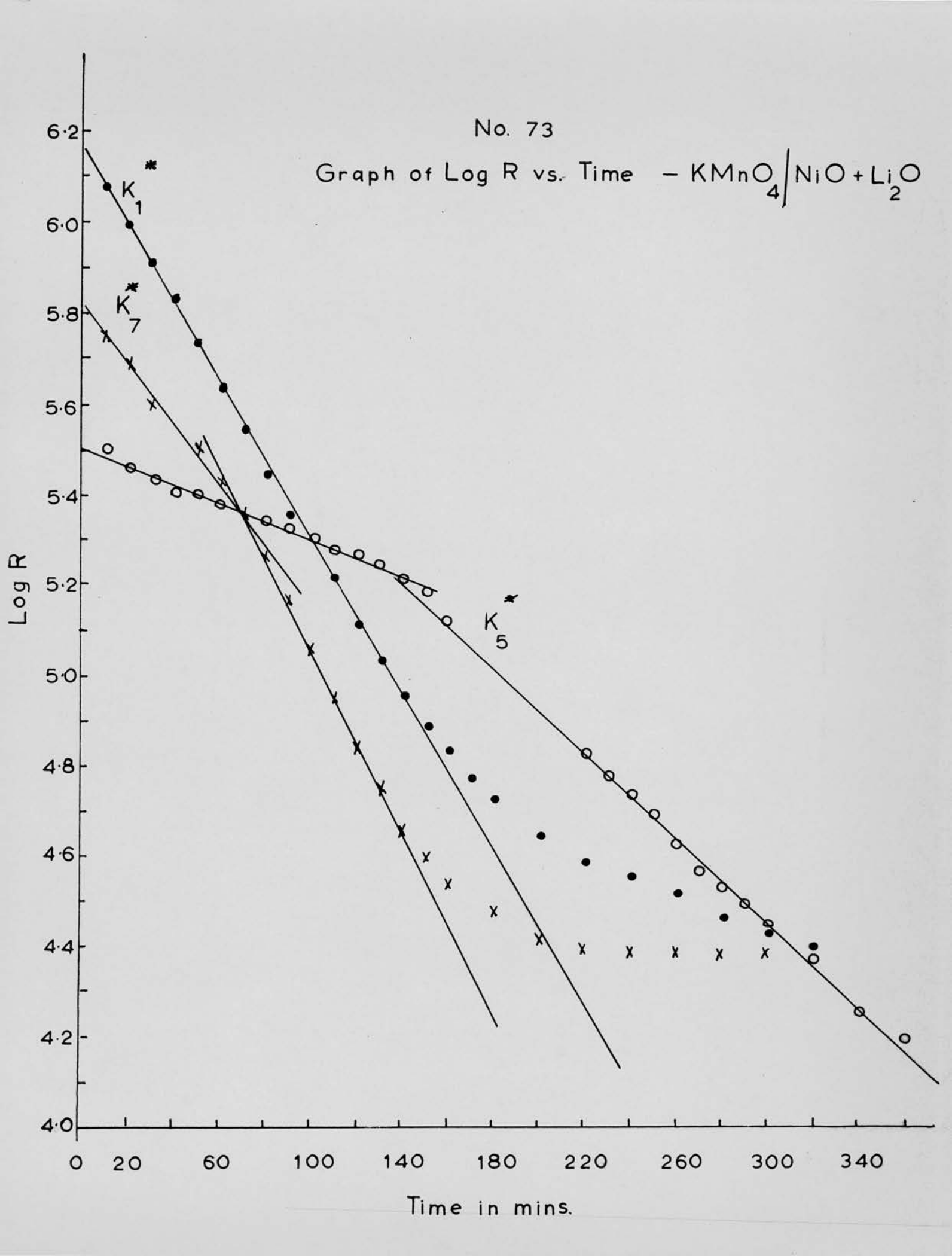
No. 73
Graph of Log R vs. Time – $KMnO_4$ / $NiO + Li_2O$
K_1
K_7
K_5
Log R
6·2
6·0
5·8
5·6
5·4
5·2
5·0
4·8
4·6
4·4
4·2
4·0
0
20
60
100
140
180
220
260
300
340
Time in mins.

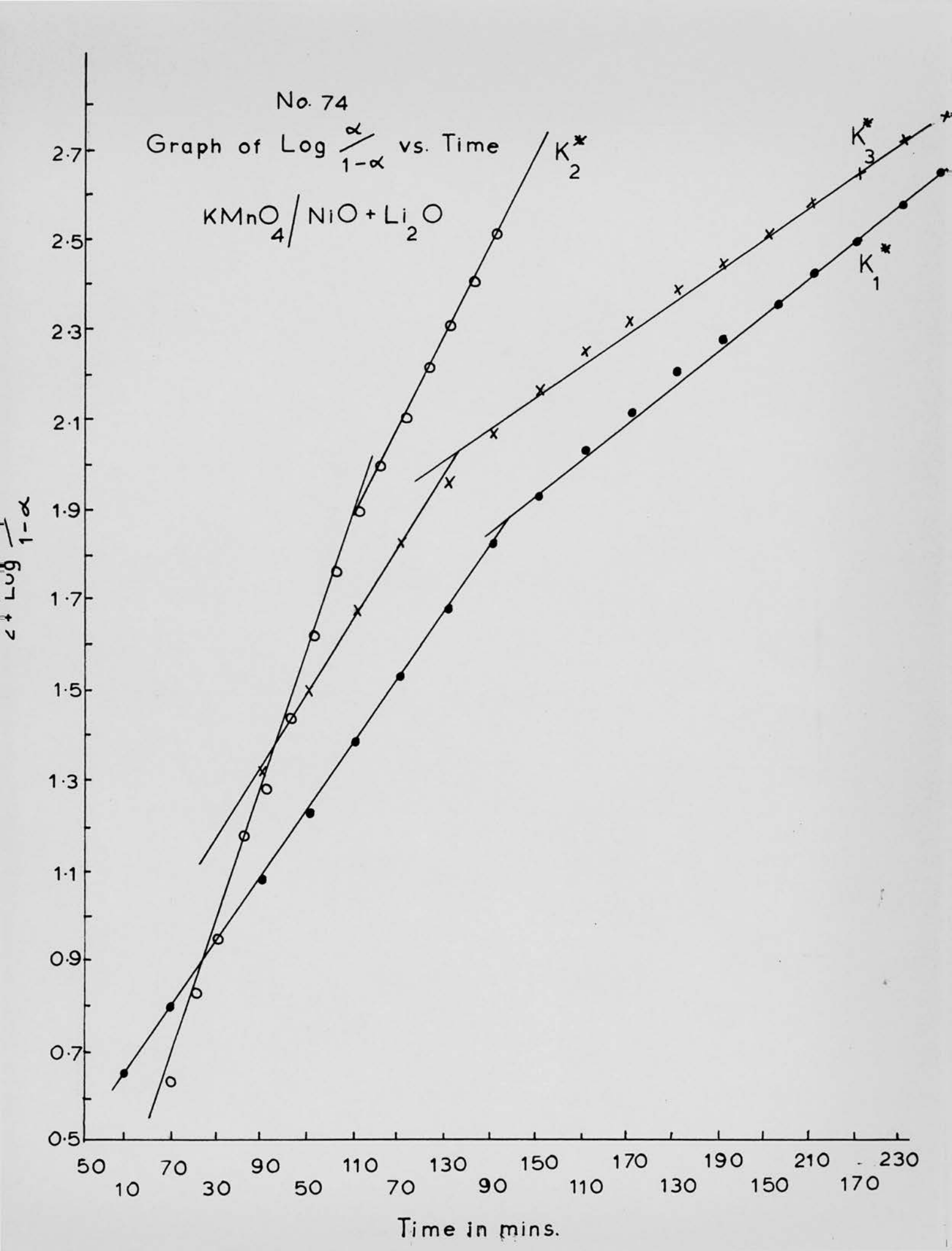
No. 74
Graph of Log α/1-α vs. Time
KMnO4 / NiO + Li2O
K*2
K*3
K*1
2·7
2·5
2·3
2·1
1·9
1·7
1·5
1·3
1·1
0·9
0·7
0·5
2.4 Log α/1-α
50
10
70
30
90
50
110
70
130
90
150
110
170
130
190
150
210
170
230
Time in mins.

No. 75

Graph of Log k_{c_2} vs. $\frac{1}{T^\circ A}$ — $KMnO_4/NiO + Li_2O$

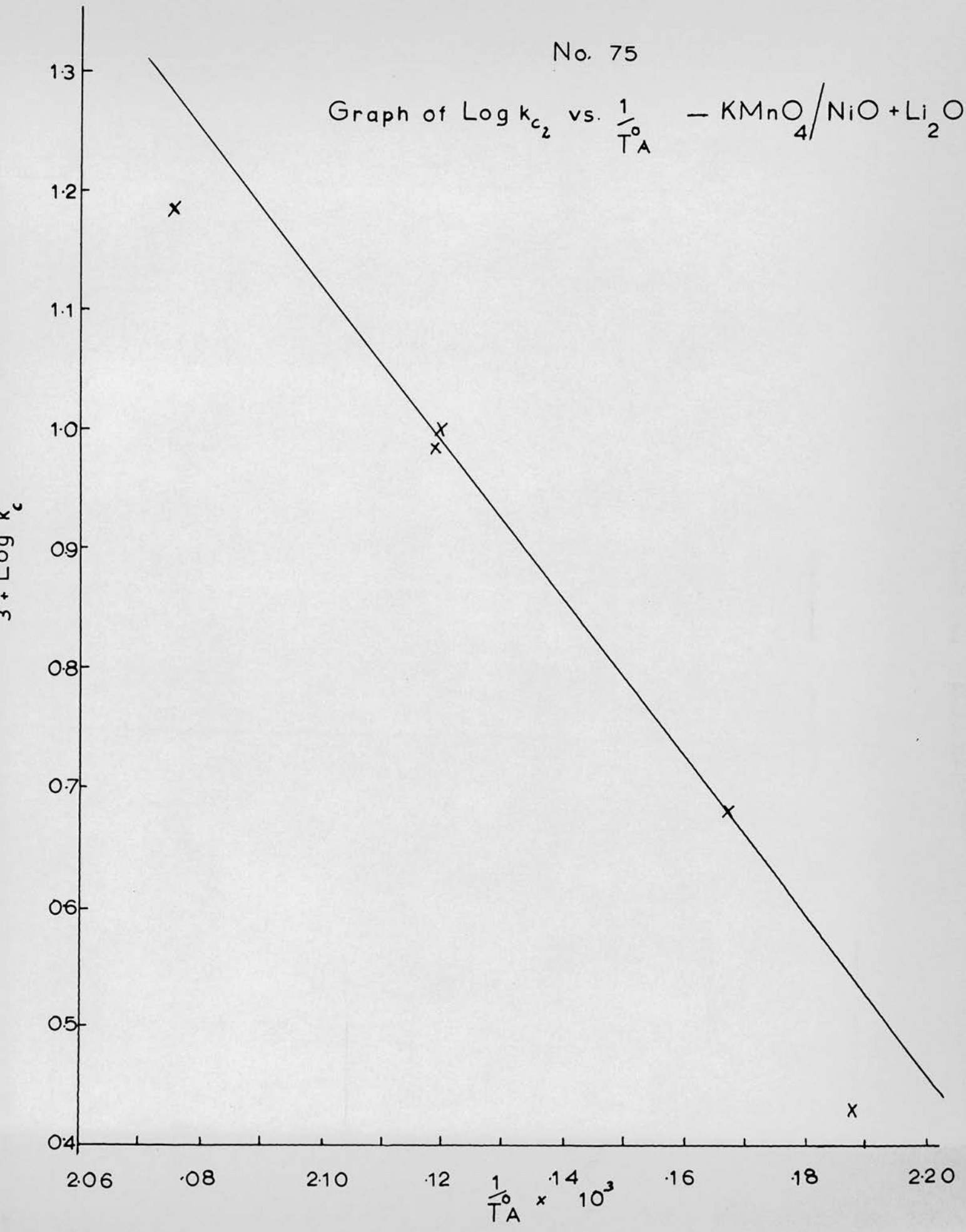

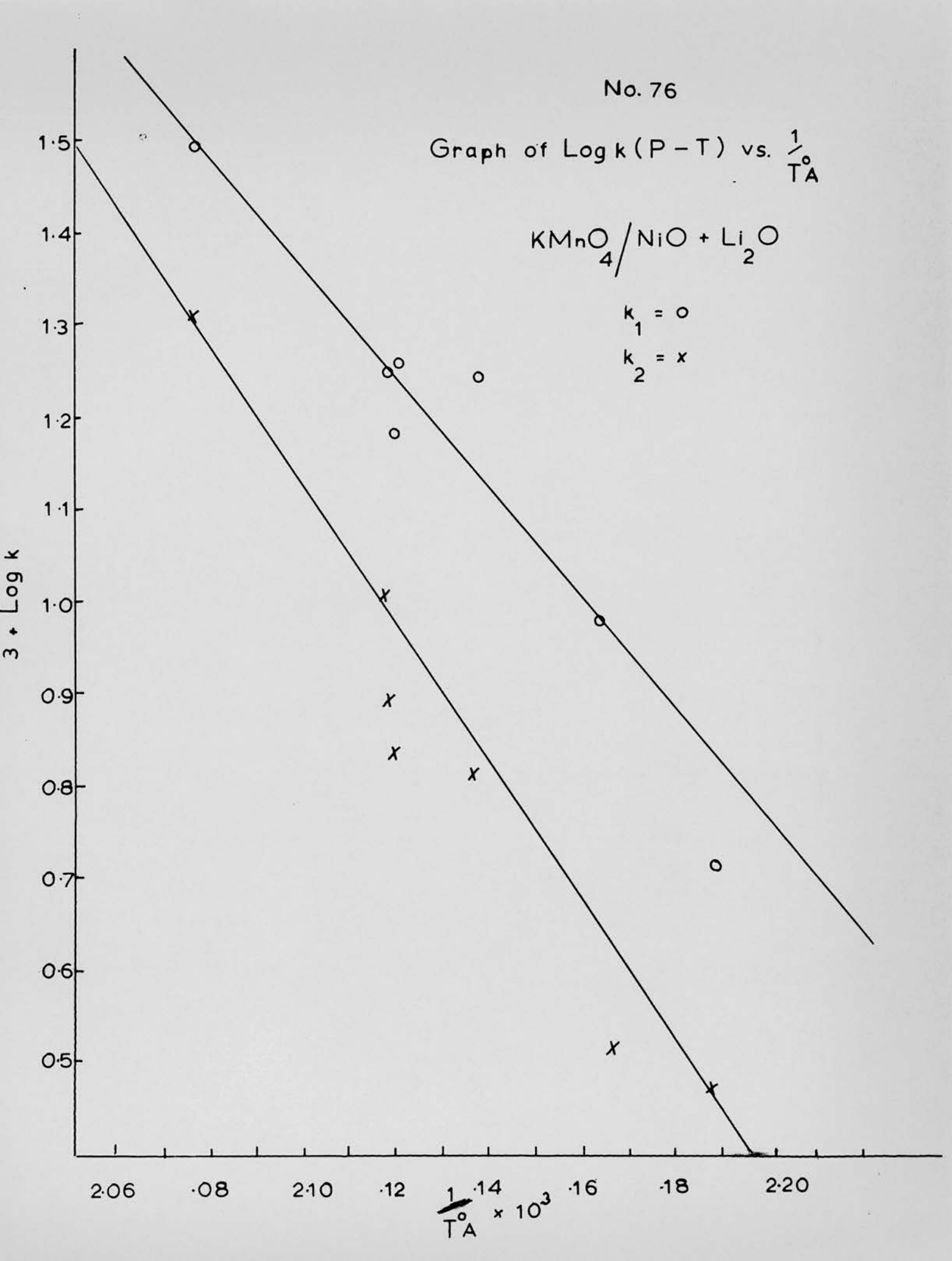
No. 76
Graph of Log k (P – T) vs. 1/T°A
KMnO4/NiO + Li2O
k1 = o
k2 = x
3 + Log k
1·5
1·4
1·3
1·2
1·1
1·0
0·9
0·8
0·7
0·6
0·5
2·06
·08
2·10
·12
·14
·16
·18
2·20
1/T°A × 10³

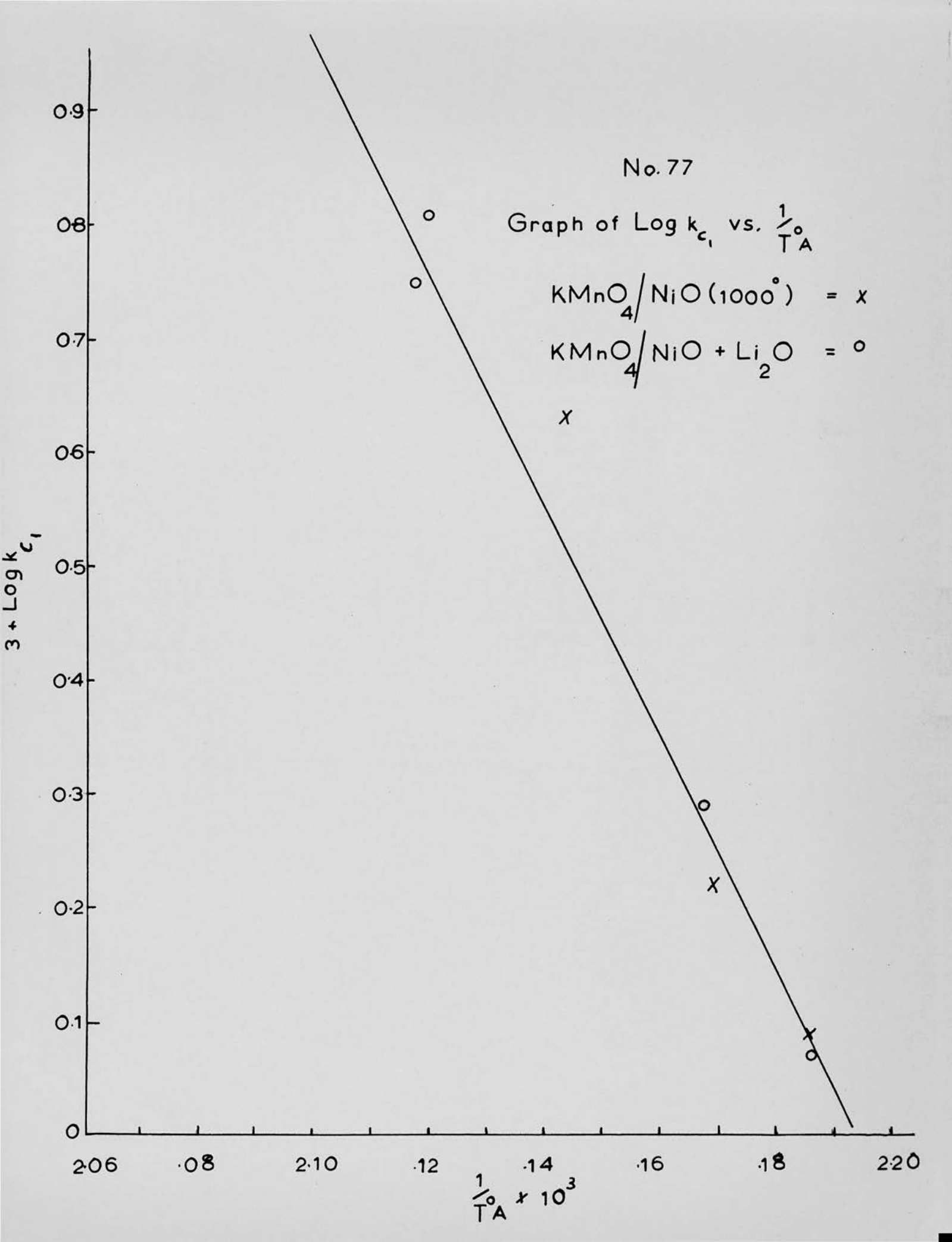
No. 77
Graph of Log k_{c_1} vs. $\frac{1}{T^\circ A}$
$KMnO_4$ / NiO (1000°) = x
$KMnO_4$ / NiO + Li_2O = o
3 + Log k_{c_1}
0·9
0·8
0·7
0·6
0·5
0·4
0·3
0·2
0·1
0
2·06
·08
2·10
·12
·14
·16
·18
2·20
$\frac{1}{T^\circ A} \times 10^3$

Table 70 Activation energies for conduction and later stages of the decomposition k cals/mole

System	E_{c_1}	E_{c_2}	E_1	E_2
$KMnO_4$	27±2	38±2	26±2	28±2
$KMnO_4/ Al_2O_3$		32±3	43±2	38±2
$KMnO_4/Fe_2O_3$		40±2		30±2
$KMnO_4/ZnO$		40±3	30±2	33±2
$KMnO_4/ZnO$ (1000°)		26±2	29±2	30±2
$KMnO_4/ZnO + Cr_2O_3$		30±2	33±2	35±2
$KMnO_4/NiO$ (1000°)	46±2	33±2	40±2	25±2
$KMnO_4/NiO + Li_2O$	46±2	34±4	28±3	32±2

4. Discussion

This work has been carried out, primarily, to investigate the effect that NiO, Fe_2O_3, ZnO, CuO, MnO_2 and α-Al_2O_3 have on the isothermal decomposition of potassium permanganate and to see if electrical conductivity measurements in conjunction with the use of "doped" oxides would provide an insight into the mechanism of the decomposition.

The kinetics of thermal decompositions must be explained in the light of modern knowledge of crystal structure. Darwin[53] was one of the first to realise that a crystal was not a perfectly ordered array of lattice points, but consisted of "mozaic blocks" of micron dimensions, which were in imperfect alignment with respect to each other. It is now considered that any crystal greater than ca. 100 μ in linear dimensions is divided into disoriented regions by subgrain boundaries which are normally in the region of 10μ apart. These boundaries are probably two dimensional arrays of edge and screw dislocations which are sites of mechanical weakness and high reactivity. The subgrains are further divided, by a network of single dislocations, into the basic mozaic blocks. Whilst these mozaic blocks contain no dislocations there are still regions of disturbance due to crystal imperfections- normally Frenkel and Schottky defects. Such a theory is necessary to explain the observed intensities of X-ray diffraction spots and also many chemical and physical phenomena in the solid state. That such a dislocation system could probably exist in a crystal was shown by Hedges and Mitchell[11] who showed that the precipitation of photolytic silver in silver bromide marked out line networks in the crystal interior which had all the expected characteristics of a dislocation system.

Application of this picture to potassium permanganate indicates that grinding to a fine powder probably reduces the crystals to subgrain size and so eliminates most of the subgrain boundaries. During pelleting due to the high pressure of compression, however, it is not entirely unforseen that the subgrain boundaries become once again contiguous and that the pellets decompose similarly to a crystal of permanganate.

From the results in sections 2.5.1. - 2.5.11. it can be seen that the oxides have a varying catalytic effect on the decomposition. The decomposition tends to split into three stages - the initial reaction which probably extends to $\alpha = 0.1$ followed by the stage $\alpha = 0.1 - 0.5$ which is best fitted by the Prout-Tompkins equation and lastly by the decay stage which is again best fitted by the Prout-Tompkins equation. For convenience therefore each stage of the decomposition will be dealt with separately although the ultimate aim is to discuss the kinetics as one unit.

The range over which the catalytic effect of the oxides extends can be seen by reference to graphs 79, 80 and 81. Graph 79 shows the rate constants, derived from the decay stage of the Prout-Tompkins equation, for most of the systems studied. The points all lie, within the experimental scatter, along one line thus showing that the oxides have little effect in the range $\alpha = 0.5 - 0.9$. This is also borne out in Table 70 which shows that there is no significant difference between the activation energies, for this stage of the decomposition, for the various systems studied with the possible exception of $KMnO_4/\alpha\text{-}Al_2O_3$.

In graph 80 are shown the rate constants derived from the "branching plate" stage of the Prout-Tompkins equation $\alpha = 0.1 - 0.5$. Here there is rather more scatter, perhaps indicating that the oxides do exert an influence in this region. However comparison of this scatter with the effect of the

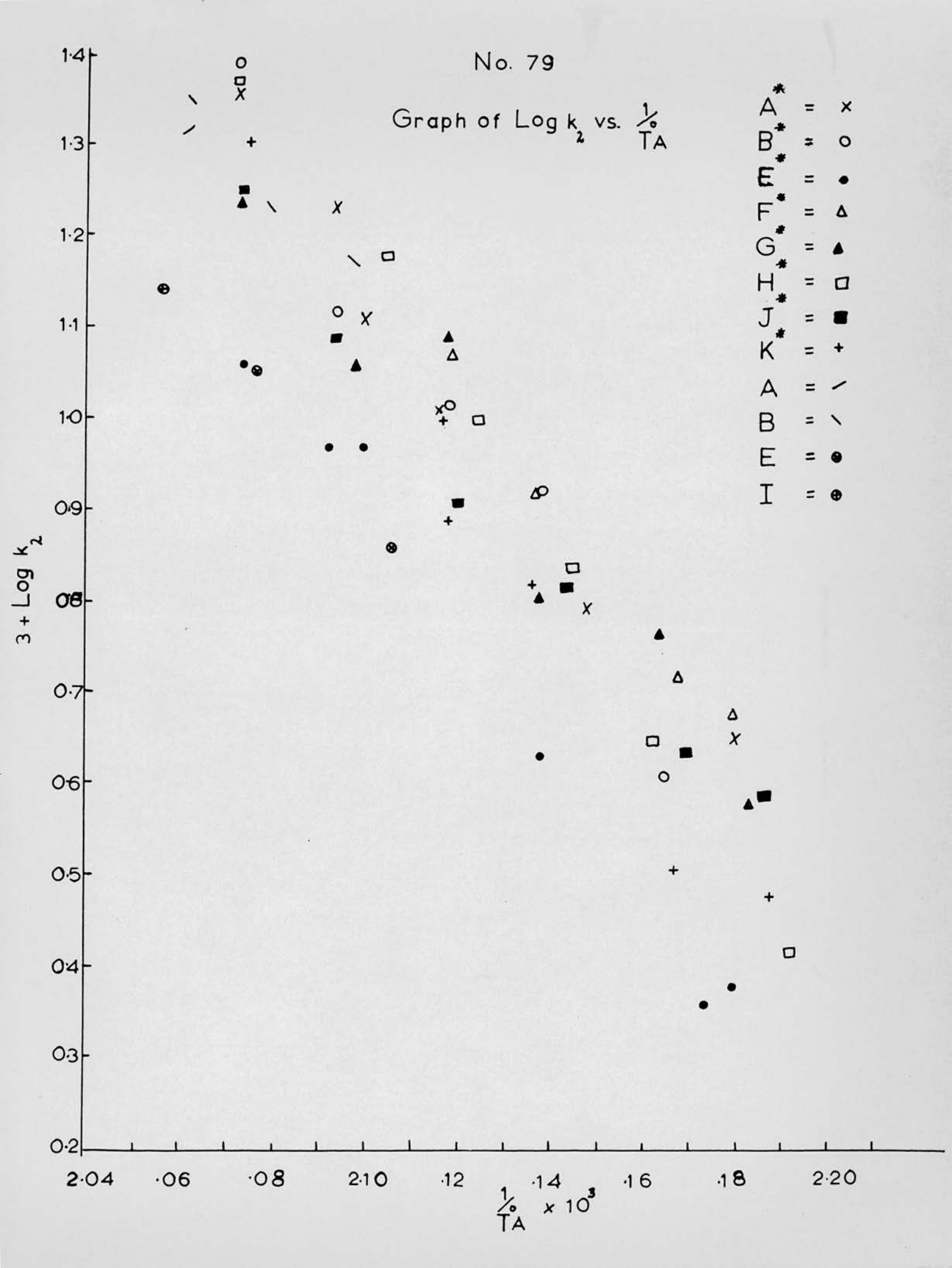
No. 79
Graph of Log k2 vs. 1/TA
A* = ×
B* = ○
E* = ●
F* = △
G* = ▲
H* = □
J* = ■
K* = +
A = /
B = \
E = ⊛
I = ⊕
3 + Log k2
1·4
1·3
1·2
1·1
1·0
0·9
0·8
0·7
0·6
0·5
0·4
0·3
0·2
2·04
·06
·08
2·10
·12
·14
·16
·18
2·20
1/TA x 10³

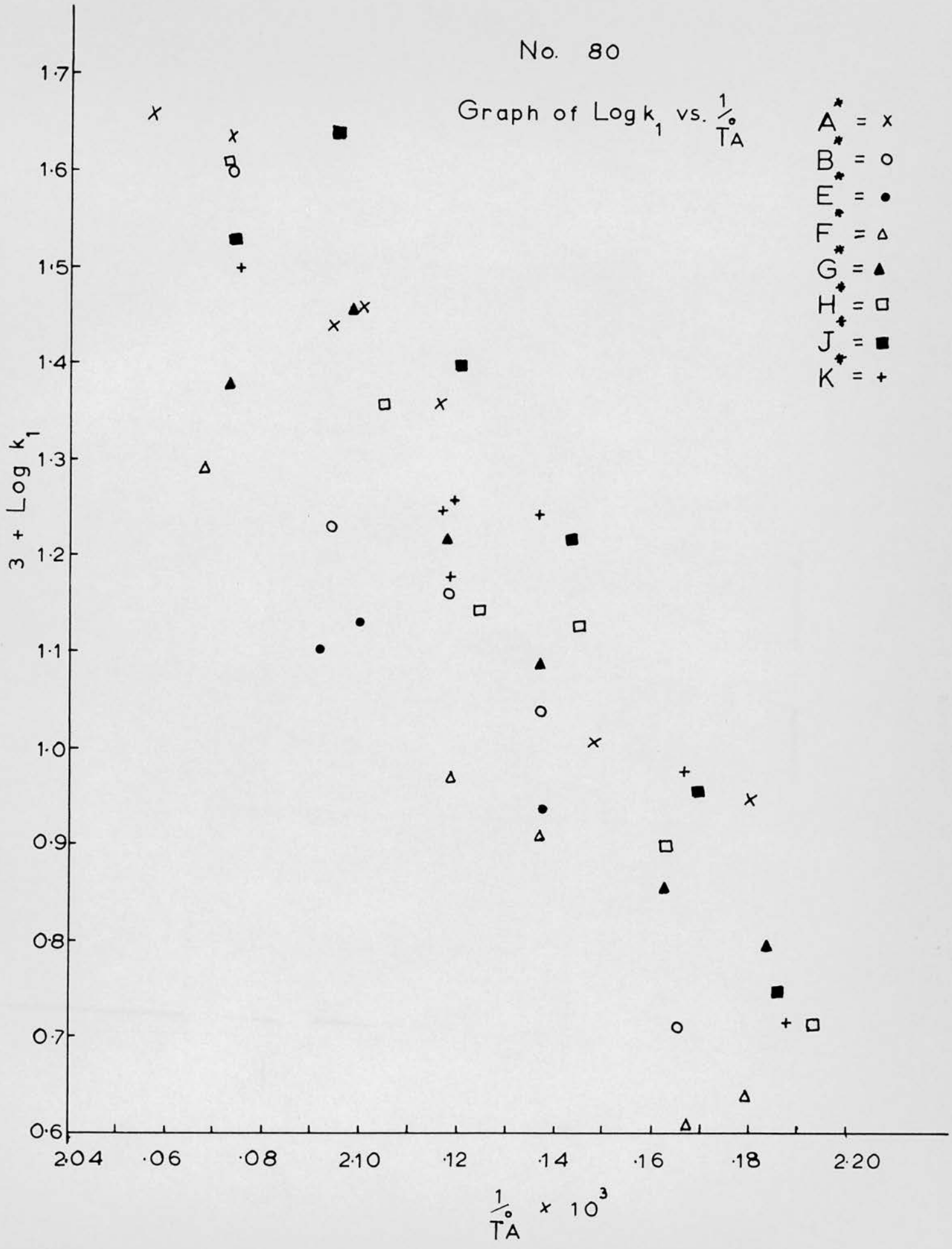
No. 80
Graph of Log k1 vs. 1/TA
A = x
B = o
E = •
F = Δ
G = ▲
H = □
J = ■
K = +
3 + Log k1
1·7
1·6
1·5
1·4
1·3
1·2
1·1
1·0
0·9
0·8
0·7
0·6
2·04
·06
·08
2·10
·12
·14
·16
·18
2·20
1/TA x 10^3

No. 81

Graph of $\text{Log}\, k_x$ vs. $\frac{1}{T_A^\circ}$

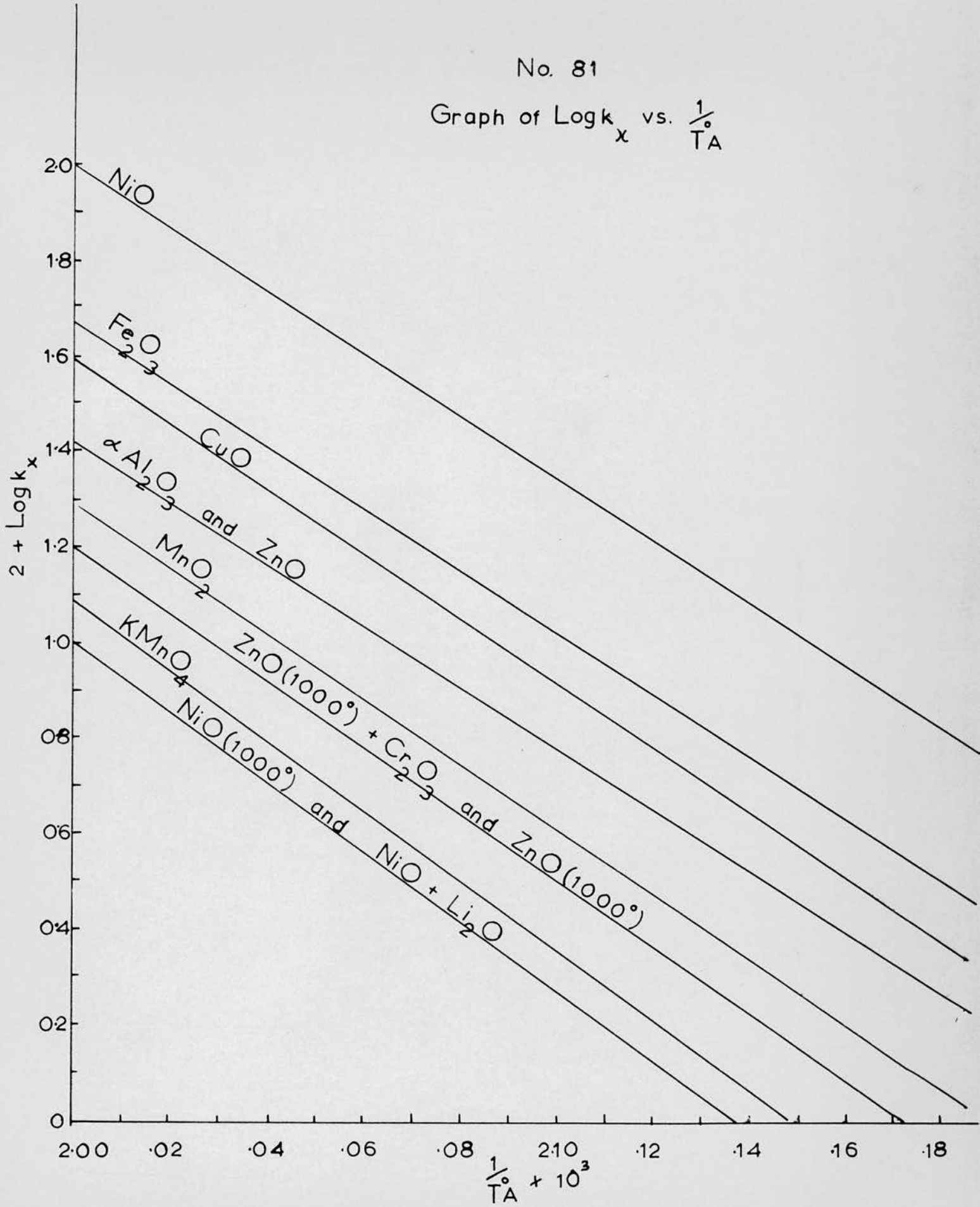

oxides on the decomposition in the range α = 0 - 0.1, which is shown in graph 81, shows that any effect of the oxides in the α- range 0.1 - 0.5 is probably small. Table 70 shows that there is also no significant change in activation energy, again with the possible exception of $KMnO_4/\alpha$- Al_2O_3 and $KMnO_4/NiO$ (1000°).

The catalytic effect is thus mainly confined to the first 10% of the decomposition. As has already been mentioned, due to the fact that in this range a common kinetic equation does not hold for all the systems studied, resort had to be made to the technique of arbitrarily selecting the inverse of the time to reach α = 0.03 as a measure of the catalytic effect in this stage. Graph 81 is the Arrhenius plot for these rate constants only the best line being shown for simplification. From this graph, the following "catalytic activity series" is arrived at:

$$NiO > Fe_2O_3 > CuO > ZnO, \alpha\text{-}Al_2O_3 > MnO_2.$$

The reliability of this series will be discussed later. However it is worth mentioning at this stage that graph 81 indicates that there should be no significant change in activation energy, between the various systems, for the initial decomposition. This is more conclusively proved in Table 38 where the activation energies, derived from the temperature coefficients of the appropriate rate constants, are tabulated.

Thus it would appear that the catalytic influence of the oxides does not extend beyond α = 0.1. It is however possible that any mechanism involving the oxides is still functioning beyond α = 0.1, but that the decomposition due to this is swamped by that due to the "branching plate" mechanism of the Prout-Tompkins equation.

The decomposition thus appears to follow a similar course to that suggested by Prout and Tompkins[20] for the decomposition of a series of alkali permanganates. The reaction is initiated mainly on the external surface leading to the formation of product molecules which have unit cells of different geometric form and dimensions from that of the unreacted permanganate. Thus whereas potassium permanganate has an orthorombic unit cell, with a = 9.99, b = 5.72 and c = 7.41 A[54]; manganese dioxide has a body centred tetragonal cell of edge 4.44A and an axial ratio of 0.651 for c/a where a is 4.38A[55]. The interfacial region will therefore be one of high energy and strain. The decomposition will therefore proceed by (1) an outward growth along the surface and (2) by penetration into the mass of the crystal, rather than by the creation of further isolated nuclei. The decomposition spikes so produced cause strain in the crystal which is relieved by the cracking of the crystal; this cracking will probably take place preferentially at dislocations, since these are positions of mechanical weakness. In support of the existance of such strain in the crystal Prout and Herley[56] have reported that Laue photographs of partially decomposed crystals of potassium and silver permanganate show asterism of the spots. They have also shown[56], in the case of silver permanganate, the existence of a surface layer of product in partially decomposed material.

The decomposition then proceeds by means of "branching planes". The controlling factor in the rate of decomposition is now the probability of branching "k", the branching of the interface reaction occurring when the interface meets a dislocation in the crystal, as was first postulated for silver oxalate[19]. The decomposition then proceeds on the freshly exposed surfaces created by the cracking. This branching of the interface, however, does not

continue unhindered; if such was the case a pure exponential relationship would result as was originally put forward by Garner and Hailes[18]. Instead, interference sets in, branching terminating when a "branching plane" meets a decomposed surface. It is this interference which leads to the Prout-Tompkins equation being required. Decomposition by such a mechanism requires that the activation energy for the initial surface reaction should be greater than that for the branching interface process. This was found to be the case: the activation energy for the initial decomposition $\alpha = 0 - 0.10$ for all the systems studied was 38 ± 3 k. cals./mole, whereas that for the branching interface reaction was with the possible exception of the system $KMnO_4/\alpha\text{-}Al_2O_3$, 28 ± 3 k. cals./mole. This last figure is lower than any previously published results and may show a continuation of the observation reported by Prout and Tompkins[20] that the grinding of potassium permanganate crystals reduced the activation energy from 38.5 k. cals to 34.5 k. cals/mole. Thus the compression of powdered permanganate may have further facilitated the "branching mechanism". Certainly comparison of the absolute values of "k" obtained in this work with those reported by Prout and Tompkins shows that the rate of decomposition is approximately doubled. Thus Prout and Tompkins report the rate at 205°C and 210°C, for ground crystals, to be respectively 1.13×10^2 min^{-1} and 1.76×10^2 $min.^{-1}$ whereas in the present work for run A*5 (204.6°C) and A*4 (209°C) the rates are respectively 2.77×10^2 $min.^{-1}$ and 4.33×10^2 $min.^{-1}$. Another possibility for this reduction in activation energy may lie in the heat treatment these samples were given, namely the gradual heating from room temperature to the reaction temperature. In this connection, however, it should be mentioned that in section 2.5.1 the sample used in run A6 was preheated for 3 hours at 120°C. This appeared to have no significant effect on the rate

of the initial decomposition (α = 0 - 0.1) nor on the rate for the initial fast growth as can be seen by reference to graphs 5 and 6. The term "initial fast growth" is used to cover faster growth rate of the nuclei in the range α = 0 - 0.002, which can be seen when the plots of $\alpha^{\frac{1}{3}}$ vs. Time are extrapolated back to zero time. It therefore seems unlikely that the heattreatment is responsible for the reduction in activation energy. In the case of the system $KMnO_4/\alpha\text{-}Al_2O_3$ the activation energy is 43±2 k. cals./mole; here owing to the fine particle size and large surface area of the oxide some interference with the "branching" may occur. Overall however it would appear that the oxides do not affect this stage of the decomposition. Graph 42 shows that no significant change, bearing in mind that each point refers to a different pellet, occurs in the rate constants for the "branching plane" stage on increasing the nickel oxide content of the pellet. If the oxides did affect this stage of the decomposition a change in the pellet composition should have led to a change in the rate constant.

The reaction thus proceeds by the "branching plate" mechanism until the maximum rate is reached, which signifies that the crystallites are now of approximately mozaic block dimensions. Branching is now no longer possible since these blocks contain no dislocations.

The decay stage of the decomposition then starts at α = 0.5. In this region the rate determining step is the amount of undecomposed permanganate with the added restriction, required by the Prout-Tompkins equation, that before an undecomposed particle can react it must be adjacent to a decomposed particle. The condition of the reaction interface will therefore be of major importance in such a mechanism. It is therefore feasible that the oxides could effect this stage of the decomposition since, providing the oxides have a reasonable surface area, merely by acting as a "filler" they could disrupt the interface, reducing the probability of contact between decomposed and

undecomposed particles and thus the rate of the decay stage of the decomposition. That nickel oxide does exhibit such an effect is shown in graph 42, where, even bearing in mind that each point refers to a different pellet, there is clearly shown a dependency of reaction rate on oxide concentration - an increase in the concentration of nickel oxide lowers the rate. If this reduction in rate is due merely to the simple mechanical filler action described above, then all the systems should show this reduction in rate. It should therefore be reflected in graph 79, where log k_2 is shown as a function of $^1/T^o$, since even if all the oxides lowered the probability of contact, and hence the rate, by exactly the same factor, there should be a significant difference between this rate and the rate for pure potassium permanganate. This is not so; as has already been stated the rate constants lie within experimental error, about one line with perhaps the rates for the systems $KMnO_4/NiO$ and $KMnO_4/Fe_2O_3$ slightly lower than the others. The oxides do not, therefore, appear to act as fillers and any effect by them on the rate of decomposition in the region $\alpha = 0.5 - 1.0$, would appear to be restricted to nickel oxide and perhaps ferric oxide. Such selectivity would appear to suggest that the reduction in rate is possibly due to a chemical interaction between the oxide and the decomposition products, which results in the disruption of the reaction interface.

It would therefore appear that only nickel oxide from all the oxides studied exert any effect on the later stages of the decomposition probably due to an interaction between the oxide and the decomposition products. Such an interaction should occur throughout the decomposition and so is in agreement with the conclusions drawn from the shape of the "α" - time curves. As

has already been stated the effect of the added oxides on the shape of the "α" - time curve, is in all the systems studied with the exception of $KMnO_4/NiO$, exhausted after $\alpha = 0.15$. This is illustrated for the system $KMnO_4/Fe_2O_3$ in graph 1. However, as is shown in graph 82, the effect of nickel oxide persists throughout the decomposition. The fact, as has already been discussed, that the decomposition rate in the region $\alpha = 0.1 - 0.5$ is not affected by the concentration of nickel oxide present does not invalidate the arguement of an interaction between oxide and products, since this rate is primarily a measure of the probability of the interface branching at a dislocation,and would thus not be affected by any interaction, and would therefore be independent of oxide concentration. This interaction with the products may, however, be the reason for the other "unusual" results which have been obtained with the system $KMnO_4/NiO$ - the fact, already mentioned in the experimental, that unlike the other systems there is no measurable change in electrical conduction during the decomposition of the permanganate-oxide pellet and also the fact, as will be discussed later, that unlike the other systems which exhibit catalysis as unpelleted powdered samples the system $KMnO_4/NiO$ requires pelleting before any catalysis is shown. Certainly any interaction between oxide and solid decomposition products would be enhanced by the greater contact which would occur as a result of pelleting.

The exact nature of the interaction is not known but it would certainly appear to be dependent on an "active surface" and on surface area, since heating of the oxide to 1000°C, which will also be discussed later, destroys the catalysis, and the shape of the "α" - time curve return to the more normal sigmoidal shape, as is shown in graph 82. It is also perhaps worth mentioning here that with the system $KMnO_4/NiO$ (1000°), it

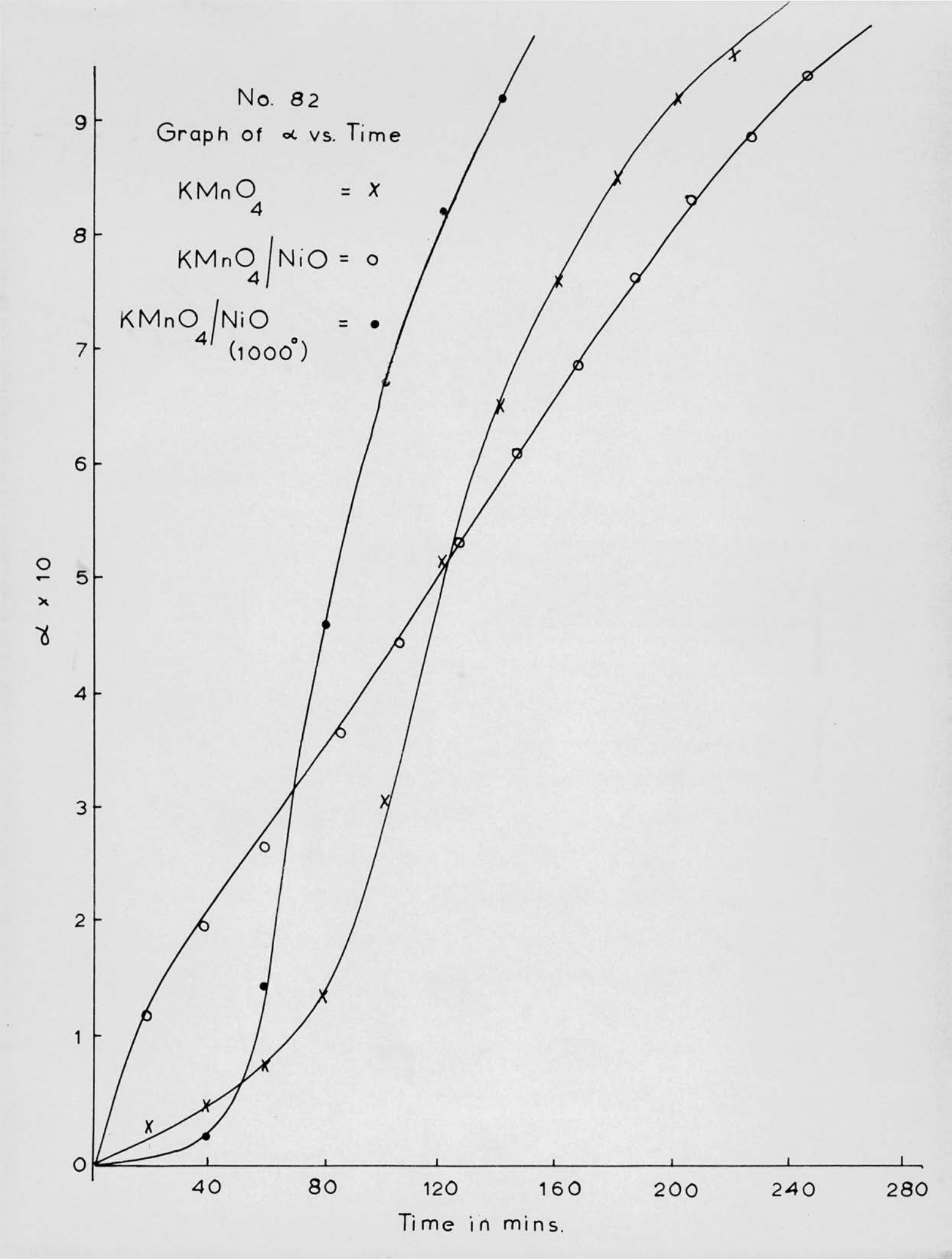
No. 82
Graph of α vs. Time
KMnO4 = X
KMnO4/NiO = o
KMnO4/NiO (1000°) = •
α x 10
0
1
2
3
4
5
6
7
8
9
40
80
120
160
200
240
280
Time in mins.

is now possible to measure a change in electrical conduction during the decomposition.

It therefore appears that in its action on the decomposition of potassium permanganate nickel oxide behaves differently from the other oxides studied.

Return is now made to the initial stage of the decomposition $\alpha = 0 - 0.1$ the region in which the catalytic influence of the oxides is greatest and where the kinetic equation required depends on the system. Since this stage is essentially a surface reaction the rate of decomposition will be heavily dependent on the exact nature and condition of the surface e.g. number of active sites and concentration of oxide present at the surface. Such factors are likely to affect the values of k_x, which is based only on the first three percent of the decomposition, more drastically than the rates based on the kinetic equations covering the first ten percent of the decomposition. This dependency of k_x and $k_{(1-\alpha)^{\frac{1}{3}}}$ on the concentration of oxide in the pellet, is shown for the system $KMnO_4/NiO$, in graph 41 where the rates increase with increasing oxide concentration up to a maximum at seventy percent oxide. It has already been stated that nickel oxide is somewhat unusual in its action, but it is probable that a similar dependency of reaction rate on oxide concentration, in this α-region, will hold for all the systems, although perhaps not in so pronounced a manner as in the system $KMnO_4/NiO$. Comparison of the values of k_x and $k_{(1-\alpha)^{\frac{1}{3}}}$ for run L5(50% NiO) with the results for system I shows a fairly high discrepancy reflecting the irreproducability of runs performed on different "pellets". This discrepancy may be due, in view of the closer correlation of $k_{(1-\alpha)^{\frac{1}{3}}}$ for run L4(40% NiO) with those for system I, to changes from one pellet to another

in the concentration of oxide at the surfaces of the permanganate particles, this despite the care taken in mixing to ensure complete homogeniety and the agreement in every case between the final oxygen pressure and the calculated weight of permanganate present which was based on the sample weight and the "known" composition of the pellet.

This must therefore throw considerable doubt on the validity of the "activity series" which was derived solely from the values of k_x. It is probably better therefore to now consider the oxides as falling into three groups - the most effective catalysts are NiO and Fe_2O_3; less effective are α-Al_2O_3, ZnO, CuO and MnO_2, and finally those with no effect are ZnO (1000^o), ZnO + Cr_2O_3, NiO (1000^o) and NiO + Li_2O - and to ignore the exact order within the groups. It is probably also important to realise that this order is strictly only applicable to the very initial stage of the decomposition; up to $\alpha = 0.03$.

These groupings are similar to those found by Roginsky and Shultz[34]. Also in agreement with these results is the dependence of the initial catalysis on, the heat treatment of the oxides. Thus by heating NiO and ZnO to 1000^oC the catalytic effect has been destroyed. The initial catalysis is also, it would appear, independent of semi-conductor properties of the oxides. Thus, the incorporation of altervalent lithium oxide and chromic oxide into the lattices of nickel oxide and zinc oxide respectively will have considerably altered their conductivities, but this led to no significant change in catalytic activity. This tends to suggest that the initial catalysis depends on an "active surface" and on oxide surface area. This would certainly explain the rather random grouping of semi-conductor types present in the

activity pattern and also the dependence on heat treatment, since the heating at 1000°C will have caused considerable sintering of the oxides and thus reduction of surface area. This dependency on surface area raises great difficulties in trying to assess the relative efficiency of each oxide: factors such as volume effects due to the different densities of the oxides (the present systems are on a weight basis), and areas of contact between the particles which in turn would be related to the particle size distribution, would have to be taken into account.

Such ideas, however, are in line with the results of Erofeev[31] and Komatsu[32] who found that the initial rate of decomposition was dependent on the surface area and particle size of the permanganate. It could be argued therefore that in the mixing of the permanganate and oxides, which was carried out by mortar and pestle, a further increase in surface area of the permanganate occurred which would be related to the surface area and abrasive character of the oxide. If this is the case pelleting of these systems would not be required for catalysis to be observed and may perhaps even hinder it.

Runs were carried out on un-pelleted samples in section 2.5.11 and showed that Fe_2O_3, α-Al_2O_3, ZnO and CuO did in fact show catalysis. Nickel oxide, however did not show any effect probably due, as has been said before, to the fact that this oxide acts by some interaction with the products and thus requires a greater degree of contact than is present in a loose powdered mixture. The much greater effect observed with the un-pelleted ferric oxide in relation to α-alumina, zinc oxide and cupric oxide probably suggests that at least in this case a further mechanism, over and above any effect due to an increase in surface area of the permanganate by grinding, is involved.

Also pointing to another mechanism occurring, although in this case not until after $\alpha = 0.03$, is the fact that whilst ZnO (1000°) and ZnO + Cr_2O_3 show no catalysis when measured by "k_x", the rate constants for these systems derived from the t^2 relationship, which holds to $\alpha = 0.10$, are comparable with those derived from the same relationship, for the system $KMnO_4/\alpha$-Al_2O_3, and are greater than those for the system $KMnO_4$/CuO. It may therefore be that the semi-conductor properties of the oxides do have some effect although not until after $\alpha = 0.03$. Whether or not such a "conduction" effect is observed with NiO (1000°) and NiO + Li_2O, which also show no catalysis as measured by "k_x", cannot be determined, since no other system is fitted by the exponential equation required by these systems in the α range 0 - 0.10. However, in view of the fact that the Prout-Tompkins equation which normally holds for pure potassium permanganate reduces at small values of "α" to such an exponential relationship as is required by the systems $KMnO_4$/NiO (1000°) and $KMnO_4$/NiO + Li_2O, it may be that in these systems only a very slight modification if any of the kinetics of pure potassium permanganate has occurred in the range $\alpha = 0 - 0.10$. It is therefore unlikely that any conduction effect does occur in the stage after $\alpha = 0.03$. It may well be that the larger catalytic effect shown by un-pelleted ferric oxide as compared with the other un-pelleted oxides is due to a "conductivity" effect.

In view of what has been said and since the activation energy for the initial decomposition ($\alpha = 0 - 0.10$) is 38 ± 3 k. cals./mole, irrespective of system studied, thus showing that the same chemical process is occurring in all, the kinetic expressions required by the different systems must reflect the number of nuclei available, whether produced by grinding or by some other mechanism and the ease of their growth in certain directions. A review

covering the kinetics of formation and growth of nuclei has been published by Jacobs and Tompkins[57].

For pure potassium permanganate a t^3 relationship was found to hold up to $\alpha = c\ 0.09$ after which the Prout-Tompkins equation was required. The t^3 relationship has two possible interpretations: either a three dimensional growth of a fixed number of nuclei at active sites on the surface, or the two dimensional surface growth of nuclei whose number increases linearly with time. In view of the quick onset of "branching" it is probable in this case that the growth is three dimensional thus creating a number of decomposition spikes which results in the cracking of the crystal. The plots of $\alpha^{\frac{1}{3}}$ vs time were found on extrapolation to give at zero time nuclei of finite size, graph 4. An attempt to calculate the activation energy for this very fast initial growth, graph 5, was made but an accurate figure could not be obtained.

With the systems $KMnO_4/\alpha\text{-}Al_2O_3$, $KMnO_4/CuO$, $KMnO_4/ZnO$ (1000°) and $KMnO_4/ZnO + Cr_2O_3$ a t^2 relationship holds up to $\alpha = c\ 0.1$. This corresponds to the two dimensional surface growth of a fixed number of nuclei. Such a surface growth is in agreement with the fact that the "branching plate" mechanism does not commence till relatively late in the decomposition (at $\alpha = c\ 0.2$). For these systems therefore conditions of growth must be such as to encourage a surface growth rather than a penetration into the mass of the sample.

In the case of $KMnO_4/ZnO$ the initial reaction proceeds linearly with time, which suggests that the decomposition proceeds by the penetration into the sample of a constant area interface. Such a course would require a greater surface concentration of nuclei than where the t^2 or t^3 kinetics apply. A more extreme example is shown by the system $KMnO_4/NiO$ which requires the "contracting sphere" expression. Such an expression requires that the particles

be approximately spherical in shape and that their surface be completely nucleated, the decomposition then proceeding by the progression of the intact interface into the crystal. Certainly for such kinetics efficient nucleation would be required, the formation of a complete surface layer of products occurring very rapidly.

For the system $KMnO_4/NiO$ (1000°) and $KMnO_4/NiO + Li_2O$ the initial decomposition proceeds exponentially and since the Prout-Tompkins equation reduces, in the initial stages, to such an expression, the kinetics in these cases indicate that conditions are very similar to those with pure potassium permanganate, only a few isolated nuclei being present initially.

The expression required by the systems $KMnO_4/Fe_2O_3$ and $KMnO_4/CuO$ for the initial decomposition is the analoge of first order decay and it would therefore appear in these systems that the rate determining step is the amount of undecomposed permanganate in contact with the oxide.

Since the kinetics of the decomposition have been explained within the framework of the Prout-Tompkins equation it is desirable to discuss the conductivity measurements also within this framework. Theoretical aspects of ionic conductance in solid salts have been treated by Tompkins and Jacobs[51] but no attempt has been made to apply these in detail in the present work, both because absolute values of conductance were unobtainable and because the main object was to observe changes in conductivity during decomposition of the samples.

Certain features in the conductivity results were common to all the systems studied: there was an initial exponential increase in conductivity with time, the exact α-range over which this held depending on the system used; also

there was little change in conductivity after approximately $\alpha = 0.6$. In many cases the conductivity change involved powers of ten, showing quite clearly that the end product had a much higher conductivity than the initial material.

These and other features can in reasonable measure be explained on the basis of the mechanism proposed by Smirnova[46], although the exact identity of the intermediate, given as MnO_4, or of the conducting species, assumed to be an electron, cannot be established. At the same time, one has to take into account the fact that the bulk of the oxygen is evolved according to Prout-Tompkins kinetics.

The mechanism proposed by Smirnova is

$$MnO_4^{'} \longrightarrow MnO_4 + e \qquad 1.$$

$$MnO_4 \longrightarrow MnO_2 + O_2 \qquad 2.$$

$$MnO_4^{'} + e \longrightarrow MnO_4^{11} \qquad 3.$$

There are therefore two reactions which could affect the electrical conductivity, the production of electrons by reaction 1 and their destruction by reaction 3. The conductivity could also be affected by the build up of solid products. The general shape of the conductivity - time graph indicates that it may be a composite figure incorporating both these effects. If the change in conductivity was entirely due to the formation of solid products then the curve would be sigmoidal similar to that for the evolution of oxygen, on the assumption that solid products are formed at the same rate as oxygen is evolved. If on the other hand the change in conduction was due entirely to the production and destruction of the conducting species then the curve would rise to a maximum and then decay to the original conductivity value, the precise shape depending

on the concentration and life-time of the conducting species. Our curves are the net result of these two effects: we suggest that the exponential increase in conductivity up to $\alpha = c\ 0.5$ corresponds essentially to the formation of charge carriers by reaction 1, and that the absence of a subsequent decrease in conductivity is due to a compensating effect caused by the formation of substantial amounts of contiguous solid products. It is suggested that the solid products cannot exercise this compensating effect until a relatively late stage in the decomposition when sufficient product has been formed so that the particles may be contiguous. With pure potassium permanganate, however, a small maximum in the conductivity curve is observed before the conductivity levels out: here we believe the effect of reaction 3, is evident causing a fall in the conductivity, before the compensating effect of the solid products comes into play. The initial rise in conductivity must, however, undoubtably be due to the greater rate of production of charge carriers to their destruction.

The Prout-Tompkins equation reduces in the early stages to an exponential equation; it is only when branching interference and overlapping of nuclei occur that the Prout- Tompkins equation is required. The reaction, after the first few percent of decomposition, accelerates therefore exponentially and provided reaction 1 continues to maintain its increase on 3 the conduction which is really a measure of the relative increase of 1 with respect to 3 should also increase exponentially. The onset of interference and overlapping should destroy this exponential increase. However in many cases the exponential increase in conduction holds to $\alpha = 0.5$, long after any interference would have started, why this should be is not known.

The analysis of the results is based on the assumption that the rate of change of conduction (in fact, the slope of the plot log conductivity vs time)

is independent of the size and thickness of the sample. Thus while the initial conductivity of the samples is dependent on size and thickness all the conductivities could be normalised by use of a multiplying factor. For any one sample, it is assumed that the normalising factor remains constant throughout the decomposition. Thus while the absolute conductivities differ, the slopes of the log conductivity - time graphs for the various samples give the relative rates of change of conduction i.e. k in the relation conductivity $\propto e^{kt}$. This assumption has been indirectly justified by the fact that Arrhenius plots constructed from the "rate of change of conduction" at various temperatures give a reasonable straight line. The activation energy from such a diagram will be the activation energy for the rate determining stage of the increase in conduction; and therefore constitutes a measure of the energy required for reaction 1.

In the case of pure potassium permanganate the exponential increase holds to $\alpha = 0.5$ but in the low temperature runs this breaks into two sections (1) $\alpha = 0 - 0.05$ where the activation energy is 26 ± 2 k. cals/mole and (2) $\alpha = 0.05 - 0.5$ with an activation energy of 38 ± 2 k. cals/mole. This initial lower activation energy probably points to the existance of a few "active" spots on the surface and it is probably at these points that the decomposition first starts; the figure of 38 k. cals represents the normal energy required for reaction 1 and is in close agreement with the activation energy for the initial decomposition as measured by oxygen evolution. This agreement suggests the conclusion that the rate determining step in the decomposition is the removal of an electron from the permanganate ion. It is surprising however that the lower figure of 26 k. cals/mole is not reflected in the very early stages of the oxygen evolution measurements, it may be therefore that the conduction in this

early range is a surface process involving a species other than that corresponding to reaction 1. Between $\alpha = 0.5$ and 0.6 the plot of log conductivity vs. time exhibits a small maximum which is due to the relative increase in rate of reaction 3 with respect to reaction 1, the continuation of the fall in conduction being cancelled by the increase due to the continued production of more solid products.

The oxide systems studied fall into two groups. The first group includes the systems $KMnO_4/Fe_2O_3$, $KMnO_4/ZnO$, $KMnO_4/NiO$ (1000°) and $KMnO_4/NiO + Li_2O$ which exhibit basically all the features of pure permanganate i.e. exponential increase which holds to $\alpha = 0.5$ and a similar activation energy of "conduction". There is however no maximum in the log conductivity - time graph. In the case of $KMnO_4/Fe_2O_3$ and $KMnO_4/ZnO$ the exponential increase holds to $\alpha = 0.5$ giving only one activation energy: 40 ± 2 k. cals as compared with 38 k. cals for pure permanganate. The oxides appear therefore to have no effect on the activation energy of the rate determining step, and their catalytic effect must arise from an increase in the pre-exponential term, probably due to an increase in the number of decomposition sites. The activation energy for the initial decomposition, as measured by oxygen evolution, should not be altered therefore by the presence of these oxides and this is in fact the case.

The absence of any maximum on the log conductivity - time curves (and this also applies to the Group 2 of the systems - see below) indicates that, in the presence of initially added oxides either the destruction of the charge carriers is more efficient or there is a greater compensating increase in conductivity due to solid products. The former suggestion corresponds to a relative increase in the rate of reaction 3, compared with 1 and the latter requires the contiguity of the particles of solid products (perhaps sandwiched between particles of added oxide) to be established at an earlier stage than in pure permanganate.

In the case of $KMnO_4/NiO$ (1000°) and $KMnO_4/NiO + Li_2O$ the exponential increase splits into two stages, the first extends to $\alpha = 0.06$ and has a high activation energy 46±2 k. cals, the second stage for $\alpha = 0.06 - 0.5$ gives an activation energy of 34±4 k. cals which is not significantly different from that for pure permanganate. The initial high energy probably reflects that the initial conducting species are trapped out by the p-type oxide, the higher energy being that required to raise the conducting species from the trap into the conduction band. Later, however, the traps become saturated or neutralised due to the production of product and the energy required for conduction then becomes the same as for pure permanganate. There should therefore be no significant change in the activation energy for the initial decomposition, as measured by oxygen evolution, and this is the case. The fact that these systems tend to show no catalytic activity as measured by "k_x" and the similarity of the initial decomposition kinetics to those for pure permanganate, are probably due to the fact that since these oxides have relatively small surface areas they are unable to activate the permanganate surface significantly and bring about any change in the pre-exponential term.

The second group consists of the systems $KMnO_4/\alpha\text{-}Al_2O_3$, $KMnO_4/ZnO$ (1000°) and $KMnO_4/ZnO + Cr_2O_3$. In this case the exponential increase only holds to $\alpha = 0.2$, after which there is a continued rise in conduction but at a slower rate, before the conductivity levels out at $\alpha = 0.6$. The initial exponential increase in these systems give a lower activation energy for conduction. Thus for $KMnO_4/\alpha\text{-}Al_2O_3$ $E_c = 32\pm3$ k. cals, for $KMnO_4/ZnO$ (1000°) $E_c = 26\pm2$ k. cals and for $KMnO_4/ZnO + Cr_2O_3$ $E_c = 30\pm2$ k. cals. These systems at first sight therefore appear to have a definite effect on the ease of production of the conducting species. Since the group 1 results have tended to support the view that this is the rate determining step for the decomposition, the lower activation energy given above for the second group should be reflected in the

activation energy for the initial stage of the decomposition, as determined from oxygen evolution measurements. This however is not so: the oxygen activation energies for these systems $KMnO_4/\alpha\text{-}Al_2O_3$ E_{O_2} = 38±2 k. cals, $KMnO_4/ZnO$ (1000°) E_{O_2} = 43±5 k. cals and $KMnO_4/ZnO + Cr_2O_3$ E_{O_2} = 43±5 k. cals are very similar to that for pure permanganate. It is perhaps noteworthy that for pure potassium permanganate in the range α = 0 - 0.05, the conduction activation energy is also "low":. C 26 k. cals/mole compared with 26 - 32 k. cals for this second group of systems. For the latter, where the added oxides are mainly n-type, it may again be suggested therefore that the conduction is by a species arising other than by reaction 1. If on the other hand, these oxides do in fact facilitate the release of an electron from the permanganate ion, then their catalytic action is readily explained and also the preference for surface growth of nuclei indicated by the t^2 kinetics found for all three systems for the initial stage of the decomposition. Coupled with the t^2 process is the postponment of the onset of the Prout-Tompkins branching until α = 0.2; with the other systems and with pure permanganate the onset normally occurs at approximately α = 0.1.

The lowering of the energy required to remove an electron from the permanganate ion may in the case of $\alpha\text{-}Al_2O_3$ owing to its large surface area, be due to the creation of many more "active" sites on the permanganate by grinding during mixing, or to some semi-conductor property of the $\alpha\text{-}Al_2O_3$. However, in the case of ZnO (1000°) and $ZnO + Cr_2O_3$, since they have relatively low surface areas, the reduction in activation energy would most probably be related to the semi-conducting properties of the oxides. It is to be noted however that no significant differences in kinetics or activation energies occur due to the incorporation of chromic oxide into the lattice of the zinc oxide.

After the exponential increase, as already stated, the conductivity continues to increase but at a slower rate. This probably reflects the return to the "normal" pure permanganate reaction, but modified slightly by an increase in rate of reaction 3, due to an increased electron concentration provided by the n-type oxides.

In conclusion therefore, these results appear to confirm that the decomposition occurs by a mechanism similar to that proposed by Smirnova, with the rate determining step the removal of an electron from the permanganate ion. The catalytic effect of most of the oxides appear not to be related to any lowering of activation energy for the rate determining step but to an increase in the pre-exponential term of the Arrhenius equation.

Comparison of the results from this work with the published results of the effect of oxides on the thermal decomposition of perchlorates[39, 40, 41, 42, 44] suggests that the decomposition of potassium permanganate is more complex. Due, perhaps, to the fact that, unlike the perchlorates, the decomposition results in the formation of an oxide, MnO_2, which will be in close contact with the unreacted permanganate. Also in contrast to the perchlorates, where the catalytic effect of the oxides is quite appreciable and extends throughout the decomposition, is the fact that with potassium permanganate the oxides, with the exception of nickel, only effect the initial stage of the decomposition up to $\alpha = C\ 0.15$. Any effect due to the semi-conductivity of the oxides also appears less important and if anything is completely opposite to that found for the perchlorates. For the perchlorate decomposition p-type oxides were found to be the most efficient catalysts. In this work increasing the p-type character of the oxides by "doping" had no effect the systems $KMnO_4/NiO$ (1000°) and $KMnO_4/NiO + Li_2O$ were no more efficient than pure permanganate whereas the

systems $KMnO_4/ZnO$ (1000°) and $KMnO_4/ZnO + Cr_2O_3$ were rather more efficient than pure permanganate.

FILTRON
EXTRA STRONG

ABSTRACT

A brief outline has been given of the present knowledge of the kinetics of the thermal decomposition of inorganic solids.

The effect of NiO, Fe_2O_3, CuO, ZnO, MnO_2 and α-Al_2O_3 on the decomposition of potassium permanganate in the solid state has been studied using pelleted samples of 1.1 mixtures, by weight, of permanganate and oxide. The decomposition, in all cases, could be accurately represented by the equation

$$KMnO_4 \longrightarrow K_2MnO_4 + MnO_2 + O_2$$

The oxides were found to catalyse the initial stages of the decomposition but their effect was exhausted, with the exception of NiO, after α = c 0.15. The decomposition in the later stages, α = 0.15 - 0.9 followed the Prout-Tompkins equation, viz.

$$\log \alpha/1-\alpha = kt + c$$

two values of k being required. This requires the acceleration or autocatalytic stage α = 0.15 - 0.5 to proceed by a "branching plane" mechanism in which the planes interfere, k being a measure of the probability of branching. The second value, k_2, is required for the decay stage of the decomposition α = 0.5 - 0.9.

Since in the α - range 0 - 0.10 a common kinetic equation did not hold for all the systems studied, it was necessary, in order to measure the relative catalytic efficiency of the oxides, to resort to arbitrarily selecting the inverse of the time required for α to reach 0.03 as a measure of the catalysis. This procedure gave the following "activity series".

$$NiO > Fe_2O_3 > CuO > ZnO, \alpha\text{-}Al_2O_3 > MnO_2$$

The activation energy for the decomposition in this region, as measured by

oxygen evolution, was 38±3 k. cals/mole; irrespective of system. The catalytic action of the oxides is therefore due to a change in the pre-exponential term of the Arrhenius equation. Their action would appear to be dependent on an "active surface" and on oxide surface area, since heating to 1000°C, in the case of NiO and ZnO, destroyed the catalysis. The semi-conductor properties of the oxides do not appear to be important: the incorporation of altervalent lithium and chromic oxide into the lattices of nickel and zinc oxide respectively led to no significant change in catalytic activity or kinetics.

The changes in electrical conductivity of the permanganate - oxide pellets were measured during the decomposition of the permanganate. The results have been explained within the mechanism proposed by Smirnova, although the exact identity of the intermediate given as MnO_4 or of the conducting species assumed to be an electron, could not be established. These results suggested that the rate determining step of the decomposition is probably the removal of an electron from the permanganate ion. The activation energy for the production of the charge carrier, 38±2 k. cals/mole, is not significantly different from that for the initial decomposition as measured by oxygen evolution. The presence of oxides, with the exception of ZnO (1000°), $ZnO + Cr_2O_3$ and α-Al_2O_3 did not alter the activation energy of conduction, confirming that the catalysis is due to changes in the A factor.

References

1. Garner, "Chemistry of the Solid State", ed. Garner(Butterworths, London 1955). Chap. 8.
2. Hailes, Trans. Faraday Soc. 29, (1933) 544.
3. Prout and Tompkins, Trans. Faraday Soc. 43, (1947) 148.
4. Garner and Gomra, J. Chem. Soc., (1931) 2123.
5. Wischin, Proc. Roy. Soc., A 172, (1939) 314.
6. N.F. Mott, Proc. Phy. Soc., B 64, (1951) 729.
7. F. Seitz, Advan. Physics, 1, 43. (1952)
8. J.S. Koehler, Phy. Rev., 60, (1941) 397.
9. D.L. Dexter, Phy. Rev., 86, (1952) 770.
10. Cottrell "Progress in Metal Physics", Vol. 1, Chap. 2. Butterworths London (1949)
11. Hedges and Mitchell, Phil. Mag., 44, (1934) 223, 357.

13. Bright and Garner, J. Chem. Soc., (1934) 1872.
14. Garner and Southam, J. Chem. Soc., (1935), 1705.
15. Garner and Reeves, Trans. Faraday Soc., 50, (1954) 254.
16. Acock and Garner, Proc. Roy. Soc., A 189, (1947) 508.
17. Avrami, J. Chem. Phys., 7, (1939) 1103; 8, (1940) 212; 9, (1941) 177.
18. Garner and Hailes, Proc. Roy. Soc., A 139, (1933) 576.
19. Finch, Jacobs and Tompkins, J. Chem. Soc., (1954), 2053.
20. Prout and Tompkins, Trans. Faraday Soc., 40, (1944) 488.
21. Herley and Prout, J. Phy. Chem., 64, (1960) 675.
22. Herley and Prout, J. Phy. Chem., 65, (1961) 208.
23. Herley and Prout, J. Phy. Chem., 66, (1962) 961.

24. Simpson, Taylor and Anderson, J. Chem. Soc. (1958), 2378.

25. Bircumshaw and Harris, J. Chem. Soc., (1939), 1637; (1948), 1898.

26. Bartlett, Tompkins and Young, J. Chem. Soc., (1956), 323.

27. Garner, Trans. Faraday Soc., 34, (1938) 979.

28. Hill, Trans. Faraday Soc., 54, (1958) 685.

29. Erofeev and Smirnova, Zhur Fiz. Khim., 26, (1952) 1233.

30. Erofeev and Smirnova, Zhur. Fiz. Khim., 25, (1951) 1098.

31. B.V. Erofeev, Proc. Inter. Symp. of Reactivity of Solids, 4th Amsterdam 1960, 273.

32. Komatsu, J. Chem. Soc. Japan, 78, (1957) 1452.

33. Hill and Welsh, Trans. Faraday Soc., 56, (1960) 1059.

34. Roginsky and Schultz, Z. Phys. Chem., A 138, (1928) 21.

35. Osinovich and Bel'kevich, Vesti. Akad. Navuk. Belarus. S.S.R. Ser. Fiz-Teckh. Navuk, (1956), No. 1, 127.

36. Smirnova, Zhur, Fiz. Khim., 30, (1956) 2649.

37. Simchen, Bull. Soc. Chim. France, (1954), 638.

38. Prout and Tompkins, Trans. Faraday Soc., 42, (1946) 468.

39. Solymosi and Krix, Journal of Catalysis, 1, 468. (1962)

40. Solymosi and Revesz, Z. anorg. Chem., 322, (1963) 86.

41. Solymosi and Revesz, Magyar Kem. Folyoirat, 68, (1962) 283.

42. Galwey and Jacobs, Trans. Faraday Soc., 55, (1959) 1165,

43. Solymosi and Kris, Magyar Kem. Folyoirat, 68, (1962) 283.

44. Hemoni and Salmon, 8th Symp. on Combustion, Baltimore, (1962), 5656.

45. Galwey and Jacobs, Proc. Roy. Soc., A 254, (1960) 455.

46. Smirnova, J. Physic Chem. U.S.S.R., 29, (1955) 135; 30, (1955) 2649.

47. B.R. Philips, PhD. Thesis, Edinburgh University, (1961).

48. Palmers, "Inorganic Chemistry", 483. Cambridge. (1954.)

49. Wagner and Hanltemann, J. Chem. Phys., 18, (1950) 72.

50. Jacobs and Tompkins, J. Chem. Phys., 23, (1955) 1445.

51. Jacobs and Tompkins, Quat. Reviews, (1952), 238.

52. Simpson, PhD. Thesis, Edinburgh University, (1957).

53. Darwin, Phil. Mag., 6, 27, (1914) 315, 675; 43, (1922) 800

54. Mooney, Physic Rev., 37, (1931) 1306.

55. St. John Physic Rev., 21, (1923) 389.

56. Prount and Herley, J. Inorg. and Nucl. Chem., 9, (1959) 232.

57. Jacobs and Tompkins, Reference 1, Chap. 7.